UNIVERSITY OF NAIROBI

THE GEOMETRY, HYDROGEOCHEMISTRY AND VULNERABILITY OF AQUIFERS TO POLLUTION IN URBAN AND RURAL SETTINGS: A CASE STUDY OF KISUMU AND MT. ELGON AQUIFERS
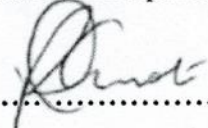
BY

JAPHET RUGENDO KANOTI
REG. NO. I80/96667/2014

A THESIS SUBMITTED IN FULFILLMENT OF THE REQUIREMENTS FOR THE AWARD OF THE DEGREE OF DOCTOR OF PHILOSOPHY IN GEOLOGY OF THE UNIVERSITY OF NAIROBI

2021

DECLARATION

I declare that this thesis is my original work and has not been submitted elsewhere for examination, award of degree or publication. Where other people's work or my own work has been used, this has been properly acknowledged and referenced in accordance with the University of Nairobi's requirements.

Signature ………………………………..……Date……23/06/2021…………………………

Japhet Rugendo Kanoti

I80/96667/2014

Department of Geology

School of Physical Sciences

University of Nairobi.

This thesis is submitted for examination with our approval as research Supervisors:

Name	Signature	Date
1. Prof. Norbert Opiyo-Akech, Department of Geology, University of Nairobi, P.O. BOX 30197-00100, Nairobi. Kenya. opiyo-akech@uonbi.ac.ke		24/6/2021
2. Prof. Daniel Olago, Department of Geology, University of Nairobi, P.O. BOX 30197-00100, Nairobi. Kenya. dolago@uonbi.ac.ke		24/6/2021
3. Prof. Christopher Nyamai, Department of Geology, University of Nairobi, P.O. BOX 30197-00100, Nairobi. Kenya. cnyamai@uonbi.ac.ke		24/6/2021

DECLARATION OF ORIGINALITY FORM

This form must be completed and signed for all works submitted to the University for Examination.

Name of Student: JAPHET RUGENDO KANOTI

Registration Number: I80/96667/2014

College: BIOLOGICAL AND PHYSICAL SCIENCES

Faculty/School/Institute: SCHOOL OF PHYSICAL SCIENCES

Department: GEOLOGY

Course Name: Ph.D. IN GEOLOGY

Title of the work: THE GEOMETRY, HYDROGEOCHEMISTRY AND VULNERABILITY OF AQUIFERS TO POLLUTION IN URBAN AND RURAL SETTINGS: A CASE STUDY OF KISUMU AND MT. ELGON AQUIFERS

DECLARATION

1. I understand what Plagiarism is and I am aware of the University's policy in this regard

2. I declare that this Thesis is my original work and has not been submitted elsewhere for examination, award of a degree or publication. Where other people's work, or my own work has been used, this has properly been acknowledged and referenced in accordance with the University of Nairobi's requirements.

3. I have not sought or used the services of any professional agencies to produce this work

4. I have not allowed, and shall not allow anyone to copy my work with the intention of passing it off as his/her own work

5. I understand that any false claim in respect of this work shall result in disciplinary action, in accordance with University of Nairobi Plagiarism Policy.

Signature: _____

Date: 23/06/2021

Dedication

I dedicate this thesis to my late father, Eliphas Ngeretha Njagi, my beloved mother, Cecilia Ciankoroi, my wife, Harriet, my daughter, Hellen and my son Vincent.

Abstract

Kenya is one of the countries in sub-Saharan Africa considered to have water scarcity, and the national per capita water is below 1,000 cubic meters. The estimated per capita by the Kenya government in 2005 was about 647 cubic meters, and in 2009 it was estimated at 534 cubic meters. Water scarcity in the country is expected to worsen by 2025, when per capita water is estimated to be about 235 cubic meters. This projected low per capita is a serious threat to socio-economic development, the ecosystems, and the efforts to achieve the Government of Kenya blueprint of Vision 2030 and the United Nations sustainable development Goal 6. The low per capita can be mitigated by the proper understanding of the finite freshwater resource in the country. Like in other parts of Sub-Saharan Africa, there is an explicit lack of information on aquifer geometry, water chemistry, groundwater vulnerability to contamination, and the timing of recharge water in both rural and urban settings in Kenya. This study aimed to appraise aquifers' aquifer geometry, hydrogeochemistry, and vulnerability to pollution in Kenya's urban and rural settings. The urban aquifer is Kisumu and the rural aquifer is Mt. Elgon. The specific research objectives were; (a) to delineate the aquifer geometry in the selected areas of study and estimation of aquifer properties, including yields, transmissivity, and storativity values through pumping tests data in selected wells, (b) to establish groundwater quality and evaluate how groundwater chemistry was modified by rock-water and surface-groundwater interactions and land uses through analysis of water samples and (c) to determine recharge sources through environmental isotope signatures in groundwater. The existing literature was reviewed and, historical borehole data and current data from selected wells was analysed to determine current knowledge and gaps. The research entailed field surveys to determine geology, in-situ physico-chemical parameters, thermotolerant coliform bacteria, and interviews with the local community to identify the location of existing water points. The study also entailed water sampling and analysis for the determination of water chemistry and isotopic composition. Geological mapping and vertical electrical sounding combined with petrographic, XRD, XRD, and interpretation of VES data using relevant software were used to determine the aquifer geometry. Test drilling for lithological samples, aquifer testing, and analyses of previously available data permitted delineation of aquifer dynamics, generalised transmissivity distribution, and interpretation of the groundwater flow system. Field measurements using relevant field kits were used to measure the physic-chemical parameters of water and bacterial loading in the water. Full chemical analysis of water and isotopic analysis for oxygen-18 and deuterium was done locally and in the United Kingdom. Relevant computer software was used

to construct the geological maps, statistical plots, chemical, and isotopic plots. The research revealed that the shallow Kisumu aquifer is extremely heterogeneous. Mt. Elgon aquifer is also heterogeneous. In an attempt to understand the hydrogeochemistry of the study areas, the origin and composition of solutes in groundwater sampled from the Kisumu and Mt. Elgon aquifers were charecterised using a range of techniques. Classical graphical methods (i.e., Gibbs, Durov, Piper, Schoeller, Stiff and Ternary plots) were utilised as interpretative tools of the main hydrogeochemical processes. The study identifies three main groundwater geochemical signatures in the Kisumu study area: cation exchange (Ca^{2+}-Na^+ and Ca^{2+}-Mg^{2+}) between aqueous and solid phases, the chemistry of recharge water, and groundwater mixing. The concentration of major ions in groundwater varied with geology and also seasonally. The dominant water facies was Na^+ - Ca^{2+} - HCO_3^- type; other hydrochemical facies include Ca^{2+}-Mg^{2+}-HCO_3^- and Na^+-HCO_3^-. Hydrochemical plots suggest that the dissolution of carbonates and halite are the other major chemical processes and cation exchange that controls the groundwater chemistry in the Kisumu aquifer. The dominant water type in the Mt. Elgon aquifer is the Na^+-HCO_3^- type. The Kisumua quifer's mineralisation was more than in the Mt. Elgon, as revealed by the saturation indices. The historical records of $\delta^{18}O$ and $\delta^{2}H$ in rainfall at Kericho from the IAEA Global Network of Isotopes in Precipitation (GNIP) database were used to plot the local meteoric water line. Stable isotope ratios in groundwater reflect orographic effects on rainfall controlling recharge, a bias to months of heavy rainfall, and evaporative enrichment in heavy isotopes associated with local, convectional rainfall derived from Lake Victoria. The isotopic tracers indicate that shallow groundwater in Kisumu is recharged directly and locally from rainfall, and there is no direct connection between Lake Victoria and groundwater. The study concluded that the current deficiencies in providing adequate water and dignified sanitation to the poor in rural and urban settings could be remedied through improved knowledge of shallow aquifer dynamics, the geological control of groundwater flow isotope hydrology, and innovative water research. Improved scientifically based evidence is the only path to achieving the UN SDG 6 and Kenya's four development pillars.

Table of Contents

List of Figures

xii

List of Tables

List of abbreviations and acronyms

AfriWatSan	African Water and Sanitation Project
EPSG	European Petroleum Search Group
GMWL	Global Meteoric Water Line
GNIP	Global Network of Isotopes in Precipitation
GoK	Government of Kenya
GPS	Global Positioning System
IAEA	International Atomic Energy Agency
IGAD	Intergovernmental Authority on Development
IHP	Intergovernmental Hydrological Programme
ISCO	*In situ* chemical oxidation
ISTT	*In situ* thermal treatment
IWMI	International Water Management Institute
JICA	Japan International Cooperation Agency
KMD	Kenya Meteorological Department
LMWL	Local Meteoric Water Line
MDG	Millennium Development Goals
Meq	Milliequivalent
mg/L	Milligrams per Litre
MNA	Monitored Natural Attenuation
NAWARD	National Water Resources Database
NGO	Non-Governmental Organization
PCA	Principal Component Analysis
SDG	Sustainable Development Goals
SSA	Sub-Saharan Africa
TTC	Thermotolerant Coliforms
UN	United Nations
UNEP	United Nations Environmental Programme
UNESCO	United Nations Educational, Scientific and Cultural Organization
UNICEF	United Nations Children's Fund
WHO	World Health Organization
WRA	Water Resources Authority

Definition of Keywords

Aquifer	An underground rock formation that can store, yield and transmit water
Aquifer geometry	Aquifer zones, well yield, hydraulic aquifer properties, groundwater levels, flow and recharge.
Base Flow	Water that seeps into a stream through porous rock or sediment unit that outcrops in the bottom or banks of the stream.
Confined Aquifer	An aquifer that exists where the groundwater is bounded between layers of impermeable rocks

Contamination	Naturally-occurring or anthropogenic substances in air, soil or water that are unfit for human consumption and can cause harm to human health or the environment.
Depletion	The loss of water from groundwater aquifers or surface water reservoirs at a rate greater than that of recharge; when water is used faster than it is replaced
Discharge	An outflow groundwater aquifer, or watershed; the opposite of recharge
Homogeneous aquifer	An aquifer is homogeneous when aquifer parameters are constant throughout the medium, i.e. the properties of the medium are independent of space.
Heterogeneous aquifer	An aquifer is heterogeneous or non-homogeneous when aquifer properties are varying with space.
Hydrochemical facies	Are used to denote the diagnostic chemical aspect of groundwater solutions occurring in hydrologic systems. The facies reflect the response of chemical processes operating within the lithologic framework and also the pattern of flow of the water.
Hydraulic conductivity	The ability of a porous material to transmit a fluid.
Isotope	One of several forms of an element. These different forms have the same number of protons but varying numbers of neutrons.
Precipitation	Stage of the water cycle when water vapour molecules become too large and heavy to remain in the atmosphere and fall to the ground in the form of rain.
Drawdown	The reduction in hydraulic head observed at a well in an aquifer, typically due to pumping.
Recharge	Water added to a groundwater aquifer. For example, when rainwater seeps into the ground. Recharge may occur naturally through precipitation or surface water or artificially through injection wells.
Storativity	The storage coefficient is the volume of water released from storage per unit decline in hydraulic head in the aquifer, per unit area of the aquifer.
Transmissivity	The rate at which water passes through a unit width of the aquifer under a unit hydraulic gradient.
Water quality	An assessment of the physical, chemical and biological characteristics of water, especially how they relate to the suitability of that water for a particular use.

Water table	A level beneath the Earth's surface, below which all pore spaces are filled with water and above which the pore spaces are filled with air. The top of the zone of saturation in a subsurface rock, soil or sediment unit.
Withdrawal	A removal of water from a surface or groundwater source for use.

CHAPTER 1 – INTRODUCTION

1.1   Background information

Water supports life, and it is an essential requirement supporting all other human activities. The importance of water has received recognition by the United Nations since 1981. The First Water Decade (1981 – 1990) that the United Nations declared brought attention to and support for clean water and sanitation worldwide (UN, 1980). In 2010, the UN General Assembly explicitly recognized water and sanitation as a human right (UN, 2010). The global community has continuously given water importance. In September 2015, the United Nations Summit adopted the 17 Sustainable Development Goals (SDGs) that replaced the Millennium Development Goals (MDGs) that climaxed in 2015. The new goals are aimed at guiding global development efforts up to the year 2030. Water and sanitation targets are in goal number 6, which seeks to "ensure access to water and sanitation for all" (UN, 2015). This explicit focus is vital because there is a silent revolution in the intensive use of groundwater in most countries (Llamas and Martínez-Santos, 2005), including a sharp increase in groundwater exploitation to meet demands for agriculture and lifestyle changes due to increase in urbanisation (Linfang *et al*., 2020; Morris *et al*., 1994).

The effect of aquifer characteristics, water chemistry, water-rock interaction and isotopic composition on groundwater evolution is well documented (e.g. Ahialey *et al*., 2016; Blomqvist, 1999; Jeong, 2001; Walter *et al*., 2017). However, water scarcity and deteriorating water quality can be attributed to many local and global issues. Two main related issues are an increase in population and climate variability. The world population is snowballing and is resulting in increased demands for finite freshwater. In 2019 the world population was about 7.7 billion and was projected to be about 8.5 billion in 2030, 9.7 billion in 2050 and 10.9 billion in 2100 (UN, 2019). Apart from demand increases, the increase in population results in increased human waste and demands for waste disposal systems. Global climate changes are expected to affect the hydrological cycle, altering surface-water levels and groundwater recharge to aquifers with various other associated impacts on natural ecosystems and related human activities (Le Treut *et al*., 2007). Global and local climate changes can affect water resources in many ways. The impacts of changes on water resources have been studied in some detail, but little is known about how groundwater will respond to these changes (e.g. (Bovolo *et al*., 2009; Green *et al*., 2011; Holman, 2006). Of particular interest are groundwater and surface water interactions and how climate change influences groundwater dynamics. Previous

studies projected that the most noticeable impacts could be changes in surface water levels and quality. There could be potential effects on groundwater quantity and quality (Le Treut *et al.*, 2007). Hence, concerted efforts are needed to understand the hydrological cycle better, emphasising the groundwater. Understanding flow paths and other aquifer characteristics should be a priority in both rural and urban aquifers. The understanding will provide information and data for sustainable management of the aquifers (Gleeson *et al.*, 2012).

A review by the WHO and UNICEF Joint Monitoring Programme in 2017 estimated that about 1.8 billion people globally used water sources that were contaminated with faecal indicators, and noted that achieving universal access by 2030 will be challenging for some countries that rely directly on rivers, lakes and irrigation canals for drinking water (WHO and UNICEF, 2017). The report further reveals that in Angola, Kenya, Madagascar, Papua New Guinea, Sierra Leone, South Sudan and Tajikistan, 20% of the population rely on surface water for drinking, a source considered unprotected. Today, as the global community strives to achieve the SDG6 targets, millions of people succumb to infectious diseases associated with drinking contaminated water. The waterborne diseases kill approximately 1.8 million people, most of whom are children below five years in developing countries (WHO, 2007), and have associated impacts on family food security, livelihood and educational opportunities for communities and societies all over the world (Kulabako *et al.,* 2010). Shifting from surface to groundwater for potable water supplies, therefore, conveys several benefits, including better protection from pollution, minor temporal variability of supply due to the large storage capacity of most ground-water aquifers, constant temperature, obtaining water close to users. The possibility of step-wise development of groundwater supplies as demand increases makes it possible to avoid significant initial investments (Macdonald *et al.,* 2005).

Africa is the second driest continent after Australia and experiences perennial water scarcity (Dos Santos *et al.*, 2017; Naik, 2017). The scarcity involves water stress, water deficit/shortage and water crisis. Groundwater is an integral part of climate change adaptation and is often a solution for people without access to safe water (Gleeson *et al.*, 2012). The rural areas and small towns rely on septic tanks and pit latrines, sources of surface and groundwater contaminants. Further, most urban and rural settings utilise shallow aquifers that are susceptible to both climate change and pollution (Xu *et al.*, 2019), while at the same time, networked sewer systems only exist in major cities. Sub-Saharan Africa (SSA) is affected most by water scarcity compared to the North African countries with high-yielding, high-storage, sedimentary

aquifers (Foster *et al*., 2018; Xu *et al.*, 2019). The shortage of water can further be attributed to inadequate investment in the water sector. Water utility companies and Central Governments set aside very little money for research in groundwater (Gronwall and Danert, 2020). Insufficient investment in research can be partly related to the traditional neglect of groundwater due to its invisibility. Therefore, apart from the transboundary aquifers, little is known about most aquifer geometry and groundwater dynamics in developing countries, especially for the smaller aquifers crucial to urban and rural settings (Olago, 2019). Relative to North Africa, there is little investment in groundwater research and monitoring systems in SSA due to high investment costs, and therefore few countries in Sub-Saharan Africa have drilled dedicated boreholes for observation and monitoring (IWMI, 2012). The only information available in most countries is from isolated individual academic research or through projects funded by development partners. Despite the low investment in groundwater research, it provides almost half of all drinking water world-wide, about 40% of water for irrigated agriculture and about 30% of water supply required for industry (Guppy *et al.*, 2018; IGRAC, 2018). It sustains ecosystems, wetlands and maintains the base-flow of rivers (Taylor *et al*., 2013).

Like the other sub-Saharan African countries, Kenya faces water challenges and is considered a water-scarce country (Naik, 2017). Surface water is diminishing due to climate variability (Mogaka *et al*., 2006) and where the rivers pass through towns, the water is heavily contaminated (Mbui *et al*., 2016). The Kenya government estimated that the water per capita in 2005 was 647 m^3 per person per year, and in 2009 it was at 534 m^3 per person per year, far below the global benchmark of 1000 m^3 per person per year (Gulyani *et al*., 2005). Water scarcity is expected to worsen by 2025 when per capita water is estimated to be below 500 m^3 per person per year in Kenya, an indicator of absolute water scarcity (Marshall, 2011; World Bank, 2011b). Due to diminishing and deteriorating surface water resources, groundwater utilization is gaining momentum. Nairobi and Kisumu are examples of cities whose water supply is strongly complemented by groundwater borehole and shallow wells (*Figure 1.1*). The availability and demand for groundwater resources in Kenya vary, spatially, temporally and sectorally (Bakker, 1997; Olago, 2019), but neither the groundwater potential nor its vulnerability to both geogenic and anthropogenic pollutants is known at the national level (Rendilicha *et al*., 2018), and information from already undertaken studies are not readily available to water stakeholders (Mogaka *et al*., 2006; World Bank, 2011a).

Figure 1.1. Queuing for water in Nyamasaria, Kisumu. The scenario is duplicated in all major towns in Kenya during the dry season

The national projected low water per capita and lack of adequate data for sustainable management of the increasingly important groundwater are severe threats to socio-economic development, the ecosystems and the efforts to achieve the Government of Kenya development blueprint, Vision 2030.

1.2   Statement of the problem

This study gives insight into two inadequately studied yet critical groundwater systems in Kisumu and Mt. Elgon. The groundwater in these areas is being exploited without adequate understanding of the aquifer extents, geometries and characteristics (Alam, 2014; Razack *et al.*, 2020; Tamunobereton-ari *et al.*, 2014), which are necessary ingredients to inform sustainable groundwater management. The scope of the geometry entails the determination of geologs during drilling to determine vertical stratigraphy from the surface to the water struck level and whether the aquifer was homogeneous or heterogeneous. Groundwater dynamics are essential in understanding aquifer characteristics (IWMI, 2012; Maurice *et al*., 2018; Sindico

4

et al., 2018). These dynamics can be estimated by mapping the geology, delineating the aquifer geometry, and determining the recharge mechanisms (Todd and Mays, 1980). Estimation of aquifer properties like yields, transmissivity, and storativity values can be achieved through pumping tests (Fetter, 2001). Groundwater recharge can also be estimated using the groundwater table fluctuation method (Varni *et al*., 2013; Yang *et al.*, 2018). This method requires long term (more than two years) monitoring of groundwater table and rainfall.

Currently, there exist only scanty and scattered information, mainly from point-located geological and geophysical surveys that are aimed at finding sites for borehole drilling (Olago, 2018), so that the principal focus has been to identify the appropriate drilling location and depth to the water table to enhance chances of getting a successful water supply well. Although test pumping is routinely done to determine the yields and, therefore, the size of the pump to be installed, data from pumping can also give information on aquifer dynamics. Still, drillers do generally not undertake this analysis. These point source data, taken collectively, can supply information on an aquifer's spatial and depth characteristics, including its geometry and flow dynamics. Further, there were no piezometers for measuring groundwater table fluctuation in Kisumu and the Mt. Elgon study sites before this study. However, during this study, six piezometers were installed in Kisumu. No piezometers were installed in the Mt. Elgon study site due to financial constraints.

Vulnerability to contamination by geogenic and anthropogenic processes is hardly studied before groundwater development (Muthoni, 2009). After the development of a borehole, the only parameters that are essentially taken into consideration are water yields and quality and suitability for human consumption, which is only accepted at the time that the well is being developed (Abdi and Osman, 2012; Coetsiers *et al*., 2008; Gicheruh, 1993; Kanda and Suwai, 2013; Mailu, 1997), and which only routinely analyse a determined suite of major and minor ions that may miss out on ions which may be necessary to be monitored based on the unique geology and anthropogenic contamination threats that are faced in a particular area. Further, there is no continuous monitoring, yet the sub-surface which hosts groundwater also acts as a repository of on-site human waste disposal, particularly in low-income areas where the majority of the population live and which are unserved with sewer systems, rendering the groundwater vulnerable to anthropogenic pollution over space and time.

The Kisumu and Mount Elgon aquifer systems vulnerability to contamination from both geogenic and anthropogenic sources as a consequence of interactions in the nexus of geology, rainfall, land-use changes and onsite sanitation, compounded by changes in flow dynamics due to over-abstraction and climate variability and change, are poorly understood (DHV Consultants, 1988; Fetter, 2001; K'oreje *et al*., 2016; Nyilitya *et al*., 2020; Opisa *et al*., 2012b). In urban settings in Kenya, including Kisumu, it has also been observed that incidences of waterborne diseases increase during rainy seasons (Angienda and Onyango, 2010; Njiru *et al*., 2016; Osiemo *et al*., 2019; WHO, 2007). However, there remains an absence of scientific evidence linking this increase to the continued use of the subsurface for sanitation and as a source of drinking water. In rural settings such as Mount Elgon, planned sewerage are rare, and the populations rely on pit latrines and, occasionally, non-lined septic tanks (Gudda *et al.*, 2019; Nakagiri *et al*., 2016; Njuguna, 2019). Shallow wells are commonly dug close to these pit latrines (Drangert *et al.*, 2002; Lapworth *et al*., 2017; Okotto-Okotto *et al*., 2015).

Finally, there is a lack of explicit knowledge of the groundwater recharge/discharge rates, source of recharge water, flow paths, residence time, and interaction between surface and groundwater for both the Kisumu and Mount Elgon aquifer systems. Isotope hydrology is a powerful tool to study these aspects, but generally, it has not been utilised due to a lack of expertise and dedicated laboratories for analysis.

This study aimed at narrowing the knowledge gap and sought answers to the following broad questions;

1. What are the aquifer characteristics in Kisumu, and what factors influence these characteristics?
2. What causes the hydrochemical modification of groundwater in Kisumu and Mt. Elgon aquifers, and how vulnerable are aquifers to faecal contamination and pollution in a changing climate?
3. What is the relationship between rainfall, recharge and groundwater in the Kisumu aquifer?

1.3   Main and specific objectives of the study

1.3.1   Main objective of the study

This study aimed to delineate Kisumu and Mt. Elgon aquifer characteristics, determine the relationship between groundwater quality, geology, rainfall, land uses and on-site sanitation, and establish the source of recharge water using environmental isotope signatures.

1.3.2   Specific objectives of the study

This study aimed at achieving the following three specific research objectives in selected study sites:

1)   To delineate the Kisumu and Mt. Elgon aquifer geometry and estimate the aquifer properties.

2)   To determine groundwater chemistry and groundwater vulnerability to contamination.

3)   To determine the relationship between Lake Victoria and groundwater and the source of the recharge water in Kisumu.

1.4   Justification and significance of the study

1.4.1   Justification of the study

At the national level, a poor understanding of groundwater undermines the sustainability of the general water resource base that can be used for the economic viability of water supply and water resources investments (Dos Santos *et al.*, 2017; Macdonald and Davies, 2000). Groundwater mapping at a national scale has never been undertaken, and the current hydrogeological map is based on geology and scattered hydrogeological survey reports. It is essential to understand the aquifer geometry and extent, which means, among other things, its length, width, thickness, vertical and lateral extensions, and flow dynamics (Todd and Mays, 1980) since these properties determine the heterogeneity or homogeneity of an aquifer and have implications on the yields and vulnerability to pollution (Fetter, 2001).

Water chemistry is one of the parameters that determine the suitability of groundwater for various uses (APHA, 1999). There is a strong relationship between rainfall, land-use changes

and groundwater quality. Rainfall recharges the groundwater either directly or through surface run-off, and land-use changes influence the infiltration rates (Abdou *et al*., 2018; Carrera and Tubau, 2010; Chung *et al*., 2010; Oiro *et al.*, 2018; Taylor *et al*., 2006). Anthropogenic activities also modify the infiltration rate and introduce contaminants into water bodies (Xu et al., 2019), including coliform bacteria, contaminating groundwater through pit latrines and open defecation (Rompré *et al*., 2002). It is essential to establish groundwater quality and evaluate how groundwater chemistry is modified by rock-water interactions, cation exchanges, dissolution, surface-groundwater interactions, and land uses through analysis of water samples and environmental isotope analysis (Adimalla and Venkatayogi, 2018; Brielmann, 2008; UNESCO, 2002), particularly for the Kisumu and Mount Elgon aquifer systems for which such studies have not been comprehensively carried out, thus compromising human health through unsafe water use, and hampering remedial actions through lack of an informed evidence-base.

Environmental isotope signatures in groundwater can evaluate recharge water sources (Gat *et al*., 2001; Mook, 2000e). These isotopes include hydrogen, deuterium, tritium, oxygen-16, and oxygen-18, which are conservative and are not influenced by other water interactions (Adelana *et al.*, 2011; Leis *et al*., 2018; Oiro *et al*., 2018). Comparison between the local meteoric water line, global meteoric water line and isotopic signature of groundwater samples can reveal the origin of the recharge water (Mook, 2000a). If it is meteoric water, the aquifer has modern water vulnerable to climate variability and anthropogenic activities (Craig, 1961; Dansgaard, 1964). The isotopic signature can also reveal the relationship between groundwater and surface water (González-Trinidad *et al.*, 2017; Tamez-Meléndez *et al.*, 2016; Zhu and Ren, 2018).

1.4.2   Significance of the study

Due to the poor understanding of groundwater, there are already demonstrable negative impacts on groundwater systems, including pollution and over-abstraction (Calow *et al*., 2009; Calow *et al.,* 2010; Lapworth *et al.*, 2017; MacDonald *et al*., 2012; Maurice *et al*., 2018). The development and use of groundwater resources sustainably from aquifers that are strategic in rural and urban settings requires assessing the aquifer dynamics, hydrogeochemistry and vulnerability to pollution (Todd and Mays, 1980). The evaluation will ensure that an economically, socially, and environmentally acceptable balance is maintained between groundwater recharge and demand (Upton *et al.*, 2019). The determination of aquifer type and aquifer properties through pumping tests and geologs provides data that guides determining

suitable groundwater development sites (Fetter, 2001). For example, in a heterogeneous aquifer, the development of boreholes in one locality will not affect water yield in the neighbouring boreholes (Fetter, 2001). In such aquifers, borehole yields are influenced by the spatial-temporal distribution of recharge, groundwater storage, and aquifer transmissivity (Upton *et al.*, 2019). Borehole yields are critically dependent on the pumped water level and how this relates to vertical aquifer heterogeneity, the nature and distribution of inflow horizons to the borehole, and features of the borehole itself, such as borehole storage, the depth of the pump and its pumping characteristics (Foster *et al*., 2017).

Due to contamination of surface water bodies, groundwater utilization is slowly gaining pace in many countries (Calow *et al*., 2009; Calow *et al.,* 2010; MacDonald and Davies, 2000). Unlike surface water, groundwater is more resilient to climate variability and therefore considered a reliable water source during extreme drought (Hulme *et al.,* 2001). Despite the importance of groundwater, little effort is being put to understand the controls and threats (Tuinhof *et al*., 2011; Bonsor *et al.*, 2018; Lapworth *et al*., 2017; Maurice *et al*., 2018). Hydrogeochemical and environmental isotope techniques are cost-effective tools in hydrological investigations and assessments and are critical in supporting effective, sustainable water resources management (Barbieri, 2019). These tracers can effectively be used to model contamination and the impacts of the climate variability and provide adaptation mechanisms to sustain the finite groundwater (Carvalho *et al*., 2018; Gleeson *et al*., 2012; Maurice *et al*., 2018; Singh, 2014; Taweesin *et al., 2018).* While available groundwater must be used for economic growth, at the same time, it is essential to avoid creating undesirable impacts leading to a decline in the value of the resource in future. There is, therefore, a need for scientific evidence to understand its hydrogeological settings, quality, recharge and discharge processes and other groundwater properties and dynamics (Todd and Mays, 1980). Investigating the two aquifers in Kenya will contribute knowledge, data and information on the pertinent groundwater issues. The protection and sustainable management of groundwater aided by data and information generated through this study will benefit societies that rely on the resource and the environment. The outputs from this research will provide the evidence base to support policies and practise that sustain the quantity and quality of groundwater supply to various demand points in urban Kisumu and rural settlements in Mt. Elgon on the Kenyan side.

1.5   Scope and limitation of the study

1.5.1   Scope of the study

The aquifer geometry, hydrochemical facies and vulnerability to contamination were the critical areas investigated during this study. The two case study areas vary in size, population, geology, agro-climatic zones and land use. Each has unique geological, hydrogeological and hydrochemical characteristics and face different groundwater challenges. The degree of detail in the evaluation of the two study sites varies in this thesis as a consequence of the limitations described in the section below: actual field research on the Kisumu aquifer was undertaken in the context of all the four specific objectives, while for the Mount Elgon aquifer, fundamental field research was undertaken only concerning its hydro-chemistry (as specified in Objective 3 of this thesis), with other parameters and factors relating to objectives 1 and 2 being derived from critical analysis and synthesis of secondary literature.

In Kisumu, the study targeted the low-income settlement areas that rely heavily on groundwater. The area extended from Nyamasaria to Kisian and was approximately 20 x 15 kilometres ($300\,\text{km}^2$). The scope in Kisumu included a monthly collection of physico- chemical data, seasonal sampling for hydrogeochemical data, monitoring of water samples for contamination and stable isotope studies. Initially, twenty-two sites were randomly selected for monitoring and sampling. Data used in this study was collected from these twenty-two sites that included springs, shallow wells, boreholes, rivers and Lake Victoria. Later, selected six piezometers were drilled and installed with data loggers for continuous water table monitoring for use by other researchers. During the drilling of the piezometers, visual logging of the drill detritus was done at a 1-meter interval to reveal changes in the sub-surface geology and drill samples were collected at 3-meter intervals or when changes in soil or rock composition were noted. Pumping tests were done to determine the aquifer properties. Two automatic rainfall stations were put up within the Kisumu study area for water table fluctuation data to estimate recharge. The piezometer and rainfall data are not included in this study. Interpretation of these data requires long-term monitoring.

In Mt. Elgon, the scope included sampling groundwater from thirty-three randomly selected sites for hydrogeochemical analysis. The sites included springs, shallow wells and boreholes. Geophysical sounding and existing borehole completion records provided data for estimating

aquifer characteristics. The water sampling points were located between Kitale and Suam in Trans Nzoia County and extended northward to Kacheliba in West Pokot County.

1.5.2   Limitations of the study

In the two study areas, the unavailability of historical hydrogeological and groundwater data limited our scope of the study. The inventory of historical borehole data from the Ministry of Water and Sanitation was incomplete in the two study sites. Most boreholes could not be located on the ground because the coordinates provided were erroneous or the boreholes were abandoned. Data on borehole construction, water flow, drawdown, pumping tests, geologs and water quality data was missing. Data on water table fluctuation was not available since no single borehole was being monitored in the two study sites. There was no existing inventory of shallow wells and springs in both the Kisumu and Mt. Elgon study areas. A rapid survey and interviews with the community had to be conducted to identify strategic borehole, wells and springs for this study.

Lack of historical geophysical, hydrogeological and groundwater abstraction data constrained the numerical model development and estimation of recharge using the groundwater fluctuation method in the Kisumu study area. Data needed for groundwater modelling include information on surface and subsurface geology, depth to the water table, precipitation, evapotranspiration, borehole yield, stream flows, soils, land use, vegetation, irrigation, aquifer characteristics and boundaries, and groundwater quality data. During this research, we drilled six boreholes, and aquifer characteristics and limits from these sites are not enough for numerical or mathematical modelling. A conceptual model was developed for Kisumu using this data together with data collected during the field sampling and geological mapping.

Mt. Elgon studies were confined to the determination of hydrochemical processes and a few geophysical profiles near Kitale due to limited funding, insecurity and inaccessibility of roads in West Pokot. The Department of Geology, University of Nairobi does not have a laboratory that could analyse water for isotopic composition or complete chemical analysis. Therefore, commercial laboratories were used for both isotopic (Elemtex Laboratory, London) and chemical water analysis (Water Resources Authority (WRA) laboratory and CropNut laboratory, both in Nairobi). Water analysis is costly, and this meant limiting the number of samples for analysis.

11

1.6   The layout of the thesis

This thesis provides a comprehensive synopsis of the study and has five chapters. These chapters are given below. The titles and abstracts of the published papers in peer-reviewed journals are presented in the appendices. Auxiliary data and comprehensive data collected or generated and used for interpretation is also shown in the appendices. Chapter 1 introduces the general information on groundwater resources, the aim of the study, problem statement, objectives of the research, scope and limitation of this study, introduction to the study area and the general layout of this thesis. Chapter 2 provides a literature review relevant to the aim of the study. The chapter includes available information on groundwater availability and challenges globally, nationally and locally. Chapter 3 describes the study sites and methods, and materials used to achieve the objectives of this research. The methods discussed include geological surveys, water sampling, geochemical surveys, geophysical survey, isotope analysis and microbial analysis of water samples. Chapter 4 gives the results obtained from the research and a discussion of the results. The chapter provides results on aquifer geometry, water chemistry, isotope ratios, source of recharge water, and groundwater quality. Chapter 5 presents the conclusion and recommendation from this study. This chapter also provides the contribution of this study to science and contribution to the residents of the study areas.

CHAPTER 2 - LITERATURE REVIEW

2.1   Introduction

This chapter critically reviews groundwater's existing and current knowledge guided by the study's overall aim and specific objectives. The sections offer information on existing knowledge and gaps in knowledge achieved through this research based on the study objectives. The subsections are aquifer geometry and characteristics, groundwater chemistry determinants, and environmental isotope use to understand groundwater recharge.

2.2   Aquifer geometry and characteristics

2.2.1   Background information

Groundwater is an essential source of water in both rural and urban settings globally due to its affordability, quality, and ability to buffer short-time climatic variability (Aladejana *et al*. 2020; Hellwig *et al.*, 2020; Hosseinizadeh *et al*., 2019; Wang *et al*., 2010). There are global efforts to understand groundwater availability and potential through water table monitoring and the acquisition of sub-surface information through geologs and pumping tests (Fiedler and Doll, 2008; Richts *et al.*, 2011; Schmoll, 2013). However, in sub-Saharan Africa (SSA), little is known about the various aquifer geometry and characteristics at the national level (Fiedler and Doll, 2008; Kehinde and Loehnert, 1989; SADC, 2011; Taylor and Howard, 2000). In Kenya, very few aquifers have been studied in details. The aquifers that have received attention include Merti aquifer in North-eastern Kenya (Blandenier, 2015; De Leeuw *et al*., 2012; Kuria and Kamunge, 2013; Lantagne *et al*., 2009), Turkana aquifer (Haines *et al.*, 2017; Nyaberi *et al*., 2019; Olago, 2019), the Coastal aquifer (Ferrer et al., 2019) and the Nairobi aquifer (Mulwa *et al.*, 2010; Oiro *et al.*, 2020).

2.2.2   Aquifer properties and characteristics

Subsurface information about the geometry of an aquifer (aquifer boundaries) can be achieved through drilling (Liu *et al*., 2020). The data can also be derived by geophysical methods (Alam and Ahmad, 2014; Overmeeren, 1981). Logging during drilling generates data on the subsurface geology (Chirindja *et al.*, 2017; Wohlgemuth *et al*., 2004). This information is crucial in understanding aquifer geometry (Wilhelm and Jean, 1995). Other aquifer properties

can be calculated or estimated based on data from the drilling logs (geologs). These properties include porosity, grain size distribution, specific yield, storativity, hydraulic transmissivity and permeability, and compressibility (Fetter, 2001; Todd and Mays, 1980; Willis, 2008). Hydraulic transmissivity and porosity are the most critical factors that determine a good aquifer. Hydraulic transmissivity values >1 m^2 per day always result in a successful borehole (MacDonald *et al*., 2010). Little is known about the aquifer properties in both Kisumu and Mt. Elgon aquifers. Only scattered hydrogeological reports compiled hydrogeological surveys. The drillers are expected to conduct pumping tests to determine yields. Other aquifer characteristics are estimated for compliance purpose with the regulatory authorities. The key aquifer characteristics in Kenya are summarised by Kuria 2013, with little mention of Kisumu and Mt. Elgon aquifers due to lack of information (Z. Kuria, 2013).

Groundwater transmissivity is mainly controlled by rock type, discontinuities due to compositional differences and fractures (joints and faults) (Fetter, 2001). Other controls include topography, depth of weathering, nature and size of the recharge and discharge areas, and the spatial relationships of these factors (Crawford and Brackett, 1995). Most igneous rocks are consolidated and therefore have low primary hydraulic transmissivity and porosity. However, secondary porosity may develop due to earth processes like fracturing, faulting and hence increase transmissivity. Old erosional surfaces between various lava flows are other good hosts of groundwater (Meinzer, 1923; Chilton and Seiler, 2006; MacDonald *et al*., 2010; Maurice *et al*., 2018; Maxwell *et al*., 2018;). When lava flow is spread out in successive sheets, the old surfaces form suitable aquifers. Water occurs in joints, cavities and zones of vesicular and fragmental material between these subsequent lava flows. Geological structures like faults provide pathways for groundwater movement. These are very important in areas subjected to tectonic movements and metamorphism (Mussa *et al*., 2020; Solder *et al.*, 2020; van Lopik *et al*., 2020).

While the presence of spatial variability of aquifer properties is widely recognized in hydrogeological parameters, most pumping test data studies are carried out assuming that the aquifer is sufficiently defined by a few parameters, such as constant transmissivity and storativity (Oliver, 1993). However, recent studies of pumping test data's sensitivity to radially symmetric non-uniform flow properties have shown that the drawdown is insensitive to transmissivity. The storativity of an aquifer is the volume of water released from storage per

unit surface area of the aquifer per unit decline in the hydraulic head (Todd and Mays, 1980; Fetter, 2001).

2.2.3 Rock type and its influence on aquifer characteristics

2.2.3.1 Consolidated rocks

Metamorphic rocks differ in the number of crevices, size and transmissivity. Therefore, most metamorphic rocks form poor aquifers (Crawford and Brackett, 1995; Singhal, 2008; Sivaramakrishnan *et al.*, 2015; Tóth, 2009). Gneisses and slates are consolidated and have low primary porosity. Metamorphic rocks are intrinsically inferior in porosity and permeability. This is because the original porosity and permeability of the original rock, if any, have been entirely erased by the metamorphic processes. Indeed, water can only pass through them with difficulty. When metamorphic rocks weather, the resultant regolith can form 1suitable aquifers (Morgan, 2018; Taylor and Howard, 1996). Metamorphic rocks only gain porosity and permeability by fracturing. Fractures give the rock porosity and permeability from metric to decametric extension, from a few fractions of millimetres to a few centimetres thick, and thus render it aquiferous.

Igneous rocks typically form at depth and have interlocking crystals. They have the lowest primary porosity. The bulk of their porosity falls in fractures in the form of secondary porosity. Of the consolidated rocks, well broken volcanic rocks with cavernous openings created by dissolution have the highest possible porosity, while intrusive igneous rocks formed under high pressure have the lowest possible porosity.

Volcanic rocks are known to form very good aquifers (*Figure 2.1*). They have various chemical, mineralogical, structural, and hydraulic features, primarily due to differences in how the rock cooled from the magma (Middlemost, 1991; Suhada and Hastuti, 2019). However, hot pyroclastic material may become welded as it settles and thus be nearly impenetrable. Silicic lavas appear to be extruded as thick, compact flows, and except where they are fractured, they have low permeability. Basaltic lavas appear to be fluid, and they form thin flows at the tops and bottoms of the flows that have substantial pore space (Arnous *et al*., 2020; Fenta *et al*., 2020; Sarma *et al*., 2020; Suhada and Hastuti, 2019). The lava flows are divided by erosional surfaces or alluvial materials that form permeable zones. Passages that allow water to travel

vertically through the basalt and related rocks build columnar joints that form in the central sections of basalt flows (*Figure 2.1*). The most active and productive aquifers are volcanic rocks of basaltic origin (Fenta *et al.*, 2020; Wright and Burgess, 1992).

Figure 2.1. Andesitic rock outcrop in Kisumu. The columnar joints and fractures increase the secondary porosity

2.2.3.2 Unconsolidated rocks

Gravel forms very productive aquifers (Alsharhan and Rizk, 2020; Eggleston *et al.*, 1996; Kempton *et al.*, 1982). Coarse clean gravel has high porosity, permeability, and specific yield. It, therefore, absorbs water readily, stores it in large quantities, and yields it freely (Todd and Mays, 1980). The yields in gravel are further modified by the degree of sorting and the type of cementing materials. The best gravelly aquifer is formed from rock debris transported over long distances to remove soft materials, and only clean, hard, and durable materials remain (Fetter, 2001).

Silt is a porous material with minute interstices with high water-retaining capacity, but because the interstices are not connected, it permits a languid movement of water (Fetter, 2001). It yields water very slowly but may supply enough water for domestic use. Silty aquifers are likely to produce hard water due to the mineralogy of silt. Water from silt formation is of good quality. The danger of groundwater contamination from these aquifers is minimal because the material is very fine-grained and rarely contains crevices connected with the surface (Winter *et al*., 1998; Zhang *et al.*, 2017).

Clay forms very poor aquifers. This is not because it contains no water, but the constituent particles of clay are tiny, and the interstices between these particles are so minute that they hold water (Fetter, 2001). Clay is impervious under normal hydrostatic pressure (Jones, 1964; Konikow, August and Voss, 2001). It is also soft and plastic when wet. This property makes the joints or other larger openings formed in it close completely under even slight pressure (Xing *et al*., 2018).

Unsorted or poorly sorted alluvium form beds of excellent water-bearing gravel. However, alluvium is most of the time not well sorted, consisting of pebbles and boulders embedded in a mixture of gritty and clayey debris matrix (Abesser *et al.*, 2008). Such poorly sorted deposits are probably the result of unpredictable conditions of streamflow, whereby an area may at one moment receives coarse material carried by a raging flood and later receives only the clayey sediments of a degenerated stream (Fetter, 2001). The clayey sediments fill the spaces between the coarser debris. As deposition continues, the river channels are shifted many times, and the gravel beds of the abandoned channels gradually become covered with more poorly sorted alluvium. This alternating sequence ultimately develops into a thick mass of poorly sorted alluvial material with numerous stringers of well-sorted gravel that may contain groundwater (Kaser and Hunkeler, 2016).

2.2.4   Other aquifer media properties and relationship to yield

Apart from the type of rock, its texture influences the specific yield (Fetter, 2001). The specific yield decreases, and retention increases as grain size decrease due to packing and compaction. The amount of water an aquifer can store depends on the grains' packing and how they are connected (Todd and Mays, 1980; Willis, 2008). Fracturing and faulting increase aquifer yield (*Figure.2.2*).

A = dry borehole, B = productive borehole in fault Zone, C and F =Dry well, D = productive borehole in fractures, E and F = seasonal well and G = productive borehole in the weathered zone
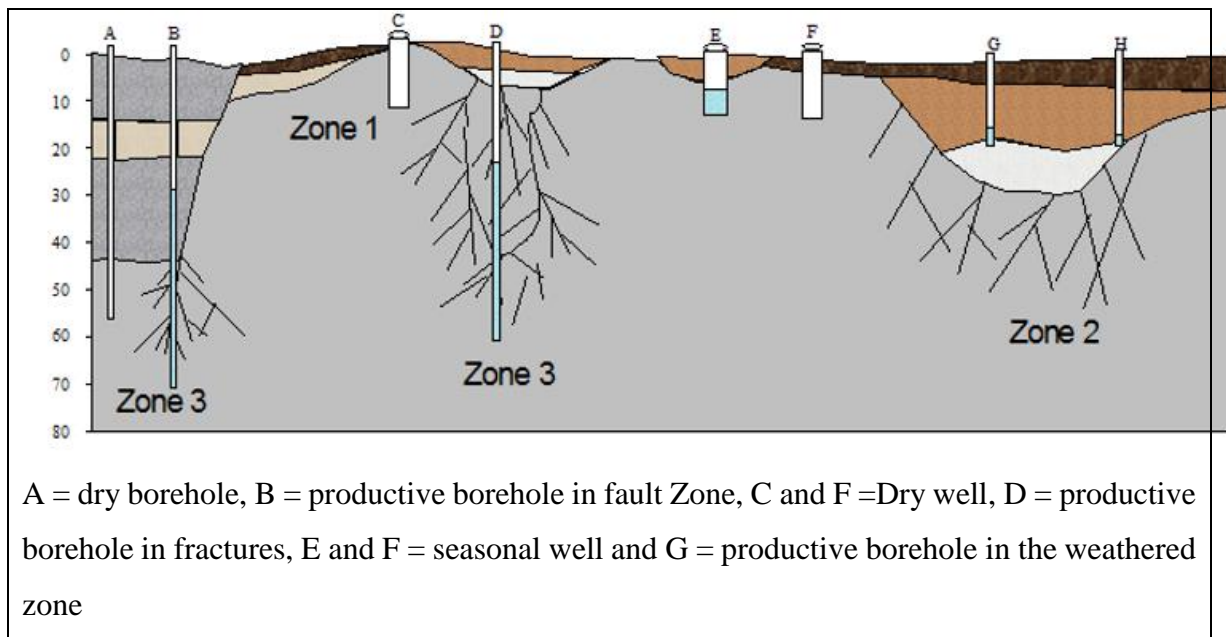
Figure 2.2. Stratified occurrence of groundwater in fractured and weathered volcanic rocks (modified from DHV Consultants, 1988)

Not all water in an aquifer is available for recovery through boreholes and wells. Part of the water will be retained within the rocks (Tessema *et al.*, 2014). The water yielding and retaining capacity of a rock or soil has great practical importance to the development of groundwater resources (Johnson, 1967). The amount of water an aquifer can yield depends on its effective porosity and permeability (Fajana, 2020; Oliver, 1993; Pierce *et al*., 2013). Consolidated rocks, such as lava flow containing good-sized cavities and solution channels or joints, may have low porosity and are excellent water sources because the openings or interstices they include are large, therefore releasing their water (Todd and Mays, 1980) freely.

2.3 Determinants of groundwater chemistry and vulnerability to contamination

2.3.1 Overview of groundwater chemistry and vulnerability to contamination

The chemical characteristics of groundwater are continuously modified by rock water interactions, rock weathering, evaporation, and ion exchanges (Dragon and Gorski, 2015; Prasanna *et al*., 2010; Vasu *et al*., 2017). The dominant rock water interaction processes within the tropics and sub-tropics are the ion exchanges (Joji, 2016; Sajil *et al.,* 2016). The unique combination of the physical and chemical characteristics of water due to its polar arrangement

of the oxygen and hydrogen atoms, in particular, its density, heat capacity, capillarity, and dissolving capacity, make it an extremely versatile and multifaceted resource (Fetter, 2001; Todd and Mays, 1980).

Aquifers exhibit complex groundwater chemistry and water types (Kassune *et al*., 2018; Modibo *et al*., 2019; Rosenthal *et al*., 1998; Tóth, 2009). The chemistry range from low ionic concentration where the residence time is short to moderately and highly mineralized water where residence time is big (Fetter, 2001). The major ion chemistry and compositional relationships among ionic species can reveal the origin of solutes and modified water chemistry processes. The chemistry provides a powerful tool for determining solute sources and describing groundwater evolution (Blanchette *et al*., 2010; Eissa *et al*., 2018; Harbison, 2007; Mossmark, 2014; Rajendra *et al*., 2012). Groundwater chemistry varies widely and is a function of the many complexes, geochemical, hydrogeological, geological and climatic factors that control chemical evolution (Shand *et al*., 2007). Water chemistry can also be modified by activities taking place within the recharge area (Fetter, 2001).

There is considerable literature on interpreting geochemical processes in groundwaters based on hydrochemical data (Li *et al.*, 2018; Lohman, 1972; Lovley and Chapelle, 1995). Hydrochemical facies denote the diagnostic chemical character of water solutions in hydrologic systems due to rock-water interaction, precipitation, or evaporation (William Black, 1966). The facies reflect the effects of chemical processes between the minerals within the lithological framework and the groundwater. Graphical plots of multiple ionic ratios, saturation indices, and ion exchange indices are used to determine the hydrochemical processes that result in different hydrochemical facies (Hem, 1985). There is an explicit lack of information on evaluating hydrochemical facies in Mt. Elgon and Kisumu study sites. However, a few studies have been conducted by researchers (Cerling, 2019; Chebet *et al.*, 2020; Davies, 1996; Kuria, 2013)

2.3.2   Natural or geogenic processes of groundwater quality modification

Groundwater quality can be modified by several geogenic processes (Falkenmark, 1990; Hirji, 2000; Opisa *et al.*, 2012a; Petersen-Perlman *et al.*, 2018; Sampat, 2000; UNESCO, 2002; WHO, 2003, 2009) such as weathering within the zone of aeration (Appelo and Postma, 2005) and geochemical reaction processes such as dissolution and precipitation of solids, cation

exchange, and adsorption, all of which contribute considerably to the variation of elemental concentration of groundwater (Dedzo *et al*., 2017; Jeong, 2001; Vasu *et al*., 2017; Yousif and El-Aassar, 2018). The chemical composition of water is also influenced by atmospheric deposition through precipitation (Wood, 2019); for example, deposition of inorganic nitrogen and sulphate has been reported in Europe and other parts of the world (Fenn *et al.*, 2015; Morales-Baquero *et al*., 2013; Waldner *et al.*, 2014). The nature and extent of interactions can significantly influence the spatial variation in the dissolved solids (Tesfamichael, 2011). Hence, the concentrations of significant groundwater ions can be used to subdivide groundwater into distinct zones or hydrochemical facies (Back, 1960).

Hydrochemical facies evaluation is instrumental in providing information about the complex hydrochemical processes in the subsurface (Kumar, 2013). Determination of hydrochemical facies has been used extensively in groundwater and surface water assessment since the 1940s. Piper made the first attempt in this direction in 1944 and Durov in 1948. Piper diagram is used to classify water into six significant types (Ca^{2+}-HCO_3^- type, Na^+-Cl^- type, Ca^{2+}-Mg^{2+}-Cl^- type, Ca^{2+}-Na^+-HCO_3^- type, Ca^{2+}-Cl^- type and Na^+-HCO_3^- type) (Freeze and Cherry, 1979). Many researchers in their studies use these water types to understand the controlling factors of the water chemistry (Fetter, 2001). Other plots like Wilcox and correlation of ions matrix are also used to classify water. No studies currently exist for the Mt. Elgon and Kisumu study sites.

2.3.3   Anthropogenic influence on groundwater quality

Anthropogenic activities that influence groundwater quality can be classified as direct and indirect. Direct anthropogenic activities are due to the direct input of substances from agricultural (nitrates, phosphates, salinity and acidity), industrial (salts, heavy metals and petroleum products) or urban (sewage, improper waste disposal and pharmaceutical products) activities as well as from accidents (e.g. oil spills) (Grutzmacher *et al.*, 2013). Beauty products and other detergents contribute to surface water and groundwater contamination. These anthropogenic products and activities can change the geochemical conditions in the subsurface and thus can also potentially mobilize hazardous geogenic substances (Appelo and Postma, 2005). For example, dewatering of mines can lead to aeration of aquifers and subsequent pyrite oxidation, increasing the total iron and sulphate concentrations whilst reducing pH (Kjøller *et al*., 2004). Nitrate is the most prevalent type of anthropogenic substance that influences water quality and has been reported in many countries worldwide (Zhou *et al.*, 2015). Consuming

water containing high nitrate concentrations can cause acute toxicity and cause methemoglobinemia risk (WHO, 2017).

2.3.4 Groundwater vulnerability to contamination

Groundwater contamination is becoming a common occurrence in sub-Saharan Africa (Howard and Karundu, 1992; Kehinde and Loehnert, 1989; Kouamé *et al*., 2019; SADC, 2011; Schmoll, 2013). It is difficult to distinguish precisely between groundwater pollution and contamination. Still, groundwater pollution can be regarded as occurring if the contaminant(s) is/are in high dosages, rendering it very dangerous to human health and the ecosystem (Morris *et al*., 2003; Stefanakis *et al.*, 2015). Groundwater contamination occurs if the magnitude is low but can still make contaminated groundwater unusable or make it slightly hazardous to life (Foster *et al*., 2002; Foster, 1984). The geology and the grade of consolidation coupled with fractures are critical factors in assessing aquifer contamination vulnerability (Sampat, 2000). Within the saturated zone, dispersion and dilution or spreading out of the contaminants play essential roles in reducing contaminant concentrations, although they are not reliable reduction mechanisms for highly toxic pollutants (Foster *et al*., 2002; Gonçalves *et al*., 2019; Morris *et al*., 2003; Stoppelenbrug *et al*., 2005).

The use of the sub-surface as a repository of solid and liquid waste generated by man is widespread in rural areas and low-income informal settlements in urban centres (Beatty *et al*., 2009; Kiptum and Ndambuki, 2012; Opisa *et al*., 2012a; Wood, 2019). The preferred mode of sanitation in these areas are traditional pit latrines and septic tanks. The pit latrines are hand dug and are most of the time not lined. Faecal loading of groundwater could be through sewerage leaks, and storm drains overflows, open defecation or pit latrines (UNESCO, 2015). The microbes from these sources are ultimately carried in various ways into the hydrological cycle, where they can survive for several weeks if conditions are favourable (Foster *et al*., 2002; Okotto-Okotto *et al*., 2015). Several researchers have noted that coliform bacteria move horizontally or vertically through the soil profile if the soil pores are saturated with water and pore sizes are large enough for bacteria to go through (e.g. Bowen *et al*.,1999; Carleton, 2010; Jayakody *et al.,* 2014). Other researchers have reported that coliform bacteria can move vertically as far as 7.5 m deep in the presence of water (e.g. Culley 2002; Stocker *et al*., 2015; Sclar *et al*., 2016). For high yielding shallow boreholes, the travel time is typically short, and

therefore contaminants take a short time to reach the water table (ARGOSS, 2001). For deeper boreholes, the travel time is longer, delaying the arrival of persistent contaminants. This substantially reduces the risk of less persistent pollutants, including many microorganisms (Egboka *et al.*, 1989; Szymkiewicz *et al.*, 2018). Little has been to evaluate groundwater contamination through a study of coliform bacteria. This is, therefore, one of the gaps this study intended to fill.

2.4   Environmental isotope and groundwater recharge

2.4.1   Analytical rationale of water isotopes

The conservative water isotopes oxygen-18 (^{18}O) and deuterium (^{2}H) provide an improved understanding of the processes associated with the source of water, transport parameters and flow dynamics (Adelana, 2011; Dansgaard, 1964; Faye *et al.*, 2019; Kraiem *et al.*, 2013; Loader and Hemming, 2004; Mook, 2000d). They provide information about evaporation, transpiration and downward infiltration problems to resolve by other techniques (Adomako *et al.*, 2010; Barbecot *et al.*, 2018; Barbieri, 2019; Yurtsever and Araguas, 1993). These isotopes are naturally abundant in precipitation, and due to fractionation effects, there is seasonal variability of water isotopes in the rain. These seasonal distributions are attenuated by transport processes in the subsurface and can still be reflected in shallow groundwater systems (Mook, 2000d; Rozanski, Araguás and Gonfiantini, 2013).

The two main physical processes a water molecule undergoes naturally are evaporation and condensation (Mook, 2000a-f). When water evaporates, the lighter isotopes of hydrogen and oxygen goes into vapour, and during condensation, the heavier isotopes will condense first. These processes cause a variation in isotopic composition in water molecules by fractionation of isotopes. These variations depend on various conditions such as temperature, humidity, and altitude. Isotopic concentrations are expressed as the difference between the measured ratios of the sample and the reference over the measured ratio of the reference (Dansgaard, 1964). Knowledge of the water isotope content of precipitation, soil water and groundwater can give information about groundwater recharge, transit times and water flow paths (Abott *et al.*, 2000; Bershaw, 2018; Calow *et al.*, 1997; Craig, 1961; Faye *et al.*, 2019; Houcine *et al.*, 2013). Stable water isotopes are powerful tools to study the global water cycle and are also a cornerstone of

paleoclimate reconstructions (Abott *et al.*, 2000; Faye *et al.*, 2019; Gat *et al.*, 2001). Isotopic composition of groundwater can be used to reveal groundwater source and water mixing from different geological terrains, varying degrees of continuity, and age (Gat *et al.*, 2001; Mook, 2001). The signature can also be used to determine groundwater compartmentalization, connectivity, zoning over depths and to choose geological stratigraphy and diagenesis (Craig, 1961; Abott *et al.*, 2000; Yu *et al.*, 2007; Levin *et al.*, 2009; Abiye *et al.*, 2015; Wirmvem *et al.*, 2017; Oiro *et al.*, 2018b). Stable isotopes are utilised to establish isotope fractionation patterns in natural systems, trace sources of groundwater, and model groundwater dynamics (Sodemann, 2006).

The variations of oxygen-18 and deuterium in natural waters show a linear relationship because their behaviour during the fractionation processes is similar; this relationship was determined by Craig in 1961 using annual average values of ^{18}O and ^{2}H. The equation was derived using average yearly values of about 40 per cent samples from North America and the rest distributed worldwide (Craig, 1961). The equation ($\delta^{2}H = 8*\delta^{18}O + 10$) is known as the global meteoric water line (GMWL) and forms the basis for comparing the isotopic composition of water from other sources (Dansgaard, 1964). The global meteoric water line is valid as an average global relation and may have different characteristic values in different climatic regions, especially the deuterium intercept. The intercept may be different due to deuterium excess (Dansgaard, 1964). The deuterium excess varies between 4 per mil to 23 per mil, for relative humidity variation range of 60 to 90 per cent and the temperature of condensation range of 0 to 20°C (Yurtsever and Araguas, 1993). Deuterium excess (*d*-excess) is computed using the Dansgaard equation (*d*-excess = $\delta^{2}H – 8*\delta^{18}O$) (Dansgaard, 1964). Its wide use in understanding climate conditions in moisture source regions is based on simple calculations showing that d-excess is determined mainly by sea surface temperature, relative humidity, and wind speed at the site of evaporation (Kopec *et al.*, 2019). The application of water isotope in the estimation of recharge is handily undertaken.

2.4.2   Utilization of environmental isotopes in groundwater recharge estimation

Many methods are used to estimate groundwater recharge. These include the Darcy Law, water balance techniques and the tracer techniques (Hubbert, 1957; Sidle, 1998; Sokolov and Chapman, 1974). The use of environmental isotopes as tracers in the water cycle increases as analytical instrumentation improves and more applications are discovered (Barbecot *et al.*,

2018; Barbieri, 2019; Porowski, 2014; Sidle, 1998). Applying this technique solves the hydrological problems that other methods cannot solve, e.g. flow-system tracing. The differences and correlations of isotopes in various water bodies (precipitation, boreholes, shallow wells, springs, and surface water) can be studied to estimate groundwater recharge sources and their interrelations (Taylor and Howard, 1996; Yeh *et al*., 2014). This can be done by comparing the mean *d*-excess values of precipitation and groundwater. Plots of precipitation isotopic signature and signatures from groundwater can reveal whether groundwater is recharged directly by rainfall (modern water) or whether recharge occurred in the past (paleowater). The signatures can also reveal whether groundwater formed through geochemical processes (Mook, 2000d).

2.5   Summary

This chapter provided the theoretical background required for understanding aquifer geometries and characteristics, water chemistry and contamination, and the importance of environmental tracers. A review of these and current knowledge gaps was necessary for deciphering the consecutive chapter on methodology. Groundwater is increasingly subjected to excessive over-exploitation and contamination in many parts of the world. It faces the challenge of balancing its multiple functions sustainably. Understanding the groundwater systems through evidence-based research is the way forward. There is a need for a multi-faceted approach to address the scientific and societal issues involving groundwater resources. Understanding the aquifer characteristics, hydrogeochemical data, threats, and stable environmental isotope data provide essential water resources management tools.

Pressure on groundwater is increasing rapidly, which calls for sustainable groundwater practices (Brunner and Kinzelbach, 2005). Finding a universally applicable definition of sustainability is complex. The Brundtland Commission defined sustainable development as meeting the needs of the present generations without comprising the future generations ability to meet theirs (Brundtland, 1988). It is possible to identify non-sustainable groundwater practices in a catchment. These include groundwater pollution, over-pumping of aquifers and destruction of recharge areas (Gaye and Tindimugaya, 2019). Sustainable groundwater management is generally challenging to implement because effective strategies are constrained by lack of data, limited technical capacities, lack of political and broader social support for regulatory interventions (Shah *et al.*, 2000), rapid population growth, and economic and

environmental changes in many parts of the world (Boretti and Rosa, 2019; Carter and Parker, 2009; Okello *et al*., 2015). These impacts are irreversible and often render groundwater interventions and remediation not applicable when sufficient data and information are available. For example, in the Thiaroye aquifer in Dakar, Senegal, the reversal of nitrate contaminations may not be practically possible in the short term (Ndao *et al*., 2019; UNEP/UNESCO, 2006), while in Nairobi, Kenya, deepening of the existing boreholes is a norm since those below 300 m are drying up (Morris *et al*., 2003; Muthoni, 2009; World Bank, 2005). Groundwater management challenges continue to emerge globally, and the developing countries bear the most significant burden (Olago, 2019; Yongxin *et al*., 2019).

There is a need to develop groundwater monitoring systems, understand groundwater-land use relationships, address climate-change impacts on groundwater, assess the effects of over-abstraction, and capacity building in groundwater management to address these challenges. This study will contribute to the sustainable management of the Kisumu and Mount Elgon aquifers by providing the critical and necessary scientific evidence base for their sustainable use and management.

Chapter 3 introduces the key aspects of the study area (e.g. location, bio-physical setting and social-economic setting) and outlines the methods and materials used to achieve this study's objectives. Desktop studies, fieldwork, laboratory analysis and data analysis techniques for each objective are presented.

CHAPTER 3 – MATERIALS AND METHODS

3.1   Introduction

This chapter present and discusses the details of the research methods used to achieve the study objectives highlighted in chapter one. It also describes the research design, research processes, method of data collection and methods used for data analysis, interpretation and presentation. The study involved structured field investigations, data collection, laboratory analysis and interpretation of data generated. The criteria used to define water sampling sites as urban settings included availability of structures such as houses, commercial buildings, roads, plots sizes and high population density that depend on non-agricultural jobs. This is typical of the Kisumu setting. The lack of the features mentioned above was used to define rural settings. There are fewer people in the Mt. Elgon rural area, and their homes and businesses are located far away from one another.

The depth of drilled boreholes for observation (piezometers) in Kisumu was between 40 and 60 meters. The existing boreholes used for monitoring were located within the deep aquifer system and ranged from 90 m to 200 meters. The hand-dug wells ranged in depth from 3 meters in Obunga to 25 meters in Mbeme. In the Mt. Elgon aquifer, the deep boreholes are located in Kacheliba and around Kitale, and they range from 80 to 150 meters. Shallow wells are hand-dug and were up to 60 meters in depth. The study materials and methods used to achieve the rural Mt. Elgon and urban Kisumu study aim and objectives are discussed in detail in the subsequent sub-topics in this chapter.

3.2   Location of the study areas

The two study areas are located on the extreme western side of Kenya. The Kisumu aquifer is on the shores of Lake Victoria, while the Mt. Elgon aquifer is on the slopes of Mt. Elgon. Kisumu County lies between longitudes 33°20' E and 35° 20' E, and latitude 0° 20' S and 0° 50' S (Figure 3.1) The County is bordered by Homa Bay County to the South, Nandi County to the North East, Kericho County to the East, Vihiga County to the North West, Siaya County to the West. The study site lies within longitude 34°39' E and 34°50' E, and latitude 0°00'07" S and 0°8'40" S. The study area is about 300 km^2 (*Figure 3.1*) and falls within the Kisumu urban boundaries. It is located on the shores of Lake Victoria, the second-largest freshwater lake in the world. The County's urbanization revolves around the City of Kisumu and the

satellite high population areas scattered in different parts of the county. Kisumu City is the significant high density and high population urban area in the county. The proportion of those residing in urban areas within the county accounts for 50.30 per cent of the total population. Forty per cent of these urban dwellers live in the informal settlements within the city, including Nyalenda, Manyatta and Obunga (Figure 3.1). The land tenure system within these informal settlements is free-hold (County Government of Kisumu, 2018a).
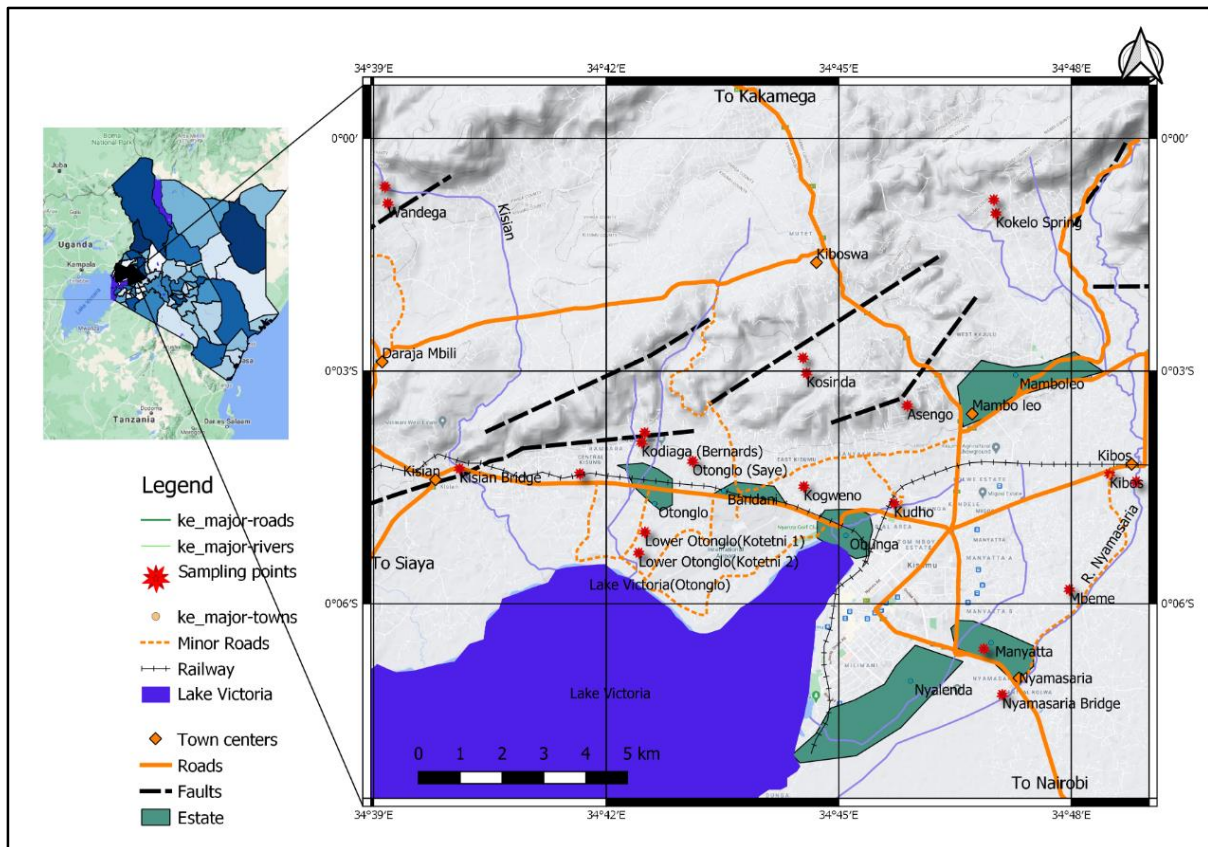
Figure 3.1. Map of the main informal settlements and the twenty-two sampling points in Kisumu.

The Mt. Elgon transboundary aquifer is located in western Kenya and straddles the Kenya-Uganda international boundary (*Figure 3.2*). It is bounded by longitude 34°48' E and 35°12' E and latitude 0°54' N and 1°30' N. The study area lies in Trans Nzoia and West Pokot Counties, and extends from Kitale to the east, Suam to the north, Kiminini to the south and Kacheliba in West Pokot to the west. The study area in Mt. Elgon has about 7500 km^2 and covers part of the Mt. Elgon conservation area and extensive arid area in West Pokot occupied by nomads. The two study sites are accessible from Nairobi via well maintained all-weather roads. Kisumu has an international airport, while in Kitale, there is an airstrip that is well maintained. Mobile connectivity by service providers is good except in far-flung villages in West Pokot.
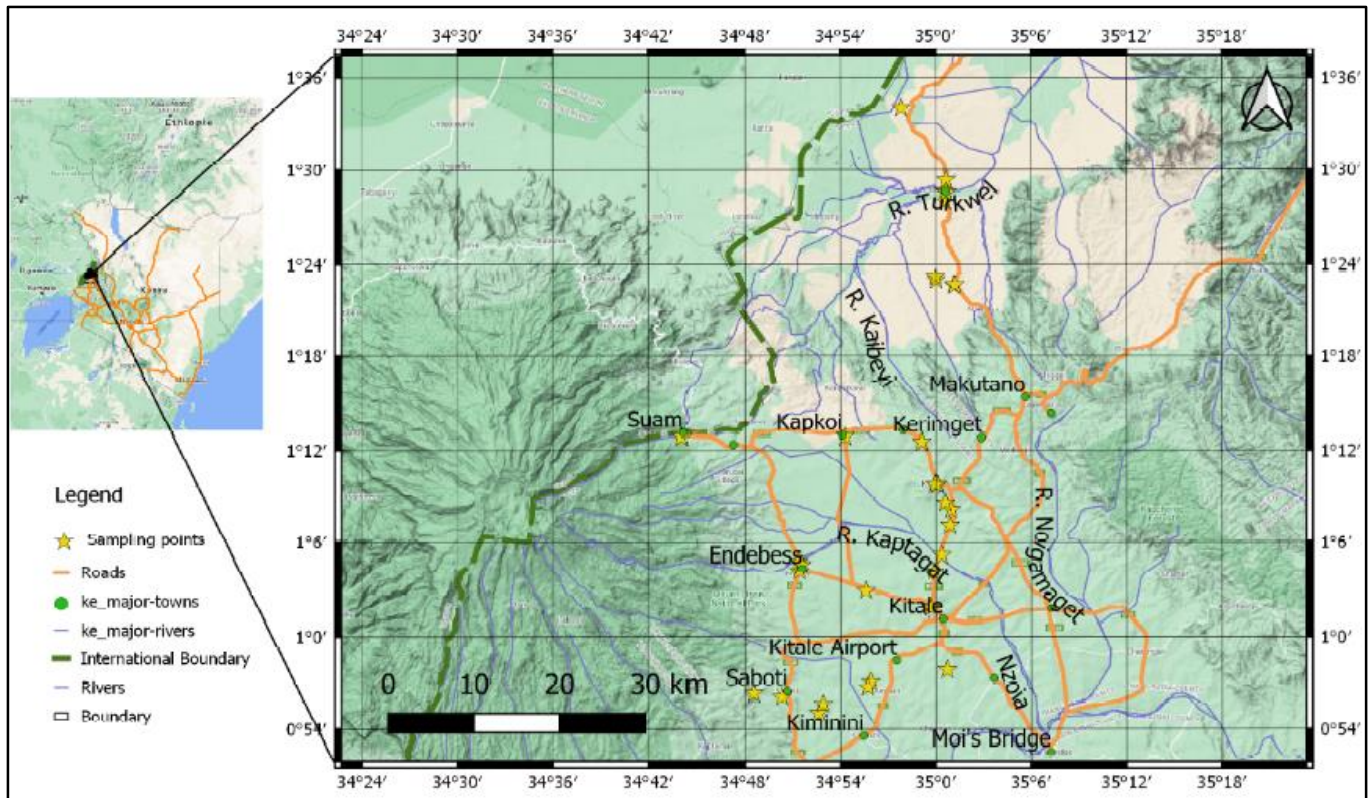
Figure 3.2. Map of the Mt. Elgon study sites. Targeted water sampling points are shown in the map

3.3   Biophysical setting of the study areas

3.3.1   Climate of the study areas

The climate in Kisumu belongs to the inland equatorial type and is modified by altitude, relief, and Lake Victoria's influence (Kendall, 1969). The cooling effect of the lake slightly lowers the temperatures from the expected actual equatorial climate (Hulme *et al*., 2001; Hulme and Turnpenny, 2004). Temperatures have a mean monthly minimum of 15° C to a mean monthly maximum of about 30° C, according to data from the Kisumu Meteorological Station (KMD, 2018). The area has four seasons comprising two relatively dry and two wet seasons. However, the seasons are constantly changing due to climate variability (Williams *et al*., 2015; Yang *et al*., 2014). The highlands like the Maseno, Riat hill, Nandi escarpment and Tinderet receive the highest rainfall. Long rains occur between March and May, while short rains occur between September and November (Mungai, 1984). The mean annual precipitation is about 1,300 mm (KMD, 2018). Due to climate variability, no month can be considered a completely dry month, but the dry peak period falls between December and February. A secondary dry peak occurs between June and September (KMD, 2018).

In the Mount Elgon study area, the climate varies depending on altitude. Trans Nzoia County has a cool temperate climate with mean maximum temperatures ranging between 23.0° C and 28.0° C and mean minimum temperatures ranging between 11.0° C and 13.5° C. The maximum and minimum extreme temperature are recorded in February and January, respectively (KMD 2018). The annual rainfall ranges from 1000 mm to 1700 mm. The yearly rainfall is distributed into three major seasons, namely, long rainfall season - March, April, May (MAM); Intermediate Season - June-July-August (JJA); and short rainfall season - October-November-December (OND). The average annual temperature in West Pokot range from 15° C to 25° C. Rainfall decreases northwards from Kapenguria to West Pokot. It ranges from 1500 mm to less than 250 mm in semi-arid parts of the county (KMD, 2018). The variability of temperature and rainfall results in alternating landslides, flooding, and dry spells that negatively impact human, livestock, food security, and the environment (Githui, 2008; Nangulu, 2009; Ngecu and Mathu, 1999).

3.3.2   Vegetation covering the study areas

Kisumu is endowed with a variety of both indigenous and exotic vegetation. White (1983) developed a simple system in which seventeen major vegetation types are recognized in five categories. The Kisumu study area has four types of vegetation based on this system. These are:

- Forests include vegetation that comprises continuous trees with heights of at least ten meter and interlocking crowns. This type of vegetation dominates the upper slopes of Nandi Escarpment and the Riat hill. However, forest cover is diminishing due to the conversion of forest land into residential areas, resulting in rapid population growth and urbanization in Kisumu.

- The plains, located on the floor of the Kavirondo Rift, are dominated by bush land. These bushes consist of trees between three and seven meters tall and a canopy cover of 40% or more.

- Grasslands dominate the lowland zones surrounding Lake Victoria. They consist of land covered with grasses and other shrubs, with woody plants covering no more than 10% of the ground.

- The water hyacinth weed and papyrus characterize the shores of Lake Victoria and swamps.

The Mt. Elgon study area is characterized by various vegetation ranging from equatorial type vegetation with tall trees within the Mt. Elgon forest to open grassland towards Kitale (Greenway, 1973). The mountain is a significant water tower in Kenya and is accorded protection by the Kenya Forest Services (Akotsi, 2004; Muhweezi *et al*., 2007). Using the White (1983) classification scheme, the main types of vegetation are;

- Forests that include vegetation comprising continuous stand of trees at least ten meters tall with interlocking crowns. This type of vegetation dominates the Mt. Elgon slopes.
- The bush land includes open stands of bushes three to seven meters tall, with a canopy cover of 40% or more. This vegetation type dominates the Kitale plains.
- Grasslands consist of land covered with grasses and other shrubs, with woody plants covering no more than 10% of the ground. This vegetation dominates the lowlands zones of the West Pokot County around Kacheliba.

3.3.3 Land uses and resources of the study areas

A built-up area with tiny open spaces dominates Kisumu City. Extensive sugarcane plantations dominate the outskirts of Kisumu. In the arid and semi-arid zones, livestock keeping is practised. The breed kept is the traditional cattle that provide little milk and fetch little money since they are small. Further, livestock keeping does not offer enough livelihood support due to frequent droughts alternating with severe floods. Rapid rural-urban migration is witnessed as a consequence of unplanned and uncontrolled urban centres (Carter and Parker, 2009; Drangert *et al.*, 2002; Okello *et al*., 2015).

On the other hand, Trans Nzoia County, on the eastern slopes of the Mount Elgon study area, is considered Kenya's food basket with extensive maize plantations for consumption and seed maize. At the same time, West Pokot is semi-arid to arid, and the main agricultural activity is livestock rearing. However, peasant farming is practised at the household level.

3.3.4 Physiography and drainage of the study areas

The physiography of Kisumu consists of hills stretching from Nandi escarpment through Riat to Kisian. The elevation of these hills varies from 1300 to 1600 meters. The lowlands from the hills' base to the lakeshore range from 1100 to 1250 meters above sea level (County Government of Kisumu, 2018a; Rakama *et al.*, 2017). The upper reaches are rocky, particularly on the steep slopes of the hills, while in the lowlands, the soil profile is loamy with rocky

patches in the gentler slopes. A progressive change in the soil types occurs from the hills towards the lake shores. The area is generally well-drained, with runoff and discharges eventually entering Lake Victoria (Awange and Ong'ang'a, 2006). The predominant soils are black cotton soils.

The main physiographic feature in the Mt. Elgon study site is the volcanic Mt. Elgon. It is a solitary extinct shield volcano straddling the border of eastern Uganda and western Kenya. The mountain has a diameter of about 80 kilometres, and its summit is at an altitude of 3,070 metres above sea level (TWAP, 2015). Abutting the foot slopes of the mountain are the Kitale plains to the east and the West Pokot Plains to the north (Pulfrey, 1960). Fertile loam soils cover the study area on the mountain and sandy soils on the metamorphic rocks terrain to the north.

3.3.5 Water resources of the study sites

(a) Kisumu aquifer area

The primary water resources in Kisumu comprise Lake Victoria, rivers, groundwater resources, springs and rainwater. Lake Victoria, the second-largest freshwater lake in the world and the largest in Africa, is the main surface water body and defines the operational framework for the Kisumu water-related activities (Sitoki *et al*., 2010). However, due to the outdated and controversial Nile Treaty, the utilization of the lake water is limited and keenly monitored by the Nile riparian countries (Lumumba, 2007). The Lake is facing other challenges that render its water unfit for domestic and human consumption without treatment (Awange and Ong'ang'a, 2006). These include untreated effluent discharges from surrounding towns, water hyacinth and other invasive plants, and the impacts of climate variability (Opande *et al*., 2004). The surface waters (lake, rivers and streams) are also heavily laden with contaminants that range from industrial waste, solid and liquid waste from the neighbouring urban centres and other types of emerging contaminants (Opisa *et al.*, 2012). The main rivers flowing through Kisumu are R. Nyamasaria, R. Kodiaga and R. Kisian (*Figure 3.1*). River water intakes constructed away from the city provide alternative water to the town. These include the Kajulu water intake and the Maseno-Kombewa intake located outside the city. Surface water pollution makes groundwater resource the primary potential water sources for domestic and commercial purposes in Kisumu (Drangert *et al.*, 2002). The exploitation of the groundwater resource is highest in the industrial and prime residential areas but limited and confined to shallow wells,

especially in areas far from the Lake. Its contribution to the overall water balance is not yet known (JICA, 2013). The urban Kisumu aquifer is a strategic groundwater resource. It supplies water to areas not served by the urban water supply from Lake Victoria (Dunga intake) and Kajulu River intake near Nandi escarpment. It also acts as a buffer in case of shortages due to pipe bursts and mechanical failures. The main Kisumu aquifer characteristics, water uses and aquifer scale, are summarized in *Table 3.1*.

Table 3.1. The main aquifer characteristics of the Kisumu aquifer (DHV Consultants, 1988)

Aquifer Parameter	Explanation
Aquifer type	Sedimentary, volcanic
Lithology	Lake/river sediments and fractured phonolite/andesite
Pollution vulnerability	Moderate-High
Depletion vulnerability	Low – Moderate
Water use	Domestic, Industrial and Irrigation
Scale	Local

In Kisumu, residential water supply coverage is 30%, while non-residual water supply coverage is 50% (County Government of Kisumu, 2018). The County has ten gazetted water supplies schemes (*Table 3.2*) and fourteen Community water supplies schemes (County Government of Kisumu, 2018). The Government developed these water schemes through various development partners, NGOs and community initiatives.

Table 3.2. The major water suppliers in Kisumu County (County Government of Kisumu, 2018)

WSP	Area of supply
Kisumu Water and Sanitation Company (KIWASCO)	Kisumu
Gulf Water and Sanitation Company	Kisumu Rural
Gulf Water and Sanitation Company	Maseno Kombewa
Gulf Water and Sanitation Company	Nyahera
Gulf Water and Sanitation Company	Mkendwa-Kanyakwar
NYANAS Water and Sanitation Company	Nyakach
NYANAS Water and Sanitation Company	Muhoroni
NYANAS Water and Sanitation Company	Tamu
NYANAS Water and Sanitation Company	Koru Mnara
NYANAS Water and Sanitation Company	Kibigori

There are also communities, institutional and faith-based private water supplies schemes. These water schemes use groundwater sources. They act as buffers during times of shortages, for example, during prolonged dry seasons or repair work on the water supply infrastructure. These self-supply schemes serve the neighbourhoods at a fee. The main communal water schemes in Kisumu are shown in *Table 3.3*

Table 3.3. The main community water supplies in Kisumu (County Government of Kisumu, 2018)

Name of Water Supply	Sub-county
Asengo Water and Sanitation Company	Kisumu West
Rabuor Water and Sanitation Company	Kisumu East
Wandiege Water and Sanitation Company	Kisumu East
Kolal	Kisumu East
Kadete	Kisumu East
Kawere	Nyakach
Olembo	Nyakach
St. Camilus	Nyando
Sangoro	Nyakach
Odino	Nyakach
Kowi	Seme
Mbaka Oromo	Kisumu West
Nyahera	Kisumu west
Paga	Seme

(b) Mount Elgon aquifer area

In Trans Nzoia, 65% of residents use improved water sources, with the rest relying on unimproved sources (Trans Nzoia County Government, 2019). The primary enhanced water sources are protected spring and wells, boreholes and piped water into the dwelling. The unimproved water sources include ponds, streams and river, unprotected wells and springs. Kiminini constituency has the highest number of residents who have access to improved water sources at 79%. This percentage is almost twice that of the Endebess constituency, which has the lowest number of residents using improved water sources. The primary water sources in the Trans Nzoia are rivers, boreholes, shallow wells, springs and rainwater harvesting. The water sources are dependent on climate and topography, and some areas are water-scarce due to distance to a source. The average walking distance to the nearest potable water source is about 1.5 km (Trans Nzoia County Government, 2019). There are four main rivers in Trans Nzoia County. These are R. Kaibeyi, R. Koitobo, R. Noigamaget and R. Kaptagat (*Figure 3.2*). These three rivers flow into River Nzoia, ultimately draining Lake Victoria (Nyadawa and Mwangi, 2011). The springs are used extensively whenever they sprout out, and most of them are protected. Shallow wells are either communal or private (Trans Nzoia County Government, 2019).

The primary water sources in West Pokot include seasonal streams, shallow wells, boreholes, sand dams, and rainwater. Most of the borehole was developed by Non-Governmental

Organisations (NGO's) and the Government of Kenya (GoK). Though the yields of these boreholes are low, they sustain the communities and the livestock. A few are solar-powered, and the majority are installed with hand pumps. The main permanent river (*Figure 3.2*) in West Pokot is R. Suam (Turkwel) that has its origin in Mt Elgon (Kenya Water Tower Agency, 2019). An estimated 59% of households in the county use rivers/streams as their source of water (County Government of West Pokot, 2018). The number of families with access to safe water is about 26,000, representing 28 per cent of the population. There are about 10,000 households with access to piped water. The average distance to the nearest water point is 5 km (County Government of West Pokot, 2018). The primary water supplies schemes in the County are Makutano - Kapenguria, Tartar - Keringet, Karas and Kabichbich - Chepareria water supply systems. These schemes are small river abstractions and are operated by gravity.

3.3.6   Geology and soils of the study areas

(a) The geology of Kisumu study site

The existing geological report and map for Kisumu (Saggerson, 1952) are over 65 years old, but the description of the rock units and geological structures is reasonably good. The main geological feature in Kisumu is the Kavirondo Rift, which branches from the main North-South oriented East African Rift Valley. This Rift trend north-eastward towards Lake Victoria. The evolution of the Kavirondo Rift involved down warping during the Miocene and rift faulting during the Pliocene to Pleistocene periods (Mboya, 1984). Faulting in the Palaeogene and Neogene sub-periods was accompanied by the eruption of phonolitic lavas found around Kodiaga prison, north of Kisumu International Airport (Saggerson, 1952).

As reported in the geological report for Kisumu by Saggerson in 1952, the primary rocks in Kisumu fall into four main groups. These groups are based on their geological age (Saggerson, 1952). They are Precambrian (Archean), Paleogene and Neogene, Pleistocene and Recent rocks. There is a significant geological hiatus between the early Precambrian and Paleogene and Neogene periods, a period of no major geological activity (Mboya, 1984). The Nyanzian rocks are the oldest and are predominantly volcanic in origin. They consist of andesitic lavas with pyroclastic rocks and tuffs (Meert *et al.*, 1994) that occupy the central part of Kisumu and also along the Kisumu-Kakamega Road. These rocks are highly weathered and have undergone various degree of metamorphism. The rocks are dark-green in colour, fine-grained in texture, and are severely sheered and altered on the margins. The pillow lava structures are evident in

these highly weathered rocks (Saggerson, 1952). The fresh rocks are dark-green, fine-grained, sheared and altered, and their original forms can hardly be recognized.

Nyalenda and central Kisumu areas are occupied by Kavirondian meta-sediments consisting of grits; the Nyanzian and Kavirondian rocks were invaded by Precambrian intrusions granitic bodies and associated quartz porphyries (DHV Consultants, 1988). The granitic intrusions are course-grained, pale, grey pinkish in colour and porphyritic (Opiyo-Akech, 1988). The granites have large pinkish or greenish feldspar phenocrysts up to one centimetre in diameter. The volcanic rocks of the Paleogene and Neogene period outcrop around Kisian and Kodiaga prison north of Kisumu International Airport (Meert *et al.*, 1994). These phonolitic lavas cover the granites related to the Neogene faulting during the Kavirondo rifting and commencement of movement along the fault lines (Mboya, 1984). These lavas have been affected by the Neogene faulting and are found at various heights on the foot-steps of the different step faults north of Kisumu (Shackleton, 1948). In the hand specimen, the phonolites are porphyritic and vary in colour from grey to greenish. The rocks are very fissile and exhibit a conchoidal to splintery fracture pattern. Laterite is a common weathering product of phonolite.

The most recent formations in the area are the Pleistocene deposits of lacustrine and fluviatile origin (Kent, 1942; Pickford, 1986; Pulfrey, 1960). During the Pleistocene, the whole of Kavirondo Rift valley was part of Lake Victoria, but since the fall of the Lake, rivers have deposited large quantities of clay and silt and extended their course (Baker *et al*., 1970; Baker *et al*., 1988; Johnson *et al*., 2000). The alluvium is of two types, the first is connected to Lake Victoria, and the second is deposition by the rivers. These deposits vary from gravels to very fine claystone (DHV Consultants, 1988). The recent soils in the area consist of black cotton soils on the alluvial flats, red laterite soils on phonolites and sandy soils on granites. Other recent deposits include talus scree, alluvium, gravel, lateritic ironstone and soils along the foothills of the Nandi escarpment (Pickford, 1986).

(b) The geology of Mount Elgon study site

The Mt. Elgon study area comprises rocks of varying age from Pre-Cambrian age, Neogene lavas to the recent surficial lateritic and black cotton soils (Gibson, 1954b; Miller, 1956). The Pre-Cambrian rocks are mainly quartzite and schist derived from the original argillaceous and arenaceous sediments deposited in a geosyncline and transformed by metamorphism and

recrystallization into quartz and feldspar-rich rocks (Miller, 1956). These rocks have abundant muscovite, biotite, and hornblende minerals. They show varying degree of weathering ranging from moderately to highly weathered rocks between Kwanza and Kapenguria. Generally, weathering is more intense in the areas underlain by schists than those underlain by gneisses (Vearncombe, 1983). The rocks exhibit good foliation with a strike trend approximately NNW-SSE.

The Mount Elgon Neogene volcanic rocks are composed of great masses of agglomerates, breccia and tuff with intercalated bands of basalts, trachyte, basanite, nephelinite, melilitite and phonolite (Simonetti and Bell, 1995; Wright, 1963). They were formed during the successive volcanic eruption during the Neogene (Wright, 1963). The agglomerate materials range from small to huge boulders. Agglomerates and lavas are composed of nephelinites with many mafic minerals such as olivine, augite, magnetite, ilmenite and perovskite (King *et al.*, 1972). The thickness of volcanic rocks thins away from the peak of Mt. Elgon, suggesting that the deposits were undoubtedly laid down on a surface sloping radially away from the peak of Mt. Elgon (Mohr and Wood, 1976; Pulfrey, 1960; Wright, 1963). The degree of consolidation of these rocks varies, giving rise to good primary porosity. Where agglomerates occur as large boulders, they often exhibit jointing, which contributes to their porosity.

3.4   Socio-economic setting of the study sites

3.4.1   Kisumu and Mt. Elgon political and administrative contexts

Kisumu County is one of the 47 Counties in Kenya. It's headquarter, Kisumu city, is the third-largest city in Kenya and is situated on the shores of Lake Victoria, the second-largest freshwater lake in the world by surface area (Awange and Ong'ang'a, 2006). Kisumu County has seven sub-counties or constituencies: Kisumu East, Kisumu West, Kisumu Central, Muhoroni, Nyando, Seme, and Nyakach. The County has thirty-five wards. The main informal settlements include Bandani, Manyatta (A and B), Nyalenda (A and B), Otonglo and Obunga (Simiyu *et al*., 2018; UN-Habitant, 2005). Due to urban population increase and demand for houses, some previously planned settlements (e.g. Mamboleo) are slowly being converted to high-rise apartments and flats (Okotto-Okotto *et al.*, 2015).

Trans Nzoia County comprises five administrative sub-counties, namely Kiminini, Saboti, Cherang'any, Endebess and Kwanza and the sub-counties are further sub-divided into twenty-five administrative wards. Kitale is the headquarters of Trans Nzoia County. West Pokot County has four constituencies and 20 administrative wards. These constituencies are Kapenguria, Kacheliba, Sigor, and Pokot South. The headquarters of West Pokot is Kapenguria.

3.4.2   National, regional and local economic setting of the study areas

In the Trans Nzoia highlands, farming is the dominant activity in cultivating crops such as maize, sugarcane, beans, bananas and tomatoes. In the lowlands around Lake Victoria in Kisumu, fishing is the dominant economic activity (Awange and Ong'ang'a, 2006; Rees *et al*., 2000). In the highlands of West Pokot, farming is the main economic activity while livestock keeping is dominant in the lowlands (Muchena and Gachene, 1988; Namboka *et al*., 2017; Rees *et al*., 2000). Trade occurs across the region, with several trading markets and town centres. Rapid urbanization has both negative and positive impacts on the area. The adverse effects include unplanned settlements, while positive consequences include the possibility of enhanced provision of services, the creation of jobs, and improved quality of life (Kempe, 2012; World Bank, 2016).

3.4.3   Socio-economic setting of the study areas

Communication infrastructures within Kisumu are well developed. They include roads, an international airport, port, fish landing bays and telecommunications facilities. All-weather roads connect Kisumu city with other towns in the neighbouring Counties. However, minor roads that link the city to the rural areas are not well maintained, and during rainy seasons, most of them are in deplorable conditions. In the Mount Elgon area, an all-weather road links Kitale and Kapenguria from Nairobi. Communication infrastructures from these counties to the rural are seasonal. They are, however, well maintained by the County Government, though they deteriorate during rainfall seasons. The road linking Kapenguria and Kacheliba is almost impassable during rains. The Kitale Suam road, linking Kenya and Uganda, in all weather. The population and distribution per sex in the study areas are shown in *Table 3.4*. Kisumu has the highest population density of 554 persons per square kilometre, while West Pokot has the lowest population density of 68 persons per square kilometre.

Table 3.4. Distribution of the population in the study area. Kisumu has a very high population density (KNBS, 2019)

County	Male	Female	Intersex	Total	Surface area (km²)	Population density (persons/km²)	No. of households	Average household
Kisumu	560,942	594,609	23	1,155,574	2,085	554	300,745	4
Trans Nzoia	489,107	501,206	28	990,341	2,495	397	223,808	4
West Pokot	307,013	314,213	15	621,241	9,123	68	116,182	5

3.4.4 Regulatory framework of water resources and related issues in Kenya

The Constitution of Kenya 2010 has had a comprehensive set of implications for the water sector and other sectors. It acknowledges access to clean and safe water as a fundamental human right and assigns water supply and sanitation service provision to 47 newly established counties (GoK, 2010). Water-related issues in the constitution were operationalized through the enactment of the Water Act 2016. The Act recognizes that water-related functions are a shared responsibility between the National Government and the County Governments (GoK, 2016). It also gives priority to the use of abstracted water for domestic purposes, over-irrigation and other uses.

Climate change is guided by Climate Change Act No. 11 of 2016. The Act stipulate the regulations to enhance climate change resilience and low carbon development for the sustainable development of Kenya (GoK, 2016). It sets out principles of climate change planning and implementation. Other laws relevant to this study include the Environmental Management and Coordination Act, 1999 (revised 2015), which provides an appropriate legal and institutional framework for managing the environment and its related matters (GoK, 2015).

3.4.5 Socio-economic vulnerabilities of study sites inhabitants

Socio-economic vulnerabilities broadly include the following; exposure to climate variability, social and economic instabilities, and lack of resilience to cope with disasters and recovery after climatic and non-climatic related disasters (Noy and Yonson, 2018). In the two study sites, floods are the common climatic disaster and the leading hydro-meteorological disaster (Benson and Clay, 2004; Mavhura, 2019; Salami *et al*., 2017). In the Kano plains and other low lying areas of Kisumu, floods cause much destruction and displacement (Okayo *et al*., 2015). Floods have also been reported in low lying areas in Trans Nzoia and West Pokot

Counties (Muricho *et al.*, 2019; Odira *et al.*, 2010; Weingärtner *et al.*, 2019). Due to climate variability, drought and the accompanying water shortage often occur in West Pokot. The area experiences related cultural conflicts with its neighbours (Turkana and Karamoja).

3.5   Groundwater conceptual framework of the study sites

Groundwater is a complicated system; hence, developing a precise conceptual framework was essential in understanding groundwater in the study sites. Disordered and lack of data and information, especially in developing countries, make the preparation of the framework difficult (Izady *et al*., 2014). The two (Kisumu and Mt. Elgon, respectively) aquifer regions each comprise hills/mountain (recharge area), (b) peri-urban/rural lowland areas (discharge/contaminant area), and (c) urban lowland areas (discharge area), *Figure 3.4*. The conceptual framework describes the groundwater flow and transport in a simplified representation. Analysis of groundwater data was key to interpreting groundwater processes and hence the derivation of information about the geometry, water type, dynamics, relationships and recharge mechanisms (Martínez-Navarrete *et al*., 2011; Yang *et al*., 2010). Within the conceptual framework, the analysis provided insight into the reaction of groundwater resources to changing conditions, like climate variability, aquifer characteristics, contamination, and flow regimes.
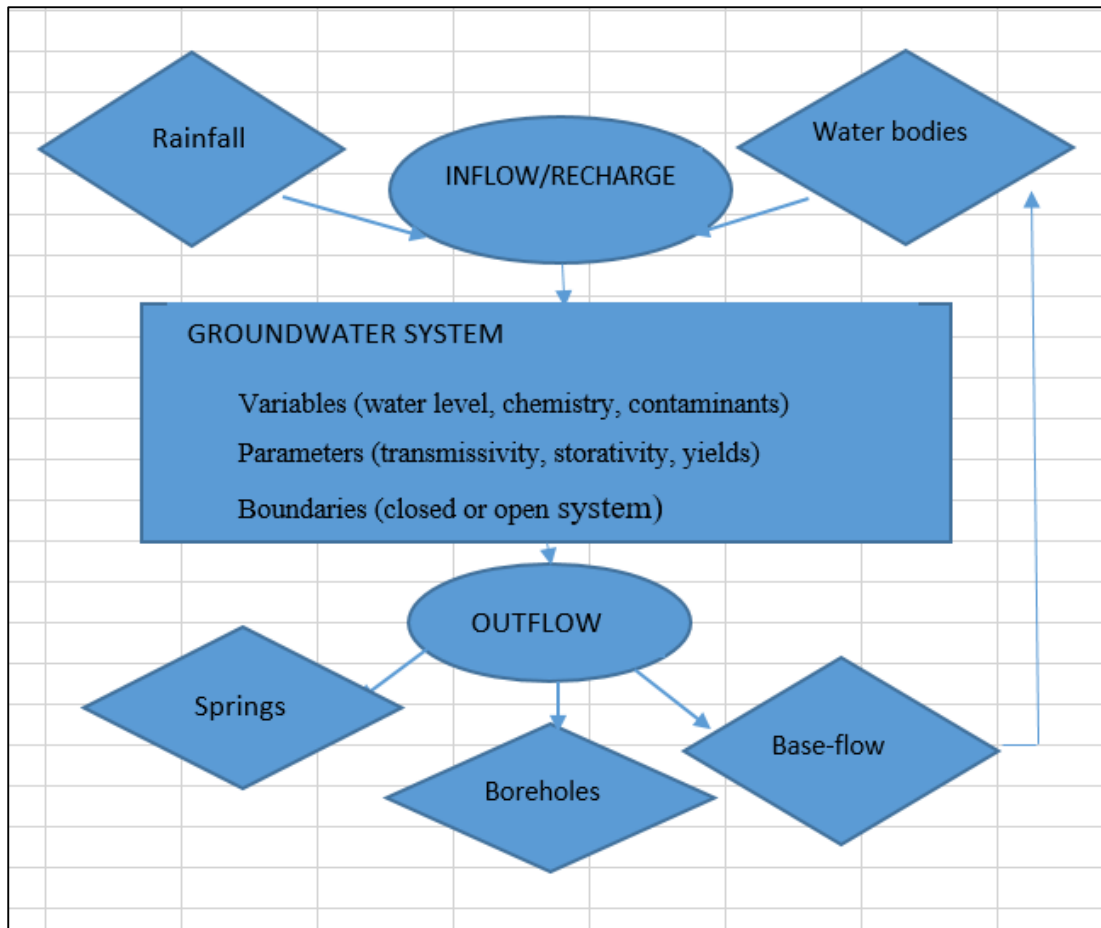
Figure 3.3. Development of the conceptual groundwater framework for Kisumu and Mt. Elgon study sites with key processes

3.6 Research methods used to achieve the objectives of the study

3.6.1 Research design, phases and activities

The research design or plan of action specifying the phase and activities for fulfilling the research objectives during this study is given in *Figure 3.4*. Several authors have argued that the research design is like a master plan, specifying the methods and procedures for collecting and analysing the needed information (Kumar, 2011). Research design techniques include surveys, experiments, secondary data and observations (Walliman, 2011). They can further be classified into exploratory and conclusive research (Kothari, 2004). The exploratory research aim was to provide insights and an understanding of the research question and provide answers. In contrast, conclusive research aims to assist the researcher in determining, evaluating and selecting the best solution to the research problem. Both the exploratory and conclusive research designs were adopted in this study.

The research design for this study, *Figure 3.4*, consisted of four different phases to address the research questions and objectives outlined in Chapter 1. For the Kisumu aquifer study area, three transects were chosen to start from the top of the Riat hills and Nandi hills, running into the low lying peri-urban areas of Otonglo, Obunga and Manyatta, *Figure 3.1*. Twenty-two sites were identified for water sampling. In the Mt. Elgon study area, twenty-three sites were selected for sampling based on accessibility and security. They consisted of boreholes, shallow well, springs and surface water sites.
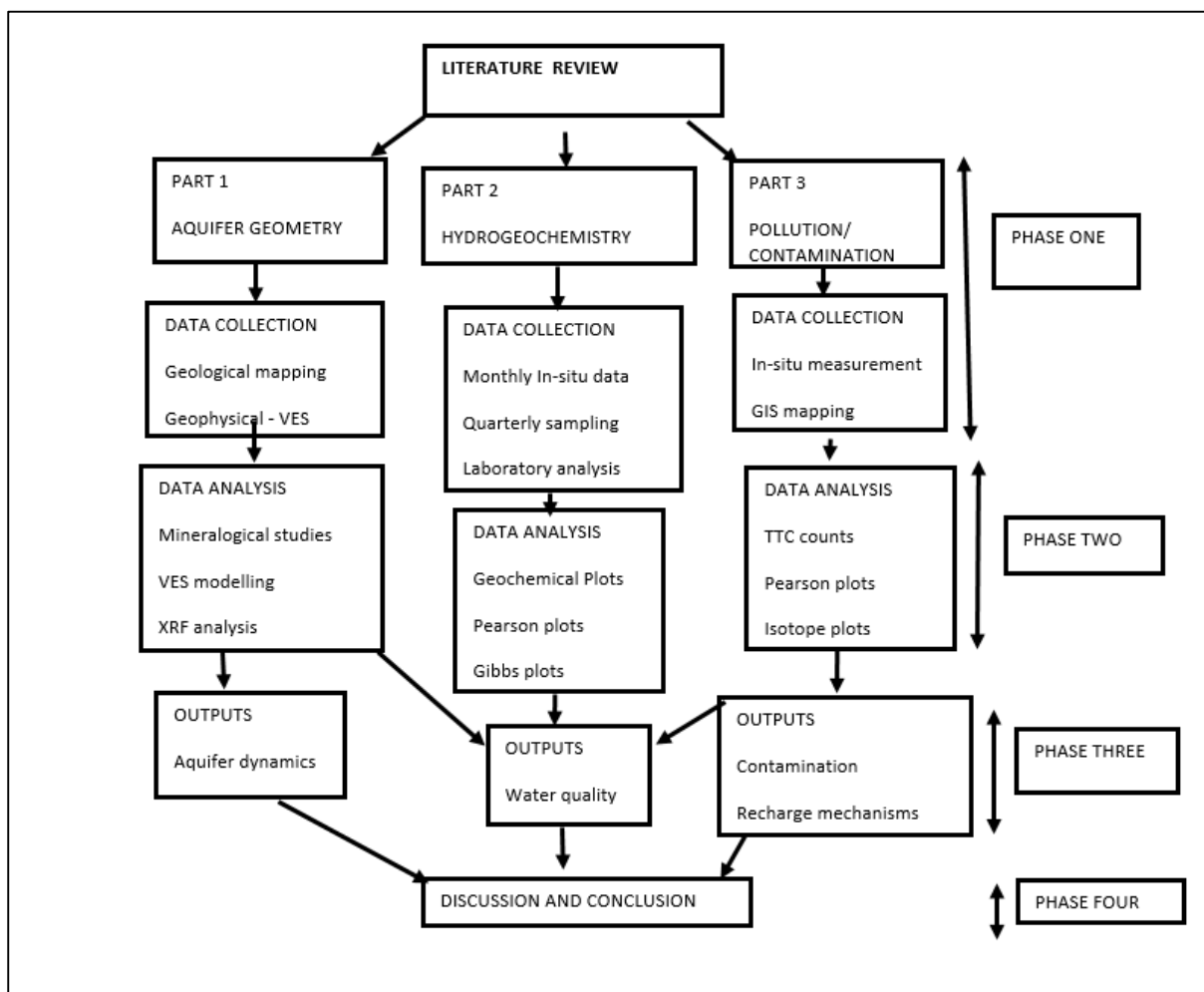
Figure 3.4. The research design used to accomplish the research objectives of this study

The first phase consisted of two broad sections. The first section reviewed the literature on the primary research thematic areas captured in the research aim, namely, aquifer geometry, water chemistry and contamination, and source of recharge. The literature review included both primary and secondary sources, *Table 3.5*. It was undertaken to establish current baseline

information and evaluate the knowledge gaps underpinning the research questions and objectives.

Table 3.5. Summary of primary and secondary data used in this study

Activity	Kisumu	Mt. Elgon
Geological field survey	Detailed geological field mapping and collection of rock sample	Reconnaissance survey without rock sample collection
Physico-chemical parameters collected in the field	pH, EC, temperature, dissolved oxygen, turbidity and salinity (sample size = 275). Data collected monthly for 12 months for Kisumu.	pH, EC and temperature (sample size = 40). Data collected once during the wet and dry season (October-November 2014 and March 2015)
Water sampling campaigns and number of samples collected	Three sampling campaign in 22 sampling points (sample size = 66)	Two sampling campaigns in 20 sampling points (sample size = 40
Sampling for isotope samples	Yes, 22 samples	No
Geophysical surveys (VES)	Yes (15 profiles)	Yes (20 profiles)
TTC enumeration in the field	Yes	No
Secondary data used	Historical borehole data and isotope data for Kericho GNIP and Lake Victoria.	Historical borehole data.
Geological maps	Geological Survey of Kenya geological map No. 21	Geological Survey of Kenya geological map No. 19, 26, 35 and 64

The second section in phase one consisted of field data collection and laboratory analysis. This was the quantitative study phase of this research. The second phase of the study entailed analysing data generated in section two of phase one. This was the qualitative/quantitative phase of the study. The third phase gives the study results, and finally, phase four of the research process summarizes the research findings, conclusion, and recommendation.

3.6.2 The research methods used to achieve objective 1 of the study

Aquifer geometry and characteristics refer to the aquifer extent, borehole yield, hydraulic aquifer properties, groundwater levels, flow, and recharge. These are derived through geophysical surveys or logging during drilling and pumping test. The approach to the delineation of the Kisumu and Mount Elgon aquifers was different in the sense that there was intensive fieldwork and monitoring wells installed in Kisumu under the AfriWatSan project, which was not the case with the IGAD funded project that only allowed for geological and groundwater sampling fieldwork in Mt Elgon aquifer, and therefore, for the latter, aquifer characteristics were inferred from re-analysis of existing secondary data for boreholes from the area, provided by the WRA.

3.6.2.1   *Desktop studies on delineating aquifer geometries and characteristics*

A review and synthesis of existing information and data on the two aquifers were done before going out to the field. This included information on the geological setting, rocks exposures, existing borehole completion data and any existing geophysical data. This information was sort from the relevant institutions. These included the Ministry of Mining and Petroleum, Ministry of Water and Sanitation and Water Resources Authority. Data from existing boreholes had the total drilled depth, and water struck levels, water rest levels and the yields. The data for the Mt. Elgon aquifer was provided in the form of borehole completion records by the WRA offices in Kitale and Kapenguria. Additional data was acquired from NAWARD (National Water Resources Database) previously hosted by the Ministry of Water and Sanitation but later transferred to WRA after the water reforms. Kisumu data was derived from NAWARD and studies by other researchers (e.g. DHV Consultants). Existing geological reports were reviewed and acted as a guide during the geological field mapping in Kisumu. In the Mt. Elgon area, geological maps were compiled using existing geological maps and reports, jointly with data acquired during the reconnaissance survey.

3.6.2.2   *Fieldwork on delineating aquifer geometries and characteristics*
Geological Mapping

Geological field studies within Kisumu involved traversing the study area on foot, mapping the various lithological units exposed on the surface and visual identification of geological structures. An e-trex30 Garmin GPS (Global Positioning System) was used to capture geographic location, and a geological hammer was used for chipping rock specimens. A Silver compass was used to determine the macro-structural properties of rocks, including preferred trends and orientations. The rock samples collected were labelled, and stored in sample bags and later transported to the laboratory for analysis. Three fieldwork campaigns were carried out in Kisumu, and twenty-six rock samples were collected. The first fieldwork was carried out between 7th and 10th June 2017, the second between 21st and 23rd September 2017, and the last fieldwork on 9th and 10th March 2018. During these fieldworks, efforts were made to identify the significant geological faults, fractures, and other lineaments and clarify uncertain lithology and boundaries. The planning of traverses in an urban setting was complex due to many factors that included buildings, perimeter walls and protected areas like the State House, Kisumu.

However, road cuttings and construction sites proved handy during the geological surveys. Eighty-two field stops were made during the geological field mapping exercise. Visual observation and interpretation of rocks and their mineralogical content based on the physical properties of minerals was made in the field.

Geophysical surveys and profiling

Combined geophysical and hydrogeological fieldwork was carried out between April and September 2017 in the Kisumu study site. During this period, geophysical surveys were conducted in fifteen locations. The main aim of the geophysical investigations was to get an insight into the hydrogeological conditions prevailing in the study site. Furthermore, an attempt was made to find the vertical extent of the water-bearing layers. A total of six locations were chosen as potential sites for piezometers construction based on profiles that were earlier selected and the budgetary constraints. The chosen areas were Kudho Primary School (2 piezometers), Kogweno springs (1), Erastus Saye well (1), Wandiege Primary School (1), Mbeme well (1) and Lake Basin Mall (1). Vertical electrical sounding (VES) was used to determine the sub-surface geology and depth to the water. The resistivity data were processed by the Interpex IX1D program using one dimensional (1D) inversion to model the vertical variations of subsurface resistivity at depths of less than 50 m.

At each site of geophysical investigation, a single sounding was carried out. The geophysical studies were mainly aimed at the determination of the following parameters:
- The lateral and vertical extent of the groundwater body,
- The texture of the aquifer deposits,
- Depth and nature of the layers below the aquifer marking the hydrogeological boundary of the shallow water.

The measurements at each site were executed in an expanding Schlumberger array, with electrode spreads ranging up to AB/2 = 50 m. This separation gives fairly reliable interpretations down to a depth of about 40 m, but only approximate solutions for resistivity layering at deeper levels. Depths beyond this level are only indicative and do not give the precise position of the measured contact zone.

A great variety of geophysical methods can assist geologists in assessing geological subsurface conditions (Reinhard, 2009). In this survey, the resistivity method (vertical electrical sounding)

was used. This method was used to probe the resistivity layering and condition of the sub-surface and confirm groundwater's existence (Fetter, 2001). The geophysical resistivity technique is based on the response of the earth material to resist the flow of electric current. It involves using a pair of current electrodes and a pair of potential electrodes to measure the resultant potential difference below the surface.

Geophysical surveys were undertaken in the Kisumu area but not in Mount Elgon. A SAS 300C terrameter model was used to carry out the resistivity measurements. The complete Schlumberger configuration was used in Kisumu with a maximum half-current electrode spread (AB/2) of between 1 and 50 m. In contrast, the half-potential electrode separation (MN/2 or a/2), *Figure 3.5*, was maintained between 0.5 and 5 m.
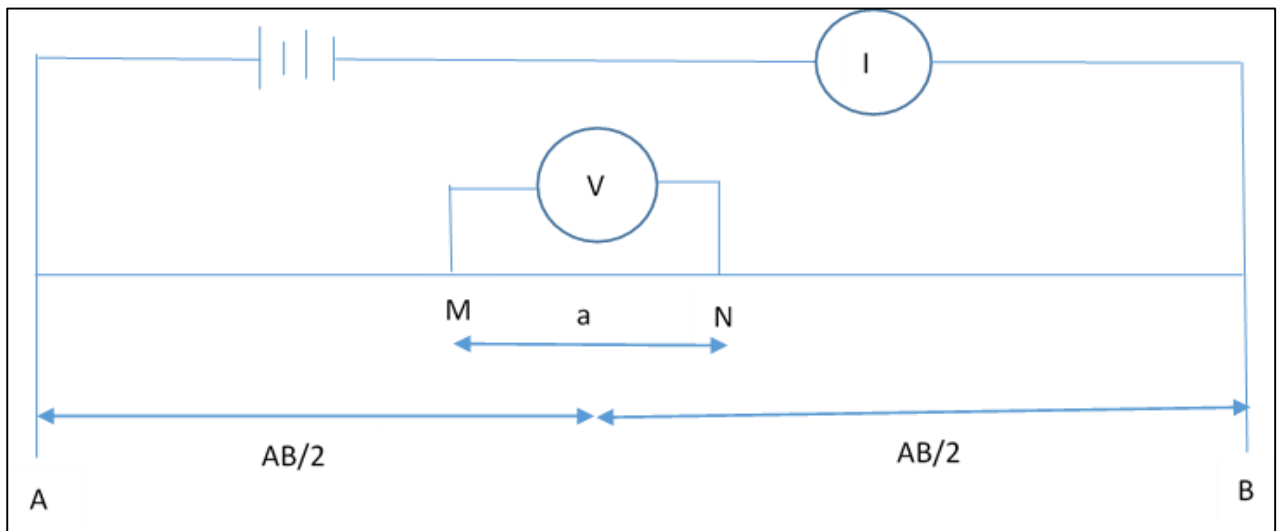
Figure 3.5. Complete Schlumberger configuration based on injecting current and measuring the potential difference created (after Moore, 2002)

The principles of the method are discussed in several books and publications on the subject (e.g. Telford *et al*., 1990; Mansour, 1996; Ewusi, 2006; Reinhard, 2009; Kurth, 2014). The method involves transmitting a current I between two grounded electrodes and measuring the induced voltage V. The apparent resistivity was then calculated as:

$$\textbf{Apparent resistivity} = \boldsymbol{k} \times \frac{V}{I}$$

Vertical electrical sounding was conducted at eleven selected sites in the study area. The method was used due to its success rates in determining aquifer systems in Kenya (DHV

Consultants, 1988). The procedure is based on a wide range of resistivity values found naturally in various geologic materials. The values range from less than one ohm-meter for metallic ore bodies to over 1,000,000 ohm-meters for igneous and metamorphic rocks. Sedimentary and unconsolidated material has resistivity ranging from 1 ohm-meter to 10,000 ohm-meter. A range of resistivity values for the different rock types occurring around the Kisumu from previous surveys is given in *Table 3.6*.

Table 3.6. Typical electrical resistivity values for various rock types found in Kisumu (modified from DHV Consultants, 1988).

Rock Type	Resistivity Range (Ohm-m)
Clay	<5
Mudstone	3 – 8
Silt/Siltstone	5 – 10
Sand/Sandstone	10 - 20
Gravel	20 - 40
Weathered or broken phonolite	50 - 150
Fresh phonolite	150 - 350
Weathered or broken granite	150 - 500
Fresh phonolite	500 - 1000

Piezometer design and construction

Piezometers were constructed in six selected sites in Kisumu to monitor groundwater table fluctuation. Small diameter piezometers are more sensitive to water table fluctuations and are suitable for manual monitoring. The big diameter is correct if installed with automatic data loggers. The Kisumu piezometers were the big diameter (125 mm) type. The six piezometers were installed with Rugged TROLL 100 type data loggers. These devices measured and logged water level, water pressure, and temperature at the programmed interval. In Kisumu, the logging frequency was set at the one-minute interval. The following were the minimum standards followed during the construction and development of piezometers in Kisumu.

1. The drilling rig was capable of and was equipped with the necessary accessories to drill the specified diameter borehole to the required depth safely. The drilling rig, water truck, and support trucks were in good mechanical condition, all with the necessary equipment to complete the specified work.

2. The piezometer drilling was undertaken via a rotary drill, although any method capable of penetrating the expected geological material could have been acceptable. Drilling diameter was chosen to enable the completion of (125 mm) diameter piezometers with sufficient space for gravel pack between it and the drilling diameter.

3. Mud drilling was not permitted, but air or degradable foam was permissible.

4. Visual logging was done at a 1-meter interval, and geological samples were collected every 3-meter interval or when soil or rocks change was noted.

5. All the piezometers were fitted with plastic (PVC) plain casing and plastic slotted screen (1 mm), allowing for a 0.5 m stickup (pedestal height) above ground level.

6. Piezometers were completed at the surface with a 1x1 m concrete pad to a depth of 0.3 m to prevent water ingress. The piezometers were adequately labelled with an identification plate immediately upon borehole completion. The identification plate was constructed of a durable, weatherproof, rustproof material and permanently secured to the well casing or protective casing where it was readily visible. The plate was permanently marked to show the following:
   - Company name and certification number of the driller who installed the well
   - Date well was completed
   - Total depth (m)
   - Casing depth (m)
   - Screened interval
   - Designator and identification number
   - Static water level.

7. Washed gravel pack of between 2 and 5 mm was installed from the base of the drilled holes to 1 m above the screen. The remaining annulus was backfilled with 0.5 m of bentonite clay then grouted to the surface.

8. Development was accomplished by airlifting with reverse air. Other acceptable methods included pumping, bailing, jetting, swabbing, or any combination of the above techniques, as specified. Only potable water was used in the development.

9. Each piezometer was air flushed for a minimum of 2 hours, and if the water was not running clear after 2 hours, then air flushing was continued until it was. Measurements taken during development were specific conductance, pH, temperature, turbidity, and yield.

10. Test pumping was undertaken at all installed piezometers. The shallow boreholes drilled were low yielding and of limited areal extent. A constant drawdown method was used during the pumping test. The pumping rate was adjusted until a constant drawdown was achieved. Pumping stabilised within 4 hours or less and, since they were not meant for production, the pumping tests were not extended for the recommended 48 hours.

Six piezometers were completed and installed with data loggers in March and June 2019 after the drilling and test pumping tests were conducted, *Table 3.7*. These piezometers are located in Wandiege, Mbeme, Kudho (2), Kogweno and Erastus Saye, *Figure 3.6*. Water table changes data was downloaded after every three months from these stations.

Groundwater fluctuation data was supplemented by rainfall data from two automatic rainfall stations commissioned in the Kisumu study site in March 2019. The rain gauges are located in the Lake Basin Development Authority and within the Kajulu Water Works, *Figure 3.6*. They have resolutions of 0.2 and 0.1 mm, respectively. Rainfall data was downloaded after every three months.

Table 3.7. Location of proposed piezometers in Kisumu and depths for monitoring fluctuations.

No	Location Name	Easting	Northing	Elevation	Recommended Depth (m)	Installed?
1	Kudho_Pri_Sch	695950	9991946	1151	40	Yes (2)
2	Kogweno_Springs	693839	9992014	1155	35	Yes
3	Erastus_Saye_well	691093	9992908	1194	50	Yes
4	Nyahera_Springs	691626	9996786	1431	50	No
5	Wandiege_Pri_Sch	698155	9988152	1136	30	Yes
6	Mbeme_well	700208	9989585	1155	30	Yes
7	KEWI_Well	701185	9991625	1171	50	No
8	Lutheran_Tech_Inst	698943	9993774	1196	35	No
9	Kokelo_Borehole	698393	9998797	1272	35	No
10	Kindu_Pri_Sch	700302	9998335	1226	35	No
11	Korando_Well	688483	9992326	1170	25	No
12	Ojola VES1	683430	9992063	1201	50	No
13	Lower Otonglo	690000	9991184	1153	35	No
14	Kodiaga-Mze Bernard	689880	9993374	1215	50	No
15	Lake Basin	697267	9992784	1181	40	(Dry)

All the probes installed in the six piezometers capture water table fluctuation at an interval of one minute. Other characteristics of the piezometers are given in *Table 3.8*.
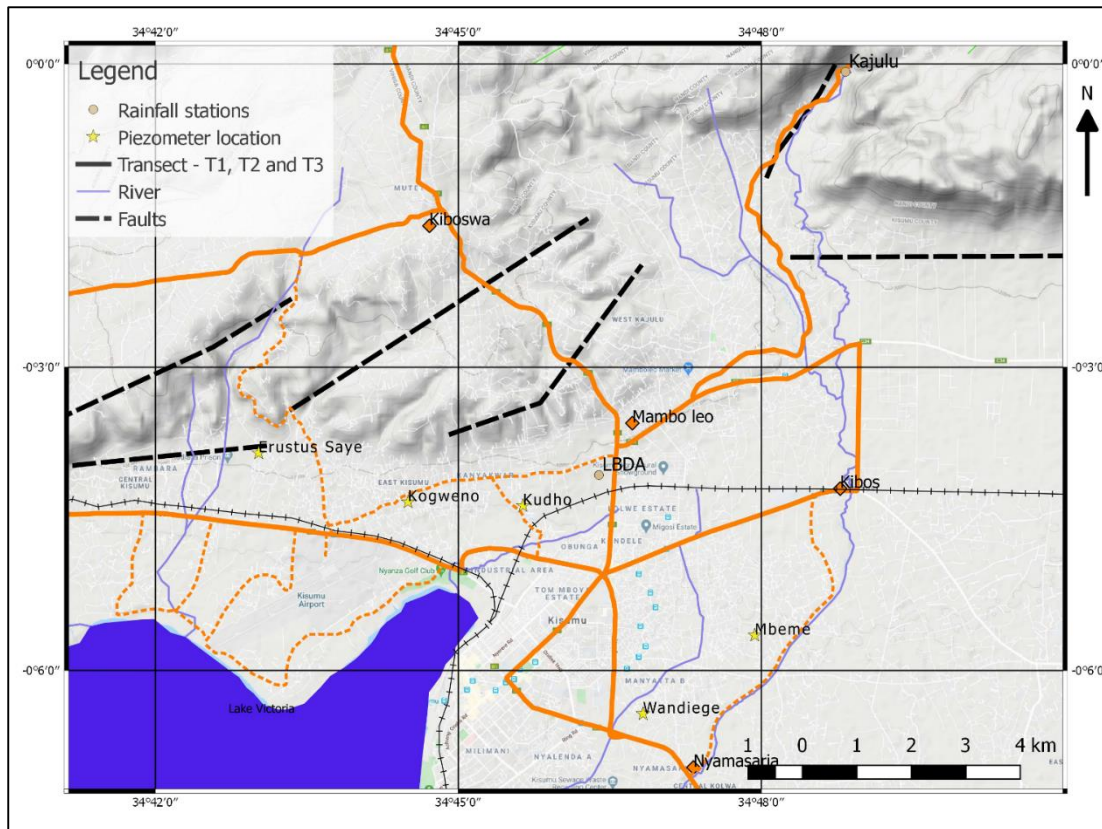
Figure 3.6. Location of piezometers and rainfall stations in Kisumu

Table 3.8. Main characteristics of the piezometers

Site name	Kotetni (Erastus Saye)	Kogweno	Kudho 1	Kudho 2	Mbeme	Wandiege
Date installed	14/6/2019	14/3/2019	14/6/2019	14/6/2019	15/6/2019	12/3/2019
Data logger (probe) type	Rugged Troll 100	Rugged Troll 100	Rugged Troll 100	Rugged Troll 100	Rugged Troll 100	Rugged Troll 100
Serial number	448508	455831	447590	448670	452014	455208
Frequency of data	1 hour	1 hour	1 hour	1 hour	1 hour	1 hour
level measurement mode	Level depth to water	Level depth to water	Level depth to water	Level depth to water	Level depth to water	Level depth to water
level reference value (m)	2.8	1.4	0.8	0.4	10.5	2.5
Depth of probe (m)	9.0	9.0	9.0	9.0	9.1	9.1
Head pressure (PSI)	12.8	12.8	12.8	12.9	12.8	12.8
Water temperature during installation(°C)	33.7	29.5	31.4	29.4	26.8	29.5

A groundwater monitoring plan was essential for the management of information collected on each piezometer. This information included the installation details and the type of data to be gathered. The monitoring plan also specified the monitoring parameters to ensure quality data was captured and stored acceptably. The details depended on what was being monitored, at what frequency and any other information. In Kisumu, the groundwater monitoring plans for each piezometer included the following:

- piezometer identification, GPS coordinates and date the data loggers were installed;
- Brief monitoring piezometer description and infrastructure details (depth to water and type of data logger);
- Drilling log details that included a description of geological characteristics encountered during drilling;
- Schedule of who, when and how often to monitor (quarterly) groundwater;
- What is being observed – water levels, temperature, physico-chemical parameters;
- Purging details of the piezometer for water quality readings (volume of water to be removed and time before sampled);
- Where will the data be stored and by whom and;
- Identification of maintenance schedule/requirements.

3.6.2.3 *Laboratory methods for delineating aquifer geometries and characteristics*

Petrographic analysis

Detailed petrographic analysis was done using a plane-polarized optical microscope once the collected rock samples were thin-sectioned at the State Department of Mining, Ministry of Petroleum and Mining Lapidary Laboratory located along Industrial Street, Nairobi, Kenya. Ten thin sections were prepared from rock samples collected in the field; the petrographic analysis aided in the identification and confirmation of various rock types in the study area. The investigation was carried out in the mineralogical laboratory of the Department of Geology, University of Nairobi. The information obtained from the mineralogical analysis supplemented the field data and facilitated the establishment of rock types in the area (Raith *et al.*, 2011).

XRD and XRF analysis

Ten rock samples were taken to the State Department of Mining, Ministry of Petroleum and Mining Geochemistry Laboratory and analysed for the major and trace elements. The ten rock sample were selected from the three major rock type, grit (3 samples), andesite (3 samples) and phonolite (3 samples), and a granite sample from Kisian. These were representative samples, and slight variation was noted after the analysis. The spectral X-ray diffraction (XRD) technique assessed minerals in rocks (Lavina *et al*., 2014; Mandile and Hutton, 1995; Wadsworth and Baird, 1989). When X-rays interact with a crystalline substance or powder, a

diffraction pattern was produced and was quantified. X-ray fluorescence spectrometry (XRF) is one of the most versatile methods for analysing major and trace elements in rock samples (Tsuchiya *et al.*, 1989). The major and trace elements analysed were **MgO, Al$_2$O$_3$, SiO$_2$, P$_2$O$_5$, MnO, Fe$_2$O$_3$, K$_2$O, CaO**, **Ti**, Zn, As, Rb, Sr, **Y**, **Zr**, **Nb**, Mo, Ta, W, Pt, and V, and the focus for this study are the bolded elements. The ratios Nb/Y (ppm) and Zr/Ti (ppm), and TAS (Total-Alkali Silica) plots were used to differentiate the rock types (andesite and phonolite) in the study area. A d2 phaser Bruker diffractometer with appropriate software and S8 LION´s simultaneous wavelength dispersive X-ray fluorescence (WDXRF) spectrometer were used. The major elements were used in determining the rock-water interactions using various plots.

3.6.2.4   *Data analysis methods for delineating aquifer geometries and characteristics*
Field data

QGIS version 3.14 software was used to make geological maps for Kisumu and Mt. Elgon. Existing scanned geological maps were georeferenced using the Georeferencer GDAL plugin. The open-source software ability to link with open Quick Map Services was utilized to create thematic layers through on-screen digitisation. During georeferencing, real-world coordinates were assigned to each pixel of the scanned raster geological maps. These coordinates were from the scanned map. Using these sample coordinates or GCPs (Ground Control Points), the scanned maps were warped and made to fit within the chosen coordinate system (EPSG 32736 for Kisumu and EPSG 4326 for Mt. Elgon). EPSG 32736 is a projected coordinate system for a region between 30° E and 36° E, southern hemisphere between 80° S and equator, while EPSG 4326 means latitude and longitude coordinate WGS84 reference ellipsoid. EPSG stands for European Petroleum Survey Group. They publish a database of coordinate system information that QGIS uses. Point data, including the location of sampling points. Point data collected during geological mapping was then added to guide the determination of geological boundaries and sampling points.

Vertical Electrical Sounding data was manipulated by inverting the apparent resistivity to the true resistivity using IX1D software to interpret the results and get layer depths. Spreadsheet data in flat ASCII files were imported into the software and modelled as either depth models or layer thickness. The values of true resistivity were then correlated with the geological layers (Loke, 2000; Olayinka and Yaramanci, 2000; Wisén *et al.*, 2008) using existing tables on resistivity to determine whether they contained water or not.

Estimation of aquifer properties

Pumping test data provided information on the hydraulic behaviour of the boreholes (Bennett and Patten, 1962; Bruin and Hudson, 1961; Gross, 2008; Mishra *et al*., 2012). The procedure involved pumping water at a constant rate and determining the drawdown. After the pump is stopped, recovery is monitored until the water label attains the initial water level. If the change in water level is speedy, the pumping rate was adjusted accordingly until the drawdown was constant. The drawdown was monitored initially at a 5-minute interval (up to 60 minutes), then 10-minutes (another 1 hour), followed by a 20-minutes interval for another 1hour and finally 30-minutes interval for 1 hour.

Test pumping can be continued for production wells up to 24 hours. The 4 hours pumping duration is acceptable for observation borehole (Bennett and Patten, 1962; Gross, 2008; Kruseman and Ridder, 2000; Richard *et al*., 2016). However, pumping may become constant after one hour or less, depending on the yields. The Kisumu pumping tests duration were;1) Kogweno, pumping 240 minute and recovery 60 minutes, 2) Kudho 1, pumping 560 minutes, recovery 50 minutes; 3) Kudho 2, pumping 240 minutes, recovery 55 minutes; 4). Wandiege, 30 minutes (well dried); 5) Erastus Saye, pumping, 240 minutes, recovery 40 minutes and 6) Mbeme, pumping 240 minutes, recovery, 40 minutes. It was a reliable way of evaluating the hydraulic properties of boreholes because the development of groundwater resources without adequate pumping test data is a theoretical approach, which may have unforeseen consequences leading to economic and social losses. Pumping tests were conducted after completing the piezometer to estimate, characterize, and define the optimal groundwater dynamics. Since the wells were low yielding, pumping tests lasted for a maximum of 240 minutes. The gathered data was then analysed to determine the hydraulic parameters, identify the distribution of hydraulic characteristics, and categorise aquifers' potential within the study area.

Pumping tests were carried out to obtain data for the following:
i)   Assess the hydraulic behaviour of boreholes and determine their ability to yield water, predict their performance, select the most suitable pump for long term use and provide an estimate of pumping costs;
ii) Determine the hydraulic properties of the aquifer; these properties included the transmissivity and hydraulic conductivity, and storage coefficient;
iii) Determine the effects of pumping on the neighbouring boreholes, streams or springs and;

iv) Obtain water quality data. Water quality characteristics may vary with time and discharge, and a pumping test provides the opportunity to determine such variations.

The aquifer properties were estimated using data derived from the pumping test. The yield or discharge was derived by calculating the number of litres of water pumped per hour. The specific capacity of the boreholes was calculated by dividing discharge in m^3/day by cumulative drawdown in meters. The Logan method (Logan, 1964) was used to estimate transmissivity. For the confined aquifer, $T = 1.22Q/s$ while for unconfined aquifer $T = 2.43Qm/s(2m-s)$. The storage coefficient was estimated using the Lohman equation (Lohman, 1972). This was done by multiplying the thickness in meters times 10^{-3}. The estimated values are not correct because no allowance is made for the aquifer's porosity and compressibility. The storage coefficient produced are however are reasonably reliable for most purposes. Such estimates may be improved upon by comparing values obtained from reliable pumping or flow tests, then extrapolated to other parts of an aquifer with adjustments for thickness if needed.

3.6.3 Research methods used to achieve objective 2 of the study.

This objective aimed at establishing the groundwater quality, rock-water and surface-groundwater interactions. It also aimed at establishing vulnerability to contamination from natural and anthropogenic sources.

3.6.3.1 Desktop studies for the determination of groundwater chemistry and vulnerability to contamination in the Kisumu and Mt. Elgon aquifers

The desktop studies included gathering information on existing water points for collecting water quality data. Existing boreholes were identified from the Ministry of Water and Sanitation database and Water Resources Authority borehole completion records. They were also identified through interviews with the local community.

3.6.3.2 Fieldwork and methods used to collect samples for the determination of groundwater chemistry and quality in the Kisumu and Mt. Elgon aquifers

Water samples for chemical analysis were collected in three sampling campaigns in Kisumu and two campaigns in Mt. Elgon. The selected sites are shown in location maps, *Figures 3.1 and 3.2*. The general practice when sampling groundwater is that boreholes should be pumped

out three or four times their holding volume to obtain a representative water sample. However, this proved difficult for the large diameter shallow wells, and therefore, water was sampled after the pH or EC of water being pumped stabilized (WRC, 2017). The sample bottles were rinsed at least twice then filled to overflow before sealing. Groundwater samples collected were put in clean, dry polyethylene plastic bottles filled to the top and capped tightly with two corks. The objective of double sealing was to protect the samples from evaporation and exchange with atmospheric water vapour. The volume of water collected for analysis two bottles (500 ml for cation determination, acidified with 2 to 3 drops of concentrated nitric acid, and 500 ml filtered (not acidified) for anion analyses).

In the Kisumu study site, the fieldwork periods were February to March 2017 and 2018, May to June 2017 and 2018, August to September 2017 and 2018 and November to December 2016, 2017 and 2018. Physico-chemical parameters were measured monthly using the portable Hydrolab Quanta field kit between November 2016 and December 2018. Four boreholes, eight shallow wells, five springs, four river sites and one site on Lake Victoria were the sampling points.

In the Mt. Elgon study area, water sampling was done between 18th of October 2014 and 3rd November 2014, 18th of March 2015 and 21st of March 2015. Physico-chemical parameters were collected using a portable Hannah kit during the collection of samples for analysis. These parameters were temperature, pH and conductivity. Six springs, four shallow wells, three river points and nineteen boreholes were sampled.

3.6.3.3 *Field studies to determine thermotolerant bacteria (TTC) in groundwater in Kisumu*

To understand the occurrence of thermotolerant bacteria (TTC) in groundwater, water samples were collected from surface water bodies, springs, shallow wells and boreholes aseptically using approved sampling methods, and stored in a cooler box at 4° C and incubated in the portable bacteriological kit within two hours after sampling. Due to the sensitivity of analysing water for micro-organisms, a portable kit, Wagtech Potatest field kit, was deployed.

A maximum of five samples was collected per day and incubated within two hours of sampling. A stainless sampling cup with a steel cable was used to fetch water from the shallow wells. This was carefully transferred to sterilised plastic bottles or sterile self-sealing plastic bags and stored in a cool box, ready for filtration and incubation. After incubation, an autoclave was used to sterilise the filtration unit, petri-dishes and other accessories. In the absence of the autoclave, 99% methanol and pressure cooker were used to sterilize the filtration kit and the accessories. The sampling procedure and incubation was repeated until all the twenty sampling sites were covered.

The sample treatment and incubation method involved filtering 100 ml of sampled water or less for highly contaminated water using a membrane filtration unit. A vacuum hand pump attached to the filtration unit was used to create suction that pulled the sample water through a sterile membrane. The membrane filter allowed water to pass through, but any bacteria present in the water were trapped on the surface of the filter membrane. The filter paper was then removed and placed on an absorbent pad in a petri dish that had been soaked in a liquid culture medium. The culture medium was to provide nutrients to the bacteria to grow while at the same time inhibiting the growth of any non-target bacteria. The loaded petri dish was then placed in the portable incubator, and the temperature set to 44.0º C. Incubation was done for 18 hours. The TTC formed were then countered and reported as CFU/100 ml of water. Tests were done in March 2017, June 2017, December 2017, March 2018 and May 2018.

3.6.3.4 *Laboratory methods used to reveal groundwater chemistry and quality in the Kisumu and Mt. Elgon aquifers*

Water sample analysis was done to establish groundwater quality and evaluate how the chemistry is modified by rock-water and surface-groundwater interactions, land uses and sanitation points. Laboratory for analysing samples included university private (CropNut, Nairobi), commercial companies (Elemtex Laboratory in the UK), and Government laboratories (WRA Central Water Testing Laboratory). At both the CropNut and WRA laboratories, major ions like Ca^{2+}, Mg^{2+}, K^+, Fe^{3+}, Mn^{2+}, Zn^{2+}, Al^{3+}, Na^+, NO_3^{2-}, PO_4^{3-}, F^-, Cl^-, HCO_3^- (reported as total alkalinity) and SO_4^{2-} were determined. Elemtex laboratory analysed for deuterium and oxygen-18. During this study, a primary selection criterion was that the laboratory has been making the desired type of analysis for several years on a routine basis and, if possible, ISO certified. CropNut laboratory was selected for water analysis because it is

ISO 1725 certified. The central WRA laboratory has been performing analysis for several years and is recognized in the water sector, and Elemtex Laboratory in the UK was recommended by Professor Taylor of University College London.

The laboratories selected have had active quality assurance/control (QA/QC) program, with documentation generally available on request. For QA/QC of sample measurements, about 5-15% of the samples were analysed in duplicate to show a constancy of results. The charge balance error acted as further proof for accuracy for the complete water analysis (Rainwater & Thatcher, 1960).

Laboratory methods

Table 3.9 and *Table 3.10* summarizes water analysis laboratory methods used during the study. The methods are laboratory specific. The laboratories used were the CropNut Kenya limited laboratory and the Water Resources Authority laboratory.

Table 3.9. Summary of the water analysis method used in the laboratory at CropNut Kenya limited (APHA, 2017)

Parameter	Method	Equipment	Summary of the method
Water P, Ca, Mg, K, Na, Mn, Fe, Cu, Mo, B, Zn, S, Si	Atomic Emission Spectrometry (ICP)	ICP-OS model	Chemical elements in water samples are detected based on the ionization of a sample by an extremely hot plasma, usually made from argon. The ions are segregated based on their mass-to-charge ratio.
Ammonium in water	Colorimetric	Auto Karl Fischer titrimeter	The concentration of a chemical element or chemical compound in a solution is determined with a colour reagent and colour change.
Nitrate Nitrogen	Colorimetric	Auto Karl Fischer titrimeter	Colour change
Nitrite Nitrogen	Colorimetric	Auto Karl Fischer titrimeter	Colour change
Chloride	Colorimetric	Auto Karl Fischer titrimeter	Colour change
Bicarbonate	Colorimetric	Auto Karl Fischer titrimeter	Colour change
Fluoride	Colorimetric	Auto Karl Fischer titrimeter	Colour change

Water samples from the Mt. Elgon aquifer were analysed at the Water Resources Authority (WRA) Water Testing Central Laboratory. The methodologies used are given in *Table 3.10*.

Table 3.10. Analytical methods used at the Water Resources Authority laboratory to analyse Mt. Elgon water samples. The codes are the standard methods abbreviations (APHA, 2017).

Parameter	Method	Equipment	Summary of the method
Water pH	SM-4500-H$^+$. Potentiometric	pH Meter: Jenway 3505	The method measured the difference in electrical potential between a pH electrode and a reference electrode.
Conductivity (25^0 C)	SM-2520 B. Electrical Conductivity Method	Conductivity meter: Jenway 3540	This method was based on the measurement of the electric potential difference between two electrodes.
Iron	SM-3500-Fe B. Phenanthroline	Jenway Calorimeter 6051	In this method, the amount of iron present in a sample was quantified by first reacting the iron with 1,10-phenanthroline to form a coloured complex and then measuring the amount of light absorbed by this complex.
Manganese	SM-3500-Mn B. Persulfate method	Titration (Calculation)	The concentration of a chemical element or chemical compound in a solution is determined with a colour reagent and colour change.
Calcium	SM 3500-Ca B.EDTA titrimetric	Titration (Calculation)	When EDTA (ethylenediaminetetraacetic acid or its salts) is added to water, calcium precipitates and indicators were used to give the indicative colour change
Magnesium	SM-3500-Mg B. EDTA titrimetric Method	Titration (Calculation)	The concentration of a chemical element or chemical compound in a solution was determined with a colour reagent and colour change.
Sodium	SM-3500-Na B. Flame photometric method	Jenway PFP7:Flame Photometer	Trace amounts of sodium were determined by flame emission photometry. Samples were nebulized into a gas flame under controlled, reproducible excitation conditions.
Potassium	SM-3500-K B. Flame photometric Method	Jenway PFP7:Flame Photometer	Like sodium, potassium was determined by flame photometer Samples were nebulized into a gas flame under controlled, reproducible excitation conditions
Total Alkalinity	SM 2320 B. Titrimetric	Titration (calculation)	Hydroxyl ions released by hydrolysis react with additions of standard acid. Alkalinity was dependent on end-point pH used.
Chloride	SM-4500-CL$^-$ B. Argentometric	Mohr method Titration and calculation	Potassium chromate was used in a neutral or slightly alkaline solution to indicate the endpoint of the silver nitrate titration of chloride. Silver chloride was precipitated quantitatively before red silver chromate was formed.
Fluoride	SM-4500-F$^-$ C. Ion-selective Electrode Method	Jenway 3345; Ion meter	The critical element in the fluoride electrode is the laser-type doped lanthanum fluoride crystal across which fluoride solutions of different concentrations establish a potential.
Nitrate	SM-4500-NO$_3^-$ B. UV spectrophotometric	UV-VIS spectrophotometer: UV Mini 1240 Shimadzu	The ultraviolet (UV) light technique measures NO_3^- absorbance at 220 nm,
Nitrite	SM-4500-NO$_2^-$ B. Calorimetric Method	Jenway Calorimeter 6051	A chemical element or chemical compound concentration in a solution is determined with a colour reagent and colour change.
Sulphate	SM-4500-SO$_4^{2-}$ Turbidimetric Method	Turbidimeter	This method measured the relative clarity of water by determining the amount of light scattered by sulphate particles in the water sample. The turbidimetric method is applicable in the range of 1 to 40 mg SO_4^{2-} /L

3.6.3.5 *Data analysis methods used to determine of hydrochemical facies and to classify water*

Univariate and multivariate data analysis techniques using IBM SPSS Statistics 25 and Excel 2013 were used to determine hydrochemical facies and classify groundwater. The data frequency descriptive statistics of central tendency that included mean, median, mode and geometric mean, and frequency dispersion (minimum and maximum) were calculated for both physico-chemical and hydrochemical data from the study sites. The descriptive (univariate data analysis) statistics were followed by multivariate analysis that included correlation and factor analysis (PCA). A KMO test for sampling adequacy and Bartlett's test of sphericity was performed for all data before correlation and factor analysis. KMO values>5 and Bartlett's test of sphericity value <0.001 are acceptable (Taherdoost *et al.*, 2014; Ul Hadia *et al.*, 2016). Once the data passed this test, it was subjected to correlation and factor analysis. Statistical analysis of chemical data was done to determine the hydrochemical facies and classify related groundwater parameters. The background processes that explain most of the original dataset's variance were achieved using Principal Component Analysis (PCA).

The processes that control natural water composition was demonstrated through hydro-chemical facies analysis. The graphical presentation was used to reveal ionic relationships and water quality regimes. These were done using Diagramme software. The classical graphical methods (Piper, Durov and trilinear, Schoeller-Berkoloff, Wilcox and Gibbs) were used as interpretative tools of the main hydro-chemical processes. In contrast, hierarchical cluster analysis (HCA) and principal component analysis (PCA) methods were used to determine subtle hydro-chemical variations and water types (Cerny and Kaiser, 1977; Helsel and Hirsch, 2002). In cluster analysis, an agglomeration schedule with five cluster solutions and the between-groups linkage method of clustering using the squared Euclidian distance was used. The variables were standardized to z-scores so that each variable contributed equally to the clusters (Sarstedt and Mooi, 2019; Yim and Ramdeen, 2015). Statistical plots were used to reveal seasonal or monthly variations in coliform contamination. Nitrates were also plotted together with TTCs to show any correlation between the two (Gosselin *et al.*, 1997; Juntakut *et al.*, 2020; Seçkin *et al.*, 2018).

Mineral saturation indices

PHREEQC software was used to estimate the saturation indexes. The mineral saturation indices for various minerals were calculated using PHREEQC software. Positive values mean that the mineral will precipitate, while negative values indicate that it will remain in solution. Chemical equilibrium for a particular mineral species can be examined by calculating the saturation index. This index is expressed as;

$$SI = \log (IAP/KT)$$

Where IAP means ion activity product and KT is the solubility constant. If the water is in thermodynamic equilibrium saturation index = 0, if over saturated, SI > 0 and when under saturated, SI< 0. Saturation indices for the groundwater samples collected from Kisumu and Mt. Elgon were carried out using the PHREEQC interactive software. The results were plotted using Microsoft Excel. Saturation indices helped identify the relationship between geochemical processes and groundwater quality (Li *et al*., 2018).

Chloro-alkaline plots

The chloro-alkaline indices provide valuable information about the ion-exchange reaction between groundwater and aquifer materials (Al-Ahmadi, 2013; Hem, 1985). These indices were calculated using the following equations;

$$CAI.1 = \frac{Cl^- - (Na^+ + K^+)}{Cl^-}$$

And

$$CAI.2 = \frac{Cl^- - (Na^+ + K^+)}{Cl^-} + (HCO_3^- + SO_4^{2-}SO4 + NO_3^{2-})$$

Where CAI 1and CAI 2 indicate ion exchange processes.

Anion and cation charge balance error determination

The error balance determination was done to confirm the accuracy of the analysis. The first step was to convert concentrations gotten from the laboratory in mg/L into milli-equivalent weights using the equation below:

$$mEq = \frac{mg}{l} \times \text{ valence} \div \text{ atomic, molecular or formula weight}$$

The charge balance error was then calculated using the equation:

$$\text{Charge Balance \%} = 100(\textstyle\sum mEq \text{ cations } - \textstyle\sum meq \text{ anions}) \Big/ (\textstyle\sum mEq \text{ cations } + \textstyle\sum mEq \text{ anions})$$

The charge of an atom is supposed to be neutral. Pauling postulated this in 1948 according to the essentials of electrical neutrality of atoms (Pauling, 1948). The charge balance error should be within $\pm 10\%$ margin using equation 2. If the charge balance is beyond $\pm 10\%$, it could mean that;

(1) There were problems or errors with field measurements,

(2) There were problems with the laboratory analysis (e.g., poor standardization or failure to correct the results for laboratory dilutions),

(3) Incorrect assignment of the charge for one or more of the significant solutes or,

(4) The list of compounds that were analysed was incomplete.

Conversion of alkalinity to bicarbonate

The methodology for converting alkalinity to bicarbonate is based on the following reaction:

$$CaCO_3 + H_2O + CO_2 = Ca(HCO_3)_2$$

Calcium carbonate has a 100 g/mole molecular weight, while calcium bicarbonate anion has a 61 g/mole molecular weight. Therefore, each mole of calcium bicarbonate corresponds to one mole of $CaCO_3$ (100 g) and contains 2 x 61 g = 122 g of bicarbonate anion. The conversion of bicarbonate alkalinity as calcium carbonate to bicarbonate alkalinity as HCO_3^- was done as in equation below;

$$(HCO_3)^- = 1.22 \times CaCO_3 \left(\frac{mg}{L}\right)$$

Conversion of electrical conductivity (EC) to total dissolved solids (TDS)

The electrical conductivity of water was measured quickly and inexpensively *in situ* by a Hydrolab Quanta portable water quality kit. However, analysis of TDS was difficult and expensive and needed more equipment and time. However, TDS analysis can illustrate groundwater quality, particularly in understanding the water interactions with rocks (Hubert and Wolkersdorfer, 2015). Hence, researchers have done various investigations to find out the precise mathematical correlation between these two parameters so that TDS concentration can be calculated from the EC value (Choo, 2019). The correlation of these parameters can be estimated by the equation below;

$$TDS \ (mgL) = k \times eC \ (\mu S/cm)$$

The value of the constant k increases with an increase in groundwater mineralisation. The typical values of the k constant are given in *Table 3.11*. The value of k = 0.55 was used in this study because the electrical conductivity measured in Kisumu and Mt. Elgon fell within the freshwater domain (Hem, 1985).

Table 3.11. Relationship between EC and TDS in various types of water (Eugene et al., 1970; Hem, 1985; Marandi et al., 2013; Walton, 1989)

EC at 25°C (µS/cm)	Ratio of TDS/EC (k)
Natural water for irrigation	0.55 – 0.75
Natural water (500 – 3,000)	0.55 – 0.75
Distilled water (1 – 10)	0.5
Fresh water (300 – 800)	0.55
Seawater (45,000 - 60,000)	0.70
Brine water (65,000 – 85,000)	0.75

3.6.4   The research methods used to achieve objective 3 of the study.

This objective three aimed at determining recharge in the Kisumu aquifer using the stable isotope data. It also aimed at determining the relationships of isotope signal from various water sources and the relationship between Lake Victoria and groundwater. Isotope data analysis did not apply for Mt. Elgon aquifer due to limited funding, as indicated in the limitation of the studies section.

3.6.4.1 Desk-top studies on the determination of water isotopes

The two main physical processes a water molecule undergoes naturally are evaporation and condensation. When water evaporates, the lighter isotopes of hydrogen and oxygen go into vapour, and during condensation, the heavier isotopes condense first (Mook, 2000b). These processes cause a variation in isotopic composition in water molecules by fractionation of isotopes. These variations depend on various conditions such as temperature, humidity and altitude. Isotopic concentrations are expressed as the difference between the measured ratios of the sample and the reference over the measured ratio of the reference (Craig, 1961).

The variations in the oxygen isotopic composition were assessed from the known four perspectives. These included the latitudinal effect that usually lowers the $^{18}\delta$ values with increasing latitude, the amount effect with more negative $^{18}\delta$ values in the rain during heavy storms, the continental effect with more negative $^{18}\delta$ values for precipitation the more inland and, the altitude effect with decreasing $^{18}\delta$ in rainfall at higher altitudes (Sodemann, 2006).

Oxygen has three stable isotopes, namely, ^{16}O, ^{17}O and ^{18}O, with abundances of 99.760%, 0.035% and 0.200%, respectively (Mook, 2000f). The concentration of oxygen-17 in water is deficient, and its ratio to oxygen-16 is low and therefore provides little information on the hydrological cycle, *Table 3.12*. Thus, the proportion of oxygen-18 to oxygen-16 (0.0020) is used in isotopic studies. Oxygen-18 is enriched in water bodies that have undergone evaporation (e.g. saline lakes) and depleted in high altitude low-temperature climates.

Table 3.12. Practical data for oxygen isotope including the natural abundances, properties, analytical techniques and standards (Mook, 2000)

Parameter	^{18}O
Stability	Stable
Natural abundance	0.00205
Abundance range in H_2O	30 ‰
Reported as	$\delta^{18}O$
Units	‰ (per mil)
Standard deviation	0.05 ‰
International standard	VSMOW
With absolute value	VSMOW 0.000052

Hydrogen has two stable isotopes, namely ^1H and ^2H. The abundance of isotopes is about 99.985% and 0.015%, respectively. The isotope ratio of ^2H to ^1H is 0.00015 (Mook, 2000). The isotope ratio of ^2H to ^1H has a natural variation of about 250‰. Like Oxygen-18, high deuterium values are reported in evaporated surface waters (saline lakes), while low deuterium values are reported in cold climates (Sodemann, 2006). Valuable data for the natural abundance, properties, analytical techniques and standards for stable and radioactive hydrogen isotopes are shown in *Table 3.13*.

Table 3.13. Practical data for the natural abundance, properties, analytical techniques and standards for stable and radioactive hydrogen isotopes (Mook, 2000)

Parameter	^2H	^3H
Natural abundance	0.00015	$<10^{-17}$
Stability	Stable	Radioactive
Abundance Range in H_2O	250 ‰	$0 - 10^{-16}$
Reported as	δ^2H or δD	^3H
Units	‰	TU, Bq/L H_2O
Standard deviation	0.5 ‰	$\geq 1\%$ at a higher level
International standard	VSMOW	NBS-SRM 4361
With absolute value	$^2H/^1H=0.0015575$	$^3H/^1H=6600$ TU

There is a strong correlation between fractionation effects of deuterium and oxygen-18. Factors responsible for the enrichment of oxygen-18 are also accountable for enriching deuterium. In natural waters, the relationship between δ^2H and $O^{18}\delta$ values is to be expected. This relationship forms the basis for the local and global water meteoric lines with an ass assumption that evaporation and condensation in nature occur in isotopic equilibrium (Dansgaard, 1964).

3.6.4.2 *Fieldwork to collect water samples for the determination of water isotopes*

Twenty-two water samples for isotope analysis were collected in March 2017, simultaneously with samples for chemical analysis as discussed in section 3.6.3.2. These samples were from boreholes (4), shallow wells (8), springs (5), river (4) and Lake (1). They were collected using heavy density 60 ml plastic bottles with double seals and stored in a dark, cool place. The bottles were filled to the rim. This was done to minimise evaporation while the samples were on transit to the laboratory. The sample size was lab-dependent, and the typical volume was 60 ml. Efforts were made to ensure that air bubbles were not trapped in the water by gentle shaking

and filling the bottle. The samples were stored in a cool dark place before shipping to the United Kingdom for analysis.

3.6.4.3   *Laboratory determination of stable water isotopes*

Due to lack of analytical equipment locally, the analysis was done in the UK by the Elemtex Company, recommended by Professor Taylor of University College London. An Isotope Ratio Mass Spectrometer (IRMS) used. This spectrometer is very precise in measuring hydrogen and oxygen isotopes in a water molecule. The stable isotope ratio mass spectrometer consisted of an inlet system, an ion source, an analyser for ion separation, and a detector for ion registration. The inlet system was generally designed to handle pure gases including CO_2, N_2, H_2, and SO_2, but some inlet systems can analyse gases like O_2, N_2O, CO, CH_3Cl, SF_6, CF_4, and SiF_4 (Brand, 2004). Neutral molecules from the inlet system were introduced into the ion source, where they were ionized via electron impact and accelerated to several kilovolts, and then separated by a magnetic field and detected by Faraday cups positioned along the image plane of the mass spectrometer (van Calsteren and Schwieters, 1995).

Hydrogen isotope measurements
The following laboratory reference materials were used to determine hydrogen isotopic ratios, *Table 3.14.*

Table 3.14.The standards used for deuterium analysis in the Elemtex laboratory

Name	Actual δ^2H	Measured δ^2H	Standard deviation
ISO63	11.26	11.26	0.29
ISO64	-98.33	-98.33	0.20
DeI	-47.29	-47.33	0.37

Oxygen isotope measurements
The following laboratory reference materials were used to determine oxygen isotopic ratios during this study, *Table 3.15.*

Table 3.15. The standards used for the determination of $\delta^{18}O$ in the Elemtex laboratory

Name	Actual $\delta^{18}O$	Measured $\delta^{18}O$	Standard deviation
ISO63	-0.42	-0.42	0.10
ISO64	-12.34	-12.34	0.05
DeI	-6.59	-6.70	0.12

3.6.4.4   *Stable isotopes data analysis*

The data generated were compared with the global meteoric water line and the local meteoric water line computed using historical rainfall records of $\delta^{18}O$ and δ^2H in Kericho. This data was collected by the International Atomic Energy Agency (IAEA) supported project on precipitation data, the Global Network of Isotopes in Precipitation (GNIP). Kericho station was chosen because it is closer to Kisumu than Entebbe. Therefore, precipitation comes from the same origin, either through relief rainfall from high altitude regions or conventional rainfall over Lake Victoria. Secondly, there is a paucity of meteoric water isotope data in Kenya. The GNIP data was used to identify the source and timing of recharge water in Kisumu. This was done by plotting Kisumu isotope data and the Kericho data and determining the relationship between the two based on the regression lines. The plots and regression analysis were done using the solver in Excel Microsoft software version 2013.

CHAPTER 4 - RESULTS AND DISCUSSION

This chapter presents the results and discussion of the results guided by the three study objectives highlighted in chapter 1. The results are presented in the first three sections, followed by a discussion of the results in section 4.4. The results section set out the critical experimental, field and laboratory results, including statistical analysis. The discussion section provide a review of this study's findings in relation to the existing literature and the gaps about the aim of the study. The discussion demonstrates the importance of key findings, the limitations of the research and the implications of the results for policy and practice.

4.1 Results of the aquifer geometry and hydrogeology of the study sites

The results and discussion of objective one of the study on aquifer geometry and hydrogeology are presented in this section. These include results on revised geological mapping and the geophysical surveys in Kisumu and Mt. Elgon study sites. The pumping tests data and the calculated aquifer parameters for the Kisumu aquifer are presented. Interpretation of selected historical boreholes records for Mt. Elgon is also given.

4.1.1   The geology of the Kisumu study site

The existing geological report and the accompanying geological map for Kisumu were done in 1952 (Saggerson, 1952). The description of rock units, structures and mineralogy in this report are superb. However, during the revised geological mapping of the area, a few rock units were renamed by this study (*Figure 4.2*) after the field observation (*Figure 4.1*) and laboratory analysis and subsequent classification using TAS and trace elements (*Figure 4.4* and *Figure 4.5*). A meta-sedimentary formation forming a ring on the southern shores of the Kavirondo Gulf, and extending along the Nairobi Kisumu Highway, and covering most of the commercial part of Kisumu, was mapped as grit. This formation was previously mapped as phonolite by Saggerson in 1952 and has evident relics of sedimentary structures like ripple marks and parting planes. It is therefore not a volcanic rock but a meta-sedimentary one due to these properties. The workability of the rocks near Dunga beach was made easier when these parting planes are targeted. It was concluded that these rocks belong to the Archaean (Kavirondian) System in age due to similarities with rocks reported in the adjacent region by previous researchers (e.g. Ngecu, 1991; Opiyo-Akech, 1988).

A distinction was also made between the formations mapped as an extensive phonolitic lava extending from Otonglo (near the Kisumu International Airport) to Kiboswa. The revised mapping showed that the area was composed of andesitic metavolcanic, and the composition ranged from 57% to 63% silica. These rocks are foliated (*Figure 4.1*) due to low-grade metamorphism and belong to the Nyanzian system. The formation was encountered along the Kisumu-Kakamega highway past the Mamboleo estate and extended to Kiboswa.

Figure 4.1. Meta-andesitic rocks outcropping along the Kisumu - Kakamega highway near Mambo Leo estate

The meta-andesites are highly fractured and have a preferred east-west orientation of fractures and joints.
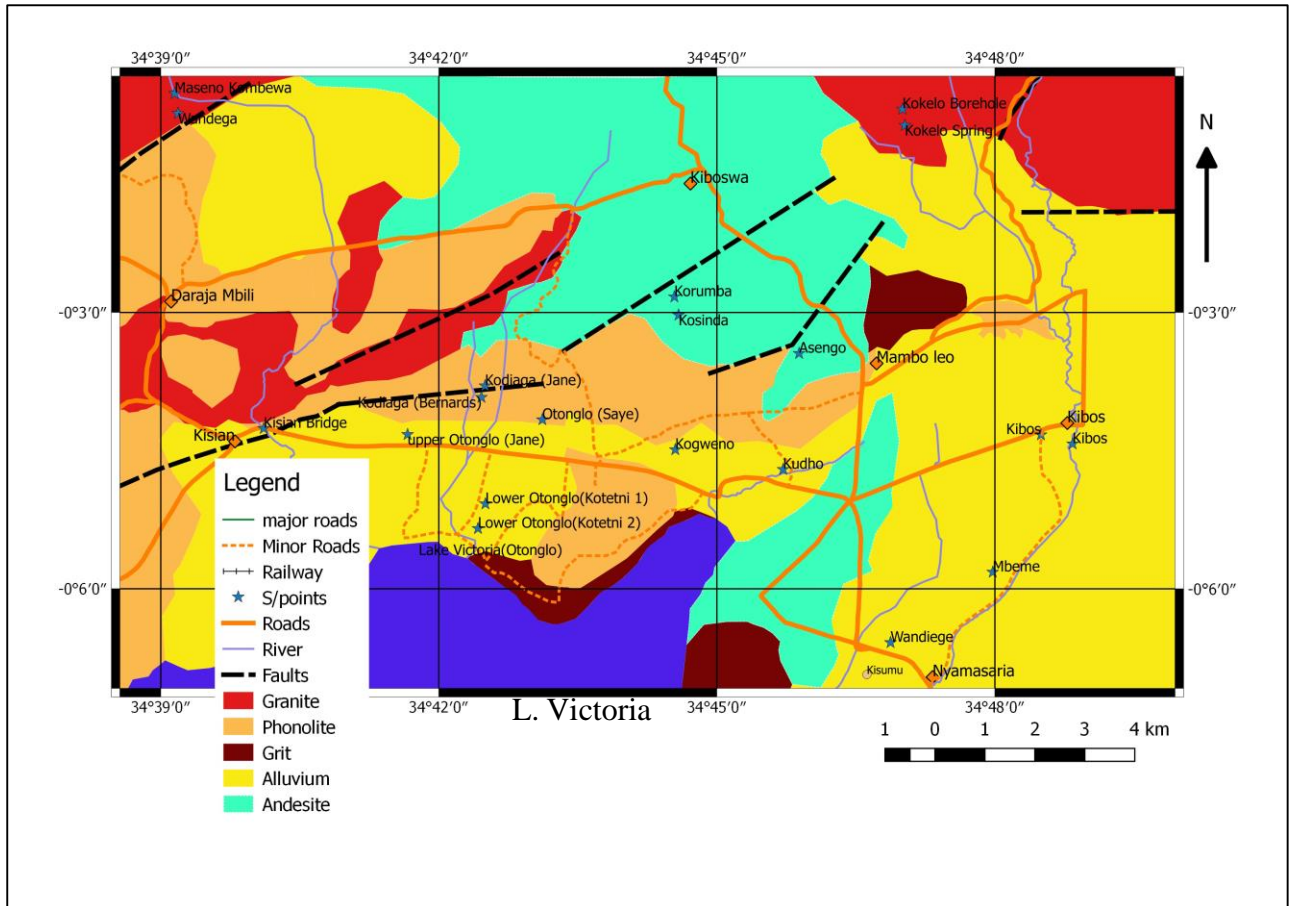
Figure 4.2. Geological map of the Kisumu study area. The main rock types are phonolite, andesite, grit, granite, unconsolidated colluvial deposits, and alluvium adjacent to river channels.

Based on the revised geology, the stratigraphy of Kisumu shows that the oldest rocks are the andesitic meta-volcanic belonging to the Nyanzian system. These are overlain by the Kavirondian grit and intruded by granitic intrusions not related to the Kavirondo rifting. Phonolititic rocks erupted during the formation of the Kavirondo Rift Valley during the Paleogene and Neogene period (*Table 4.1*). The rifting is associated with the formation of the East African Rift Valley. The structural deformation of the rift consists of normal and oblique faults, a monoclinal flexure and a syncline. These confirm the Rift to be due to crustal extension. The rift probably formed from gradual but continuous tectonic movements that started as early as the early Miocene (Mboya, 1983).

Table 4.1. A summary of the stratigraphy of the Kisumu study area. The periods, rock system, major lithology and geological events are summarized.

Period	Rock system	Lithology	Major geological event
Quaternary	Recent	Superficial deposits and soils	Erosion and sedimentation
		Alluvium and laterite	
Palaeogene-Neogene	Pliocene	Phonolite Basaltic-phonolite (trachyte)	Kavirondo rifting with the formation of major faults
Archaean	Kavirondian	Granite Intrusion	Formation of major African cratons
		Meta-grit	
	Nyanzian	Meta-andesites	

4.1.2 The geology of Mt. Elgon study site

The geological map of the Mt. Elgon area (*Figure 4.3*) was compiled using existing geological reports and maps (Gibson, 1954; Miller, 1956; Sanders, 1963; Searle, 1952). The area comprises rocks of varying ages (*Table 4.2*), ranging from Pre-Cambrian metamorphic rocks, Palaeogene-Neogene lavas to the Recent surficial sandy and black cotton soils (Gibson, 1954; Miller, 1956). The Pre-Cambrian rocks are mainly quartzite and gneisses of varying composition derived from the original argillaceous and arenaceous sediments. These sediments were deposited in a geosyncline and later transformed through metamorphism and recrystallization into quartzites and feldspar-rich metamorphic rocks (Miller, 1956). These rocks have abundant muscovite, biotite, and hornblende minerals. They show varying degree of weathering ranging from moderately to highly weathered rocks between Kwanza and Kapenguria (Searle, 1952). Generally, weathering was more intense in the areas underlain by schists than those underlain by gneisses (Vearncombe, 1983). The rocks exhibited good foliation with strike trend approximately NNW-SSE, in conformity with the general direction of Proterozoic Mozambique Belt rocks. Between Kitale and Kapenguria, fresh rock outcrops are scarce due to weathering.
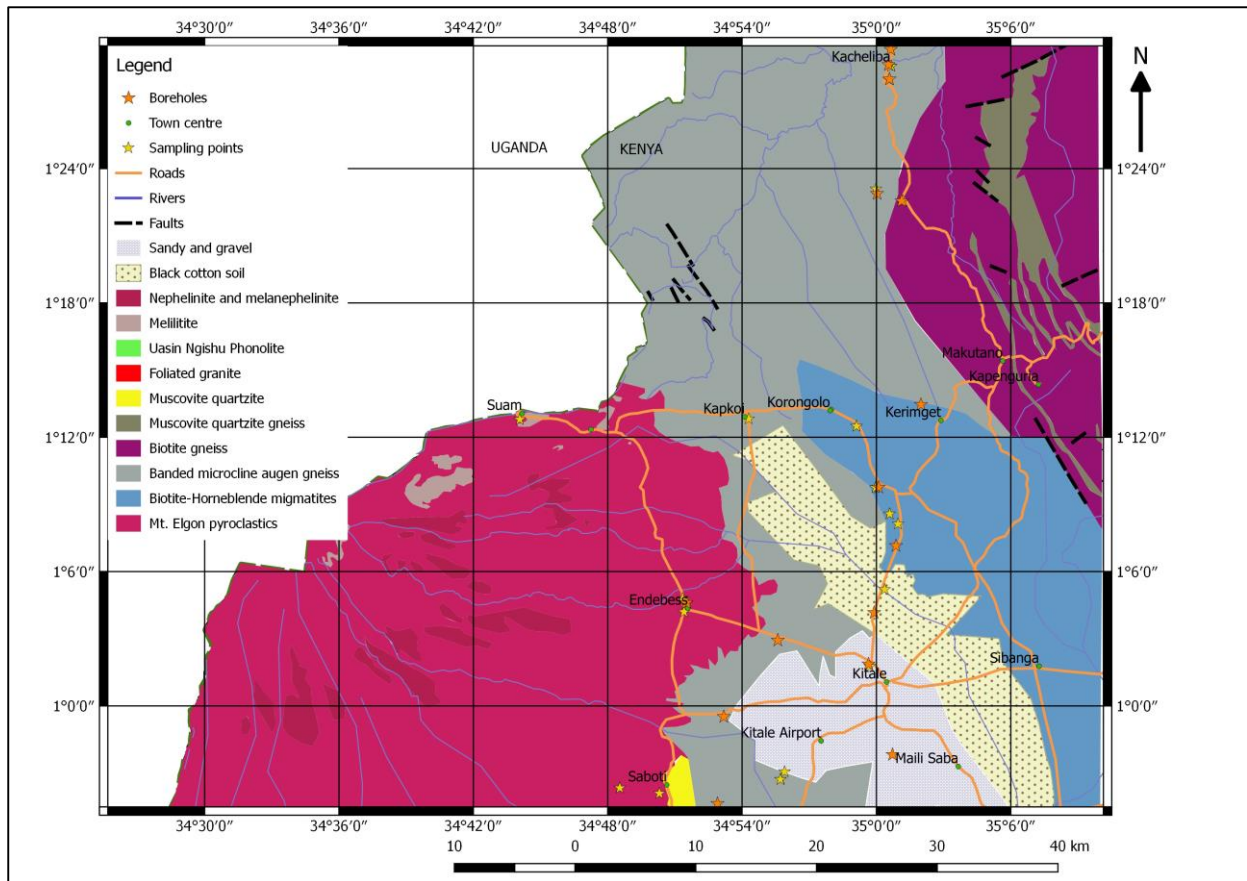
Figure 4.3. Geological map of Mt. Elgon study area (modified from (Gibson, 1954; Miller, 1956; Sanders, 1963)

The Mount Elgon Tertiary volcanic rocks are composed of great masses of pyroclastic, agglomerates, breccia and tuff with intercalated bands of basalts, trachyte, basanite, nephelinite, melilitite and phonolite (Simonetti and Bell, 1995; Wright, 1963). The thickness of volcanic rocks thins away from the peak of Mt. Elgon, suggesting that the rocks were undoubtedly laid down on a surface sloping radially away from the peak of Mt. Elgon (Mohr and Wood, 1976; Pulfrey, 1960; Wright, 1963). The mountain slopes are characterised by high cliff sections formed of Tertiary age lavas, tuffs and agglomerates that were challenging during geological mapping and geophysical surveys.

Table 4.2. Stratigraphy of Mt. Elgon study site. The dominant rocks are the Tertiary Mt. Elgon volcanic rocks.

Period	Rock system	Lithology	Major geological event
Quaternary	Recent	Superficial deposits and black cotton Soils	Erosion and sedimentation
		Sandy soils and gravel	
Palaeogene-Neogene	Pliocene	Pyroclastic and agglomerate	Volcanic eruption and formation of Major alkaline mountains in Africa
	Miocene	Melilitite, basalts, trachyte, basanite, nephelinite, melilitite and phonolite	
Pre-Cambrian	Neoproterozoic	Schists, gneisses, quartzite, Granite	Formation of Neo-Proterozoic Mozambique Belt

4.1.3   Characterisation of Kisumu geologic formations

The volcanic rocks dominate the elevated areas of Kisumu, while the lowlands have sediments of various ages and different origin. The rocks range from the Nyanzian meta-andesite, basaltic meta-andesite to Paleogene-Neogene phonolites and basaltic phonolites (trachytes). The meta-andesite belongs to a family of fine-grained, extrusive igneous rocks commonly dark grey.

The andesites in Kisumu are foliated with a preferred orientation due to weak metamorphism. The meta-andesite contain plagioclase feldspar, biotite, pyroxene, or amphibole. Phonolites are fine-grained, undersaturated, intermediate igneous rocks, with or without phenocrysts, consisting primarily of alkali feldspars and feldspathoids together with pyroxenes and amphiboles, usually sodic varieties. Thin section analysis of phonolite sample had cryptocrystalline feldspathoids and fines constituting 50%, aegirine augite 20%, sodalite 20%, Fe- oxides about 05% and quartz less than 05%.

These alumina-silicate rocks are generally rich in alkali earth and silica. The result of the XRF analysis of 10 representative rock samples is given in *Table 4.3*.

Table 4.3. Major (wt %) and trace (ppm) element composition of selected rock samples from the study area analysed using the XRF method.

Elements	Grit	Andesite			Basaltic phonolite (trachytes)		Phonolite			
SiO_2	65.1	63.5	64.4	62.3	65.2	64.9	64.6	64.5	64.8	64.1
Al_2O_3	21.7	23.4	23.0	25.1	21.5	22.4	22.2	22.9	22.7	22.5
K_2O	6.2	6.3	6.3	6.3	6.1	6.9	6.0	6.4	6.5	6.5
F_e2O_3	4.4	4.6	4.2	4.1	4.2	4.0	3.6	4.0	3.4	4.4
CaO	1.7	1.2	1.2	1.6	2.2	1.2	2.7	1.1	1.7	1.6
MnO_2	0.2	0.3	0.2	0.4	0.2	0.3	0.3	0.3	0.3	0.3
TiO	0.2	0.2	0.4	0.2	0.4	0.2	0.2	0.2	0.2	0.2
Zr	870	940	730	770	800	860	800	790	780	780
Nb	360	390	350	320	340	330	310	320	280	330
Rb	230	260	260	220	210	230	210	270	220	250
Zn	250	170	210	210	220	220	170	210	160	180
Y	90	170	120	90	110	140	70	120	70	70
V	60	150	50	120	60	50	60	80	50	50
Sr	80	90	60	80	0	0	220	60	120	80
Ta	30	50	20	20	0	20	20	20	20	20
Mo	20	10	20	30	10	10	20	10	0	10
As	10	0	0	10	10	10	0	20	20	10
P	0	0	0	0	0	0	90	0	460	170
W	0	0	0	0	0	0	10	20	0	0
Pt	0	0	0	10	10	0	0	0	0	10

The high content of alkaline earth metals in these rocks indicates richness in plagioclase, pyroxene and biotite. The Winchester and Floyd (1977) volcanic rock classification scheme was used to determine the type of rocks using data from ten samples analysed, *Figure 4.4*. This scheme was used because it is ideal for altered (metamorphosed) rocks as these plots use the immobile trace elements zircon, titanium, niobium and yttrium. A comparative plot of the samples using the Le Bas (1986) Total Alkali and Silica (TAS) plot was also used in *Figure 4.5*.
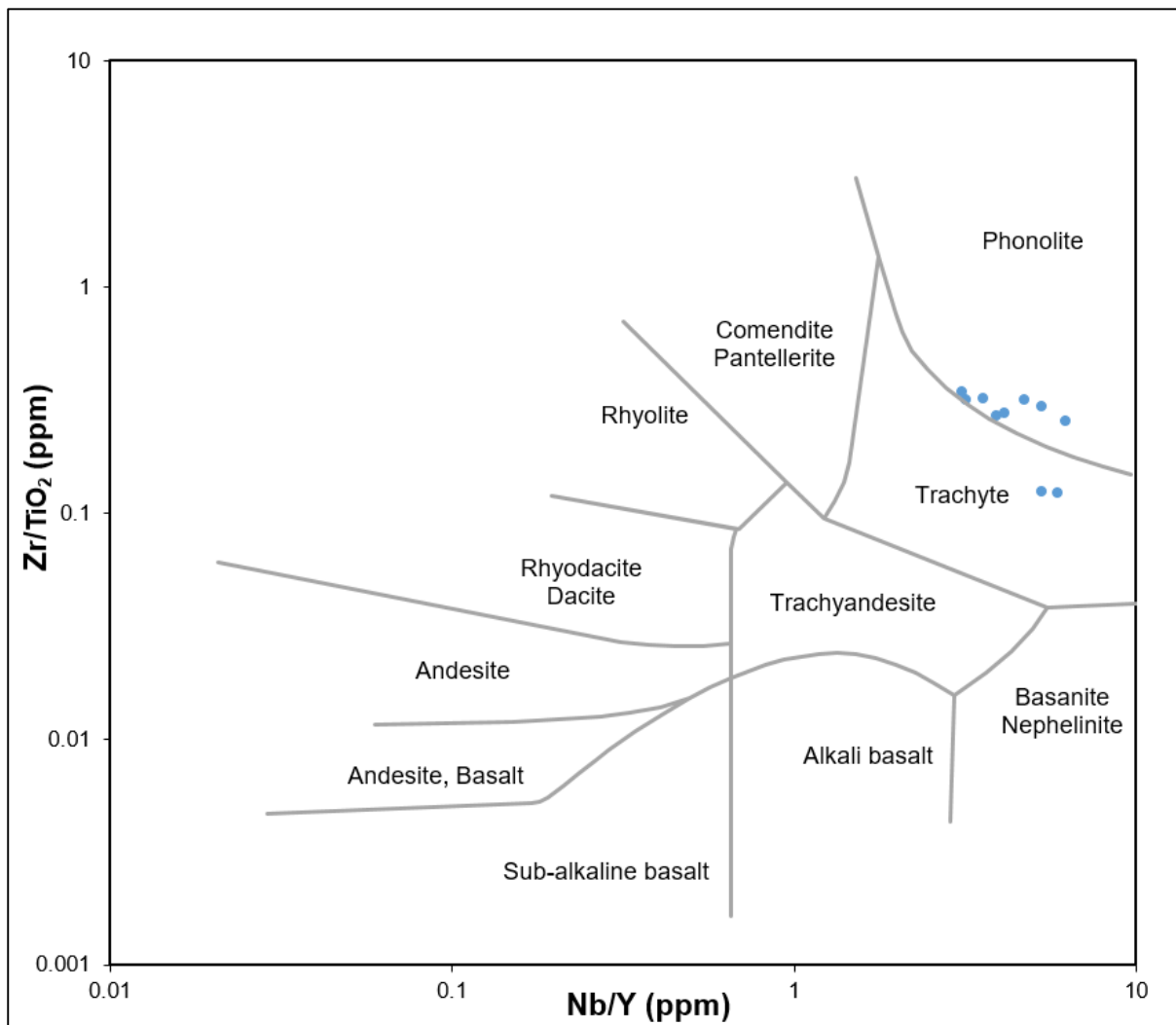
Figure 4.4. Result of Winchester and Floyd Zr/TiO2 (ppm) versus Nb/Y (ppm) classification scheme of Kisumu rocks. Eight samples plotted within the phonolite field, and two samples plotted within the trachyte field (Winchester & Floyd, 1977).

The Winchester and Floyd plot was chosen because the phonolitic rocks in the study area were altered, and the plot uses the immobile trace elements Zr, Ti, Nb and Y. Using the TAS (total alkali-silica plot) plot the rock samples plotted within the andesite and dacite field. However, due to alteration and metamorphism, the hand specimen characteristics were closer to andesite than dacite, *Figure 4.5*. Based on the two plots, it was concluded that phonolite and andesites were the dominant volcanic rocks in the area. The explanation for samples not plotting on the andesite field is that the primary melt was phonolitic but transforms to andesite due to enrichment of silicates while passing through granites and metamorphosed grit. During this process, the andesite retains the trace element marker of phonolitic melt but modified by interaction with pre-existing rock.
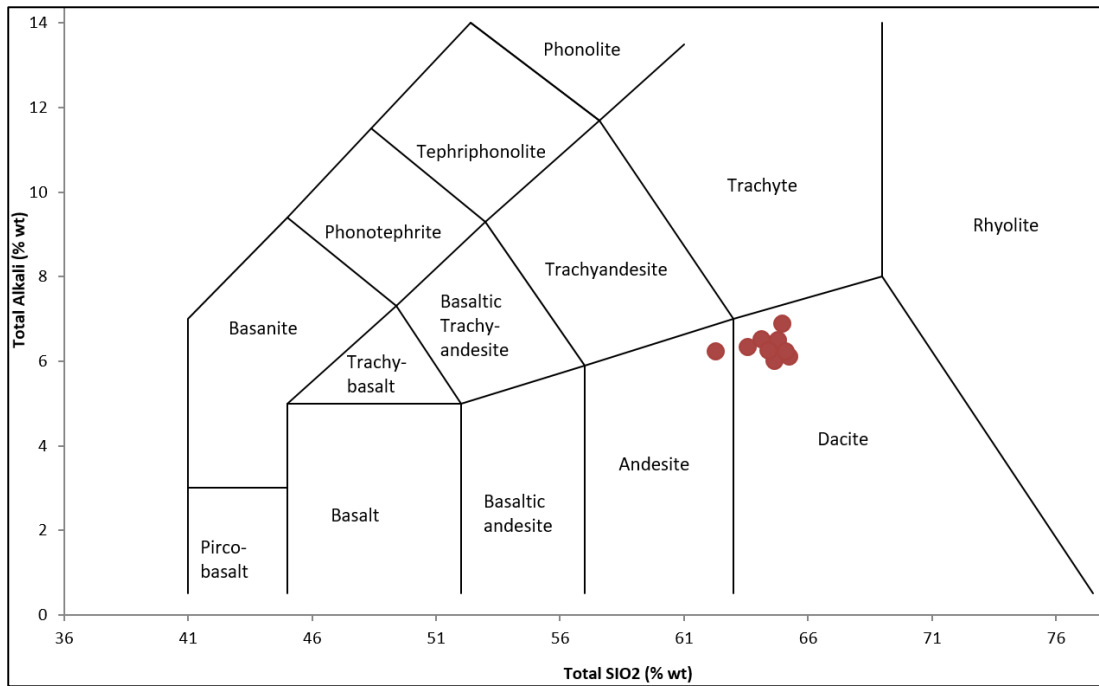
Figure 4.5.TAS plot for the selected samples (Le Bas et al., 1986). The rocks plot within the dacite but closer to andesites. The rocks have gone metamorphism are not true andesite.

4.1.4 Geophysical surveys and geologs

4.1.4.1   *Kisumu geophysical survey and geologs*

The geophysical surveys were conducted to determine the depth of the shallow water table, *Figure 4.6.*

Figure 4.6. VES survey in Kisumu using the Schlumberger configuration, with a maximum AB/2 of 50 meters.

Vertical electrical sounding (VES) resistivity values indicate that volcanic rocks and sedimentary rocks underlie the area in some sites with intercalations of clayey layers. The influence of the top surface material on the VES values is also quite apparent. *Table 4.4* shows a typical geological profile for the Kisumu study site. It matches well with the VES interpretation presented in the subsequent sub-section.

Table 4.4. Typical geological profile in Kisumu based geo-logs from historical boreholes in the area.

Formation	Depth range
The top layer of alluvial sediments and soil	0.0 – 2.0 m
A thick layer of Pleistocene sediments and laterites (location of a most shallow well)	2.0 – 4.0 m
Clay (derived from weathered pyroclastic and phonolites)	4.0 – 30.0
Weathered phonolites (some shallow aquifers location)	30.0 – 40.0
Possibly phonolite and andesite (fresh)	Beyond 40.0 m

The location of VES sites in Kisumu is shown in *Figure 4.7*. A detailed presentation of the results from sites chosen for drilling follows.
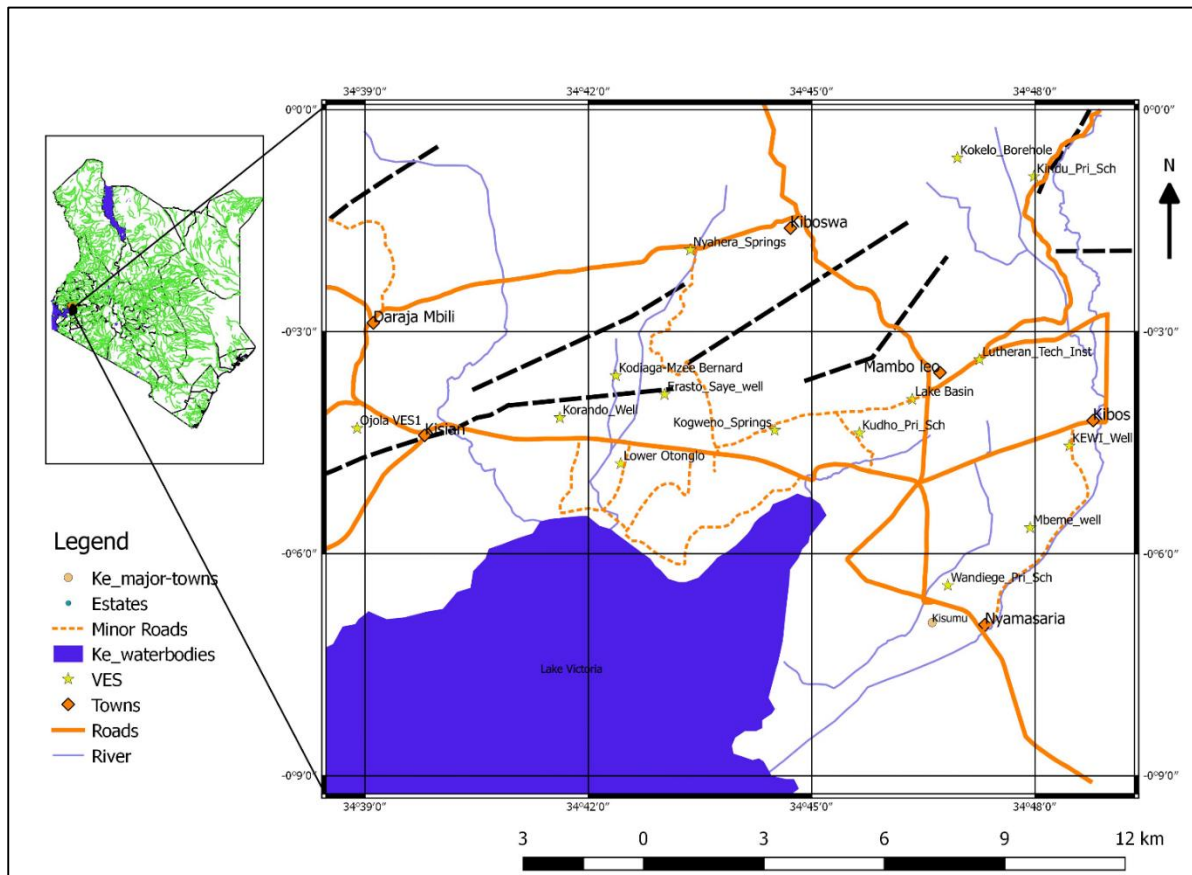
Figure 4.7. Location of VES sites in Kisumu

75

All the VES soundings have characteristics curves with low resistivity plateaus indicative of fresh groundwater (or wet clay) apart from Kindu and Kokelo sites located within granite and Kudho and Lutheran located within phonolite, *Figure 4.8*.
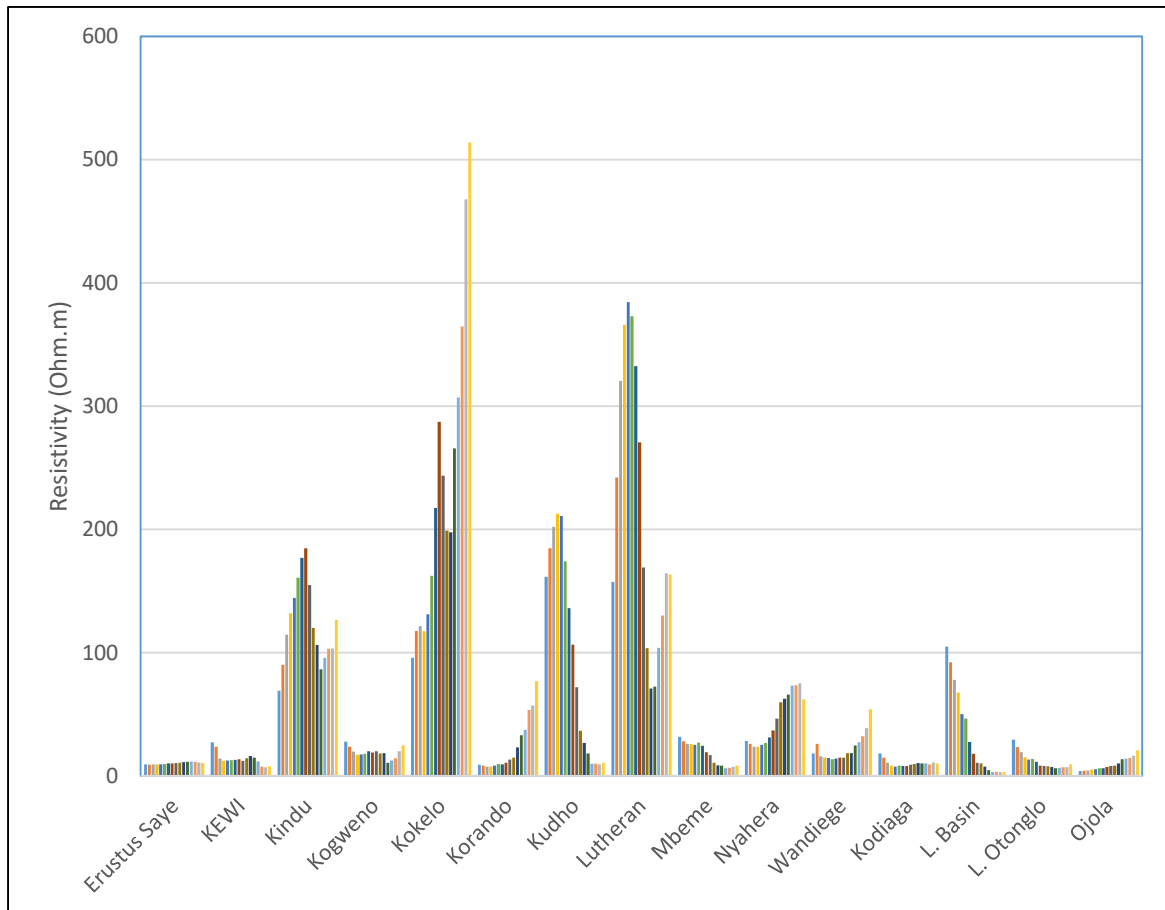
Figure 4.8. Fifteen VES sites in Kisumu. The resistivity values are typical of alluvium and weathered rocks, apart from the Kindu, Kokelo, Kudho and Lutheran sites, that have hard rock high resistivity signals.

The detailed interpretation of the VES data where piezometers were installed is presented in the sub-headings below. The VES signal interpretation used the standard resistivity reference values of materials by Hunt (2005), *Table 4.5*. The vertical rock strata below the VES sites were interpreted using the common resistivity values for various rocks and confirmed by geologs during the drilling of the piezometers.

Table 4.5. Standard resistivity value of materials. These values were derived from Geotechnical Engineering Investigation Handbook by Roy Hunt (Hunt, 2005)

Material	Resistivity (Ohm.m)
Clay soils; wet to moist	1.5 to 3.0
Silty clay and silty soils; wet to moist	3 .0 to 15.0
Silty and sandy soils; moist to dry	15.0 to 150.0
Bedrock; well fractured to slightly fractured with moist soil-filled cracks	150.0 to 300.0
Sand and gravel with silt	About 300.0
Sand and gravel with silt layers	300.0 to 2400.0
Bedrock; slightly fractured with dry soil-filled cracks rock	300.0 to 2400.0
Sand and gravel deposits: coarse and dry deposits	> 2400.0
Bedrock; massive and hard rocks	>2400.0
Freshwater	20.0 to 60.0
Seawater	0.18 to 0.24

Kudho site

The results of the geo-electric model, *Figure 4.9,* indicated the presence of a soil profile up to a depth of 1.2 meters. Laterites underlay this layer from a depth of 0.5 to 3.8 meters, indicating some permeable zones within its matrix. The moist sandy clay that formed the first aquifer was encountered at a depth between 3.8 and 24 meters. However, predicting the yield from this lithology was uncertain due to suspected clay particles in the matrix.
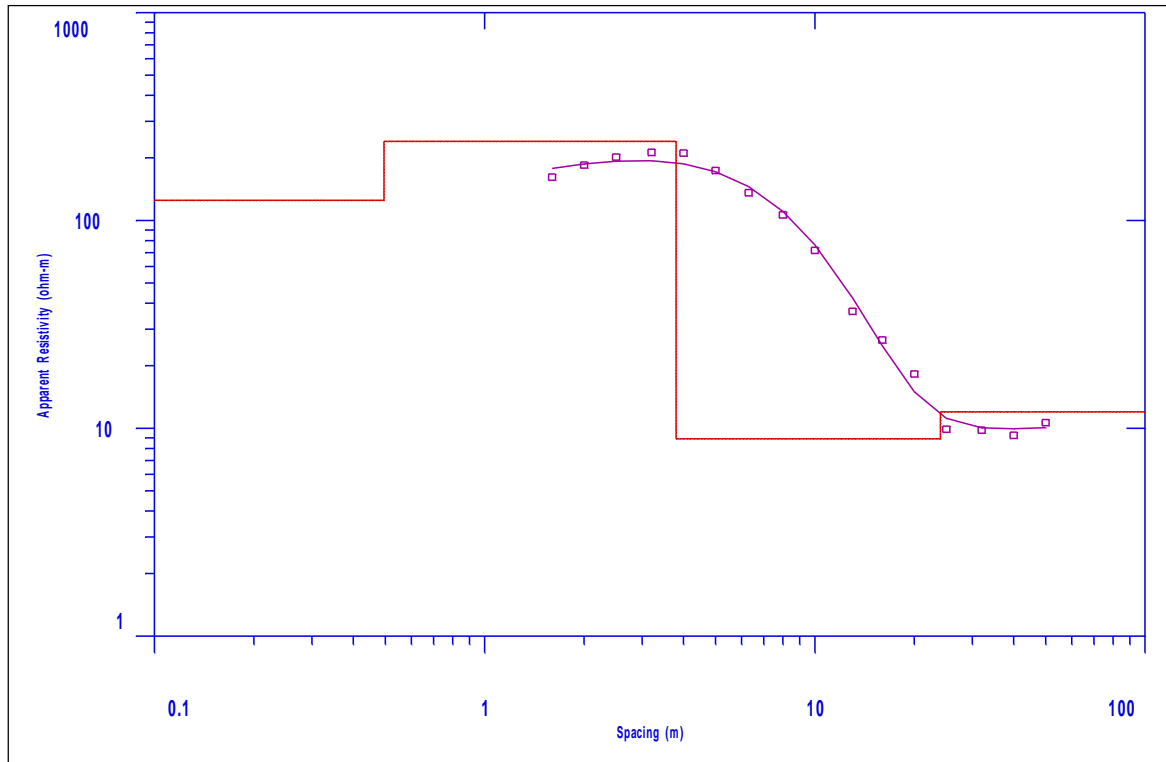
Depth (m)	Resistivity (Ohm.m)	Interpretation	Aquiferous?
0.0 – 0.5	125.0	Clayey topsoil	No
0.5 – 3.8	240.0	Pleistocene sediments (laterite)	No
3.8 – 24.0	8.9	Sandy clay	Yes, but uncertain yields
>24.0	12.0	Fine sands	Yes,(?)

Figure 4.9. Vertical Electrical Sounding (VES) for Kudho Primary School. It was interpreted as a four-layer profile consisting of a high resistivity top layer and low resistivity layer between 3.8 meters to 24.0 meters.

The basal layer geologically comprised of fine sands that occurred up to a depth of 24.0 meters. The texture of these sands indicated permeable zones and hence a good aquifer. Consequently, drilling of a monitoring well was recommended to a depth of 40.0 meters. The geoelectric model matched well with the geo-logs gathered during drilling, but the high yielding aquifer predicted at 24.0 meters was not encountered. The shallow aquifer was encountered between 2.0 and 5.0 meters from the surface during drilling, *Table 4.6.*

Table 4.6. Kudho site geologs collected during drilling of the piezometer. The shallow aquifer was encountered at 4 m below the ground surface.

Depth (m)	Lithological descriptions
0.0 – 2.0	Topsoil consisting of brown laterite
2.0 – 5.0	Brown coloured laterite (aquiferous) mixed with clay (mudstone)
5.0 – 7.5	Pebble sized brown coloured sands mixed with laterite
7.5 – 9.0	Silty clay
9.0 – 12.5	Brown colour gravel mixed with laterite
12.5 – 15.0	Medium-grained dark brown wet laterite with clay (slightly plastic)
15.0 – 20.0	Weathered phonolite
20.0 – 30.0	Dark grey fresh phonolite
30.0 – 3 5.0	Baked phonolite
35.0 – 40.0	Fresh rock, phonolite

The aquiferous layer occurred between 2 and 5 meters, and no other water-bearing layer was encountered. Springs, with similar properties as water in this borehole, occur 100 meters southwards.

Kogweno site

The interpreted geo-electric model, *Figure 4.10*, indicated moist topsoil up to a depth of 1.5 meters. The wet sandy layer underlying the topsoil had a resistivity of 19.5 Ωm. A 10 meters thick layer of clay dominated the site to a depth of 18.4 meters. The resistivity of the clay layer (6.2 Ωm) indicated the presence of minor sandy particles in the matrix, thus making the clays slightly permeable and probably with saline water. The basal layer comprised the laterites. Therefore, drilling of a monitoring well in this site was recommended to a maximum of 35.0 meters.
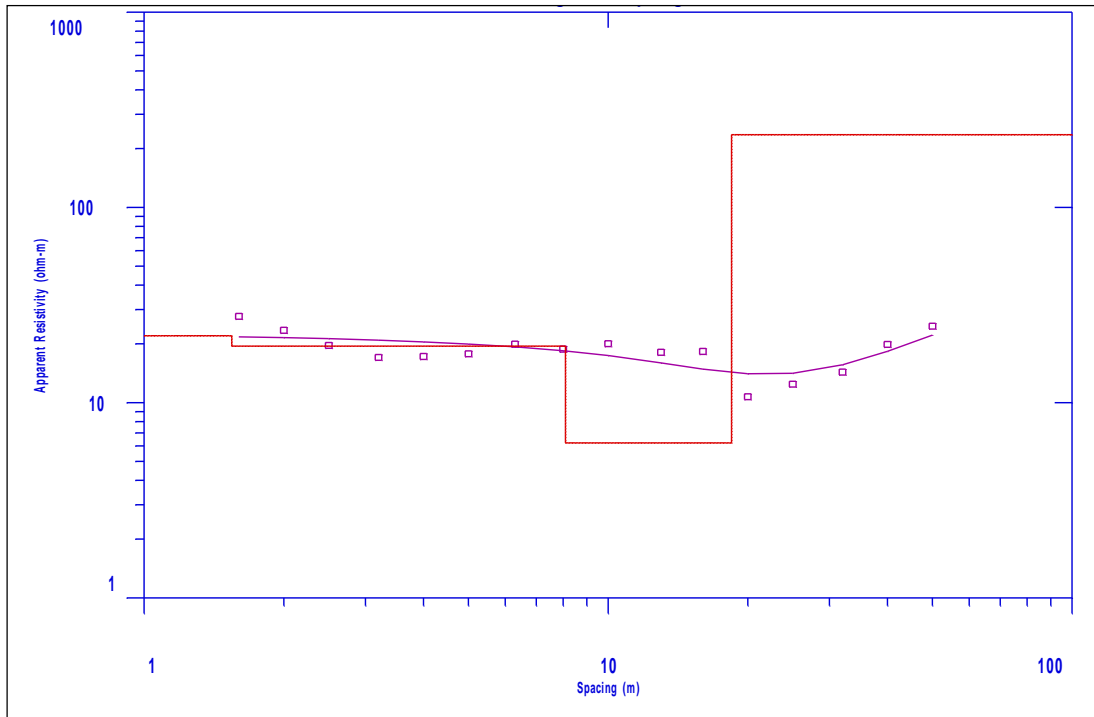
Depth (m)	Resistivity (Ohm.m)	Interpretation	Aquiferous?
0.0 – 1.5	22.0	Moist topsoil	No
1.5 – 8.1	19.5	Moist sands	No
8.1 – 18.4	6.2	Clay with minor sandy particles	Yes, but uncertain yields
>18.4	23.6	Pleistocene Sediments (laterite)	No

Figure 4.10. VES curve and layer model for Kogweno site. VES predicted a shallow aquifer at between 8.0 and 19.0 meters below the ground surface.

The geoelectrical model interpretation in this site was not in conformity with the geo-logs during drilling. The resistivity of the sub-surface layers was low, on average 20 Ohm.m, and was difficult to discriminate. The alternating thin layers of sediments encountered during drilling could be interpreted as episodic alluvium deposited in a changing river channel. A thin, confined aquifer was encountered during drilling at about 34 meters from the surface, *Table 4.7*.

Table 4.7. Kogweno geologs constructed during the drilling of the piezometer. Water was encountered at between 30 and 33 meters below the ground surface.

Depth (m)	Lithological descriptions
0.0 – 2.0	Topsoil
2.0 – 5.0	Wet laterite
5.0 – 10.0	Highly weathered volcanic rock grading into fine sands
10.0 – 11.0	Dark brown sediments
11.0 – 12.0	Losaguta type phonolite
12.0 – 15.0	Slightly weathered phonolite
15.0 – 17.0	Weathered phonolite
17.0 – 20.0	Greyish-brown sediments
20.0 - 22.5	Dark grey phonolite
22.5 – 25.0	Dark grey to black sediments derived from phonolite
25.0 – 27.5	Dark grey to black sediments (aquiferous?)
27.5 – 30.0	Slightly plastic grey-black sediments
30.0 – 33.0	Fractured phonolite (aquiferous)
33.0 – 40.0	Fractured phonolite mixed with volcanic ash (clay)

This was an example of a confined aquifer located within a zone of fractured phonolite, sandwitched between fresh phonolite. The thickness of the aquifer was about three meters.

Erastus Saye site

The interpreted geo-electric model, *Figure 4.11,* indicated moist topsoil reaching a depth of 1.2 meters similar to that of the Kudho site. A sandy clay layer overlaid the topsoil to a depth of 8 meters. This sandy clay layer constituted a minor aquifer. This layer was underlain by fine sands that characterized the site up to a depth ranging from 7.9 to 18.7 meters. A layer of clay dominated the area from a depth of 18.7 to 35.0 meters. Though the layer's resistivity (6.2 Ωm) was low, it indicated minor sandy particle that enhanced permeability. The principal aquifer was encountered from a depth of 35 meters comprising essentially of fine sands. Drilling of monitoring well was therefore recommended to a depth of 50 meters.
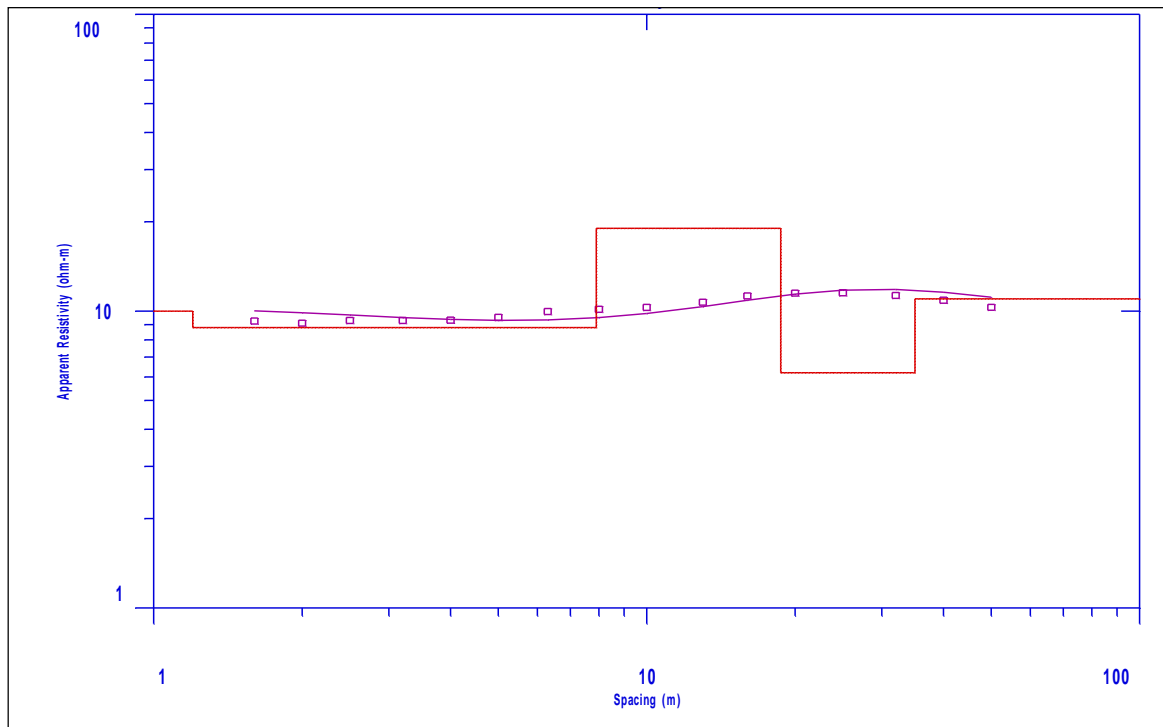
Depth (m)	Resistivity (Ohm.m)	Interpretation	Aquiferous?
0.0 – 1.2	10.0	Moist topsoil	No
1.2 – 7.9	8.8	Sandy clay	Yes, minor
7.9 – 18.7	19.0	Fine sands	Yes
18.7 – 35.0	6.2	Clay with minor clay particles	Yes, but uncertain yields
>35.0	11.0	Sandy clay	Yes

Figure 4.11. The Vertical Electrical Sounding model of Erastus Saye Site. The site is located in Otonglo, 2 km northwest of Kisumu International Airport.

The VES model and the geologs obtained during drilling matched. The shallow aquifer was encountered at a depth greater than 35 meters, *Table 4.8*.

Table 4.8. Erastus Saye site lithological description from the drilling geologs collected during drilling of the piezometer

Depth (m)	Lithological descriptions
0.0 – 2.0	Topsoil consisting of dark brown clay
2.0 – 7.5	Lateritic horizon
7.5 – 10.0	Laterite mixed with phonolite
10.0 – 12.5	Relatively fresh phonolite
12.5 – 15.0	Greenish moderately weathered phonolite mixed with laterite
15.0 – 17.5	Clayey laterite mixed with gravel
17.5 – 20.0	Laterite
20.0 – 25.0	Weathered laterite
25.0 – 30.0	Clayey laterite
30.0 – 35.0	Highly weathered phonolite mixed with clayey laterite
35.0 – 40.0	Gravelly material
40.0 – 50.0	Very wet clay
50.0 – 55.0	Fractured phonolite mixed with gravelly laterite (aquiferous)
55.0 – 60.0	Fresh phonolite

The aquiferous layer was encountered between 50.0 and 55.0 meters and was defined by fractured phonolite mixed with gravelly laterite.

Wandiege primary school site

The interpreted geo-electric model, *Figure 4.12*, indicated moist topsoil to a depth of 1.1 meters. The topsoil layer was composed of sandy clay encountered at a shallow depth of about 5.6 meters. The basal layer comprised of laterite. Consequently, drilling of a monitoring well was recommended to a depth of about 35.0 meters.
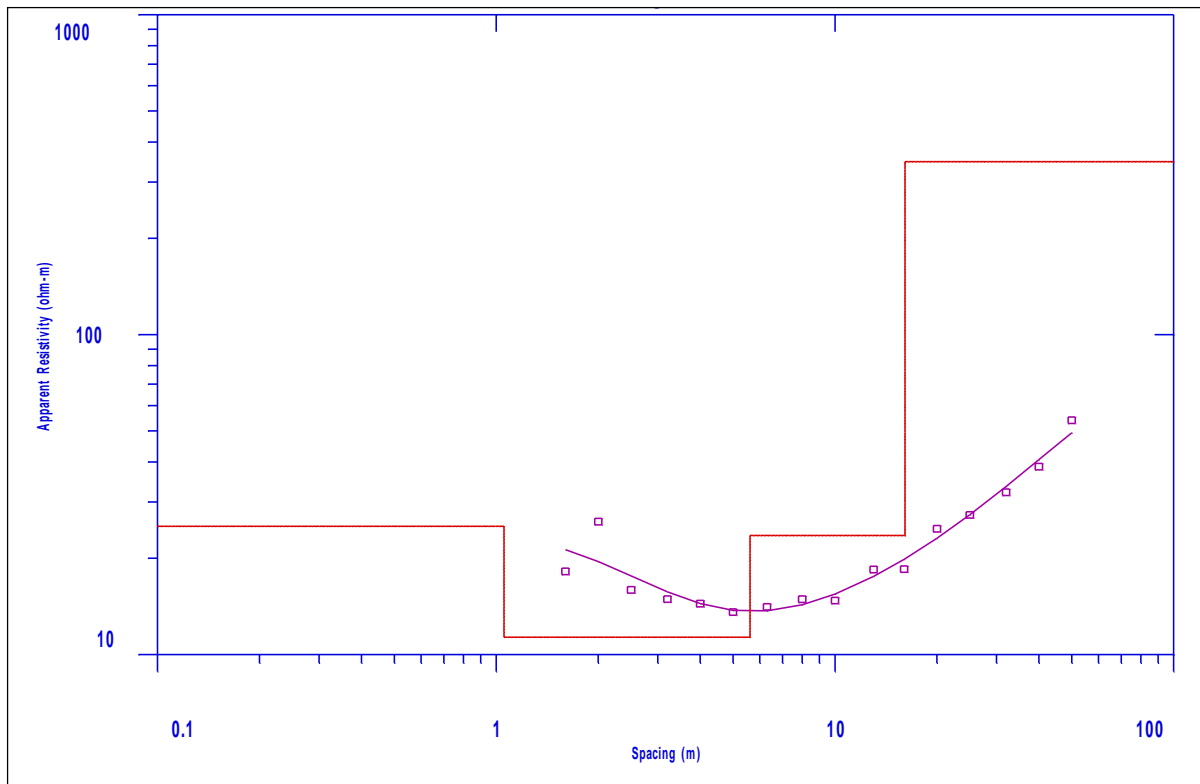
Depth (m)	Resistivity (Ohm.m)	Interpretation	Aquiferous?
0.0 – 1.1	25.2	Moist topsoil	No
1.1 – 5.6	11.3	Sandy clay	No
5.6 – 16.1	23.6	Fine sands	Yes
>16.1	347.2	Pleistocene Sediments (laterite)	Yes

Figure 4.12. Vertical Electrical Sounding model of Wandiege site. The site is located near Nyamasaria in the Manyatta estate.

The geoelectrical model and the geologs in this site did not match, and the borehole drilled was dry. Phonolite was encountered from shallow depths up to the maximum drilled depth of 10 meters, *Table 4.9*. The resistivity values for Wandiege were low, ranging from a maximum of 54.0 Ohm.m to a minimum of 14.9 Ohm.m. These resistivity signals are for fresh groundwater.

Table 4.9. Wandiege geologs are indicating the lithology encountered during drilling. No aquiferous formation was encountered in this site during drilling.

Depth (m)	Lithological descriptions
0 .0– 2.5	Topsoil consisting of coarse-grained, brown sand mixed with laterite and pebbles
2.5 – 5.0	Fairly fresh phonolite
5.0 – 10.0	Grey fresh phonolite
10.0 – 12.5	Grey rock (phonolite)
12.5 – 22.5	Brownish grey weathered rock (phonolite)
22.5 – 25.0	A rock that reacts with HCl (carbonatite?)
25.0 – 40.0	A dark grey rock that is slightly moist (phonolite)

The dry well is located on a massive volcanic rock (phonolite) from the surface up to the maximum drilled depth of 40.0 meters. Groundwater in this locality could occur at greater depth as indicated by the Wandiege borehole (120.0 meters depth) located about 100 meters from this site.

Mbeme site

The interpreted geo-electric model, *Figure 4.13*, indicated moist topsoil reaching a depth of 1.1 meters similar to that of the Wandiege site. Sandy clay underlay the topsoil to a depth of 5.6 meters. Below the sandy clays, a layer of thick wet clay characterized the site up to a depth of 23.8 meters. This layer was interpreted as largely impervious due to the persistence of the clay particles. However, the basal layer, which constituted the major aquifer, was composed of fine sands from a depth of about 24.0 meters. Drilling of monitoring well was recommended to a depth of 50.0 meters.
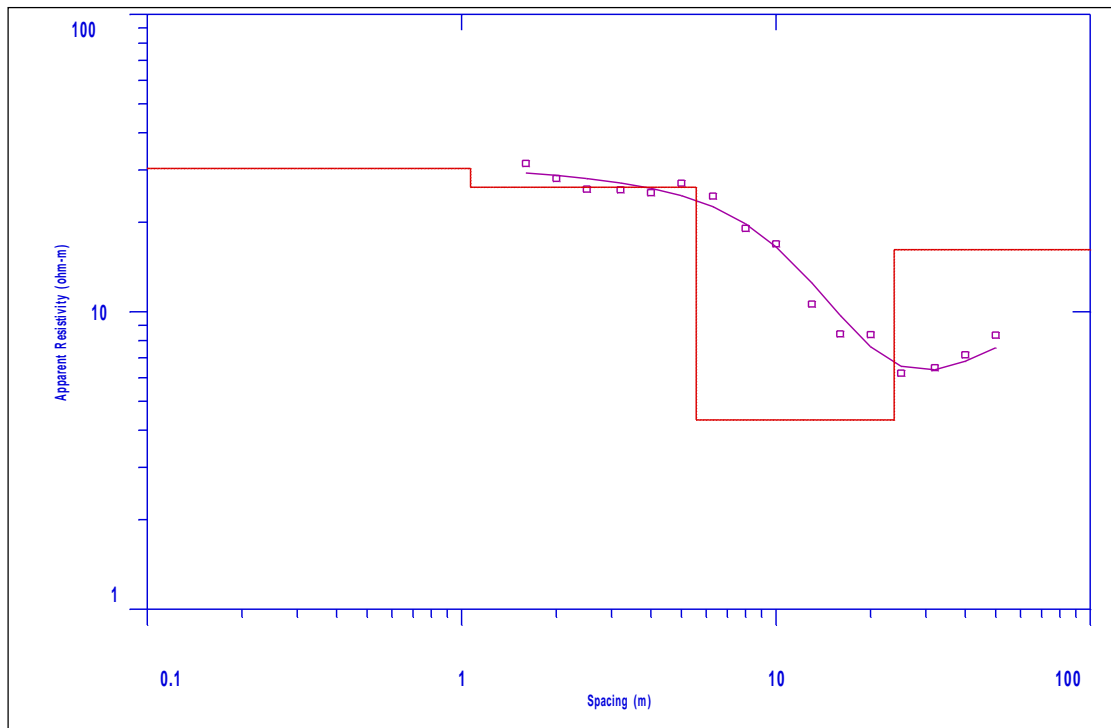
Depth (m)	Resistivity (Ohm.m)	Interpretation	Aquiferous?
0.0 – 1.1	30.3	Moist topsoil	No
1.1 – 5.6	26.2	Sandy clay	No
5.6 – 23.8	4.3	Clay	No
>23.8	16.2	Gravelly sands	Yes

Figure 4.13. The VES model of Mbeme Site. The model predicted a shallow water table at about 24.0 meters

The VES model matched well with the geologs, *Table 4.10* and water was encountered in the gravelly sandy deposits at 29 meters. The yield of this borehole (2 m^3/hour) was good enough to sustain the households in its vicinity.

Table 4.10. Mbeme geolog acquired during drilling. The geo-logs matched well with the VES interpretation in Figure 4.11.

Depth (m)	Lithological descriptions
0.0 – 2.0	Topsoil, grey
2.0 – 5.0	Very consolidated clay (mudstone)
5.0 – 9.0	Clayey fine silts
9.0 – 10.0	Very coarse-grained dark brown wet sandy deposits (slightly plastic)
10.0 – 11.0	Medium-grained dark brown wet sandy deposits (slightly plastic)
11.0 – 20.0	Slightly plastic orange-brown gravelly sands
20.0 – 22.5	Brown sandy clay
22.5 – 25.0	Light cream silt
25.0 – 35.0	Gravelly sandy sediments (aquiferous)
35.0 – 40.0	Fresh phonolite

Lake Basin site

The interpreted geo-electric model, *Figure 4.14*, indicated moist topsoil reaching a depth of 1.9 meters. The sandy clay underlay the topsoil to a depth of about 7.7 meters, which constituted a minor aquifer. The sandy clays were underlain by a very thick layer of wet clay that characterized the site to a depth ranging from 7.7 to 42.6 meters. This layer was largely impervious, impeding direct vertical recharge. The principal aquifer was encountered at a depth of about 43.0 meters and comprised mainly of coarse sands. Therefore, drilling of a monitoring well was recommended to a depth of 40.0 meters.
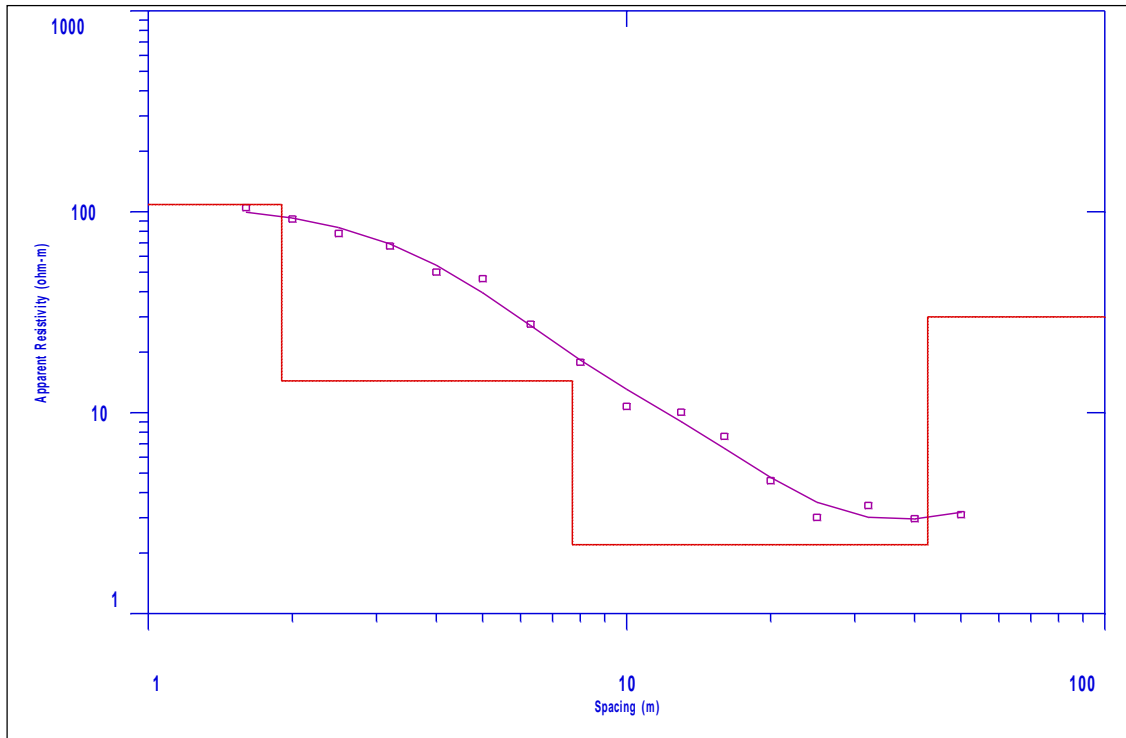
Depth (m)	Resistivity (Ohm.m)	Interpretation	Aquiferous?
0.0 – 1.9	108.6	Moist topsoil	No
1.9 – 7.7	14.4	Sandy clay	Yes, minor
7.7 – 42.6	2.2	Heavy clay	No
> 42.6	30.0	Coarse sands	Yes

Figure 4.14. VES model of Lake Basin Site. The site is located within the Lake Basin Mall, near the Mamboleo estate

The VES model interpretation at this site matched the geological logs during drilling. The heavy clay predicted to occur between 7.7 and 42.6 meters was encountered during drilling, and the drilling bit was trapped in it several times. Drilling up to 60.0 meters yielded no water. At this depth, thick wet clay was probably were mistaken for freshwater during interpretation of the VES signal. A systematic description of the well geological logs collected during the drilling process is given below, *Table 4.11*.

Table 4.11. Lake Basin lithological description from the drilling geologs.

Depth Interval (m)	Lithological descriptions
0.0 – 5.0	Topsoils: orange-brown, coarse-grained laterite mixed with clay.
5.0 – 10.0	Light brown clays mixed with laterite
10.0 – 11.0	Vey coarse-grained, brown sandy sediments mixed with gravel
11.0- 20.0	Brown sediments mixed with clays and laterite
20.0 – 22.0	Brown sandy sediments (medium-grained)
22.0 – 35.0	Clayey laterite
35.0 – 60.0	Brown compacted clay

This site was located on deep sediments and probably on a geosyncline (Mboya, 1983).

4.1.4.2   *Geophysical survey interpretation for Mt. Elgon study site*

Vertical electrical sounding was carried out in a broad Mt. Elgon aquifer during IGAD sponsored geophysical survey. The site selected for VES probing extended from Kiminini to the south, Kitale to the east, Kwanza to the North and Suam. The site chosen covered the Neo-Proterozoic metamorphic rocks and the Tertiary Mt. Elgon volcanic rocks. The profiles were oriented north-south, and the electrode spacing was 500 meters on either side. The configuration allowed for a maximum of about 333.3 meters of depth probing. The location of the sites, *Figure 4.15*, was based on available cut lines or uncultivated grounds that extended 500 meters on either side from the terrameter. A total of 20 vertical profiles were done, and results are presented in the combined plot, *Figure 4.16*.
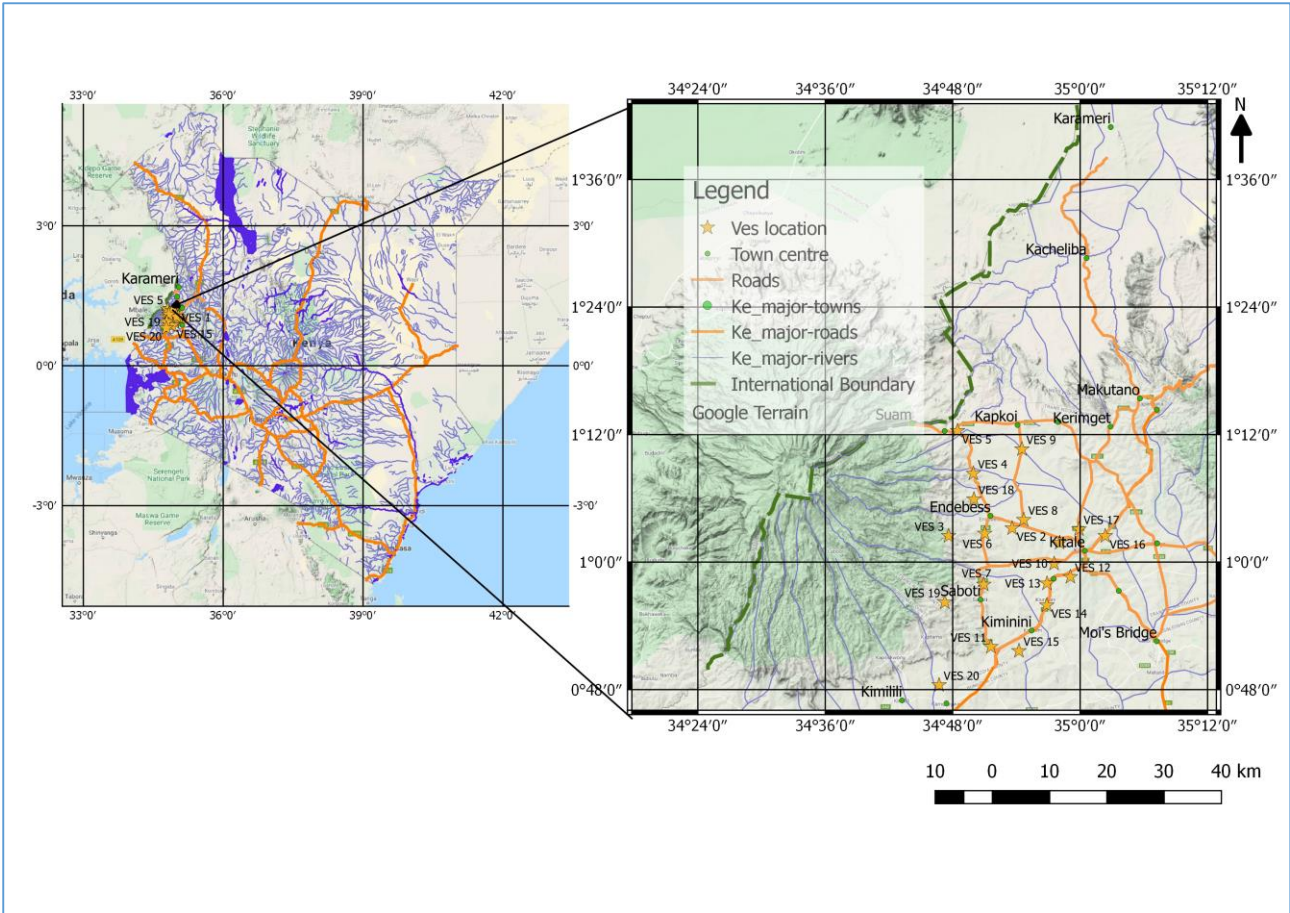
Figure 4.15. Location of VES sites in the Mt. Elgon study area

The combined plot for the 20 electrical soundings, *Figure 4.16*, clearly distinguishes the volcanic rock and metamorphic rock terrains. Low resistivity values are a signal of groundwater occurrence, while the high resistivity values are typical of hard, fresh rocks.
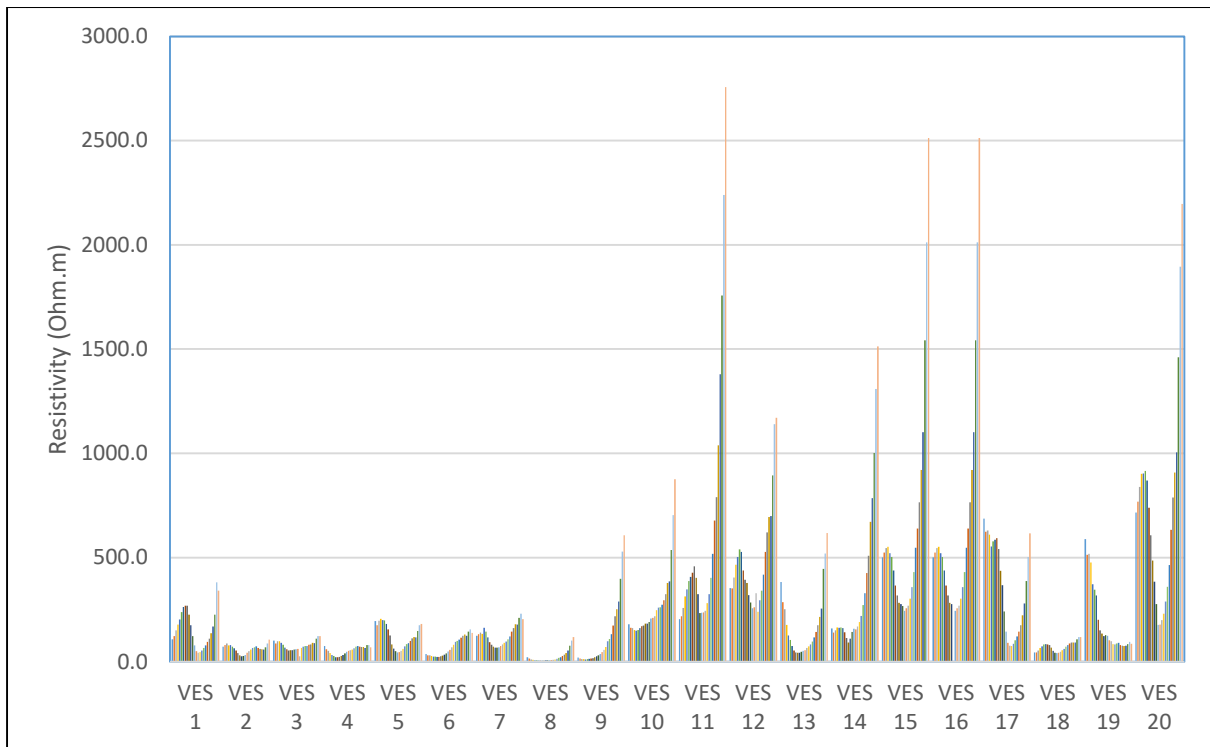
Figure 4.16. A comparative plot of the twenty profiles from Mt. Elgon. VES 1 to 9 are within the volcanic while VES 10 to 20 are within the metamorphic rocks.

A few selected VES are interpreted and shown below. These were chosen to demonstrate groundwater in the volcanic contact of volcanic and metamorphic rocks and within the metamorphic rocks.

VES 1

VES 1 was located near Kitale town, within the alluvium. The interpreted geo-electric model, *Figure 4.17*, indicated moist topsoil reaching a depth of 2.4 meters. The sandy clay underlay the topsoil to a depth of about 31.7 meters. This constituted the principal aquifer. The sandy clays were underlain by fresh bedrock consisting of metamorphic rocks. The high resistivity values of over 6000 Ω.m implied that this layer was largely impervious, impeding direct vertical recharge from the rainwater. It is unlikely that this layer is weathered.
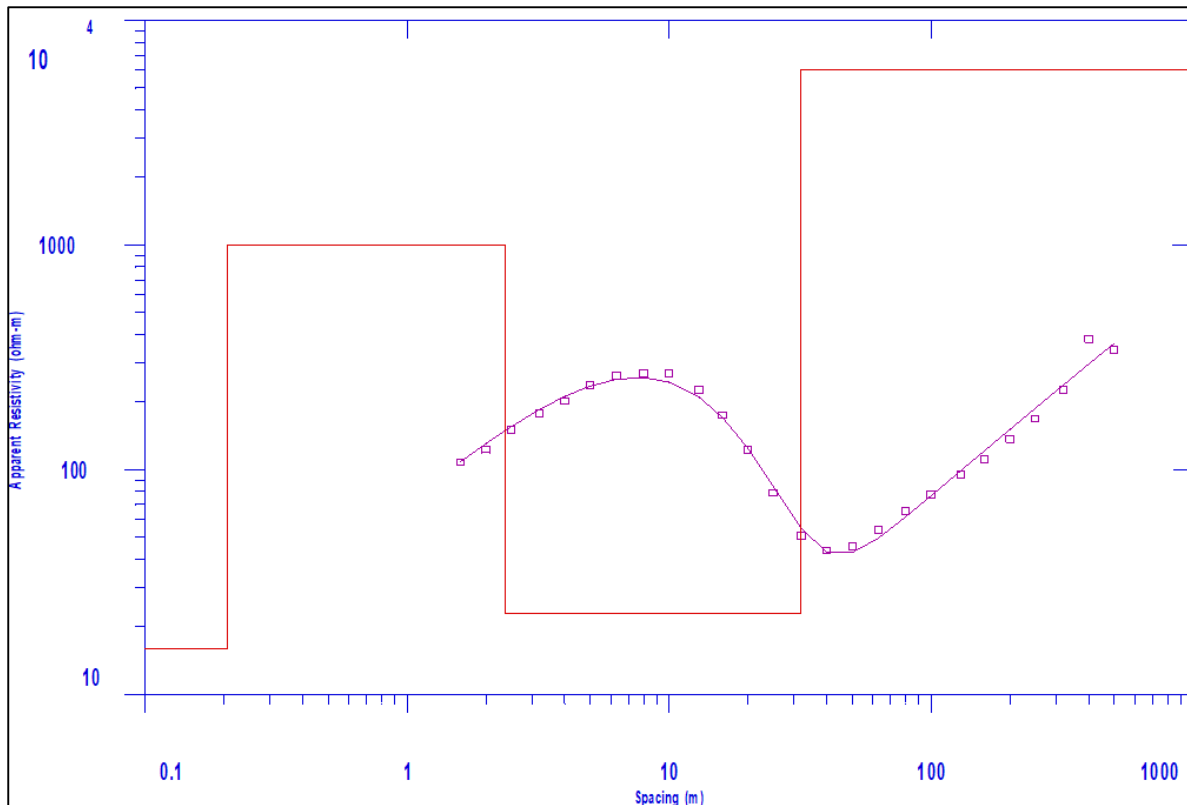
Depth	Resistivity Ohm.m	Interpretation	Aquiferous?
0.2	15.98	Moist topsoil overlying sandy clay	No
2.4	997.51	Sand and gravel with silt	No
31.7	22.99	Wet and moist silty sand	Yes
>31.7	6011.40	Fresh rock (gneiss)	No

Figure 4.17. Interpretation VES 1 near the contact of volcanic rocks and metamorphic rocks near Kitale, located in a floodplain

VES 3

The profile is located within the Mt. Elgon forest reserve near the Kenya Wildlife Services (KWS) entry gate into the game reserve. The surface geology consists of basaltic and agglomeritic volcanic tuffs. The interpreted geo-electric model, *Figure 4.18*, indicated dry topsoil composed of volcanic ash and debris, reaching a depth of 2.4 meters. The unconsolidated agglomerate underlies the top volcanic ash to a depth of about 26.0 meters. This layer constituted the principal aquifer. The aquiferous layer was underlain by a very thick wet agglomeritic tuffaceous layer intercalated with clay that characterized the site to a depth of 171 meters. Beyond 171 meters, the site was composed of fractured basalt.
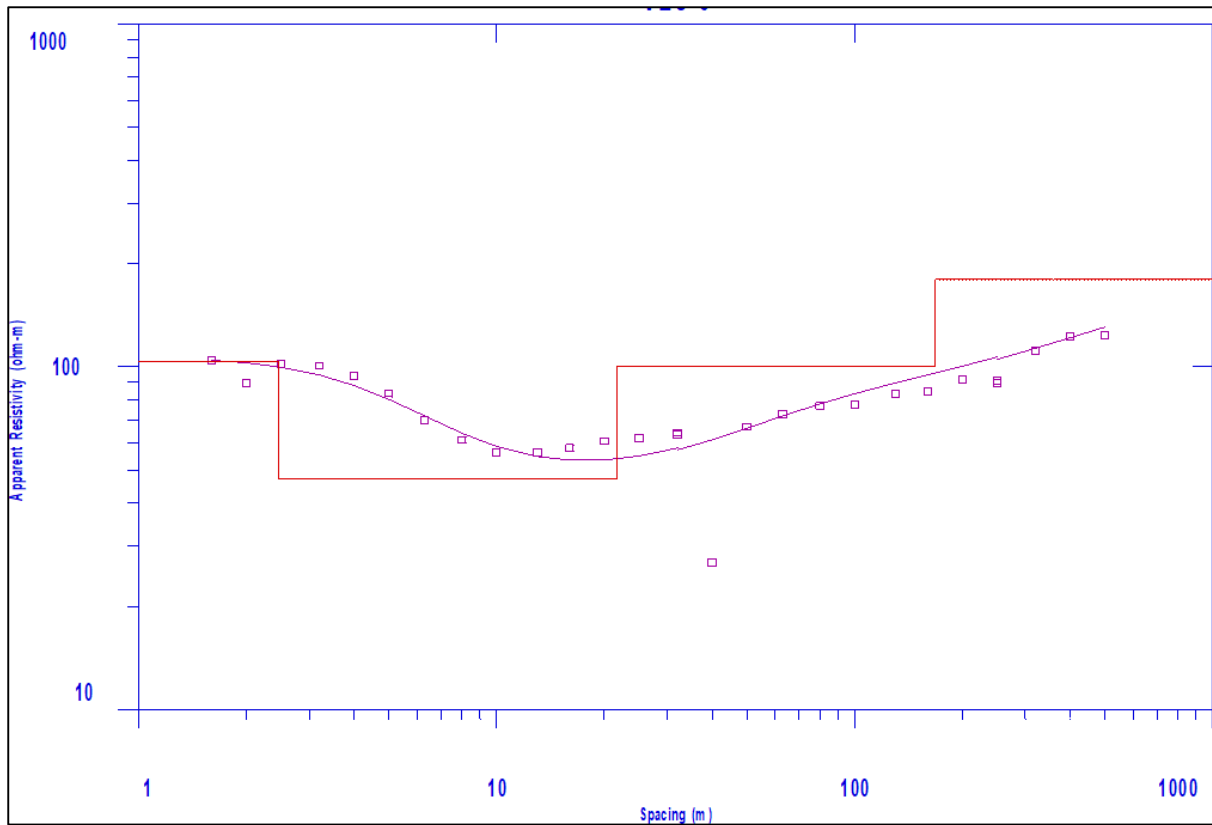
Depth	Resistivity Ohm.m	Interpretation	Aquiferous?
2.4	102.54	Agglomerate and volcanic tuff (dry)	No
26.0	49.38	Wet volcanic ash and pyroclastic	Yes
171.4	89.80	Wet agglomerate and volcanic tuff	No
>171.4	187.23	Fractured basalt	No

Figure 4.18. Interpretation of VES 3 located within the volcanic rocks near the KWS gate

VES 4

The profile was located near Endebess at the contact between the volcanic rocks and the metamorphic rocks. The interpreted geo-electric model, *Figure 4.19*, indicated a dry top, sandy soil reaching a depth of 3.8 meters. Sandy clay underlies the top, sandy, silty soil to a depth of about 23.0 meters, which constituted a minor aquifer. In turn, the sandy, silty soil was underlain by a very thick layer of clayey agglomerate that characterized the site to a depth ranging from 23.0 to 40.0 meters. This layer was largely pervious, allowing direct vertical recharge. This layer overlies a fractured basaltic layer that constitutes the main aquifer.
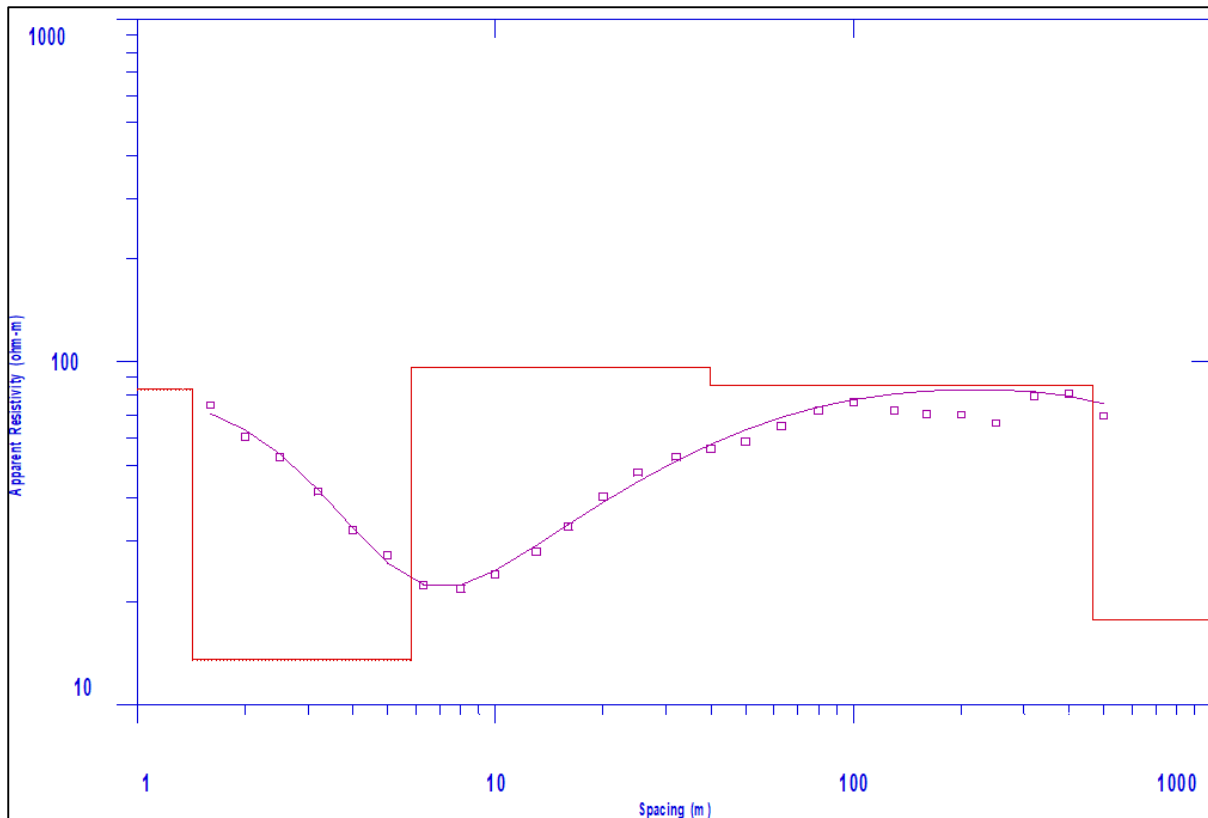
Depth	Resistivity (Ohm.m)	Interpretation	Aquiferous?
1.4	83.05	Dry sandy soil	No
5.8	13.50	Wet sandy, silty soil	Yes
39.7	96.69	Clayey agglomerate	No
466.1	85.43	Fractured basalt/phonolite	Yes? But low yielding perched aquifer
>466.1	17.61	Regolith and fractured bedrock	Yes

Figure 4.19. Interpretation of VES 4 located in Endebess near the contacts between agglomerate and metamorphic rocks

VES 6

The interpreted geo-electric model, *Figure 4.20*, indicated a dry top, sandy soil reaching a depth of 2.3 meters. Sandy silty soils underlie the top, sandy soil to a depth of about 8.3 meters, which constituted the main aquifer. The silty sand soils were underlain by a thick layer of fractured clayey agglomeritic basalt that characterized the site to a depth of 26.0 meters. Beyond 26 meters, the site consists of fractured basalts with clay-filled fractures. The site probably has a deeper aquifer beyond 300 m, indicated by the change of the resistivity curve.
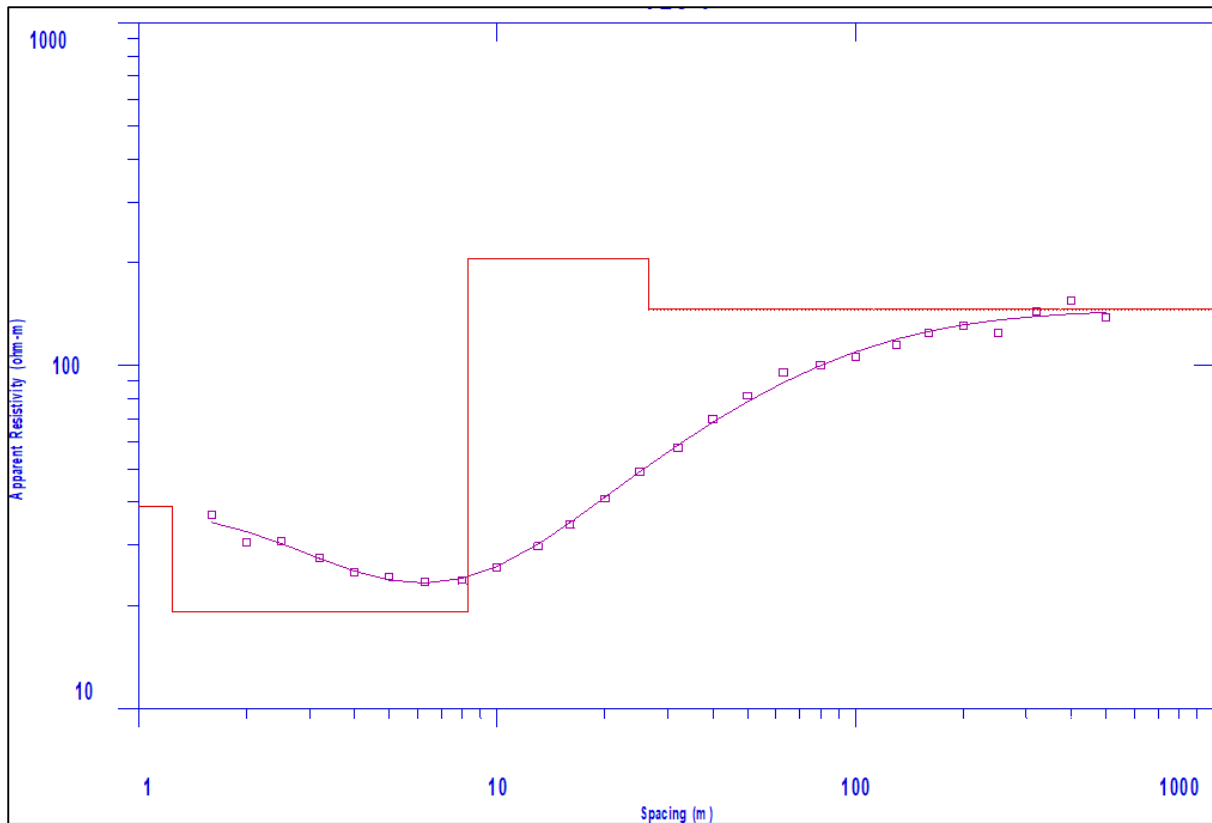
Depth	Resistivity (Ohm.m)	Interpretation	Aquiferous
1.2	38.77	Dry sand soil	No
8.3	19.15	Wet sandy clay soil	Yes
26.6	205.77	Fractured rock (agglomerate) filled with sandy particles	No
>26.6	145.89	Fractured clayey bedrock	Yes

Figure 4.20. VES6 interpretation located within ADC farm and Kenya seeds near Endebess.

VES 9

The VES was located within metamorphic rocks. The interpreted geo-electric model, *Figure 4.21*, indicated a dry top, sandy soil reaching a depth of 5.3 meters. Sandy clay underlies the topsoil to a depth of about 20.0 meters, which constituted the main aquifer. Beneath the sandy clay is a very thick layer of clayey sandy regolith that characterized the site to a depth of 130.0 meters. This layer was largely impervious, impeding direct vertical recharge of rainwater. A fresh metamorphic rock formed the bedrock beyond 130 meters.
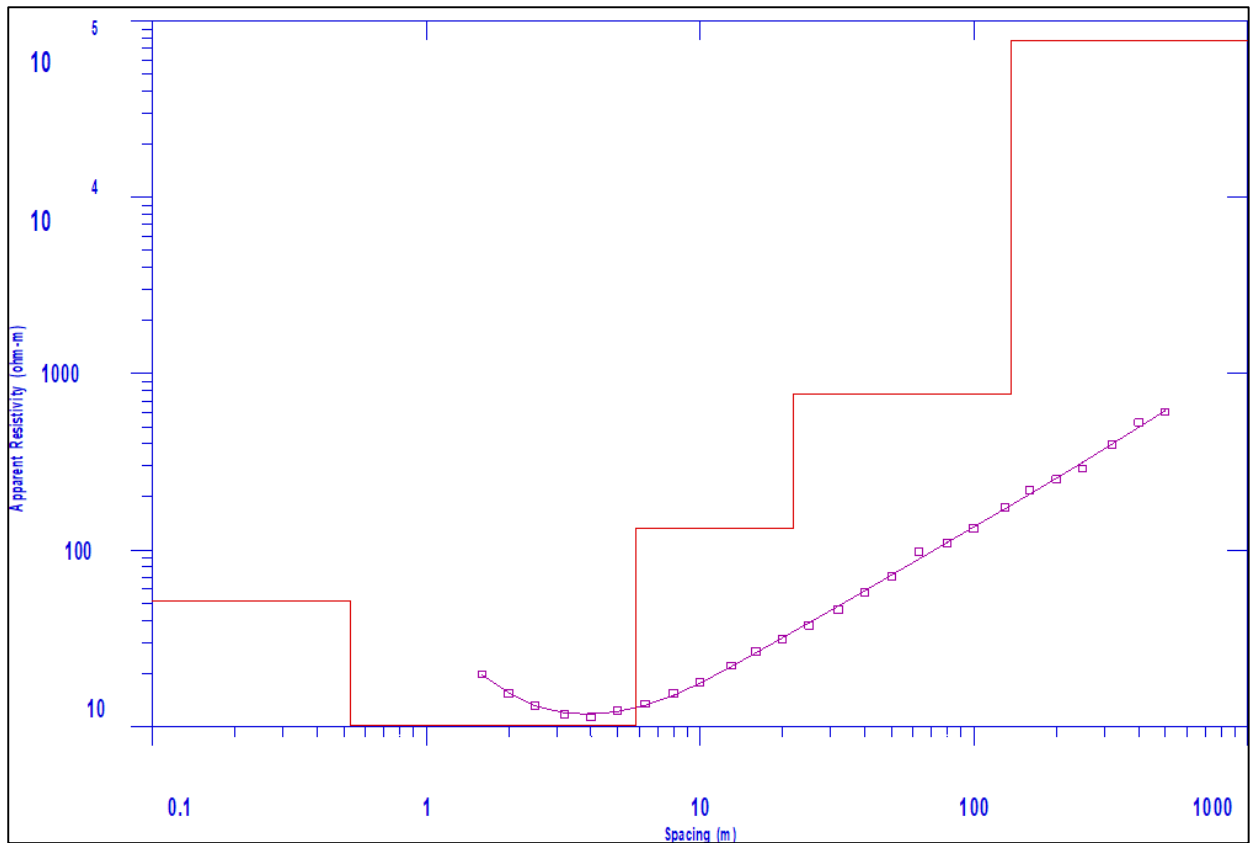
Depth	Resistivity (Ohm.m)	Interpretation	Aquiferous
0.53	51.35	Dry sandy soil	No
5.84	10.21	The wet clayey sandy layer	Yes
21.96	133.57	Wet clayey weathered regolith	No
137.36	763.30	Dry regolith	No
>137.36	77713.00	Fresh metamorphic rock	No

Figure 4.21. Interpretation of VES 9 located in Kapkoi within the metamorphic rocks

VES 16

The interpreted geo-electric model, *Figure 4.22*, indicated a dry silt-filled fractured rock reaching a depth of 3.0 meters. Fresh rock underlay this layer to a depth of about 6.0 meters. A fractured agglomeritic rock is present between 6.0 and 28.0 meters. This constituted the principal aquifer. Fresh impervious agglomeritic layer occurred beyond 28 meters.

96
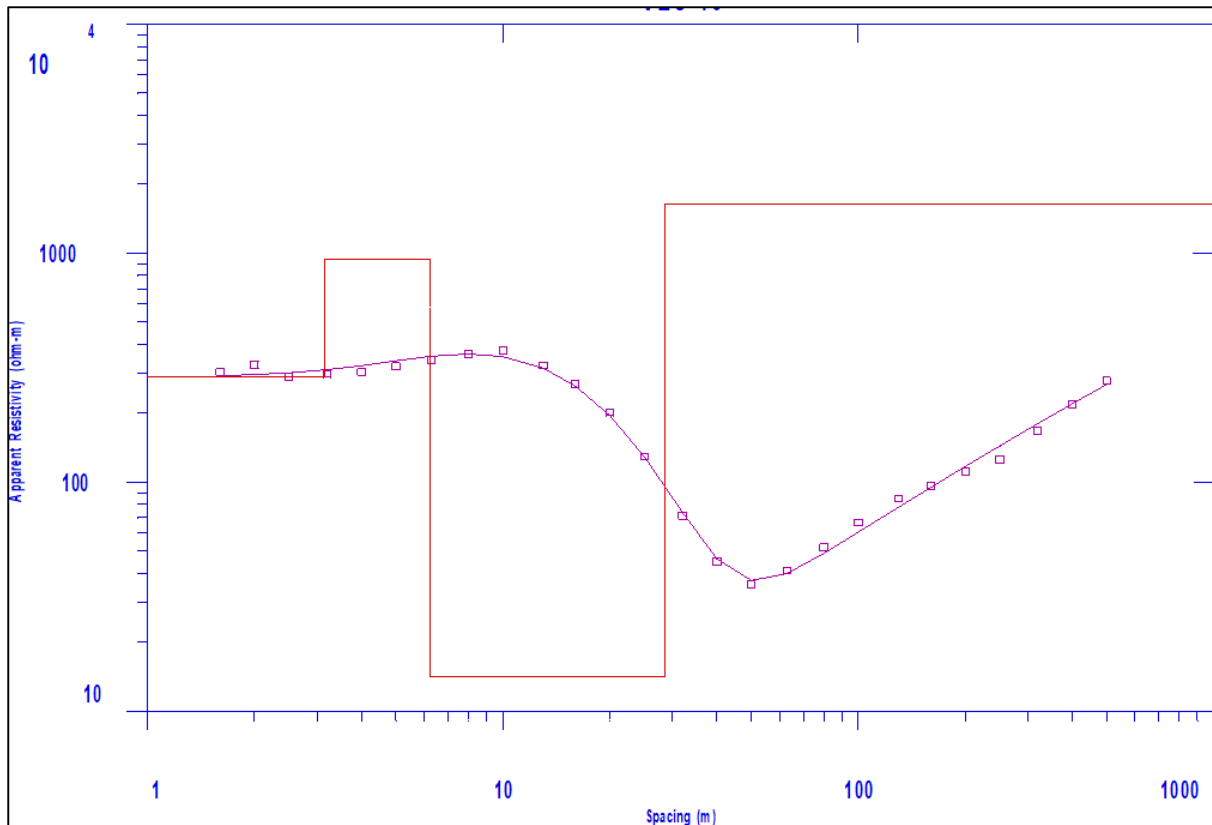
Depth	Resistivity (Ohm.m)	Interpretation	Aquiferous
3.15	288.30	Dry silty agglomerate	No
6.24	936.74	Fresh agglomeritic phonolite	No
28.65	14.20	Fractured agglomeritic phonolite	Yes
>28.65	1645.60	Fresh agglomeritic phonolite	No

Figure 4.22. VES 16 interpretation of geoelectric sounding located within agglomeritic phonolite volcanic rocks

4.1.5   Aquifer properties and characteristics from the pumping test

This sub-section discusses the results of pumping tests on the five boreholes drilled in the Kisumu study site and equipped with data loggers, *Figure 4.23*. The results from six borehole completion records from Water Resources Authority Kitale and Kapenguria are also presented for Mount Elgon.

4.1.5.1 Kisumu aquifer

The location of the six piezometers in Kisumu is shown in *Figure 4.23*. Kudho site has two piezometers, one of which was designed to monitor effluent discharge from pit latrines within Kudho primary school.
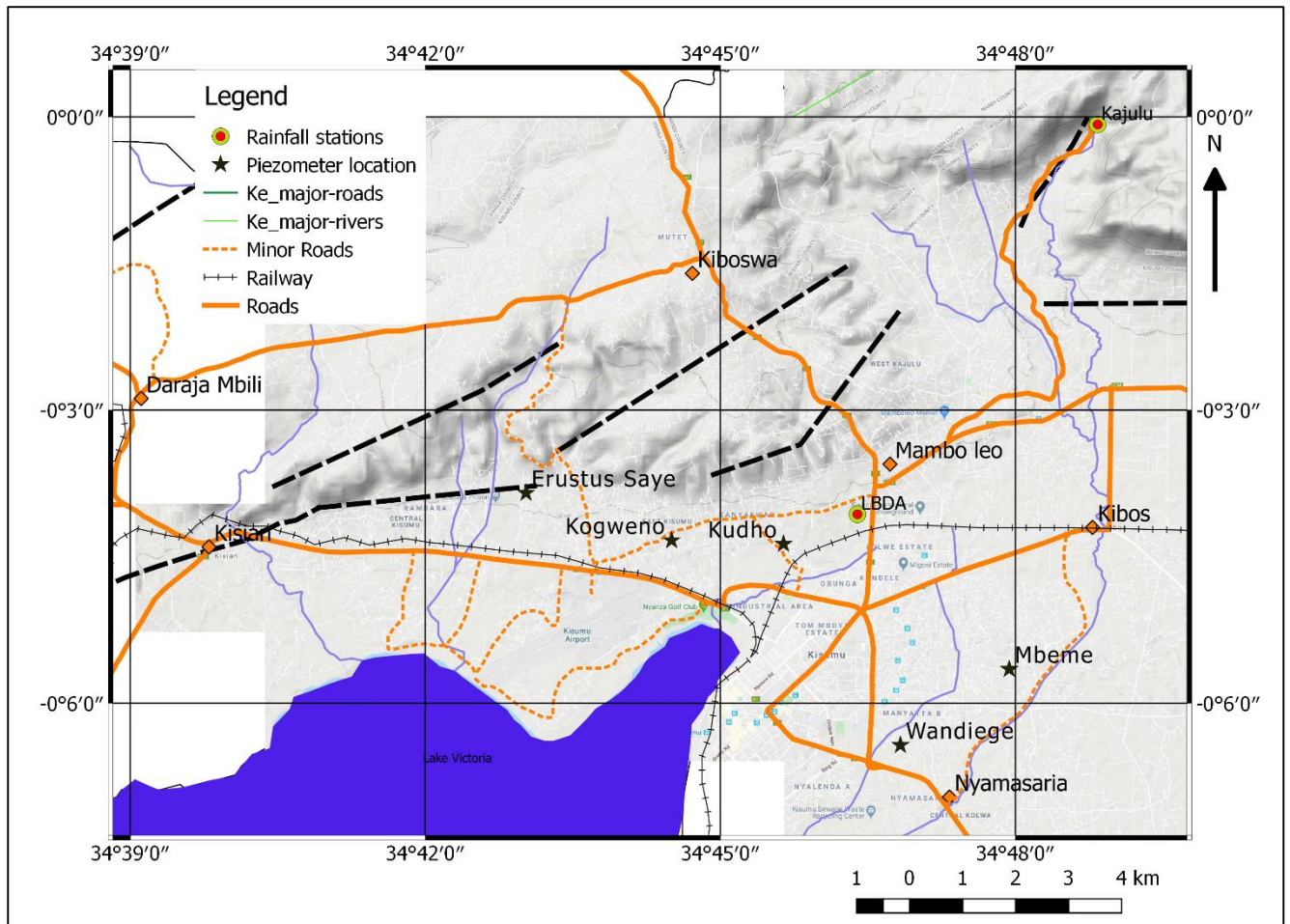
Figure 4.23. The location of the piezometer in Kisumu

A total of six piezometers were drilled from selected sites. The newly drilled boreholes were test pumped using the constant drawdown and recovery test method (Bennett and Patten, 1962; Kruseman and Ridder, 2000; Mishra *et al*., 2012; Richard *et al*., 2016) to characterize and define the optimal pumping capacity of the borehole and determine other aquifer properties.

Approximation of aquifer parameters in Kisumu

The pumping test analysis provides information on hydraulic parameters such as specific capacity, transmissivity, and the yield of boreholes.

Erastus Saye well

The pumping test summary is given in *Table 4.12,* followed by the results of the well characteristics.

Table 4.12. Erastus Saye pumping test summary

Borehole Depth (m)	60.0
Pump Type Used	DS 3-17
Pump setting Depth (m)	45
SWL (m)	2.5
Pumping Water level (m)	40.5
Pumped – discharge capacity (m³/hr)	1.5 (Average Discharge)
Cumulative Drawdown (m)	38.0

Specific capacity

The specific capacity of this borehole was calculated as follows;

$$\text{Discharge per day: } 24\ hours * \frac{1.5m3}{hr} = 36m3/day$$

$$\text{Specific capacity: } \frac{36m3}{day} \div 38m = 0.947\ m2/day$$

Transmissivity of the aquifer

This is the flow rate of water under a unit hydraulic gradient through a cross-section of unit width across the entire saturated section of the aquifer. The Logan formula(Logan, 1964) was used to estimate transmissivity:

$$T = 1.22 * \Delta S$$

Where;

T = Transmissivity (m²/day),

Q = Discharge or yield (m³/day),

ΔS = Change in water level (drawdown per log cycle of time in meters)

The ΔS change in water level (drawdown per log cycle of time in meters) was taken at 10 minutes and 40 minutes which are 17.86 m and 31.24 m, respectively. These values are from the pumping test data. Therefore,

$$\Delta S = 31.24 - 17.86 \text{ m} = 13.38\text{m}$$

Now the T value is determined as follows;

$$T = 1.22 \text{ } Q/\Delta s$$

$$T = (1.22 * 36 \text{ m}^3/\text{day})/13.38 \text{ m} = \textbf{3.28 m}^2\textbf{/day}$$

This value is moderate and suggests that the aquifer is relatively fractured and recharge is fair.

Kogweno borehole

The borehole summary for the Kogweno borehole is shown in *Table 4.13*.

Table 4.13. Kogweno borehole pumping test summary

Borehole Depth (m)	40.0
Pump Type Used	DS 3-17
Pump setting Depth (m)	30.0
SWL (m)	1.5
Pumping Water level (m)	27.8
Pumped – discharge capacity (m³/hr)	0.2 Average Discharge
Cumulative Drawdown (m)	26.3

Specific capacity

The specific capacity of this borehole was calculated as follows;

$$\text{Discharge per day} = 24 \text{ hours} * 0.2\text{m}^3/\text{hr} = 4.8\text{m}^3/\text{day}$$

$$\text{Specific capacity} = (4.8\text{m}^3/\text{day})/26.34 \text{ m} = \textbf{0.182 m}^2\textbf{/day}$$

Transmissivity of the aquifer

The Logan formulae were used to estimate transmissivity.

$$T = 1.22 \text{ } Q/\Delta s \text{ where Q is discharge or yield (m}^3/\text{day), and } \Delta S \text{ is the change in water level (drawdown per log cycle of time in meters).}$$

The change in water level for this borehole (drawdown per log cycle of time in meters) was taken at 10 minutes and 40 minutes. These were 23.70 m and 32.0 m, respectively.

Therefore, ΔS = 32.0 m – 23.7 m = 8.3 m

Therefore,

$$T = (1.22 * 4.8 \text{ m}^3/\text{day})/8.3 \text{ m} = \textbf{0.71 m}^2\textbf{/day}$$

Wandiege borehole

The Wandiege characteristics are summarized in *Table 4.14* and discussed in subsequent sub-headings.

Table 4.14. Wandiege borehole pumping test summary

Borehole Depth (m)	40.0
Pump Type Used	DS 3-17
Pump setting Depth (m)	37.0
SWL (m)	4.0
Pumping Water level (m)	38.0
Pumped –discharge capacity (m³/hr)	0.05 (Average Discharge)
Cumulative Drawdown (m)	34.0

Specific capacity

Discharge per day; 24 hrs * 0.05 m^3/hr = 1.2 m^3/day

Therefore:

Specific capacity = (1.2 m^3/day)/34 m = **0.035 m^2/day**

Transmissivity of the aquifer

Using the Logan formula: T = 1.22 Q/Δs

Q = Discharge or yield (m^3/day), and ΔS is the change in water level (drawdown per log cycle of time in meters). The ΔS was taken at 10 minutes and 40 minutes which are 19.24 m and 34.98 m, respectively. Therefore, ΔS = 34.98 – 19.24 m = 15.74 m

Therefore:

T = (1.22 * 1.2 m^3/day)/15.74 m = **0.093 m^2/day**

Mbeme borehole

Table 4.15 summarizes the pumping test data for the mbeme well, followed by the results of borehole characteristics.

Table 4.15. Mbeme borehole pumping test summary

Borehole Depth (m)	40.0
Pump Type Used	DS 3-17
Pump setting Depth (m)	33.0
SWL (m)	10.4
Pumping Water level (m)	31.5
Pumped –discharge capacity (m³/hr)	2.8 (Average Discharge)
Cumulative Drawdown (m)	21.1

Specific capacity

The specific capacity of this borehole was calculated as follows;

Discharge per day = 24 hours * 2.8 m³/hr = 67.2 m³/day

Therefore

Specific capacity; {67.2 m³/day}/21.1 m = **3.18 m²/day**

Transmissivity of the aquifer

The Logan method was also used to estimate transmissivity in this borehole.

$T = 1.22 \ Q/\Delta s$

Where; T = Transmissivity (m²/day), Q = Discharge or yield (m³/day), and ΔS = change in water level (drawdown per log cycle of time in meters). The ΔS - change in water level (drawdown per log cycle of time in meters) is taken at 10 minutes and 40 minutes which are 16.70 m and 25.80 m, respectively. Therefore, $\Delta S = 25.80 - 16.70 \ m = 9.10 \ m$

Therefore:

$T = (1.22 * 67.2 \ m^3/day)/9.1 \ m =$ **9.01 m²/day**

Kudho borehole

The Kudho borehole characteristics summary are given in *Table 4.16,* and how these characteristics were calculated is discussed in the subsequent section.

Table 4.16. Kudho borehole pumping test summary

Borehole Depth (m)	40.0
Pump Type Used	DS 3-17
Pump setting Depth (m)	39.0
SWL (m)	10.4
Pumping Water level (m)	10.0
Pumped –discharge capacity (m^3/hr)	1.0 Average Discharge
Cumulative Drawdown (m)	37.5

Specific capacity

Discharge per day = 24 hours * 1.0 m^3/hr = 24 m^3/day

Therefore:

Specific capacity; (24m^3/day)/37.50 m = **0.64 m^2/day**

Transmissivity of the aquifer

Based on the Logan formula, T = 1.22 Q/Δs

Where; T = Transmissivity (m^2/day),

Q = Discharge or yield (m^3/day) and ΔS = change in water level (drawdown per log cycle time in meters). The ΔS or change in water level (drawdown per log cycle of time in meters) were taken at 10 minutes and 40 minutes which are 19.40 m and 23.90 m, respectively. Hence, ΔS = 23.90 m – 19.40 m = 4.5 m

Tranmissivity is therefore;

T = (1.22 * 24 m^3/ day)/4.5 m = **3.24 m^2/day**

Table 4.17. Pumping test summary and aquifer characteristics of the five observation boreholes in Kisumu. The sixth well in Kudho was shallow and was not test pumped.

Parameter	unit	Kogweno	E. Saye	Wandiege	Mbeme	Kudho
Borehole depth	m	40.0	60.0	40.0	40.0	40.0
Pump type		DS 3-17	DS 3-17	DS 3-17	DS 3-17	DS 3-17
Depth of pump intake	m	30.0	45.0	37.0	33.0	39.0
Static water level	m	1.5	2.5	4.0	10.4	10.4
Pumping water level	m	27.84	40.5	38.0	31.5	10.0
Discharge	m^3/hr	0.2	3.0	0.05	2.8	1.0
Cumulative draw down	m	26.34	38.0	34.0	21.1	37.5
Specific capacity	m^2/day	0.182	0.947	0.03	3.18	0.64
Transmissivity	m^2/day	0.71	3.28	0.10	9.01	3.24

The pumping test analysis provided information on hydraulic parameters such as specific capacity, transmissivity, and the yield of boreholes. The observation boreholes (piezometers) were later equipped with data loggers for monitoring water table fluctuation. A close relationship between the specific capacity and transmissivity values, based on data from the five sites, was noted, *Figure 4.24*.
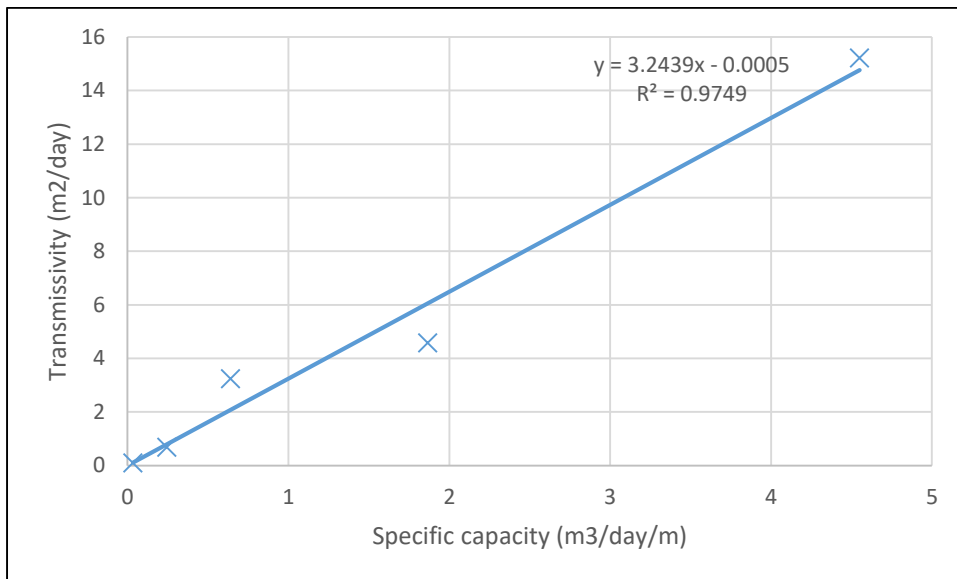
Figure 4.24. The relationship between transmissivity data and specific capacity data for the five piezometers in Kisumu.

Ideally, transmissivity, specific capacity and borehole yield data should be taken from a constant-rate pumping test of at least 24 hours duration (Graham e*t al*., 2009). The shallow aquifer in Kisumu was not very productive, and therefore the maximum pumping duration was 4 hours to attain a constant drawdown and flow. In yield data, the maximum drawdown in the

test must be less than 20% of the initial depth of water in the borehole. This was achieved in all the five observation boreholes drilled.

The relationship between the borehole yield data to the corresponding values of specific capacity reasonably closely related, although there is a significantly weaker correlation than was found between specific capacity and transmissivity, *Figure 4.25*. The student T-test in Excel based on 2-tail analysis and equal variance shows that the significance of the correlation between yield and specific capacity is 0.3 and between yield and transmissivity is 0.9. This indicates that the correlations are not significant.
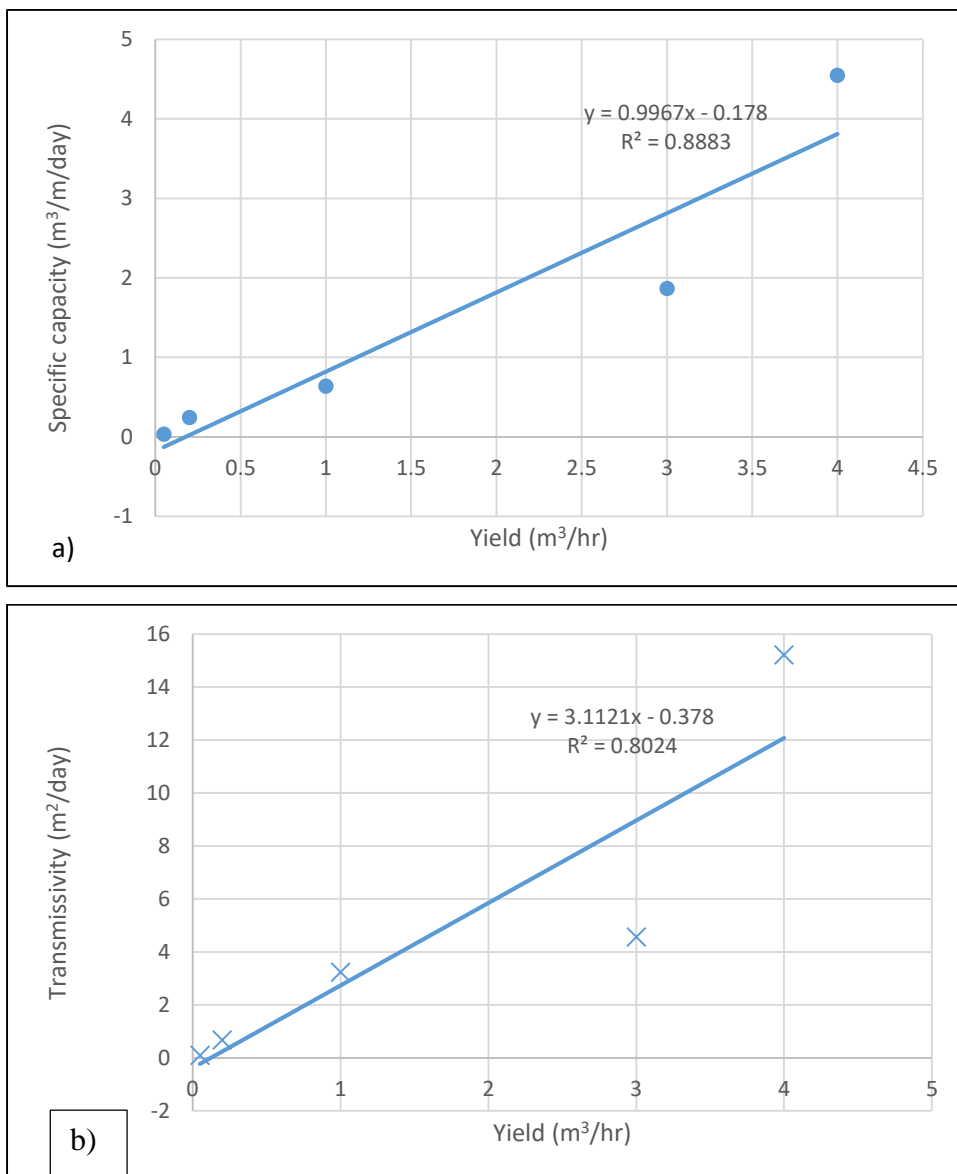
Figure 4.25. Relationship between (a) specific capacity and borehole yields and (b) transmissivity and yield

The relationship between borehole yields data to the corresponding values of specific capacity and transmissivity showed a correlation. The higher the transmissivity, the more the yields.

Historical data from the Ministry of Water and Sanitation was reviewed and compared with the results from this study. Most of these boreholes were drilled by the Lake Basin Development Authority (LBDA) in 1991 (e.g. C8118 in Mbeme, C8119 in Alendu and C8062 in Lola). Borehole number C3797 is located within Kisumu cotton mills (KICOMI) and was drilled in 1971. C10600 was drilled in 1996 within Kisumu General Hospital but was dry. These boreholes are abandoned due to broken-down pumps, and some dried up, and others collapsed due to poor development after drilling. A sample of borehole completion records for Kisumu from the Ministry of Water and Sanitation database is given in *Table 4.18*.

Table 4.18. Selected Kisumu historical borehole properties

No	Depth (m)	Water Struck Level (m)	Static Water Level (m)	Yield (m³/hr)	Draw down (m)	Specific Capacity (m³/hr/m)	Formation
C3794	34	6	6	3.4	3	1.13	Sediments
C8062	100	93.0, 98.0	18	12	8	1.5	Phonolite
C8063	92	84.0, 92.0	20	8	24	0.33	Phonolite
C8064	53	15.0, 25.0, 38.0, 47.0	7.4	14.4	21	0.69	Sediments
C8065	83	31.0 ,64.0	12	9	32	0.28	Phonolite
C8118	68	43.0, 47.0 , 5.02, 60.0	10	14.4	23	0.63	Phonolite
C8119	46	31.0, 37.0, 40.0	7.6	18	4.4	4.09	Phonolite
C10179	94	10.0, 70.0	8	8.6	50	0.17	Sediments
C10600	169	75		0	Dry		Phonolite
C11508	109	64	90	3.6	60	0.06	Basalt
C11947	70	20	15	0.6	45	0.01	Phonolite

The sampled boreholes in *Table 4.18* above have an average depth of 84.0 m and a mean yield of 8.4 m³/hr. Borehole number C11947 yielded only 0.6 m³/hour, while borehole number C10600 is dry. The wide range in tested yields is caused by geological differences between lithologies underlying the area. This shows the heterogeneity of the aquifer. Boreholes drilled through phonolitic lavas are dry or very low yielding, while boreholes within the sediments have high yields.

4.1.5.2   Mt. Elgon aquifer

The pumping test summary and aquifer characteristics of the six boreholes in the Mt. Elgon area was reviewed to summarise borehole characteristics, *Table 4.19*. Borehole completion records were availed by Water Resources Authority (WRA) offices in Kitale and Kapenguria.

Table 4.19. Pumping test summary and aquifer characteristics of the six boreholes in the Mt. Elgon area

Parameter	Unit	Saboti Sub-District Hosp.	Kacheliba Hosp.	Kitalakapel (C6252)	Waitaluk/ Sirende (C14737)	Patrick Khaemba	Kitale Municipality
Total depth	m	153	70	63	80	80	57
Aquifer (water struck level) – main aquifer coloured.	m	78.0, 84.0, 90.0, 130.0, 132.0, 138.0, 134.0	55.2	36	18.0, 28.0	38.0, 68.0	45.0, 49.0
Static water level		45.7	55.2	29.72	9	11.9	17.5
Type of pump		QF 12-17	Not given	Not given	SP 2A-18	Not given	Not given
Depth of pump intake	m	132	60.6	58	62	26	54
Discharge	m^3/hr	9.5	1.7	0.4	2.5	1.5	2.3
Pumping water level		116.8	62	60	51.4	23.2	52.9
Cumulative draw down	m	71.1	55.2	60.2	52.94	11.25	46.8
Specific capacity	m^3/day/m	2	0.7	0.2	1.2	1.6	1
Transmissivity	m^2/day	18.1	0.3	3.7	23.2	3.5	0.8

The relationship between transmissivity and specific capacity for the six boreholes from a different geological formation in the Mt. Elgon site is challenging to decipher. There is very little correlation between the two, *Figure 4.26*.
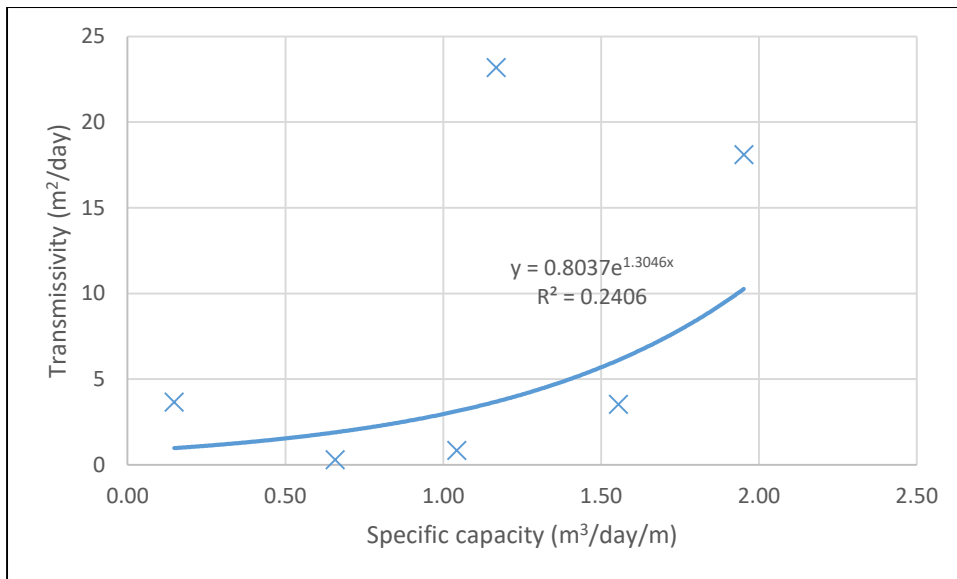
Figure 4.26. Relationship between the specific capacity and transmissivity for the Mt. boreholes

The plot shows a weak correlation ($r^2 = 0.24$) between specific capacity and transmissivity. This could be due to the unreliability of pumping test data reported by local drillers or differences in aquifer formation. This could also suggest that the aquifer is fracture controlled.

4.1.6 Aquifer geometry deduced from geology and geophysical surveys

The shallow aquifer in Kisumu and Mt. Elgon occurs at a maximum depth of 50 meters. This was confirmed in Kisumu by drilling to bedrock and VES interpretation. The aquifer sequence comprises clay, silt, different grades of sand and gravel in varying proportions. The aquifer characteristics calculated from the pumping tests are varied, demonstrating the heterogeneity of the shallow aquifer. VES interpretation alone is insufficient to identify productive points due to very thick wet clays in some sites. For example, around the Lake Basin near Mambo Leo, VES modelling showed water presence, but drilling encountered wet clay at recommended drilling depth.

The vertical electrical sounding and geology indicate that in Mt. Elgon, the aquifer is fracture controlled, and productive boreholes can be drilled in fracture zones with gravelly sands. From a sample of borehole completion records, groundwater occurs in Quaternary alluvium, multiple fractures system within the volcanic rocks, and regolith within the gneisses. The aquifer geometry varies consistently from Mt. Elgon slopes toward the lowlands and the plains. Within the mountain slopes, the depth to the water table decreases toward the lowland in Endebbes

and Kitale. At the contacts between a lava flow and the metamorphic rocks, permanent and high yielding springs sprouts. The depth to the metamorphic rocks become shallower as the volcanic thins downslope and towards the Kitale plains.

4.2 Results on hydrochemistry and water quality

This sub-chapter presents the results and discussion of the hydrochemistry and water quality in the selected study sites in Kisumu and Mt. Elgon aquifers. This objective aimed to establish groundwater quality and evaluate groundwater chemistry modified by rock-water and surface-groundwater interactions. The results of field measurements, laboratory analysis and hydrochemical facies, rock-water interactions are presented in the first part of this chapter. In the second part of the sub-chapter, the results on water quality, including groundwater contamination and microbial contamination, are presented.

4.2.1   Physico-chemical properties

4.2.1.1   *Results of physic-chemical measurements in the Kisumu study site*

Physico-chemical indicators are the traditional water quality indicators. The parameters collected in Kisumu include dissolved oxygen, pH, temperature, turbidity conductivity and salinity, *Figure 4.27*.

Figure4.27. Collection of physico-chemical data in Kisumu using Hydrolab Quanta multi-parameter kit.

These were collected *in-situ* using a portable field kit. The full results are shown in appendix 6. The descriptive statistics are shown below in *Table 4.20* and *Table 4.21*. The median temperature and pH were 25.4°C and 7.3, respectively. The monthly monitoring of the physico-chemical quality of groundwater in Kisumu shows that there were slight or negligible monthly or seasonal fluctuations apart from the turbidity that increased tremendously during rainy seasons.

Table 4.20. Descriptive statistics of physico-chemical parameter in all water samples from Kisumu

Parameter	Temp (°C)	eC (μS/cm)	DO (mg/L)	pH (Units)	Salinity (PSS)	DO (%)	Turbidity (NTU)
Mean	25.3	593.8	3.8	7.2	0.3	44.0	88.8
Standard Error	0.1	37.0	0.1	0.0	0.0	1.2	14.4
Median	25.4	326.0	3.5	7.3	0.2	42.0	16.2
Mode	26.0	68.0	2.3	7.0	0.1	26.0	9.2
Standard Deviation	2.0	613.4	2.0	0.7	0.3	20.7	239.5
Kurtosis	0.6	5.0	0.8	-0.1	7.1	-0.8	38.3
Skewness	0.4	1.9	0.9	-0.5	2.3	0.3	5.8
Range	10.4	3456.0	10.2	3.3	2.0	87.3	2000.0
Minimum	20.3	54.0	0.7	5.5	0.0	8.3	0.0
Maximum	30.8	3510.0	10.8	8.8	2.0	95.6	2000.0
Count	275	275	275	275	275	275	275

The median for turbidity was 16.2 NTU. A high level of turbidity was noted during the wet seasons. The median for electric conductivity was 326 μS/cm. The distribution of physic-chemical parameters with a negative kurtosis value indicates that the distribution has lighter tails than the normal distribution. These parameters include pH and DO but vary with individual water type as shown in the following tables per water type.

Table 4.21. Descriptive statistics of physico-chemical properties per water type, namely, boreholes, shallow wells, springs, rivers and lake water from Kisumu

1. Boreholes

Boreholes	Temp (°C)	eC (µS/cm)	DO (mg/L)	pH (Units)	Salinity (PSS)	DO (%)	Turbidity (NTU)
Mean	26.4	715.2	4.4	7.4	0.4	52.9	9.2
Standard Error	0.4	55.8	0.2	0.1	0.0	1.8	1.3
Median	26.7	512.5	4.2	7.4	0.3	54.5	7.8
Mode	30.6	512.0	3.0	6.9	0.2	61.3	8.6
Standard Deviation	3.1	394.2	1.5	0.5	0.2	12.8	8.9
Kurtosis	-1.5	-1.7	0.9	-1.0	-1.8	-0.2	34.6
Skewness	0.1	-0.1	0.9	0.2	-0.1	-0.2	5.4
Range	9.7	1054.0	6.9	1.9	0.6	59.0	66.0
Minimum	21.1	143.0	1.8	6.5	0.1	21.1	0.0
Maximum	30.8	1197.0	8.7	8.4	0.6	80.1	66.0
Count	50.0	50.0	50.0	50.0	50.0	50.0	50.0

2. Shallow wells

Shallow wells	Temp (°C)	eC (µS/cm)	DO (mg/L)	pH (Units)	Salinity (PSS)	DO (%)	Turbidity (NTU)
Mean	25.8	1081.2	3.3	7.2	0.5	36.8	17.3
Standard Error	0.1	69.3	0.2	0.0	0.0	1.3	2.6
Median	26.0	969.0	2.8	7.3	0.5	32.2	11.1
Mode	26.0	800.0	2.0	7.3	0.3	31.9	9.2
Standard Deviation	1.1	689.2	1.6	0.4	0.4	12.7	26.2
Kurtosis	2.9	2.9	1.6	3.0	4.1	0.2	53.0
Skewness	-0.6	1.6	1.3	-1.1	1.9	0.8	6.6
Range	7.1	3307.0	8.4	2.4	2.0	68.2	237.9
Minimum	22.7	203.0	0.7	5.5	0.0	8.3	1.1
Maximum	29.7	3510.0	9.1	7.9	2.0	76.5	239.0
Count	99.0	99.0	99.0	99.0	99.0	99.0	99.0

3. Springs

Springs	Temp (°C)	eC (µS/cm)	DO (mg/L)	pH (Units)	Salinity (PSS)	DO (%)	Turbidity (NTU)
Mean	25.20	205.56	2.43	6.33	0.10	28.26	57.18
Standard Error	0.15	11.87	0.16	0.06	0.01	1.96	9.66
Median	24.78	178.50	2.05	6.39	0.09	24.40	27.75
Mode	24.22	104.00	4.43	7.09	0.08	55.30	10.50
Standard Deviation	1.21	94.97	1.29	0.51	0.05	15.67	77.25
Kurtosis	1.87	0.08	-0.84	-1.03	0.07	-0.32	11.17
Skewness	1.20	1.02	0.66	0.07	0.87	0.87	3.01
Range	6.13	360.00	4.39	1.77	0.21	56.60	449.60
Minimum	23.64	101.00	0.68	5.52	0.01	8.80	6.40
Maximum	29.77	461.00	5.07	7.29	0.22	65.40	456.00
Count	64	64	64	64	64	64	64

4. Rivers

Rivers	Temp (°C)	eC (µS/cm)	DO (mg/L)	pH (Units)	Salinity (PSS)	DO (%)	Turbidity (NTU)
Mean	23.2	109.4	6.1	7.9	0.1	70.7	351.7
Standard Error	0.2	13	0.3	0	0	2.3	66.8
Median	23.1	87.5	5.6	7.9	0	72.9	170
Mode	22.9	68	5.6	7.7	0	72.2	2000
Standard Deviation	1.6	91.9	2	0.3	0	16.6	472.1
Kurtosis	-0.3	23.4	0.9	-0.5	10.6	3.4	5.6
Skewness	0.3	4.5	0.2	-0.1	3	-1.6	2.4
Range	6.6	585	9.4	1.4	0.1	78	1974.7
Minimum	20.3	54	1.4	7.2	0	17.6	25.3
Maximum	26.9	639	10.8	8.6	0.2	95.6	2000
Count	50	50	50	50	50	50	50

5. Lake

Lake	Temp (°C)	eC (µS/cm)	DO (mg/L)	pH (Units)	Salinity (PSS)	DO (%)	Turbidity (NTU)
Mean	25.9	156.3	3.3	7.8	0.1	39.8	82.3
Standard Error	0.4	16.1	0.3	0.2	0.0	5.2	6.1
Median	26.1	140.0	3.4	7.9	0.1	43.6	90.3
Standard Deviation	1.5	55.8	1.1	0.7	0.0	18.1	21.1
Kurtosis	2.2	11.1	0.9	0.7	10.8	-1.1	3.4
Skewness	0.9	3.3	-0.6	-0.7	3.2	-0.3	-1.7
Range	5.8	206.0	4.2	2.5	0.1	56.4	75.1
Minimum	23.7	125.0	1.0	6.3	0.1	11.0	27.9
Maximum	29.5	331.0	5.3	8.8	0.2	67.4	103.0
Count	12.0	12.0	12.0	12.0	12.0	12.0	12.0

Student t-Test shows a statistically significant correlation between EC and salinity at p-value <0.05 and between pH and dissolved oxygen with a p-value < 0.05. Groundwater was of good quality considering the parameters measured compared to WHO and local KEBS standards (KEBS, 2015; WHO, 2017). Electrical conductivity (3510 µS/cm) beyond the maximum recommended level by the standards was noted in one well in Otonglo, close to Lake Victoria. The shallow well is located within black cotton soil, and the interaction between clay minerals and groundwater could be the cause of high EC.

The correlation between the physico-chemical parameters are further shown in Table *4.22* and *Figure 4.28*

Table 4.22. Correlation matrix of the Kisumu water samples physico-chemical parameters. Statistically significant relationships are highlighted in bold text.

Parameter		Temp (°C)	EC (µS/cm)	Dissolved oxygen (mg/L)	pH (pH units)	Salinity (PSS)	Dissolved oxygen (%)	Turbidity (NTU)
Correlation	Temperature (°C)	1	0.48	-0.25	0.07	0.33	-0.22	-0.28
	EC (µs/m)	0.48	1	-0.22	0.04	**0.67**	-0.25	-0.26
	Dissolved oxygen (mg/L)	-0.3	-0.22	1	0.49	-0.13	0.88	0.4
	pH (pH units)	0.07	0.04	0.49	1	0.05	**0.62**	0.2
	Salinity (PSS)	0.33	**0.67**	-0.13	0.05	1	-0.11	-0.18
	Dissolved oxygen (%)	-0.2	-0.25	0.88	**0.62**	-0.11	1	0.37
	Turbidity (NTU)	-0.3	-0.26	0.4	0.2	-0.18	0.37	1
Sig. (1-tailed)	Temperature (°C)		0	0	0.12	0	0	0
	Electrical conductivity (µS/m)	0		0	0.24	0	0	0
	Dissolved oxygen (mg/L)	0	0		0	0.02	0	0
	pH (pH units)	0.12	0.24	0		0.22	0	0
	Salinity (PSS)	0	0	0.02	0.22		0.04	0
	Dissolved oxygen (%)	0	0	0	0	0.04		0
	Turbidity (NTU)	0	0	0	0	0	0	
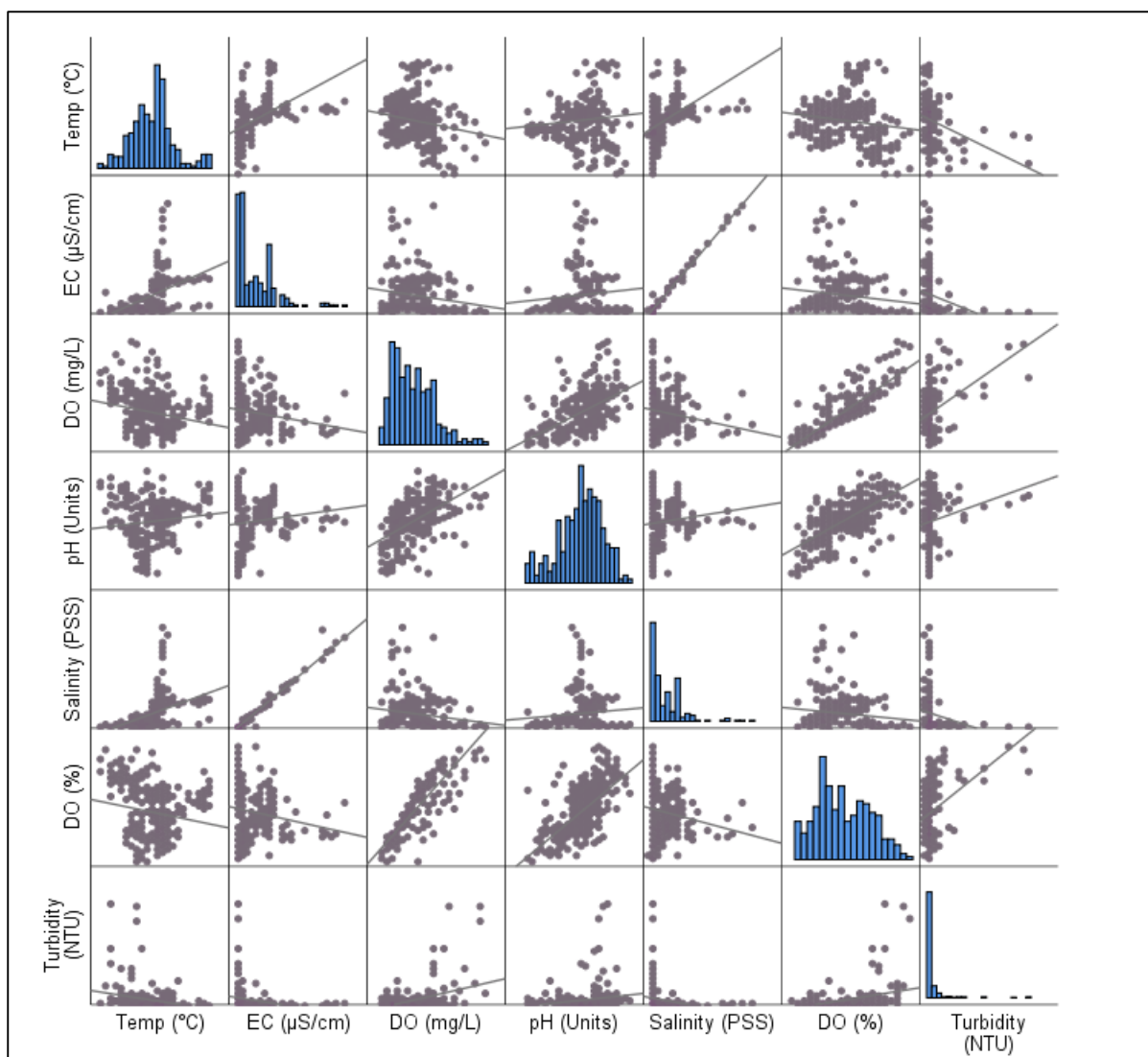
Figure 4.28. Scatter plot matrix for the physico-chemical parameters in Kisumu. Regression lines are shown in the plots. The diagonal bar charts are the respective data plots showing data skewness.

The KMO value for sampling adequacy was 0.65, and Bartlett's test of sphericity was 0, *Table 4.23*. The results were therefore satisfactory for factor analysis (PCA). Small values of the sphericity test of less than 0.05 of the significance level indicate that the factor analysis helps correlate data.

Table 4.23. KMO Bartlett's test for Kisumu physico-chemical data

Kaiser-Meyer-Olkin Measure of Sampling Adequacy.		0.650
Bartlett's Test of Sphericity	Approx. Chi-Square	852.135
	df	21
	Sig.	0.000

PCA analysis shows that the initial number of factors is the same as the number of variables used in the factor analysis, *Table 4.24*. There are six variables, and therefore six components are defined. However, only the first two factors are retained with an eigenvalue greater than one as determined during loading. The total eigenvalues for these first two components are 4.306, accounting for 71.76% of the variance.

Table 4.24. Total variant explained and depicting the six components equal to the number of variables. The first two components account for 71.76 eigenvalues.

Component	Initial Eigenvalues			Extraction Sums of Squared Loadings		
	Total	% of Variance	Cumulative %	Total	% of Variance	Cumulative %
1	2.684	44.729	44.729	2.684	44.729	44.729
2	1.622	27.032	71.760	1.622	27.032	71.760
3	.759	12.652	84.412			
4	.505	8.413	92.825			
5	.332	5.530	98.355			
6	.099	1.645	100.000			

The scree plot further shows the six principal components showed in *Figure 4.29*.
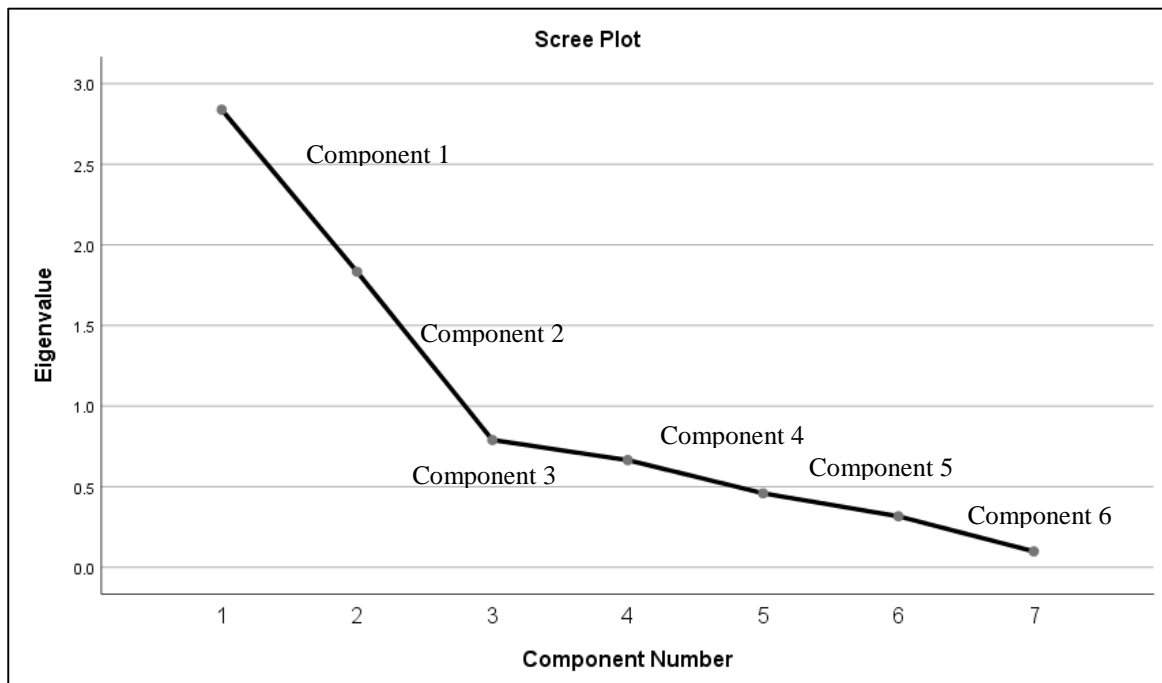
Figure 4.29. Scree plot for the physico-chemical data from Kisumu. The six components are shown.

From the third factor on, the line is almost flat, meaning that each successive factor accounts for smaller and smaller amounts of the total variance. The first component is dominated by

dissolved oxygen, pH, and turbidity, while the second component has EC, salinity, and temperature, *Table 4.25*.

Table 4.25. PCA matrix for Kisumu study site. DO, pH and turbidity from the first cluster, while EC, salinity and temperature form the second cluster

Parameter	Component 1	Component 2
Dissolved oxygen (%)	0.928	
Dissolved oxygen (Mg/L)	0.888	
pH (pH units)	0.786	
Turbidity (NTU)	0.479	-0.376
Electrical conductivity (µS/cm)		0.878
Salinity (PSS)		0.811
Temperature (°C)		0.706
Extraction Method: Principal Component Analysis.		
Rotation Method: Varimax with Kaiser Normalization.		
a. Rotation converged in 3 iterations.		
Component	1	2
1	0.816	-0.578
2	0.578	0.816
Extraction Method: Principal Component Analysis. Rotation Method: Varimax with Kaiser Normalization.		

4.2.1.2   *Results of physico-chemical measurement in the Mt. Elgon study site*

The full results for physico-chemical parameters are given in Appendix 7 and a summary of statistics in *Table 4.26.*

Table 4.26. Descriptive statistics for the physico-chemical data in Mt. Elgon

Parameter	Temp (ºC)	pH	Turbidity (N.T.U.)	EC (µS/cm)
Mean	24.0	7.6	7.9	367.1
Standard Error	0.5	0.2	2.5	49.2
Median	23.4	7.4	3.3	248.0
Standard Deviation	3.2	1.2	15.5	310.9
Kurtosis	2.4	5.3	16.3	0.3
Skewness	-0.6	2.0	3.9	1.1
Minimum	13.8	6.1	0.0	12.5
Maximum	31.1	11.9	83.3	1214.0
Count	40.0	40.0	40.0	40.0

The median water temperature, pH, turbidity and electrical conductivity are 23.4, 7.4, 3.3, and 248.0, respectively. These values are within the KEBS and WHO limits for drinking water. To

understand the relationship between the physico-chemical parameters, a correlation was carried out. This was preceded by the determination of the suitability of data for correlation. The KMO (0.43) test showed that the sample size was not very good for correlation, but Bartlett's test of sphericity ($p < 0.05$) showed that the data was statistically significant, *Table 4.27*.

Table 4.27. KMO and Bartlett's test for the physico-chemical data in Mt. Elgon

Kaiser-Meyer-Olkin Measure of Sampling Adequacy.		0.43
Bartlett's Test of Sphericity	Approx. Chi-Square	44.77
	df	6
	Sig.	0.000

There is a correlation between EC and temperature and EC and pH, *Table4.28*. The P-values (p=0) are statistically significant. There is no statistically significant relationship between turbidity and other parameters. The p-value is more than 0.05.

Table 4.28. Pearson correlation matrix and p-values for the physico-chemical data in Mt. Elgon. Statistically significant correlations are in bold font.

		Temperature (ºC)	pH	Turbidity (N.T.U)	EC (µS/cm)
Correlation	Temperature (ºC	1.000	0.151	-0.026	**0.599**
	pH	0.151	1.000	0.132	**0.660**
	Turbidity (N.T.U)	-0.0026	0.132	1.000	0.061
	EC (µS/cm)	**0.599**	**0.660**	0.061	1.000
Sig. (1-tailed)	Temperature (ºC)		0.176	0.436	**0.000**
	pH	0.176		0.208	**0.000**
	Turbidity (N.T.U)	0.436	0.208		0.355
	EC (25ºC)	**0.000**	**0.000**	0.355	

Student t-Test was used to determine the statistical significance of the correlation between EC, pH and temperature. The result shows that the correlation was statistically significant, *Table 4.29.*

Table 4.29. Student t-Test, two-sample assuming equal variance. The p-value is 0, and therefore the correlation is significant.

t-Test: Two-Sample Assuming Equal Variances		
	EC (25ºC)	*Temp (ºC*
Mean	367.1	24.0
Variance	96654.4	10.1
Observations	40	40.0
Pooled Variance	48332.2	
Hypothesized Mean Difference	0.0	
df	78.0	
t Stat	7.0	
P(T<=t) one-tail	0.0	
t Critical one-tail	1.7	
P(T<=t) two-tail	**0.0**	
t Critical two-tail	2.0	

t-Test: Two-Sample Assuming Equal Variances		
	EC	*pH*
Mean	367.1	7.6
Variance	96654.4	1.5
Observations	40	40.0
Pooled Variance	48327.9	
Hypothesized Mean Difference	0.0	
df	78.0	
t Stat	7.3	
P(T<=t) one-tail	0.0	
t Critical one-tail	1.7	
P(T<=t) two-tail	**0.0**	
t Critical two-tail	2.0	

Two principal components are defined for the Mt. Elgon parameters with a cumulative eigenvalue of 75.72%, *Table 4.30*. The PCA 1 comprises EC (0.948), temperature (0.734) and pH (0.727) while PCA 2 is composed of turbidity (0.906) and pH (0.402).

Table 4.30. Explanation of total variance and contributing parameters for Mt. Elgon physico-chemical data

Component	Initial Eigenvalues			Rotation Sums of Squared Loadings		
	Total	% of Variance	Cumulative %	Total	% of Variance	Cumulative %
1	1.980	49.489	49.489	1.958	48.940	48.940
2	1.049	26.231	75.721	1.071	26.781	75.721
3	.791	19.764	95.485			
4	.181	4.515	100.000			

Parameter	Component	
	1	2
EC (µS/cm)	0.948	
Temperature (ºC)	0.734	-0.290
pH	0.727	0.402
Turbidity (NTU)		0.906
Extraction Method: Principal Component Analysis.		
Rotation Method: Oblimin with Kaiser Normalization.		

4.2.2   Results of water chemistry from Kisumu and Mt. Elgon study sites

The complete results of the chemical analysis for Kisumu and Mt. Elgon groundwater samples are given in appendix 1 and 2, respectively. The interrelationships between the various aspects of geochemistry and between water chemistry and geology (rocks) are discussed. The description of the origin and interpretation of the significant elements, and some minor ones, that affect water quality are presented. Univariate methods like descriptive statistics, distribution analysis, and stochastic connections with correlation analysis are shown. The results on the principal component analysis and classical plots depicting the water classifications, interactions and seasonal variations are also presented in this section.

4.2.2.1   Kisumu water chemistry

The descriptive statistics for the ionic composition of water samples from the Kisumu study site is shown below, *Table 4.31*. The total number of samples are 66 (3 sampling campaigns in 22 areas).

Table 4.31. Descriptive statistics for the Kisumu water chemistry

Parameter	Fe^{3+}	Mn^{2+}	Ca^{2+}	Mg^{2+}	Na^{2+}	K^+	HCO_3^-	Cl^-	F^-	NO_2^-	NO_3^{2-}	SO_4^{2-}
Mean	0.77	0.18	44.07	8.67	89.76	10.67	329.49	55.80	1.38	2.34	10.35	35.76
Standard Error	0.38	0.03	6.01	1.13	11.88	1.10	32.94	14.72	0.19	0.67	2.98	6.02
Median	0.06	0.04	22.90	4.52	40.55	8.96	223.87	15.25	0.84	1.28	5.67	8.35
Standard Deviation	3.06	0.28	48.83	9.19	96.53	8.93	267.61	119.62	1.50	5.46	24.20	48.91
Kurtosis	35.56	3.35	2.86	4.16	1.44	0.29	-1.10	21.20	4.10	47.24	47.31	4.81
Skewness	5.84	1.94	1.78	1.97	1.42	1.05	0.61	4.36	2.01	6.54	6.54	2.08
Minimum	0.00	0.00	0.78	0.14	4.96	0.45	45.63	1.64	0.20	0.16	0.71	0.23
Maximum	21.30	1.13	196.00	42.40	412.00	34.90	871.08	752.00	7.29	42.60	189.00	223.00
Count	66	66	66	66	66	66	66	66	66	66	66	66

The mean and geometric means show that water is of good quality, but fluoride level (mean of 1.38 and median of 0.84) was beyond the KEBS and WHO recommended minimum level. The iron level was also beyond the minimum recommended values in some sites, especially those located within laterite, e.g. in Obunga (21.3 mg/L). The plots of the concentration of ions in mg/L shows that the alkaline metals exceed the alkaline earth metals, and the weak acids greatly exceeds strong acids, *Figure 4.30.* Alkaline metals are more soluble in water than alkaline earth metals.
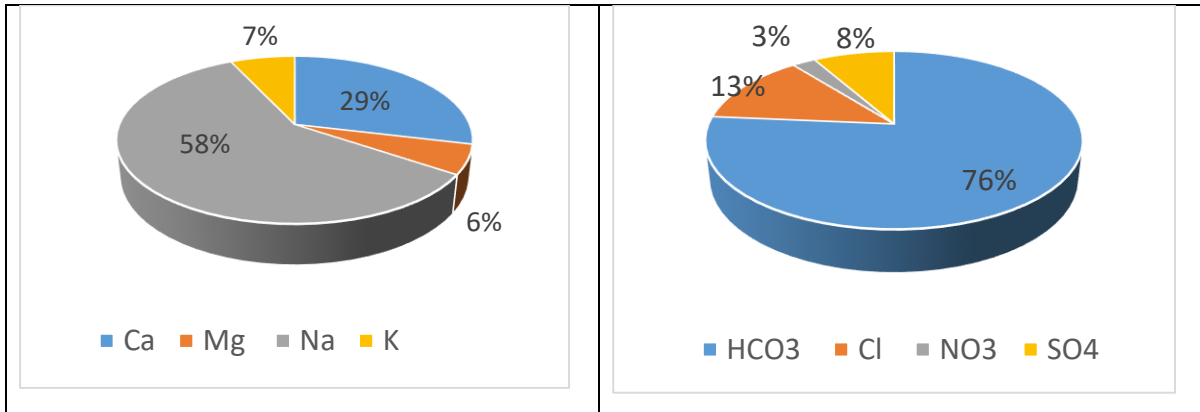
Figure 4.30. Concentrations of ions in Kisumu water (mg/L). Note the high concentrations of sodium (58%) and bicarbonates (76%) in Kisumu water.

A scatter plot and correlation matrices were done to show the relationship between ions (*Figure 4.31 and Table 4.32).* The scatter plot shows a positive relationship between the parameters. The outliers from the scatter plot are results from a deep borehole (130 m depth) in Wandiege.
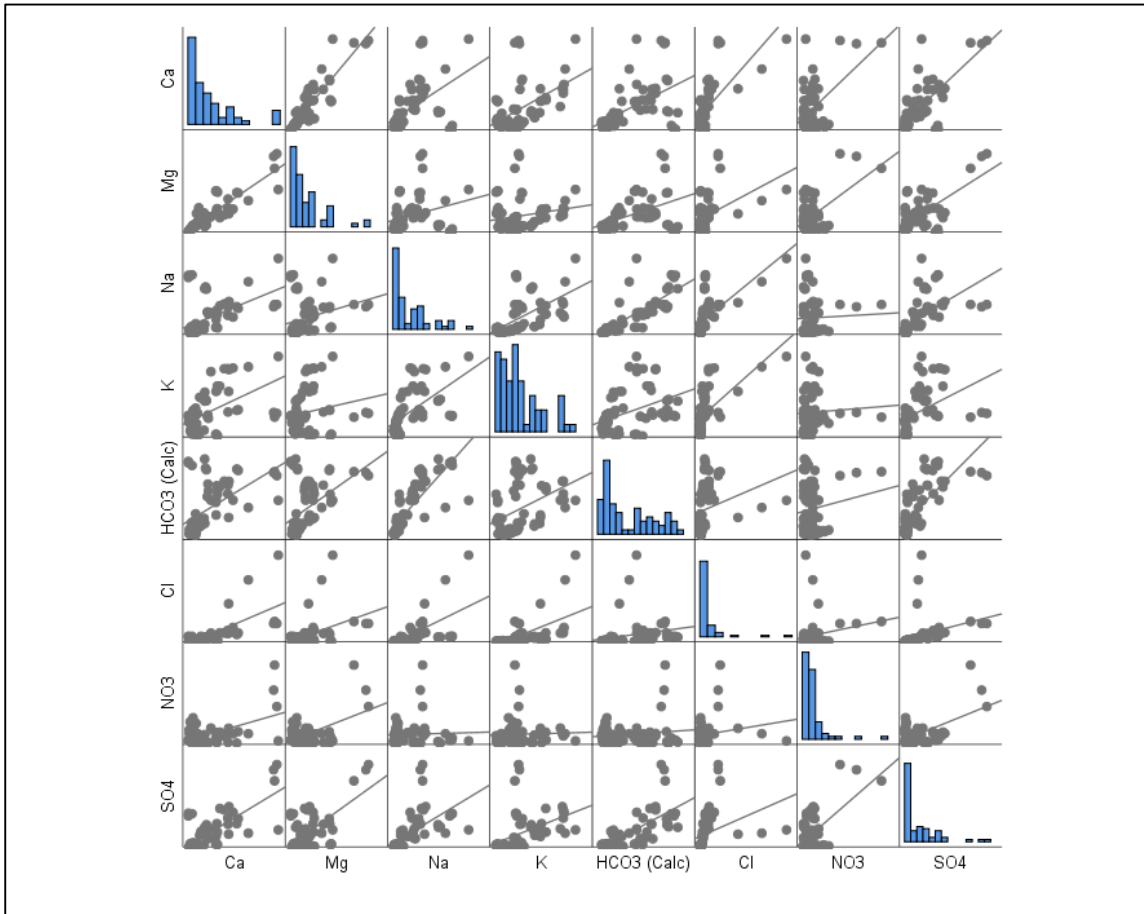
Figure 4.31. Scatter plot matrix for the main cations and anions in Kisumu water. The correlation between ions is shown in regression lines. The bar charts show the skewness in the distribution of ions.

Table 4.32. Correlation matrix for the main ions in Kisumu water. Statistically significant correlations are in bold font.

Correlation Matrix													
		Fe^{3+}	Mn^{2+}	Ca^{2+}	Mg^{2+}	Na^+	K^+	HCO_3^-	Cl^-	F^-	NO_2^-	NO_3^{2-}	SO_4^{2-}
Correlation	Fe^{3+}	1.000	0.015	-0.173	-0.148	-0.149	-0.059	-0.018	-0.082	-0.096	-0.038	-0.046	-0.139
	Mn^+	0.015	1.000	-0.011	0.152	-0.330	-0.424	-0.287	-0.098	-0.369	-0.048	0.070	-0.096
	Ca^{2+}	-0.173	-0.011	1.000	**0.901**	**-0.518**	**0.516**	**0.553**	**0.697**	0.150	0.243	**0.525**	**0.754**
	Mg^+	-0.148	0.152	**0.901**	1.000	0.283	0.188	0.487	0.435	-0.001	0.231	**0.538**	**0.677**
	Na^+	-0.149	-0.330	0.518	0.283	1.000	**0.594**	**0.807**	**0.635**	**0.709**	.005	0.040	**0.596**
	K	-0.059	-0.424	0.516	0.188	0.594	1.000	0.421	**0.597**	0.447	0.135	0.049	0.448
	HCO_3^-	-0.178	-0.287	0.553	0.487	**0.807**	0.421	1.000	0.241	**0.764**	0.024	0.134	**0.738**
	Cl^-	-0.082	-0.098	0.697	0.435	0.635	0.597	0.241	1.000	0.072	0.036	0.186	0.336
	F^-	-0.096	-0.369	0.150	-0.001	0.709	0.447	0.764	0.072	1.000	0.062	-.0183	0.408
	NO_2^-	-0.038	-0.048	0.243	0.231	0.005	0.135	0.024	0.036	0.062	1.000	0.404	0.211
	NO_3^{2-}	-0.046	0.070	0.525	0.538	0.040	0.049	0.134	0.186	-0.183	0.404	1.000	0.593
	SO_4^{2-}	-0.139	-0.096	**0.754**	0.677	0.596	0.448	0.738	0.336	0.408	0.211	0.593	1.000
Student t-Test Sig. (1-tailed)	Fe^{3+}		0.452	0.083	0.118	0.116	0.319	0.076	0.256	0.223	0.381	0.356	0.133
	Mn^+	0.452		0.464	0.111	**0.003**	**0.000**	0.010	0.217	0.001	0.351	0.289	0.221
	Ca^{2+}	0.083	0.464		**0.000**	**0.000**	**0.000**	**0.000**	**0.000**	0.114	0.025	**0.000**	**0.000**
	Mg^+	0.118	0.111	**0.000**		**0.011**	0.065	**0.000**	**0.000**	0.497	0.031	**0.000**	**0.000**
	Na^+	0.116	**0.003**	**0.000**	0.011		**0.000**	**0.000**	**0.000**	**0.000**	0.484	0.373	**0.000**
	K	0.319	**0.000**	**0.000**	0.065	**0.000**		**0.000**	**0.000**	**0.000**	0.141	0.348	**0.000**
	HCO_3^-	0.076	**0.010**	**0.000**	**0.000**	**0.000**	**0.000**		**0.026**	**0.000**	0.424	0.141	**0.000**
	Cl^-	0.256	0.217	**0.000**	**0.000**	**0.000**	**0.000**	0.026		0.281	0.386	0.067	**0.003**
	F^-	0.223	0.001	0.114	0.497	**0.000**	**0.000**	**0.000**	0.281		0.311	0.070	**0.000**
	NO_2^-	0.381	0.351	0.025	0.031	0.484	0.141	0.424	0.386	0.311		**0.000**	**0.044**
	NO_3^{2-}	0.356	0.289	**0.000**	**0.000**	0.373	0.348	0.141	0.067	0.070	**0.000**		**0.000**
	SO_4^{2-}	0.133	0.221	**0.000**	**0.000**	**0.000**	**0.000**	**0.000**	**0.003**	**0.000**	**0.044**	**0.000**	

The correlation matrix shows the strength of the relationship between parameters. For example, there is a strong relationship between calcium and magnesium (0.901), between calcium and sulphate (0.754), between sodium and bicarbonate (0.807) and between magnesium and sulphate (0.677). The student two-tail T-test confirms the significance of correlations, *Table 4.33*, *Table 4.34* and *Table 4.35.*

Table 4.33. Student t-Test between K+ and Na+, and between Ca2+ and Mg2+ for Kisumu water chemistry

t-Test: Two-Sample Assuming Equal Variances		
	K	*Na*
Mean	10.67	89.76
Variance	79.73	9317.45
Observations	66	66
Pooled Variance	4698.59	
Hypothesized Mean Difference	0.00	
df	130.00	
t Stat	-6.63	
P(T<=t) one-tail	0.00	
t Critical one-tail	1.66	
P(T<=t) two-tail	**0.00**	
t Critical two-tail	1.98	

t-Test: Two-Sample Assuming Equal Variances		
	Ca	*Mg*
Mean	44.07	8.67
Variance	2384.09	84.48
Observations	66	66
Pooled Variance	1234.29	
Hypothesized Mean Difference	0.00	
df	130.00	
t Stat	5.79	
P(T<=t) one-tail	0.00	
t Critical one-tail	1.66	
P(T<=t) two-tail	**0.00**	
t Critical two-tail	1.98	

Table 4.34. Student t-Test for statistical significance of the correlation between sodium and bicarbonate ions and between sodium and fluoride ions

t-Test: Two-Sample Assuming Equal Variances		
	Na^+	HCO_3^-
Mean	89.76	329.49
Variance	9317.45	71616.49
Observations	66	66
Pooled Variance	40466.97	
Hypothesized Mean Difference	0.00	
df	130.00	
t Stat	-6.85	
P(T<=t) one-tail	0.00	
t Critical one-tail	1.66	
P(T<=t) two-tail	**0.00**	
t Critical two-tail	1.98	

t-Test: Two-Sample Assuming Equal Variances		
	Na^+	F^-
Mean	89.76	1.38
Variance	9317.45	2.26
Observations	66	66
Pooled Variance	4659.86	
Hypothesized Mean Difference	0.00	
df	130.00	
t Stat	7.44	
P(T<=t) one-tail	0.00	
t Critical one-tail	1.66	
P(T<=t) two-tail	**0.00**	
t Critical two-tail	1.98	

Table 4.35. Student t-Test for the significance of the correlation between HCO_3^- and SO_4^{2-}, and between HCO_3^- and F^- ions

t-Test: Two-Sample Assuming Equal Variances		
	HCO_3^-	SO_4^{2-}
Mean	329.49	35.76
Variance	71616.49	2392.26
Observations	66	66.
Pooled Variance	37004.37	
Hypothesized Mean Difference	0.00	
df	130.00	
t Stat	8.77	
P(T<=t) one-tail	0.00	
t Critical one-tail	1.66	
P(T<=t) two-tail	**0.00**	
t Critical two-tail	1.98	

t-Test: Two-Sample Assuming Equal Variances		
	HCO_3^-	F^-
Mean	329.49	1.38
Variance	71616.49	2.26
Observations	66.	66.
Pooled Variance	35809.38	
Hypothesized Mean Difference	0.00	
df	130.00	
t Stat	9.96	
P(T<=t) one-tail	0.00	
t Critical one-tail	1.66	
P(T<=t) two-tail	**0.00**	
t Critical two-tail	1.98	

The scatter plot, *Figure 4.32,* shows the calcium and magnesium relationship. Potassium has a strong relationship with all the other parameters apart from the nitrates. The correlation is statistically significant as demonstrated by the student t-Tests, $p < 0.05$. The outliers are from a deep borehole located in Wandiege (depth = 130 m). The bar charts are included to show the distribution of ions. All the ions show skewed distribution toward low values.
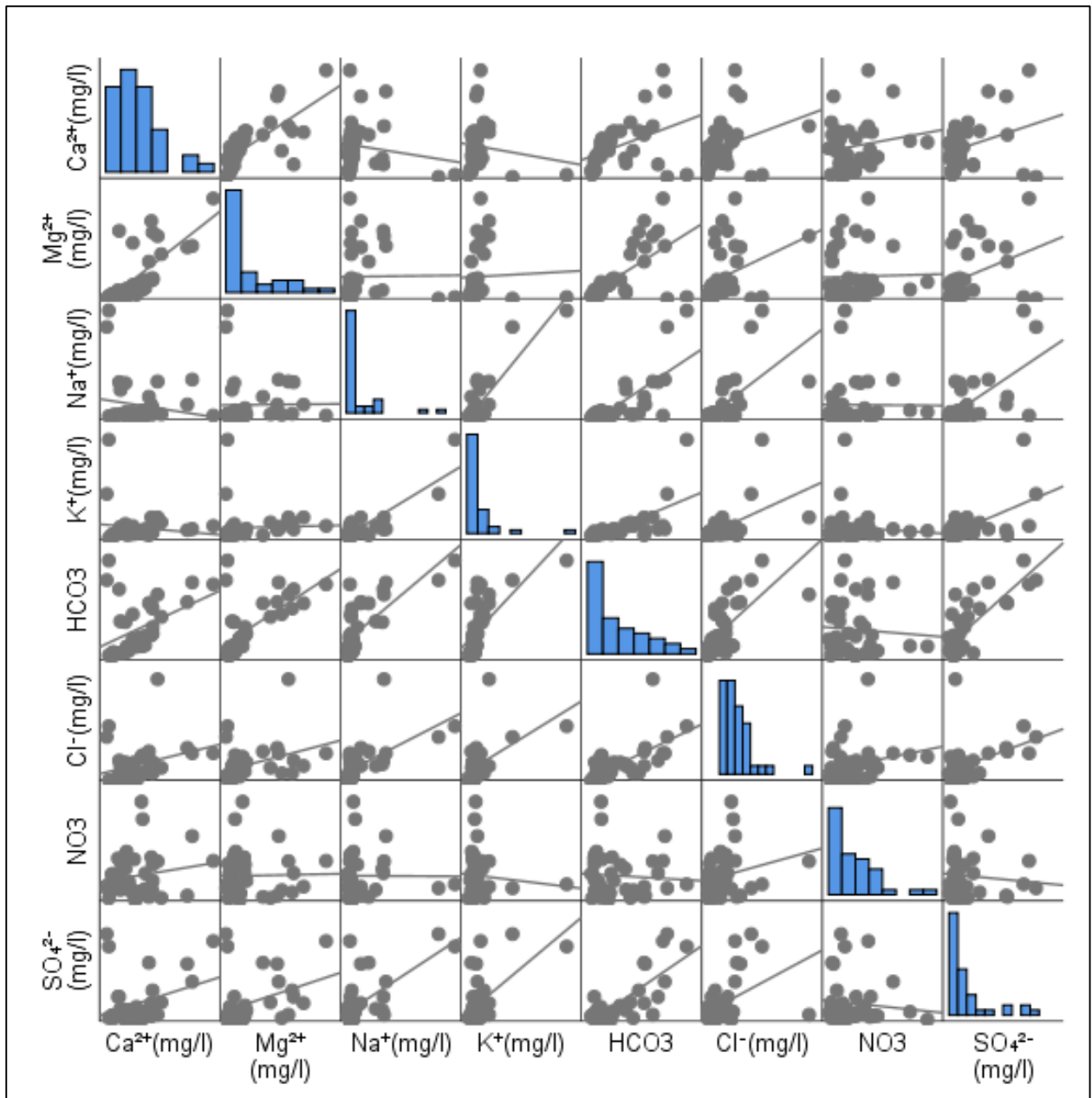
Figure 4.32. The correlation between major ions in Mt. Elgon water. The diagonal bar charts show the concentration of ions and their respective skewness. The regression lines indicate the type of relationship between ions.

The KMO measure of sampling adequacy shows that data was adequate for principal component analysis and sphericity test. The p-value (0) show that the sphericity test was statistically significant for analysis, *Table 4.36*.

Table 4.36. Test for sampling adequacy and sphericity for Kisumu water chemistry

Kaiser-Meyer-Olkin Measure of Sampling Adequacy.		0.543
Bartlett's Test of Sphericity	Approx. Chi-Square	822.584
	df	66
	Sig.	0.000

The rotated PCA matrix shows four principal components. The extraction method used was the principal component analysis. (PCA) Moreover, the rotation method was varimax with Kaiser Normalization, *Table 4.37*. The first and foremost component comprises chlorides, calcium and potassium, sodium magnesium and sulphates. The relation between these ions is high. Three other components are defined.

Table 4.37. Rotated PCA components for the main ions in Kisumu water. Four components are defined.

	Component			
	1	2	3	4
Cl	0.951			
Ca	0.745		0.474	0.413
K	0.651	0.589		
F		0.853		0.385
Mn		-0.735		
Na	0.525	0.660		0.403
NO3			0.819	
NO2			0.797	
Mg	0.510		0.530	0.530
HCO3 (Calc)		0.629		0.685
SO4	0.366	0.311	0.539	0.575
Fe				-0.497
Extraction Method: Principal Component Analysis.				
Rotation Method: Varimax with Kaiser Normalization.				
a. Rotation converged in 14 iterations.				

Component Transformation Matrix				
Component	1	2	3	4
1	0.627	0.478	0.389	0.476
2	0.142	-0.765	0.624	0.073
3	-0.766	0.262	0.451	0.377
4	0.025	0.342	0.506	-0.791

The scree plot clearly shows the four PCA components (*Figure 4.33*). The four components are above the eigenvalue of one, defined during the loading of data for analysis. They comprise 78.4 % of total eigenvalues.
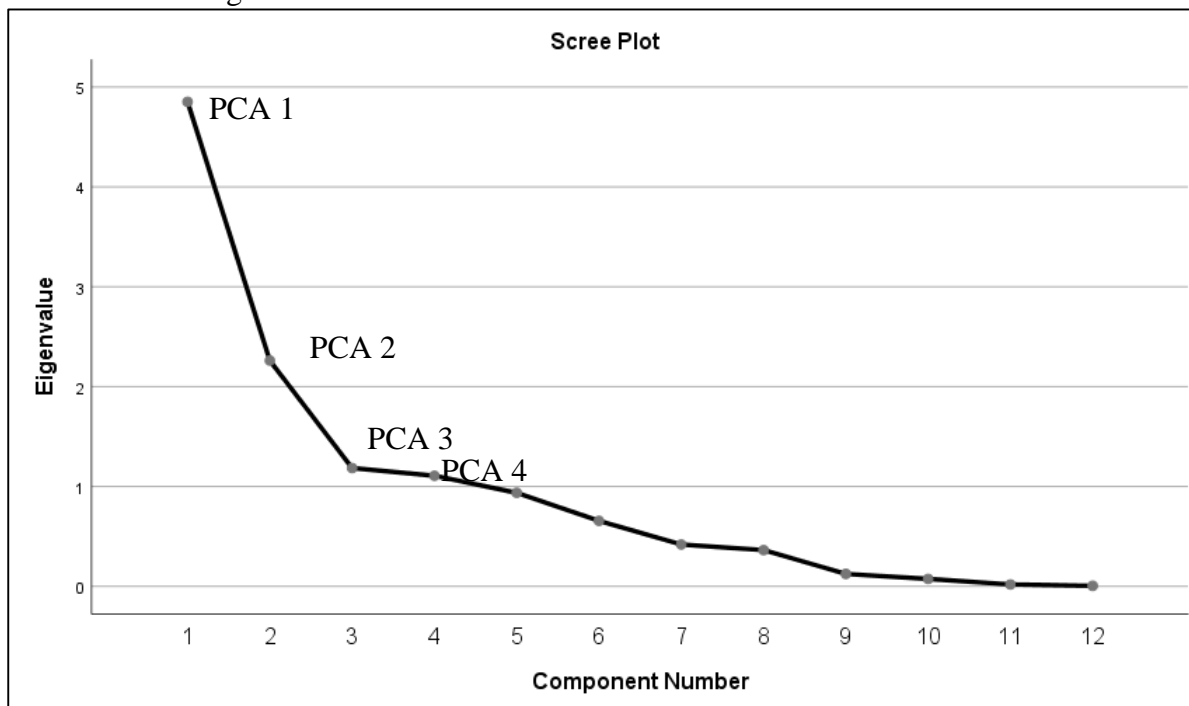
Figure 4.33. Scree plot of the four principal components.

Principal components numbers 5 to 12 accounts for only 21.6% of the eigenvalues, *Table 4.38*.

Table 4.38. Total variance for Kisumu water chemistry

	Initial Eigenvalues			Rotation Sums of Squared Loadings		
Component	Total	% of Variance	Cumulative %	Total	% of Variance	Cumulative %
1	4.851	40.428	40.428	2.648	22.067	22.067
2	2.261	18.840	59.268	2.645	22.042	44.109
3	1.184	9.871	69.139	2.139	17.824	61.933
4	1.107	9.227	78.366	1.972	16.433	78.366
5	0.936	7.804	86.170			
6	0.655	5.461	91.630			
7	0.419	3.491	95.121			
8	0.363	3.025	98.146			
9	0.124	1.037	99.184			
10	0.074	0.619	99.803			
11	0.019	0.156	99.959			
12	0.005	0.041	100.000			

4.2.2.2   Mt. Elgon water chemistry

The chemistry shows low mineralization for water samples from Mt. Elgon and higher values for samples from the metamorphic rocks. The descriptive statistics reveal that the mean and median ionic composition is within the recommended KEBS and WHO levels, *Table 4.39*.

Table 4.39. Descriptive statistics for Mt. Elgon ionic composition

Parameter	Fe^{3+}	Mn^{2+}	Ca^{2+}	Mg^{2+}	Na^+	K^+	HCO_3^{3-}	Cl^-	F^-	NO_3^{2-}	SO_4^{2-}
Mean	0.08	0.01	20.18	13.89	31.81	5.39	193.30	8.46	0.57	4.62	3.23
Standard Error	0.03	0.01	2.32	2.53	8.16	1.15	25.90	1.61	0.16	0.64	0.64
Median	0.00	0.00	17.60	6.32	11.30	3.30	134.20	7.00	0.13	3.30	1.54
Standard Deviation	0.22	0.04	14.85	16.18	52.24	7.37	165.85	10.29	1.02	4.03	4.13
Kurtosis	11.59	9.88	2.49	1.53	9.92	24.21	0.04	10.88	9.86	2.76	3.28
Skewness	3.40	3.23	1.37	1.55	3.06	4.63	1.04	2.81	3.02	1.54	2.04
Minimum	0.00	0.00	0.80	0.00	2.40	0.60	24.40	0.00	0.03	0.08	0.00
Maximum	0.97	0.20	69.60	64.67	250.00	46.00	641.72	56.00	5.06	18.29	16.10
Count	41.00	41.00	41.00	41.00	41.00	41.00	41.00	41.00	41.00	40.00	41.00

Ionic plot (*Figure 4.34*) and the correlation matrix (*Table 4.40)* confirm that the alkali metals (Na and K) dominate the alkali earth metals Ca and Mg while the weak acids strongly dominate the strong acids (Cl and SO_4).
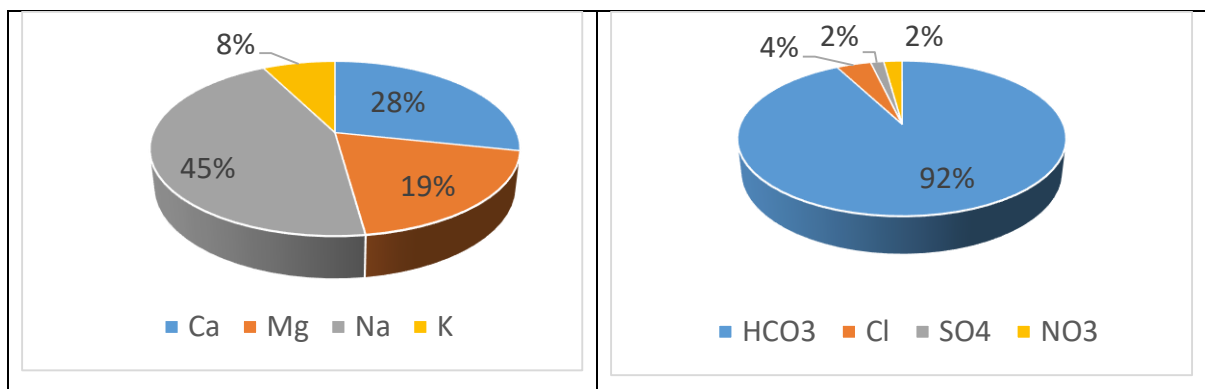
Figure 4.34. The plot of the main cations and anions in the Mt. Elgon water.

The student t-test shows a significant statistical relationship between the alkali ions and alkali earth ions, *Table 4.40*. There is a strong relationship between bicarbonate ions and fluoride and sulphate ions, *Table 4.41*. Fluoride shows a significant correlation with sodium and potassium,

Table 4.40. Correlation matrix for major ions from Mt. Elgon water

		Fe²⁺ (mg/L)	Mn²⁺ (mg/L)	Ca²⁺ (mg/L)	Mg²⁺ (mg/L)	Na⁺ (mg/L)	K⁺ (mg/L)	HCO₃⁻ (mg/L)	Cl⁻ (mg/L)	F⁻ (mg/L)	NO₃²⁻ (mg/L)	SO₄²⁻ (mg/L)
Correlation	Fe²⁺ (mg/L)	1.000	0.280	0.037	0.060	0.229	0.284	0.201	0.480	0.157	-0.080	-0.061
	Mn²⁺ (mg/L)	0.280	1.000	0.046	-0.049	-0.036	-0.088	-0.036	-0.125	0.096	0.070	-0.066
	Ca²⁺(mg/L)	0.037	0.046	1.000	**0.721**	-0.160	-0.126	0.420	0.302	0.029	0.176	0.325
	Mg²⁺(mg/L)	0.060	-0.049	**0.721**	1.000	0.012	0.036	**0.640**	0.353	0.175	0.025	0.371
	Na⁺(mg/L)	0.229	-0.036	-0.160	0.012	1.000	**0.864**	**0.749**	**0.628**	**0.826**	-0.007	**0.665**
	K⁺(mg/L)	0.284	-0.088	-0.126	0.036	**0.864**	1.000	**0.669**	**0.534**	**0.788**	-0.091	**0.598**
	HCO₃⁻ (mg/L)	0.201	-0.036	0.420	**0.640**	**0.749**	**0.669**	1.000	0.664	**0.748**	-0.070	**0.784**
	Cl⁻(mg/L)	0.480	-0.125	0.302	0.353	**0.628**	**0.534**	0.664	1.000	0.401	0.238	0.447
	F⁻(mg/L)	0.157	0.096	0.029	0.175	**0.826**	**0.788**	**0.748**	0.401	1.000	-0.016	**0.667**
	NO₃²⁻ (mg/L)	-0.080	0.070	0.176	0.025	-0.007	-0.091	-0.070	0.238	-0.016	1.000	-0.101
	SO₄²⁻(mg/L)	-0.061	-0.066	0.325	0.371	**0.665**	**0.598**	**0.784**	0.447	**0.667**	-0.101	1.000
Student t-Test Sig. (1-tailed)	Fe²⁺ (mg/L)		**0.040**	0.410	0.357	0.078	0.038	0.106	**0.001**	0.166	0.312	0.353
	Mn²⁺ (mg/L)	**0.040**		0.388	0.381	0.413	0.294	0.412	0.222	0.277	0.335	0.343
	Ca²⁺(mg/L)	0.410	0.388		**0.000**	0.162	0.219	**0.003**	**0.029**	0.429	0.139	**0.020**
	Mg²⁺(mg/L)	0.357	0.381	**0.000**		0.470	0.412	**0.000**	**0.013**	0.140	0.440	**0.009**
	Na⁺(mg/L)	0.078	0.413	0.162	0.470		**0.000**	**0.000**	**0.000**	**0.000**	0.484	**0.000**
	K⁺(mg/L)	0.038	0.294	0.219	0.412	**0.000**		**0.000**	**0.000**	**0.000**	0.288	**0.000**
	HCO3- (mg/L)	0.106	0.412	**0.003**	0.000	0.000	0.000		0.000	0.000	0.333	**0.000**
	Cl⁻(mg/L)	**0.001**	0.222	**0.029**	0.013	**0.000**	**0.000**	**0.000**		**0.005**	0.069	**0.002**
	F⁻(mg/L)	0.166	0.277	0.429	0.140	**0.000**	**0.000**	**0.000**	0.005		0.462	**0.000**
	NO32- (mg/L)	0.312	0.335	0.139	0.440	0.484	0.288	0.333	0.069	0.462		0.268
	SO₄²⁻(mg/L)	0.353	0.343	0.020	**0.009**	**0.000**	**0.000**	**0.000**	**0.002**	**0.000**	0.268	

Table 4.41. Student t-Test for relationship between anions

t-Test: Two-Sample Assuming Equal Variances		
	K⁺(mg/L)	*Na⁺(mg/L)*
Mean	5.39	31.81
Variance	54.26	2729.02
Observations	41.00	41.00
Pooled Variance	1391.64	
Hypothesized Mean Difference	0.00	
df	80.00	
t Stat	-3.21	
P(T<=t) one-tail	0.00	
t Critical one-tail	1.66	
P(T<=t) two-tail	**0.00**	
t Critical two-tail	1.99	

t-Test: Two-Sample Assuming Equal Variances		
	Ca²⁺(mg/L)	*Mg²⁺(mg/L)*
Mean	20.18	13.89
Variance	220.40	261.75
Observations	41.00	41.00
Pooled Variance	241.07	
Hypothesized Mean Difference	0.00	
df	80.00	
t Stat	1.83	
P(T<=t) one-tail	0.04	
t Critical one-tail	1.66	
P(T<=t) two-tail	**0.05**	
t Critical two-tail	1.99	

Table 4.42. Student t-Test between bicarbonate and sulphate and between bicarbonate and fluoride ions

t-Test: Two-Sample Assuming Equal Variances		
	SO₄²⁻(mg/L)	*HCO3⁻ (mg/L)*
Mean	3.23	193.30
Variance	17.04	27505.00
Observations	41.00	41.00
Pooled Variance	13761.02	
Hypothesized Mean Difference	0.00	
df	80.00	
t Stat	-7.34	
P(T<=t) one-tail	0.00	
t Critical one-tail	1.66	
P(T<=t) two-tail	**0.00**	
t Critical two-tail	1.99	

t-Test: Two-Sample Assuming Equal Variances		
	F⁻(mg/L)	*HCO3⁻ (mg/L)*
Mean	0.57	193.30
Variance	1.03	27505.00
Observations	41.00	41.00
Pooled Variance	13753.01	
Hypothesized Mean Difference	0.00	
df	80.00	
t Stat	-7.44	
P(T<=t) one-tail	0.00	
t Critical one-tail	1.66	
P(T<=t) two-tail	**0.00**	
t Critical two-tail	1.99	

Table 4.43. Student t-Test for the significance of the correlation between fluoride and alkali ions

t-Test: Two-Sample Assuming Equal Variances				t-Test: Two-Sample Assuming Equal Variances		
	F⁻	**Na⁺**			**F⁻**	**K⁺**
Mean	0.57	31.81	Mean		0.57	5.39
Variance	1.03	2729.02	Variance		1.03	54.26
Observations	41.00	41.00	Observations		41.00	41.00
Pooled Variance	1365.03		Pooled Variance		27.65	
Hypothesized Mean Difference	0.00		Hypothesized Mean Difference		0.00	
df	80.00		df		80.00	
t Stat	-3.83		t Stat		-4.15	
P(T<=t) one-tail	0.00		P(T<=t) one-tail		0.00	
t Critical one-tail	1.66		t Critical one-tail		1.66	
P(T<=t) two-tail	0.00		P(T<=t) two-tail		0.00	
t Critical two-tail	1.99		t Critical two-tail		1.99	

The KMO and Bartlett's test of sphericity, *Table 4.44*, shows that the data can be subjected to factor analysis. The PCA showed four principal components *Table 4.45*.

Table 4.44. KMO test for sampling adequacy and Bartlett's test of sphericity for Mt. Elgon chemical data

Kaiser-Meyer-Olkin Measure of Sampling Adequacy.		.531
Bartlett's Test of Sphericity	Approx. Chi-Square	403.448
	df	55
	Sig.	.000

Principal component 1 has alkali metal ions, fluoride, bicarbonates, sulphates and chlorides.

Table 4.45. PCA matrix and components for major ions.

	Component			
	1	2	3	4
Na$^+$(mg/L)	.965			
K$^+$(mg/L)	.924			
F$^-$(mg/L)	.879			
HCO$_3^-$ (mg/L)	.815	.542		
SO$_4^{2-}$(mg/L)	.760	.393		
Cl$^-$(mg/L)	.628	.307		.500
Ca^{2+}(mg/L)		.921		
Mg^{2+}(mg/L)		.917		
Fe^{2+} (mg/L)			.840	
Mn^{2+} (mg/L)			.736	
NO$_3^{2-}$ (mg/L)				.912
Extraction Method: Principal Component Analysis.				
Rotation Method: Varimax with Kaiser Normalization.				
a. Rotation converged in 5 iterations.				

Component	1	2	3	4
1	.934	.336	.095	.069
2	-.339	.922	-.056	.180
3	-.102	-.053	.923	.368
4	.037	-.187	-.370	.910

The scree plot clearly shows the four PCA components, *Figure 4.35*. The four components are above the eigenvalue of one, defined during the loading of data for analysis.
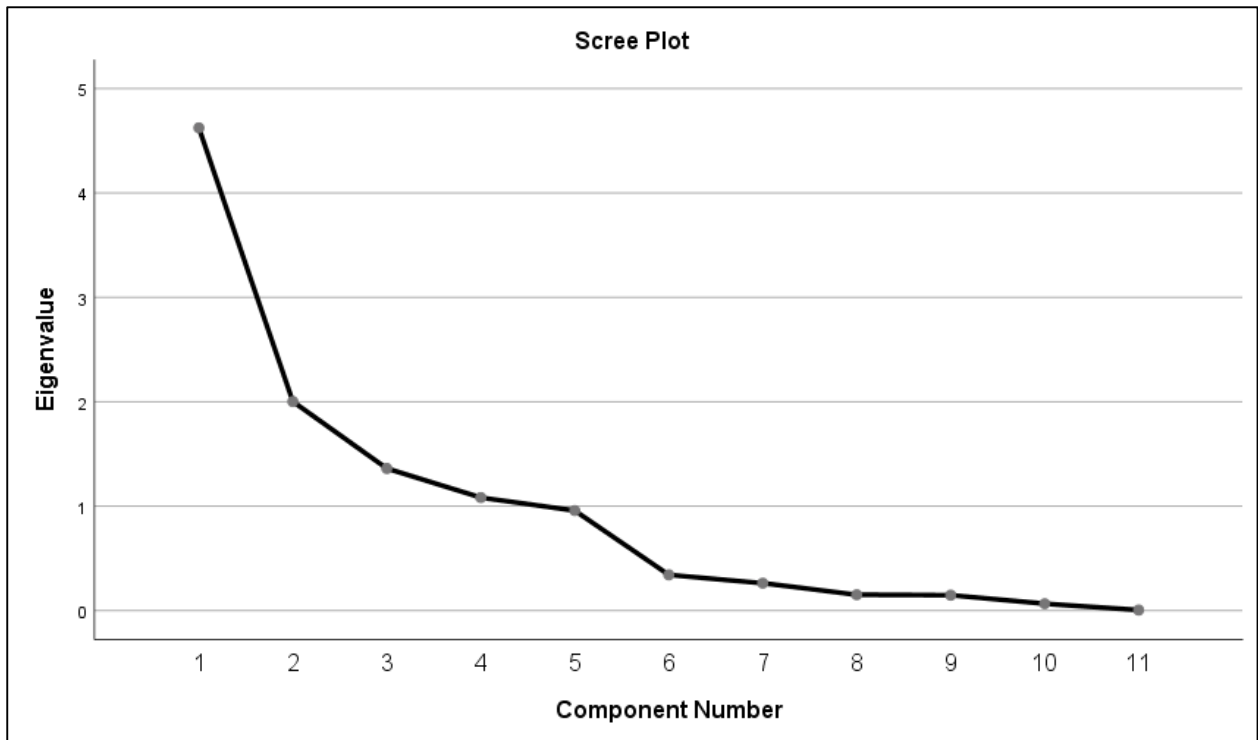
Figure 4.35. Scree plot for the four main components with eigenvalue of more than 1

4.2.3 Multivariate statistical analysis of water chemistry data for Kisumu study site

Multivariate statistical methods applied to groundwater chemistry provide valuable insight into the main hydrochemical species, hydrochemical processes, and water flow paths critical to groundwater evolution. Various results are presented in the subsequent sub-sections.

4.2.3.1 Piper plot for Kisumu water chemical data

The Piper plot (*Figure 4.36*) show the various water types Kisumu. The plot shows that all water types in Kisumu are dominated by bicarbonate. Sodium and calcium are the main cations. The sodium and potassium bicarbonate/carbonate water is, therefore, the primary type in Kisumu.

133
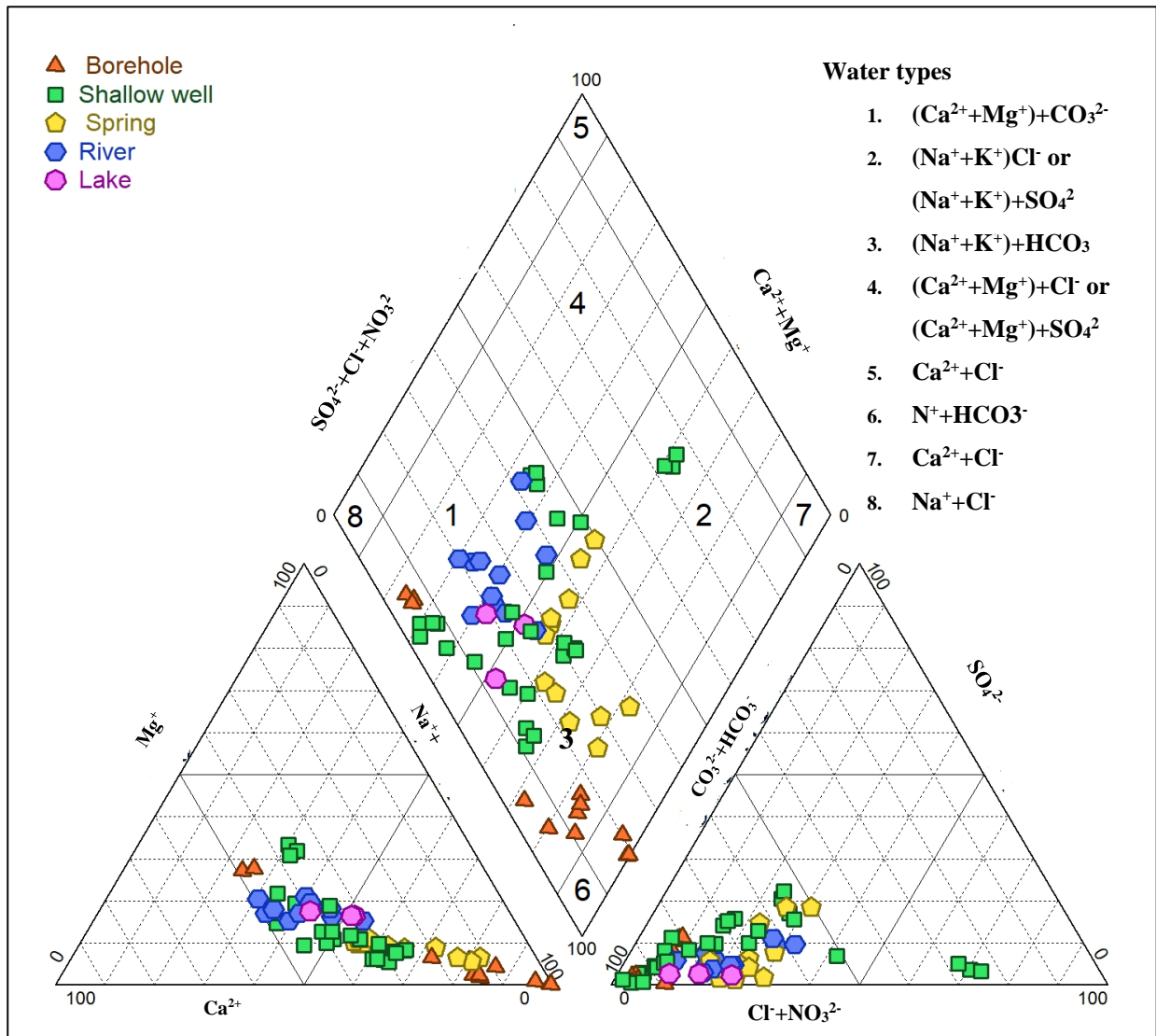
Figure 4.36. Piper trilinear diagram describing the chemical composition of water samples of the studied sites in Kisumu.

4.2.3.2   *Stiff plot for Kisumu water chemistry*

The Stiff diagram was constructed by plotting the milli-equivalents per litre (meq/L) of three cations ($Na^+ + K^+$, Ca^{2+} and Mg^{2+}) and three anions (Cl^-, $HCO_3^- + CO_3^{2-}$ and $SO_4^{2-} + NO_3^{2-}$). These plots were used to show changes in water quality at a single location over some time, *Figure 4.37*.
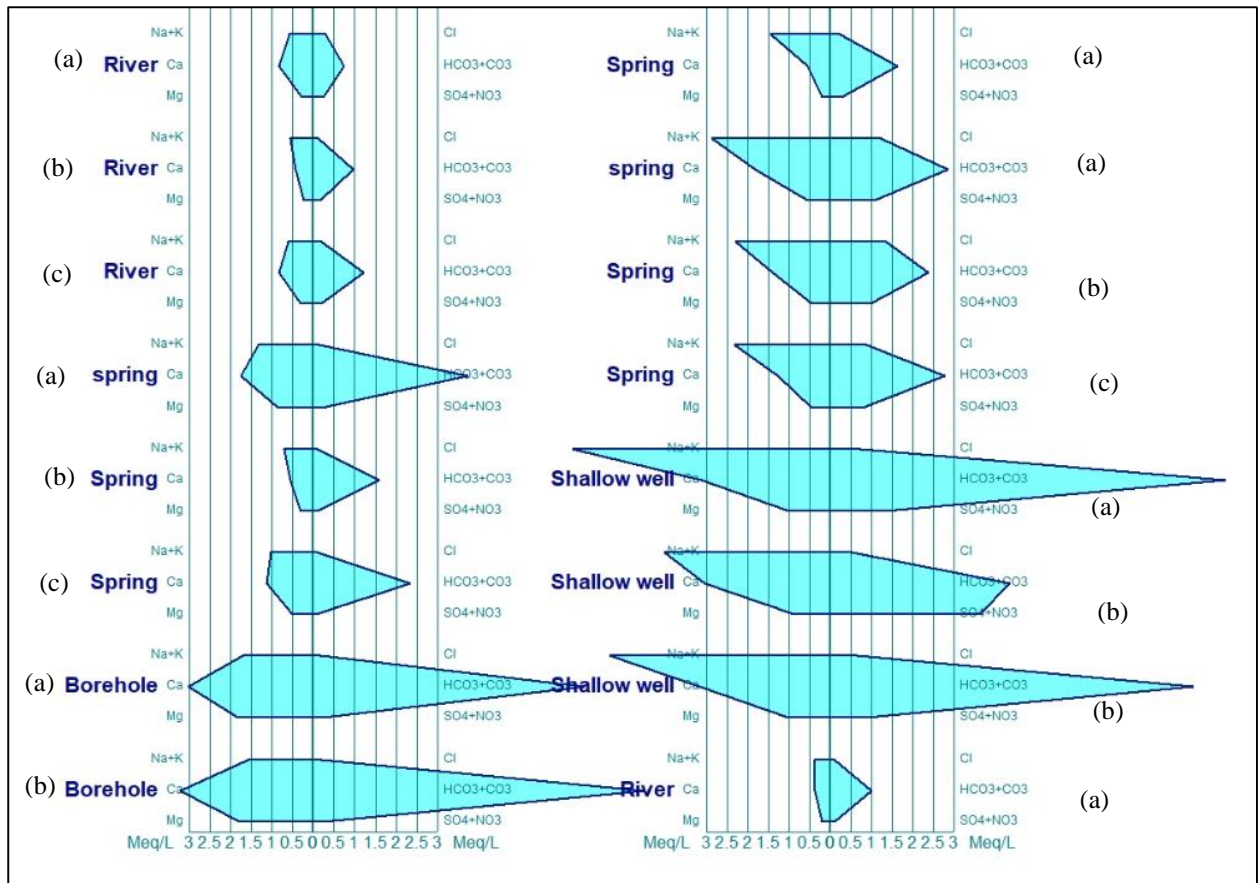
Figure 4.37. The stiff plot of Kisumu water showing very little change in water chemistry at single locations (river, spring, borehole and shallow well) during 2017 sampling campaigns in (a) March, (b) June and (c) September.

4.2.3.3   Schoeller Berkaloff plot for Kisumu water chemistry

A maximum of 14 samples can be plotted at once using the Diagramme Software. A selected plot (*Figure 4.38*) of 14 samples from the five water types in Kisumu comprising river water, lake water, borehole water, spring water and river water is given. The result reveals that the Kisumu water is dominated by sodium and bicarbonate type. This supports the earlier conclusion made after evaluating the Piper plot.
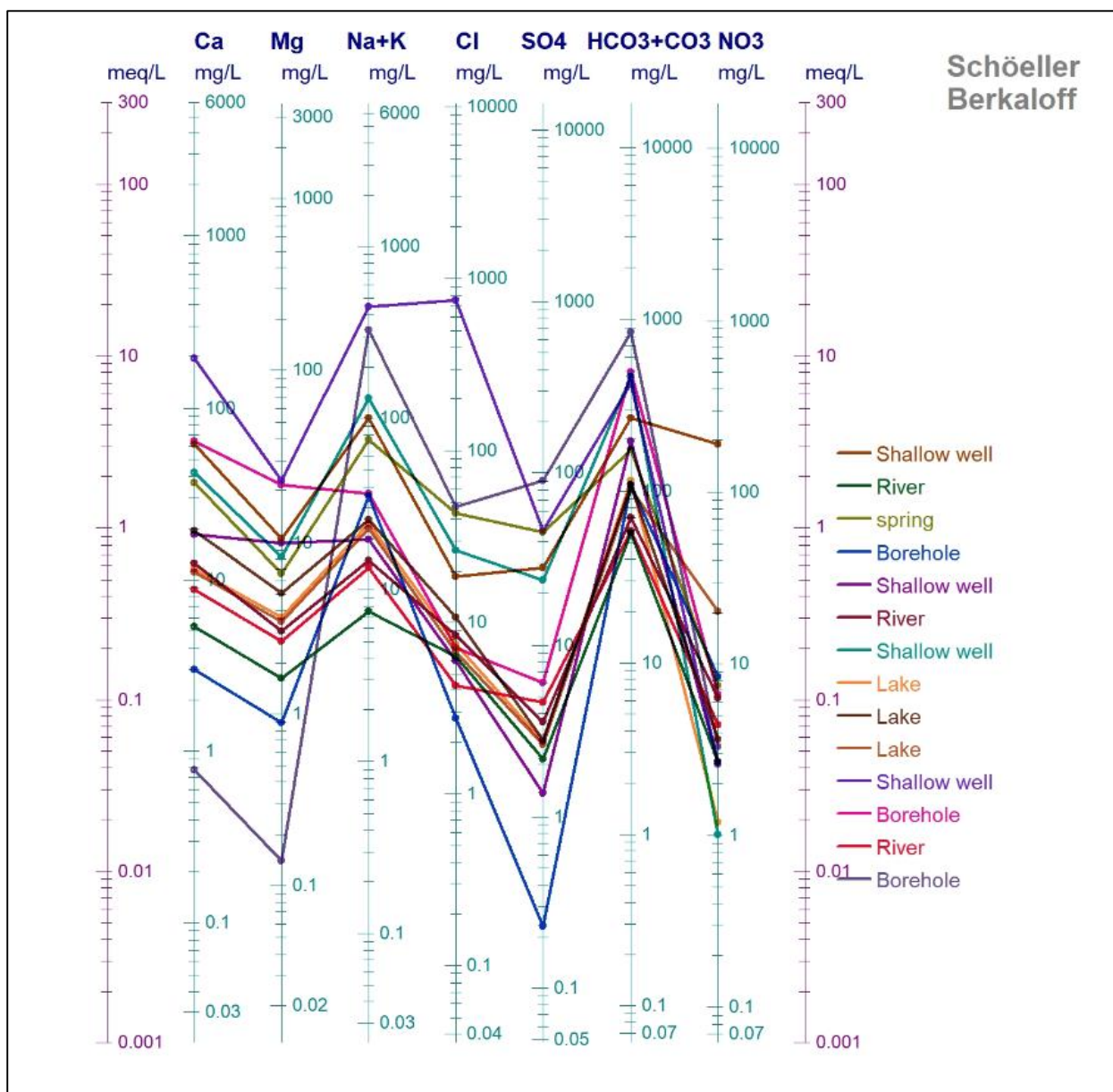
Figure 4.38. Shoeller Berkaloff plot for Kisumu water. The water is dominated by the Na⁺+K⁺ bicarbonate water

4.2.3.4   *Wilcox plot for Kisumu water chemistry*

The Wilcox plot (*Figure 4.39*) was used to determine the suitability of Kisumu water for irrigation and lately for domestic use (Hwang *et al*., 2017; Jeon *et al*., 2020; Selvakumar *et al*., 2017). Based on this plot, Kisumu water is suitable for domestic and irrigation use. However, water from a shallow well in Otonglo, which has very high conductivity values, was classified as unsuitable. Wandiege borehole water had very high sodium levels, and hence it is a bit saline

to the taste. Other parameters from this borehole were within the KEBS/WHO maximum recommended levels (KEBS, 2015; WHO, 2017).
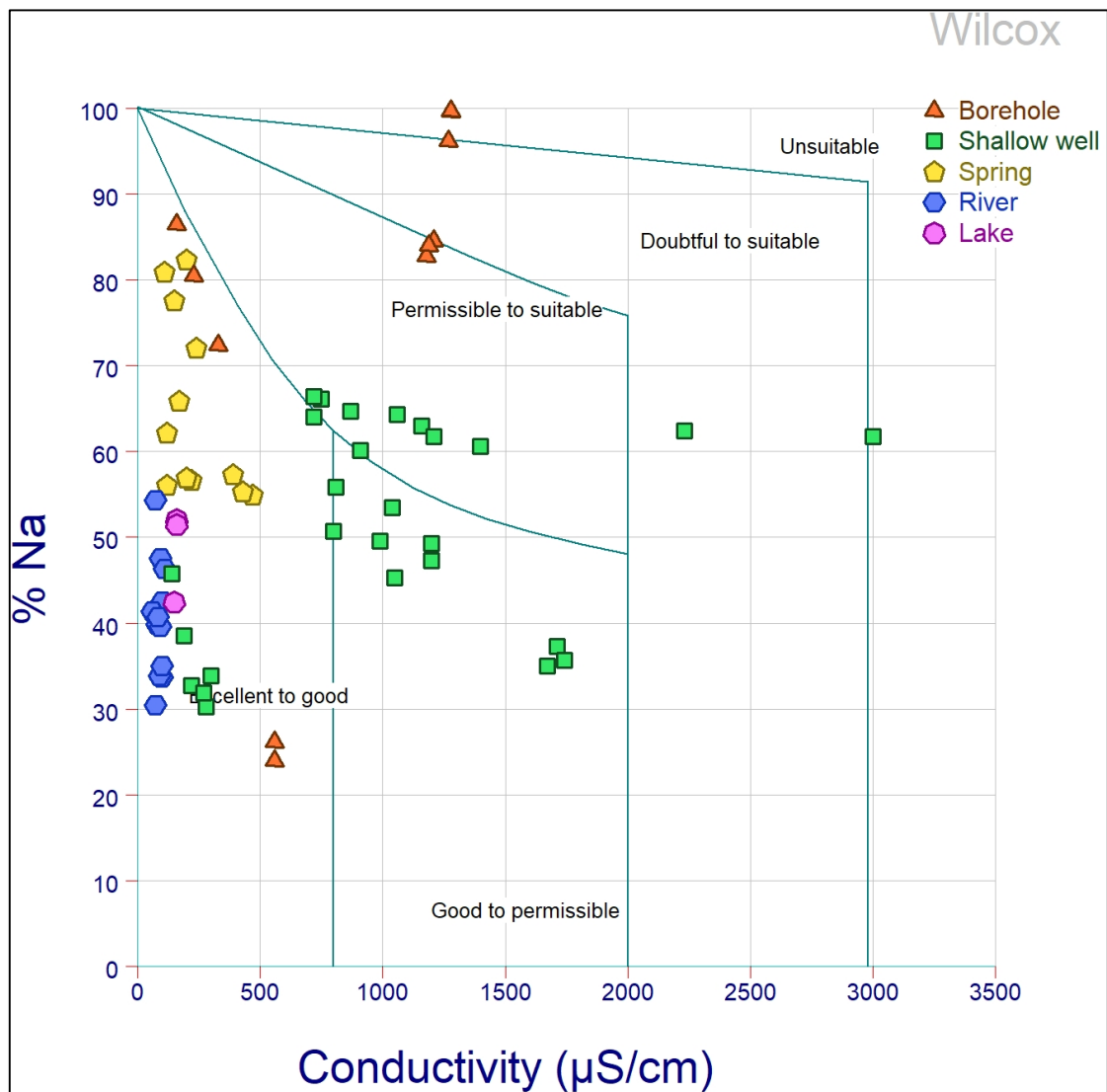
Figure 4.39. Wilcox classification of Kisumu water. The groundwater is suitable for domestic use. However, a high sodium level is noted in one borehole (Wandiege), making it doubtful for direct use.

4.2.4 Multivariate statistical analysis of water chemistry data for Mt. Elgon study site

4.2.4.1 Piper plot for Mt. Elgon water chemistry

The hydrochemical facies for Mt. Elgon water indicates that the dominant water is type 1, $(Ca^{+}+Mg^{+})$ - HCO_3^{-} type, *Figure 4.40.* However, borehole water is highly mineralized and is of type 3: $(Na^{+}+K^{+})$ - HCO_3^{-}.
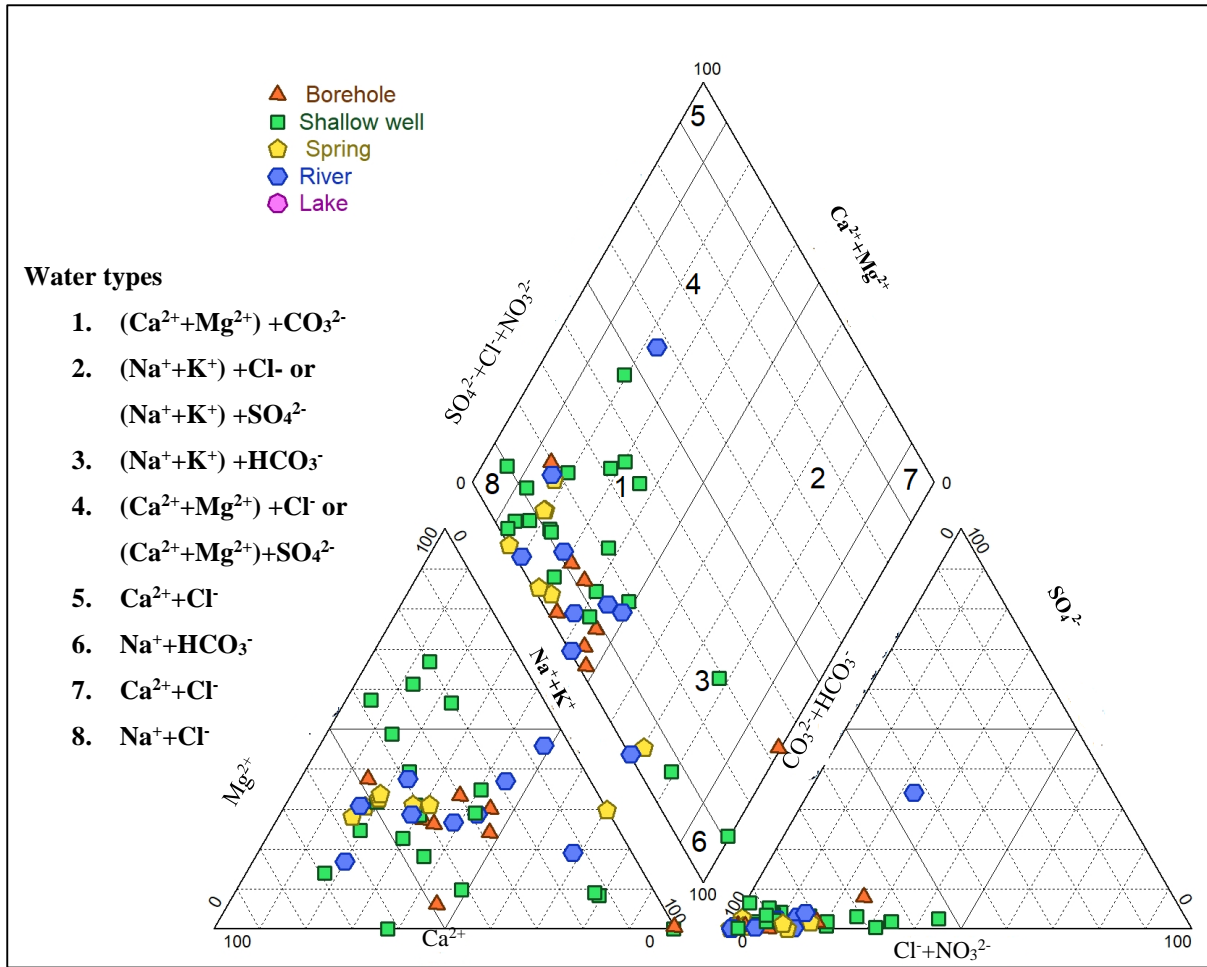
Figure 4.40. Piper plot of the major cations and anions for Mt. Elgon water sample. The dominant water types are type 1 and type 8.

4.2.4.2   Schoeller-Berkaloff plot for Mt. Elgon water chemistry

The most outstanding feature of the Schoeller-Berkaloff plot for Mt. Elgon water, *Figure 4.41*, was the presence of waters dominated by the (Na^+ + K^+) and HCO_3^-. This plot supports results from the Piper plot discussed earlier in figure 4.40.
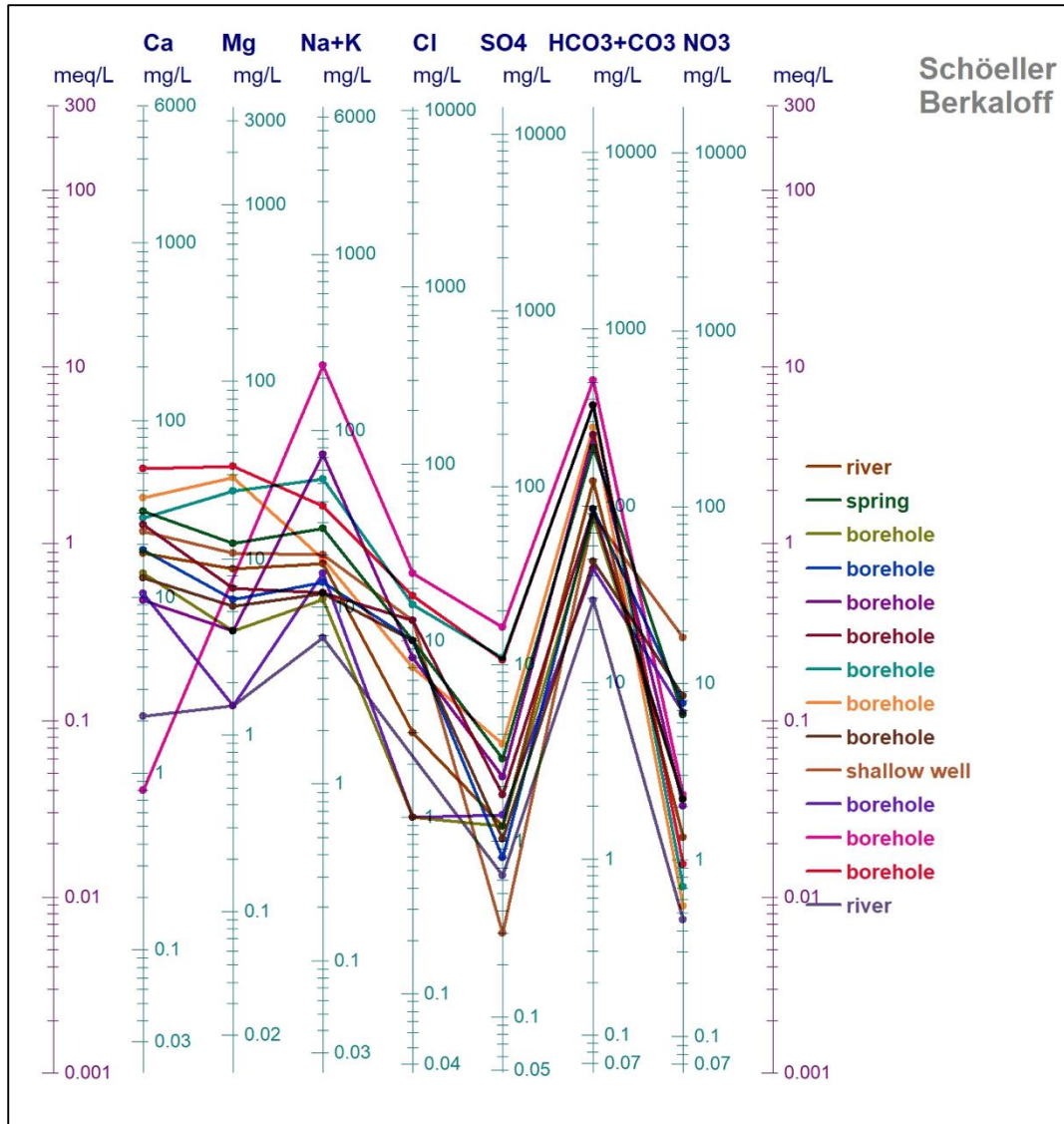
Figure 4.41. Schoeller-Berkaloff plot for Mt. Elgon water. This confirmed the dominance of the bicarbonate in the water.

4.2.4.3   Stiff plot for Mt. Elgon water chemistry

The Stiff plot, *Figure 4.42,* showed the dominance of bicarbonate water in the volcanic Mt. Elgon aquifer. The dominant cations are sodium and potassium. Calcium appears to dominate the shallow wells, while samples from borehole, rivers and springs had low values.
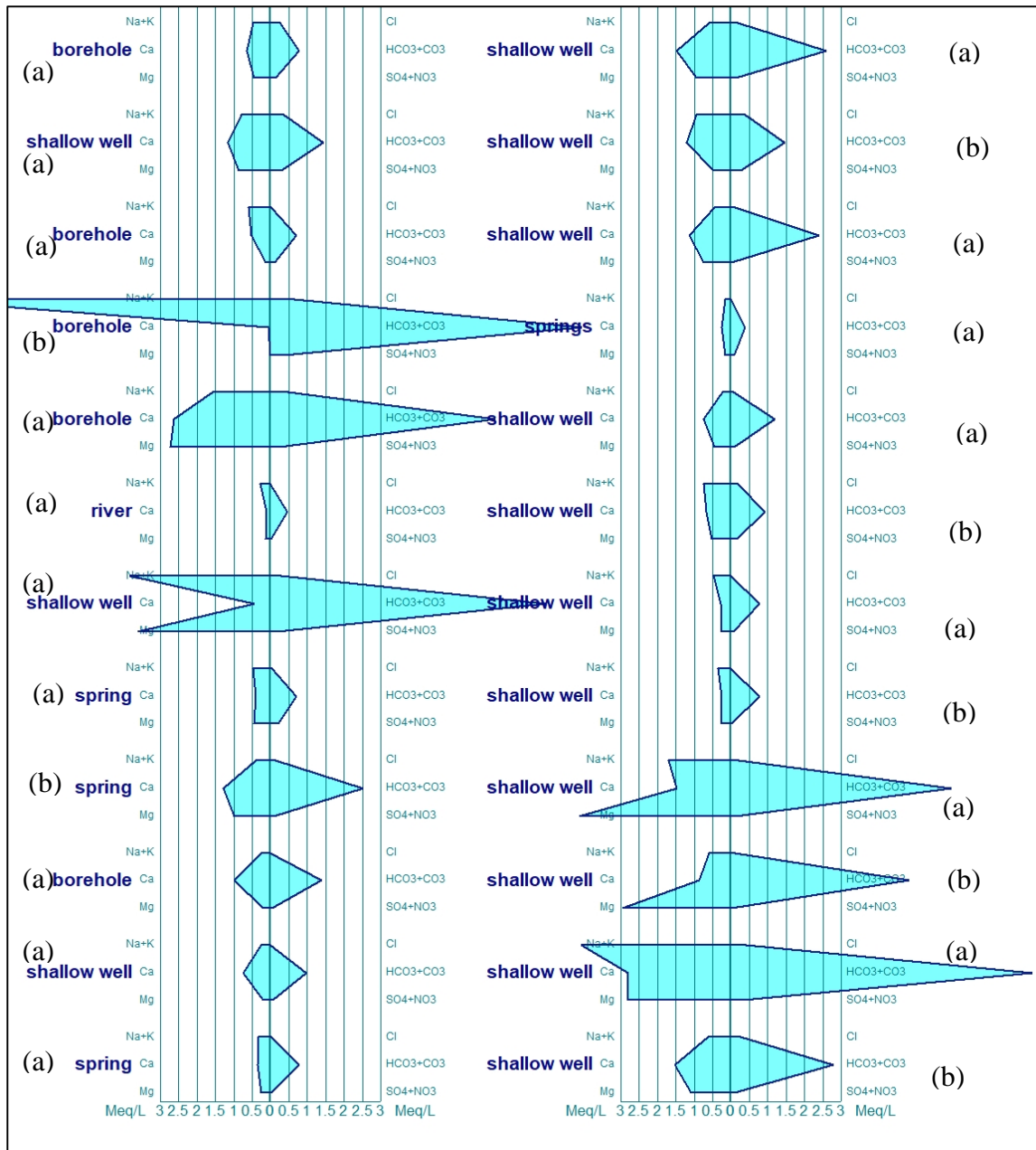
Figure 4.42. The stiff plot of Mt. Elgon water shows the dominance of the bicarbonate in all water types in the study sites for March and May 2014.

4.2.4.4   Wilcox plot for Mt. Elgon water chemistry

Wilcox plot, *Figure 4.43*, showed that Mt. Elgon water is suitable for domestic and agricultural use. Water is chemically ideal for domestic and irrigation use (Wilcox, 1955). However, a

borehole located within metamorphic rocks has high salinity and is unsuitable for domestic and irrigation use.
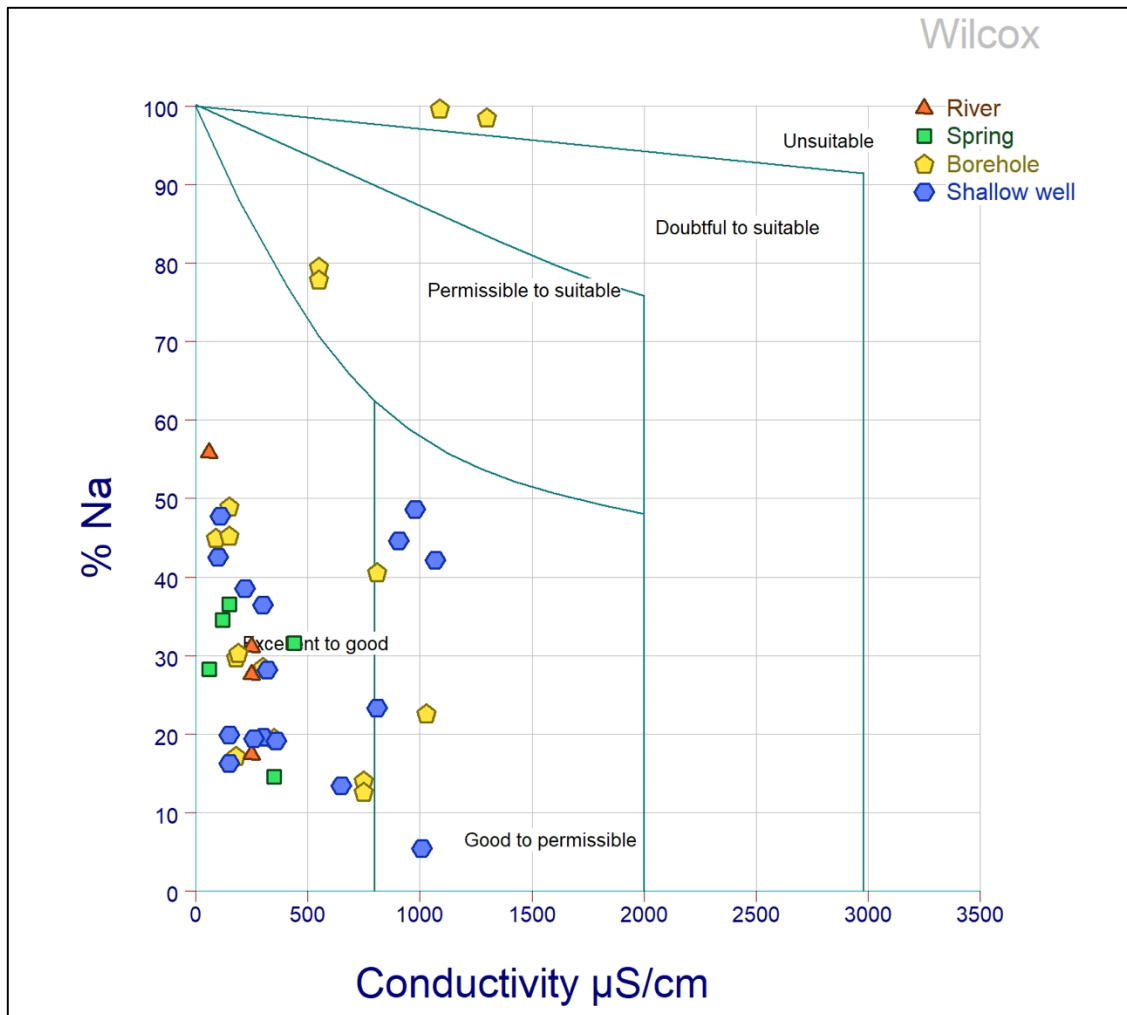
Figure 4.43. Wilcox plot suitability classification of Mt. Elgon water. The water is suitable for irrigation and domestic use (Hwang et al., 2017; Jeon et al., 2020; Selvakumar et al., 2017). One borehole (Saboti) has water (March and May) unsuitable for agriculture and domestic use.

4.2.5   Results on ion exchanges in the Kisumu aquifer

Gibbs diagrams, *Figure 4.44* and *Figure 4.45* distinguish rock-water interactions and ion exchanges as critical geochemical processes in the study area (Gibbs, 1970a). The plot of TDS against $(Na^++K^+)/(Na^++K^++Ca^{2+})$ revealed that the dominant processes are the rock-water interaction and precipitation through ion exchanges. Rock-water interaction entails weathering and dissolution of rock-forming minerals and has the greatest influence on the groundwater

quality using a dissolution of rocks in the study area. The dominance of ions is in the order of $Na^+ > Ca^{2+} > K^+ > Mg^{2+}$ and $HCO_3^- > Cl^- > SO_4^{2-} > NO_3^{2-}$. Evaporation dominance indicates an increase in ionic content due to groundwater evaporation, increasing ionic content within the aeration zones. In contrast, precipitation dominance means releasing or crystallising dissolved salt in the precipitation or rainfall into the groundwater.
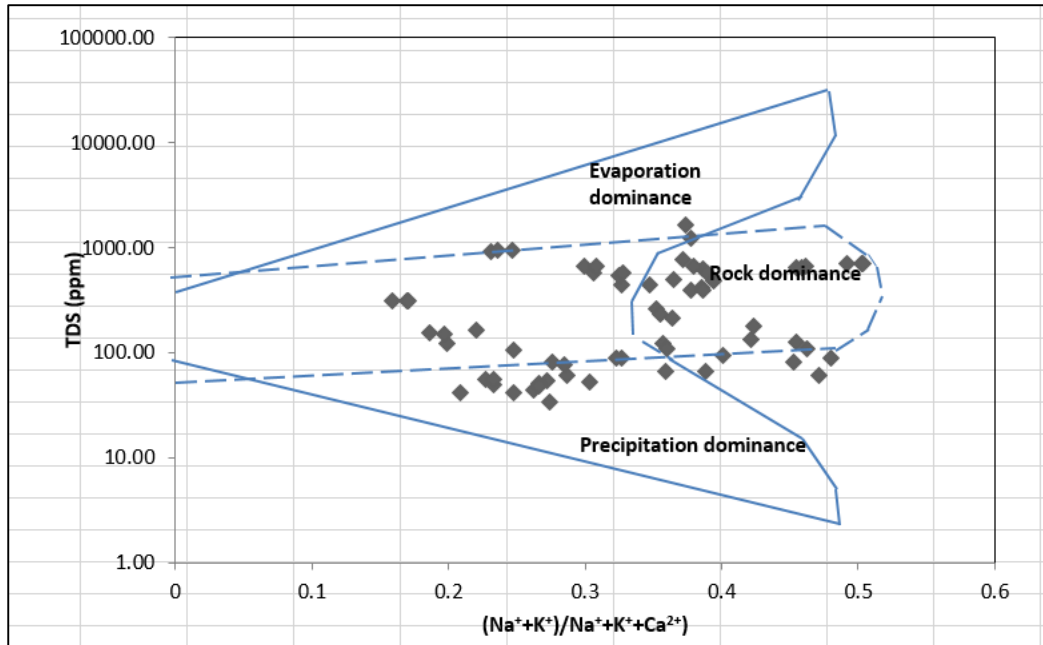
Figure 4.44. Gibbs plot showing the dominant hydrogeochemical processes. These are rock water interaction and precipitation. Precipitation dominate surface water samples with TDS less than 100 mg/L. (these are R. Kibos, Kokelo spring, Kosinda spring, Asengo spring, L. Victoria and Kisian river samples).

The plot of Cl^- against $(Cl^- + HCO_3^-)$ confirms that the dominant processes modifying the water chemistry are the rock-water interaction and precipitation.
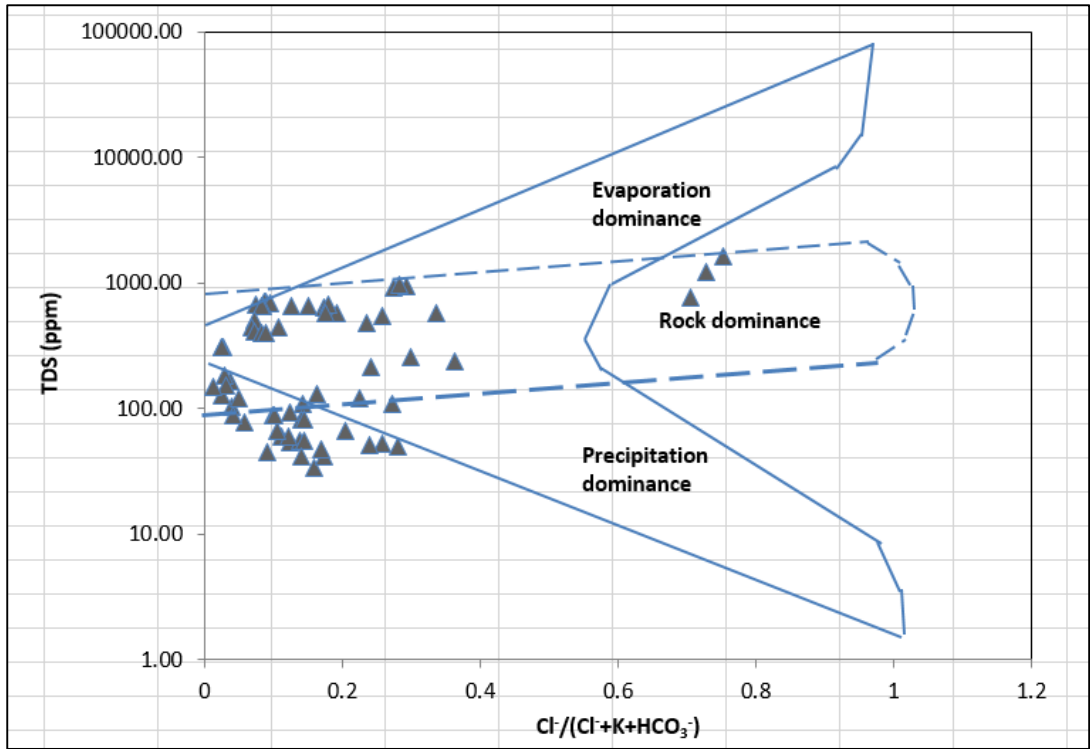
Figure 4.45. Gibbs plot supporting the main geochemical processes. These are rock interactions and precipitation

The strong linear relation between a total cation, alkali and alkali earth ions in the Kisumu study site, earlier shown to be statistically significant, indicates that weathering is the primary geochemical process, *Figure 4.46*. The areas contributing near-zero or zero values and the outliers are shown in *Figure 4.47*. The relationship between the alkali, alkali earth and total cations in the study area indicates that most of the samples plotted near the equal line. This shows that silicate weathering geochemical processes contribute sodium and potassium ions to the groundwater (Sarin *et al*., 1989; Stallard and Edmond, 1983).
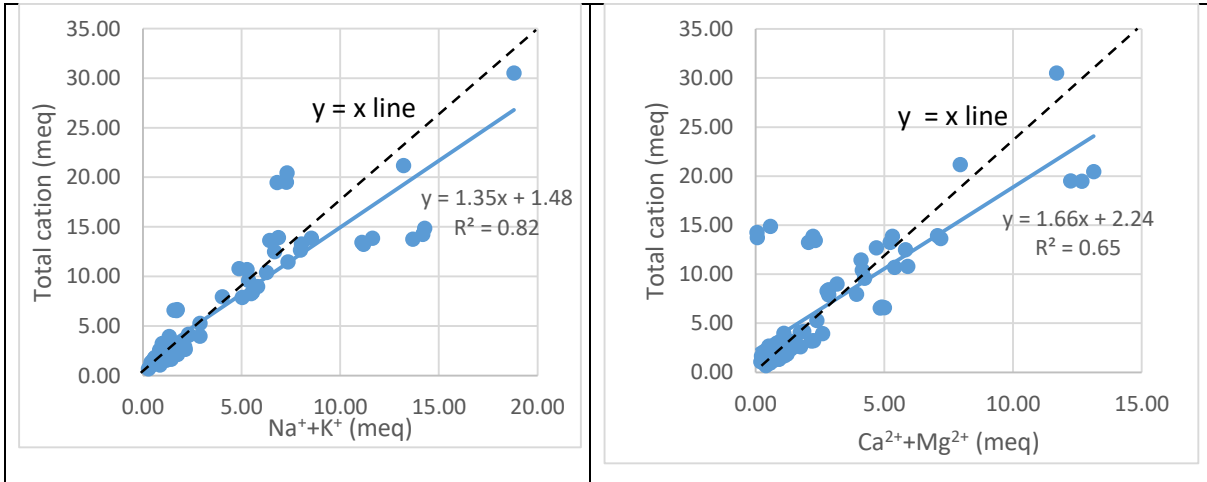
Figure 4.46. Plots of total cation against alkalis and total cations alkaline earth metals. The trend line with a near 1:1 relationship (dotted black line) suggests silicate weathering is the main source of ions in the groundwater.
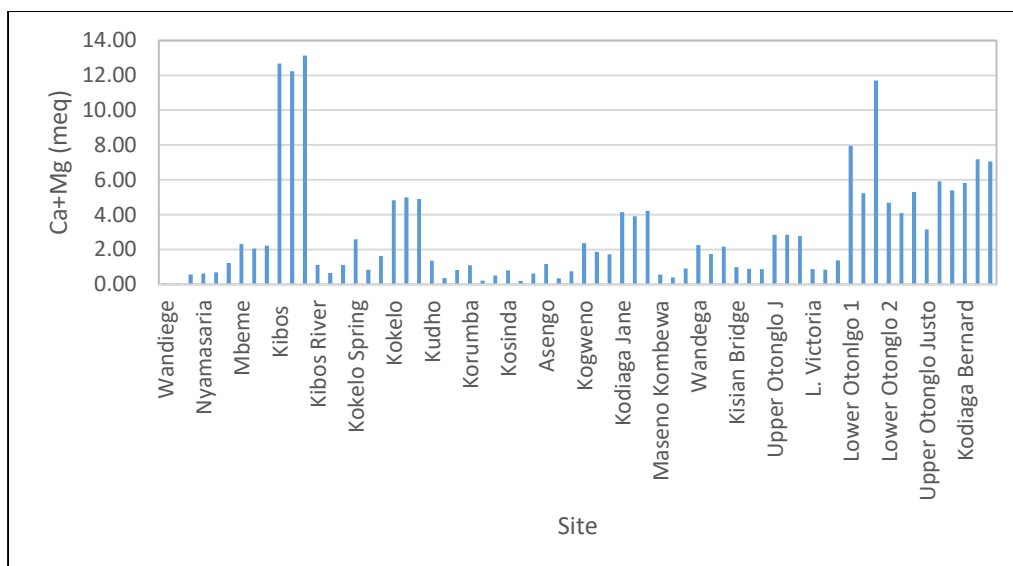
Figure 4.47. The sites contributing low calcium and magnesium total (zero or near zero) and those contributing outliers. Kibos, Kodiaga (Jane and Bernard) and Otonglo are shallow wells.

The plot, *Figure 4.48*, of total alkali versus water type show that near-zero or zero-sum is contributed by surface water bodies including rivers (Kibos, Kisian and Maseno Kombewa), Lake Victoria and springs (Kokelo, Kosinda, Asengo and Wandega)
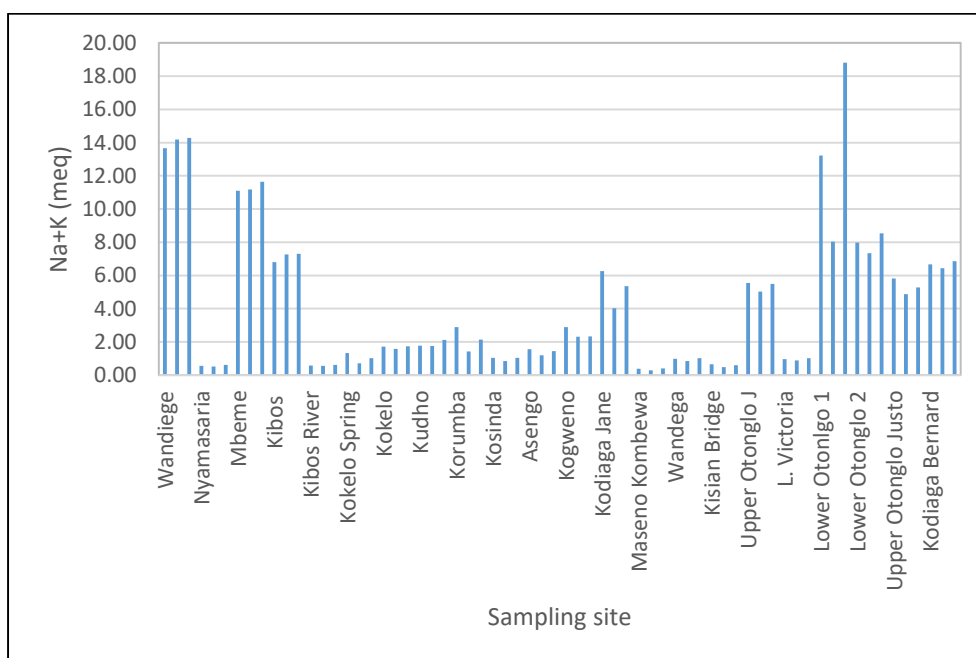
Figure 4.48. The contributors of zero or near zero-sum of alkali ions, in meq, in the study area, and the sites are contributing outliers (Wandiege and Lower Otonglo).

The Na+/Cl- versus EC plot shows the influence of evaporation of shallow groundwater, *Figure 4.49*. The plot indicates a decreasing Na^+/Cl^- ratio with increasing EC. The decreasing Na^+/Cl^- ratio can be explained by increasing Cl- either from atmospheric deposition or anthropogenic processes.
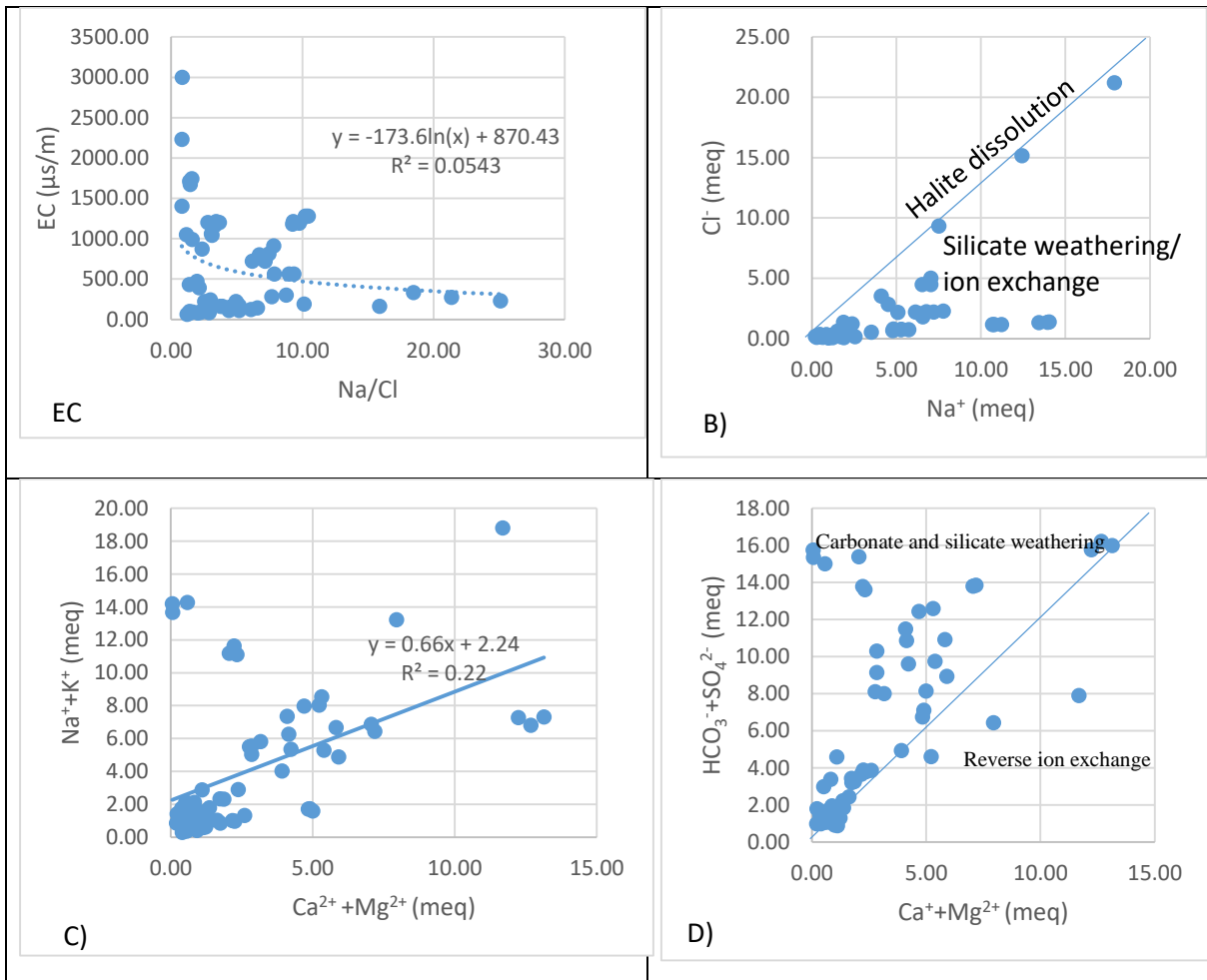
Figure 4.49. The main chemical processes in Kisumu. A) Na^+/Cl^- versus EC; B) Cl^- versus Na^+; C) $Ca^+ + Mg^{2+}$ versus $Na^+ + K^+$ and. D) $Ca^{2+}+Mg^{2+}$ versus $HCO_3^- + SO_4^{2-}$

4.2.6   Results of ion exchanges in the Mt. Elgon aquifer

The main geochemical processes are rock water interactions and precipitation, *Figure 4.50* and *Figure 4.51*.
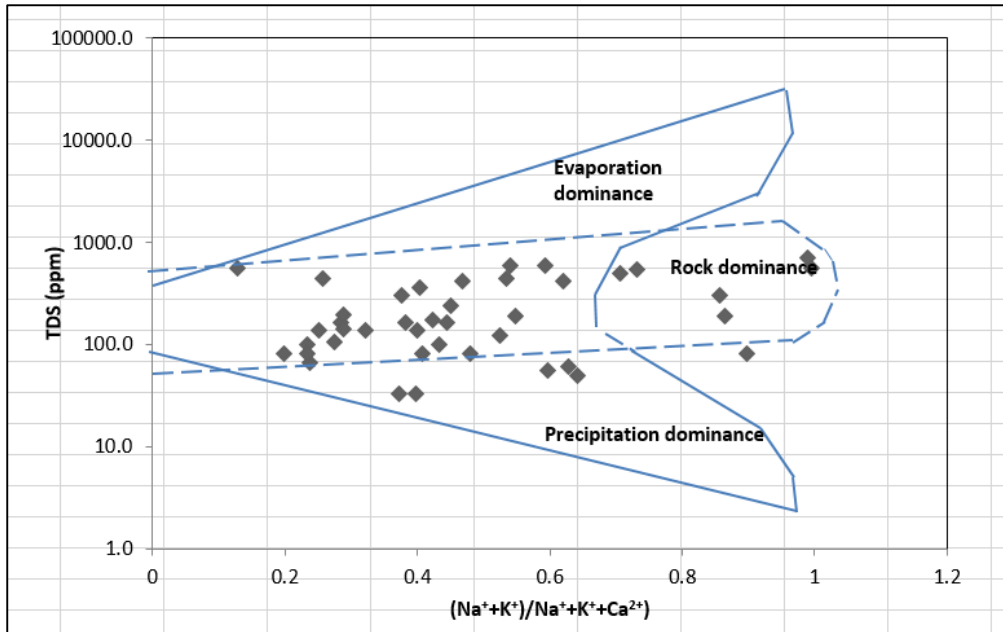
Figure 4.50. The dominance of rock water interaction (boreholes, shallow wells and springs) and precipitation (surface water) as key geochemical processes in the Mt. Elgon study area

The plot suggests that the dominant geochemical processes are rock water interactions and precipitation.
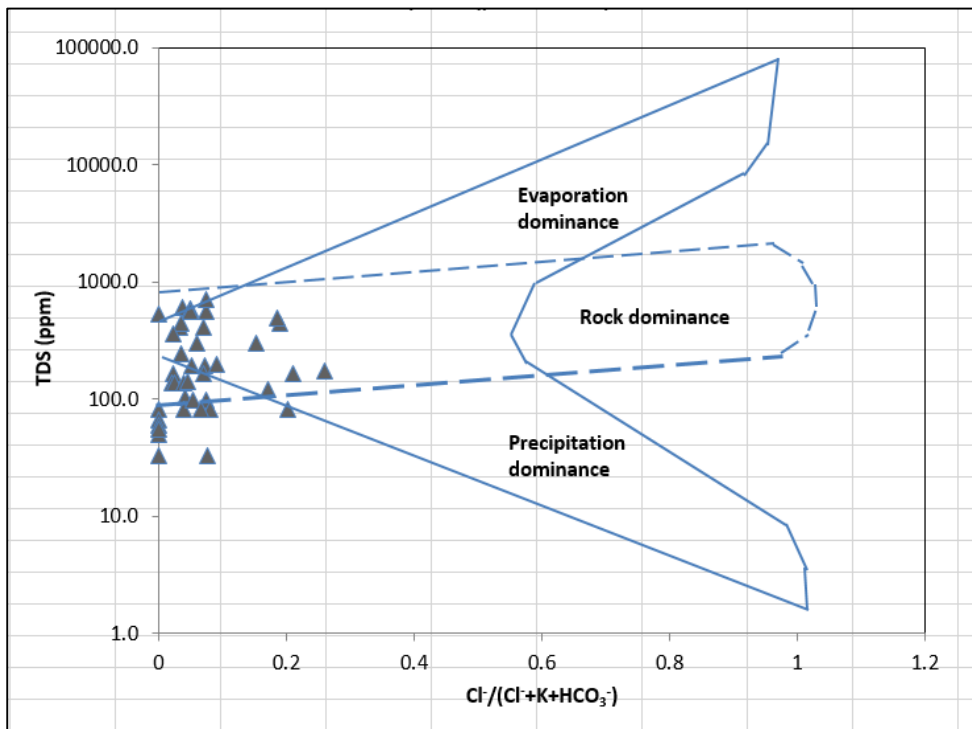
Figure 4.51. The dominance of rock-water interaction and precipitation in Mt. Elgon water samples

The relationship between total cation and alkali and total cation and alkali earth ions reveal that silicate weathering contributes cations to the groundwater, *Figure 4.52*.
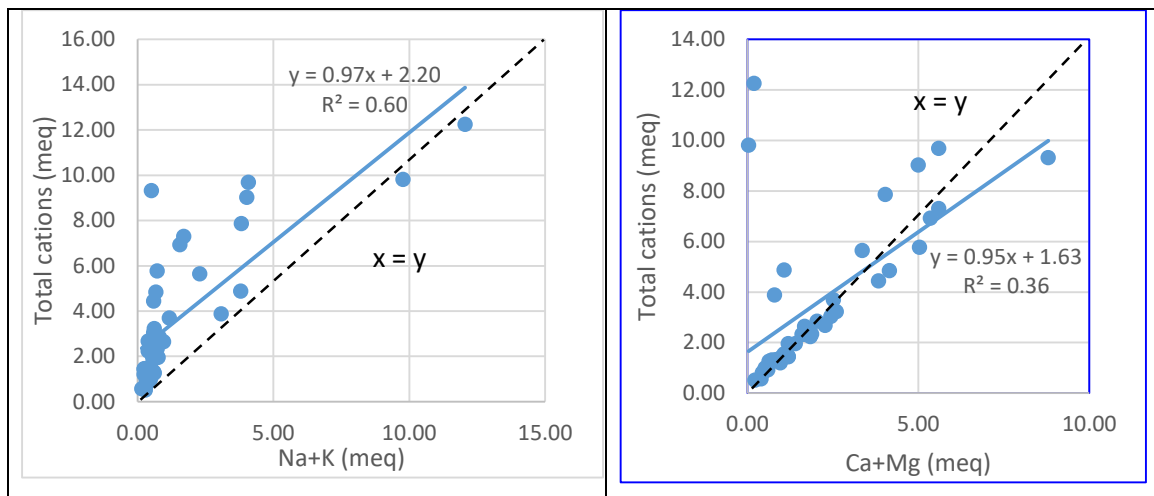
Figure 4.52. The plot of total cations against alkalis and alkaline earth metals. The near 1:1 relationship (dotted black line) suggests silicate weathering is the main source of ions in water. The two samples with no Ca or Mg are from Suam, at the source (from direct precipitation).

Various contributors of the alkali and alkali earth ions are shown in *Figure 4.53* and *Figure 4.54*. Boreholes and shallow wells located within the metamorphic rocks have high values of the alkali and alkali earth ions due to longer residency time and rock water interactions.
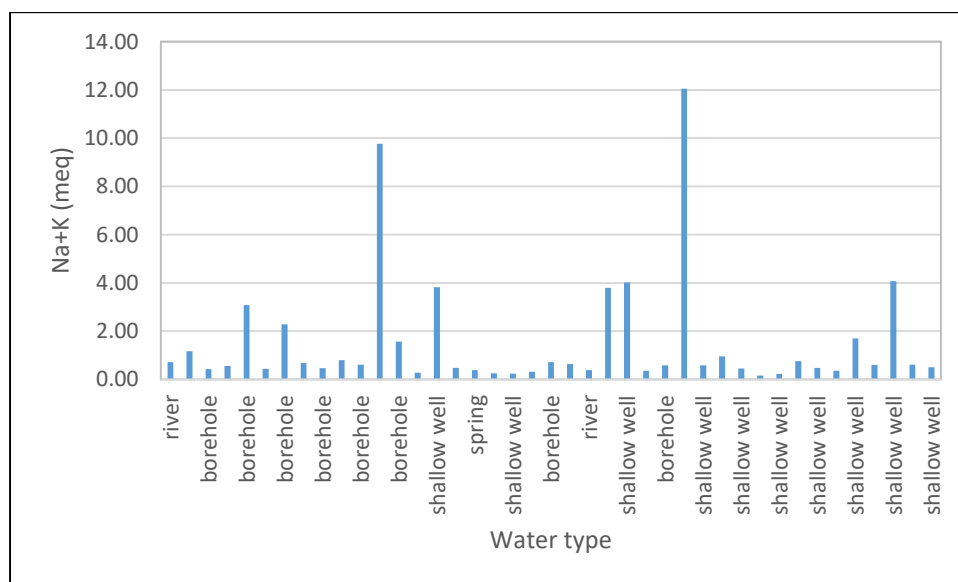
Figure 4.53. Alkali ion sources based on water types in Mt. Elgon. The boreholes are the main contributors to the peaks.
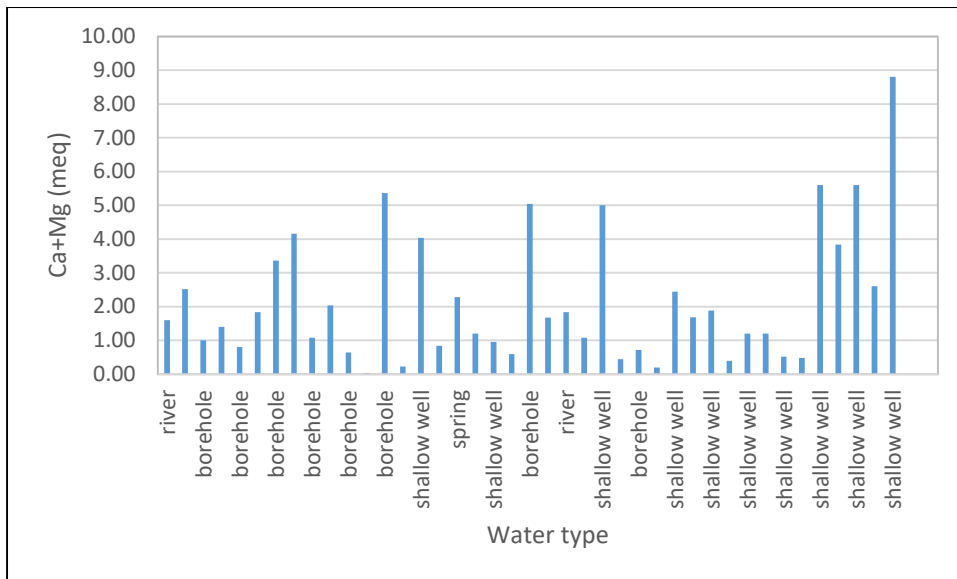
Figure 4.54. Alkali earth ion sources based on water types in Mt. Elgon. Both shallow wells and boreholes are contributors.

Evaporation is expected to affect electrical conductivity while the sodium to chloride ratio remains constant (Subramani *et al.*, 2010). The plot of EC against Na^+/Cl^- shows a correlation implying no evaporation and that Na^+ and Cl^- are coming from the dissolution of rocks. There is also a correlation between Cl^- and Na^+ as demonstrated in the plot of Na^+ and Cl^-, *Figure 4.55*. This shows that there is no addition of chloride from anthropogenic activities or from the atmospheric deposition that would have led to a preferential increase in Cl^-. The source of chloride is the rock water interactions.
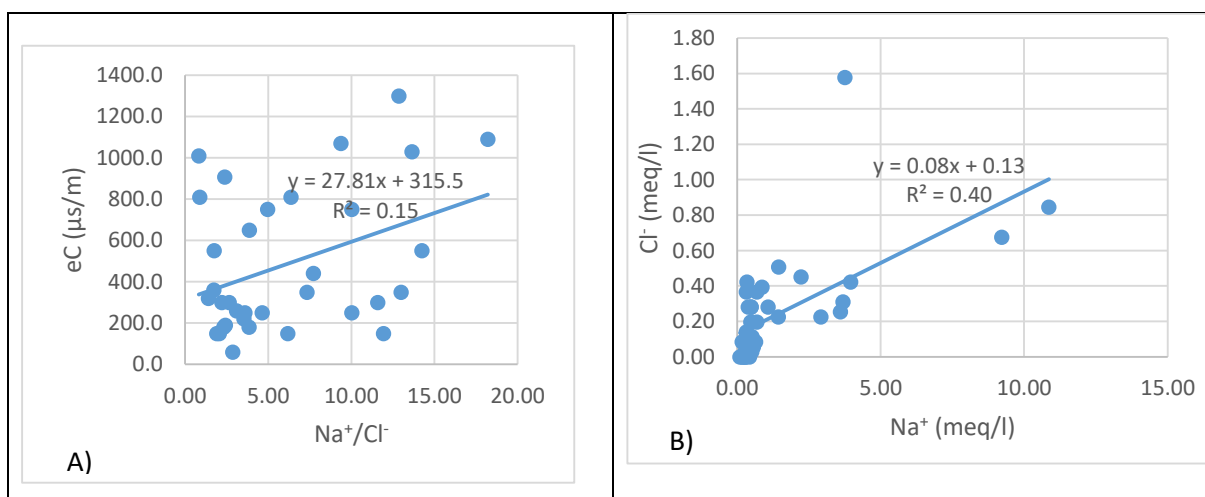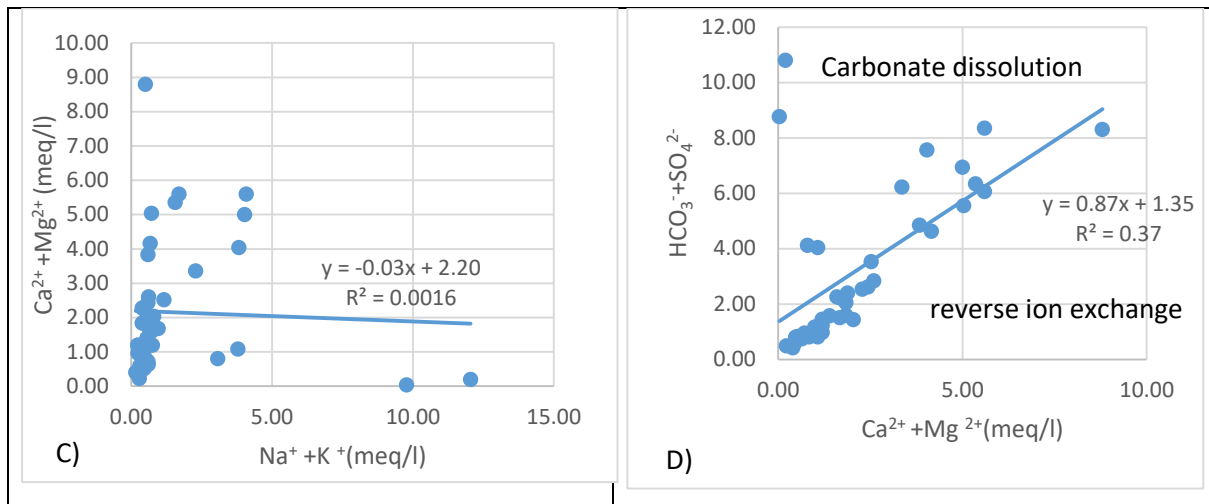
Figure 4.55. Ionic plots showing the main chemical processes in Mt. Elgon. A) Na$^+$/Cl$^-$ versus EC; B) Cl$^-$ versus Na$^+$; C) Ca^{2+}+Mg^{2+} versus Na$^+$+K$^+$ and, D) Ca^{2+}+Mg^{2+} versus HCO$_3^-$ +SO$_4^{2-}$

The test for statistical significance of the correlation between sodium and chloride is positive (0.01 for two tail t-Test and 0.00 for the one-tail test) while that between chloride and potassium is weak (0.12 for one tail and 0.12 to two tail t-Test), *Table 4.46*.

Table 4.46. Student t-Test for the correlation between the sodium, potasium and chloride ions in Mt. Elgon

Parameter	Na$^+$(mg/L)	Cl$^-$(mg/L)	Parameter	K$^+$(mg/L)	Cl$^-$(mg/L)
Mean	31.81	8.46	Mean	5.39	8.46
Variance	2729.02	105.90	Variance	54.26	105.90
Observations	41.00	41.00	Observations	41.00	41.00
Pooled Variance	1417.46		Pooled Variance	80.08	
Hypothesized Mean Difference	0.00		Hypothesized Mean Difference	0.00	
df	80.00		df	80.00	
t Stat	2.81		t Stat	-1.55	
P(T<=t) one-tail	**0.00**		**P(T<=t) one-tail**	**0.06**	
t Critical one-tail	1.66		t Critical one-tail	1.66	
P(T<=t) two-tail	**0.01**		**P(T<=t) two-tail**	**0.12**	
t Critical two-tail	1.99		t Critical two-tail	1.99	

4.2.7   Results of rock-water interactions

This subsection presents several processes modifying water chemistry in Kisumu and Mt. Elgon, including rock-water interactions and precipitation of minerals.

4.2.7.1   Chloro-alkaline indices

The chloro-alkaline indices provide valuable information about the ion-exchange reaction between groundwater and aquifer materials (Al-Ahmadi, 2013; Hem, 1985). These indices were calculated using the following equations;

$$CAI.1 = \frac{Cl^- - (Na^+ + K^+)}{Cl^-}$$

And

$$CAI.2 = \frac{Cl^- - (Na^+ + K^+)}{Cl^-} + (HCO_3^- + SO_4^{2-}SO4 + NO_3^{2-})$$

Where CAI 1and CAI 2 indicate ion exchange processes.

An exchange between Na^+ and K^+ in the groundwater with Ca^{2+} and Mg^{2+} in the aquifer material will result in a positive chloro-alkali index indicating reverse ion exchange. On the other hand, the exchange between Na^+ and K^+ in the aquifer material and Ca^{2+} and Mg^{2+} in groundwater will result in a negative index. The average values of CAI 1 and CAI 2 in the Kisumu study area are -4.94 and 1.08, respectively, *Figure 4.56*. This shows no reverse ion exchange between (Na^+ and K^+) in the groundwater with (Ca^{2+} and Mg^{2+}) in the aquifer material.
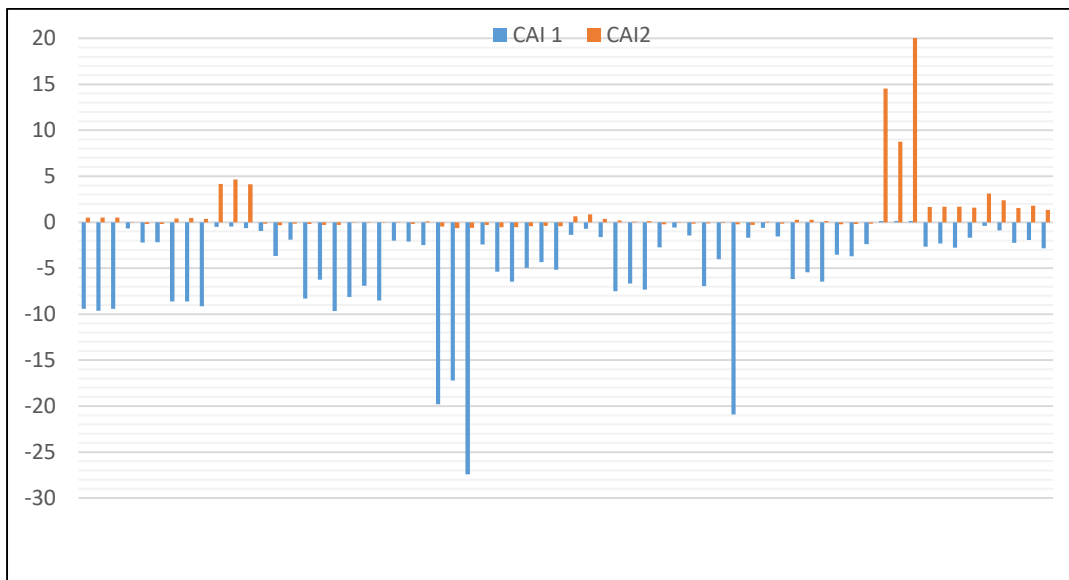
Figure 4.56. Chloro-alkaline indices (CAI 1 and CAI 2) for Kisumu water.

The dominant process in all water samples in Kisumu is an exchange between (Na^+ and K^+) in the aquifer material and (Ca^{2+} and Mg^{2+}) in groundwater (negative indices). However, a few

wells (Kibos shallow well and shallow wells in Otonglo) showed positive indices. The sites and their contribution are shown in *Figure 4.57* and *Figure 4.58*.
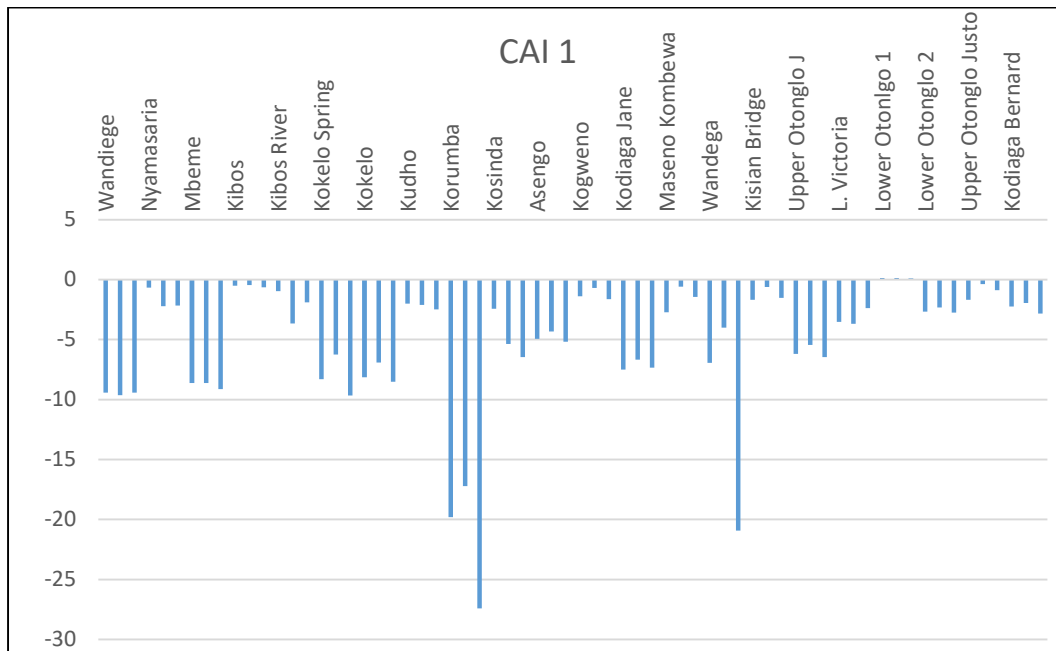
Figure 4.57. Borehole (Wandiege, Korumba and Korumba contribute highly to the CAI 1 while surface water contribution is low

The CAI 1 plot suggests an exchange between Na+ and K+ in the aquifer material and Ca2+ and Mg2+ in groundwater
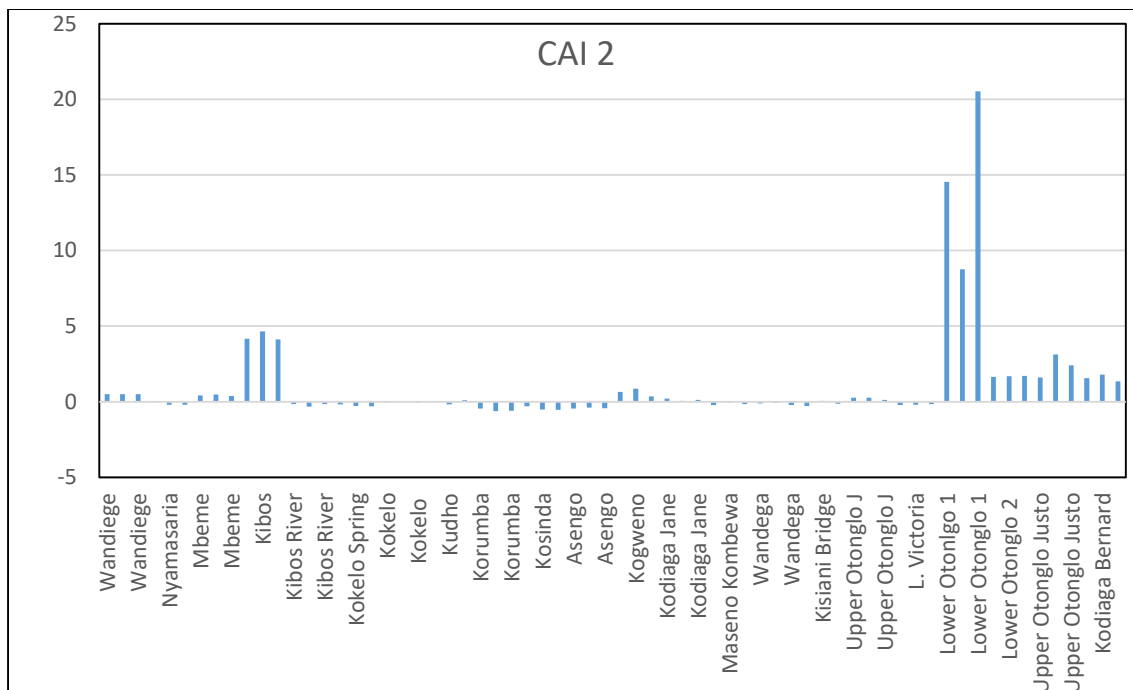
Figure 4.58. The main contributors to positive CAI 2 are shallow wells (Kibos and Lower Otonglo and Upper Otonglo). An exchange between Na+ and K+ in the groundwater with

Ca2+ and Mg2+ in the aquifer material results in a positive chloro-alkali index indicating reverse ion exchange.

The chloro-alkaline indices (CAI 1and CAI 2) for Mt. Elgon water, *Figure 4.59,* indicate the exchange of cations between aquifer material and groundwater. This implies that groundwater is under-saturated with respect to the major cations.
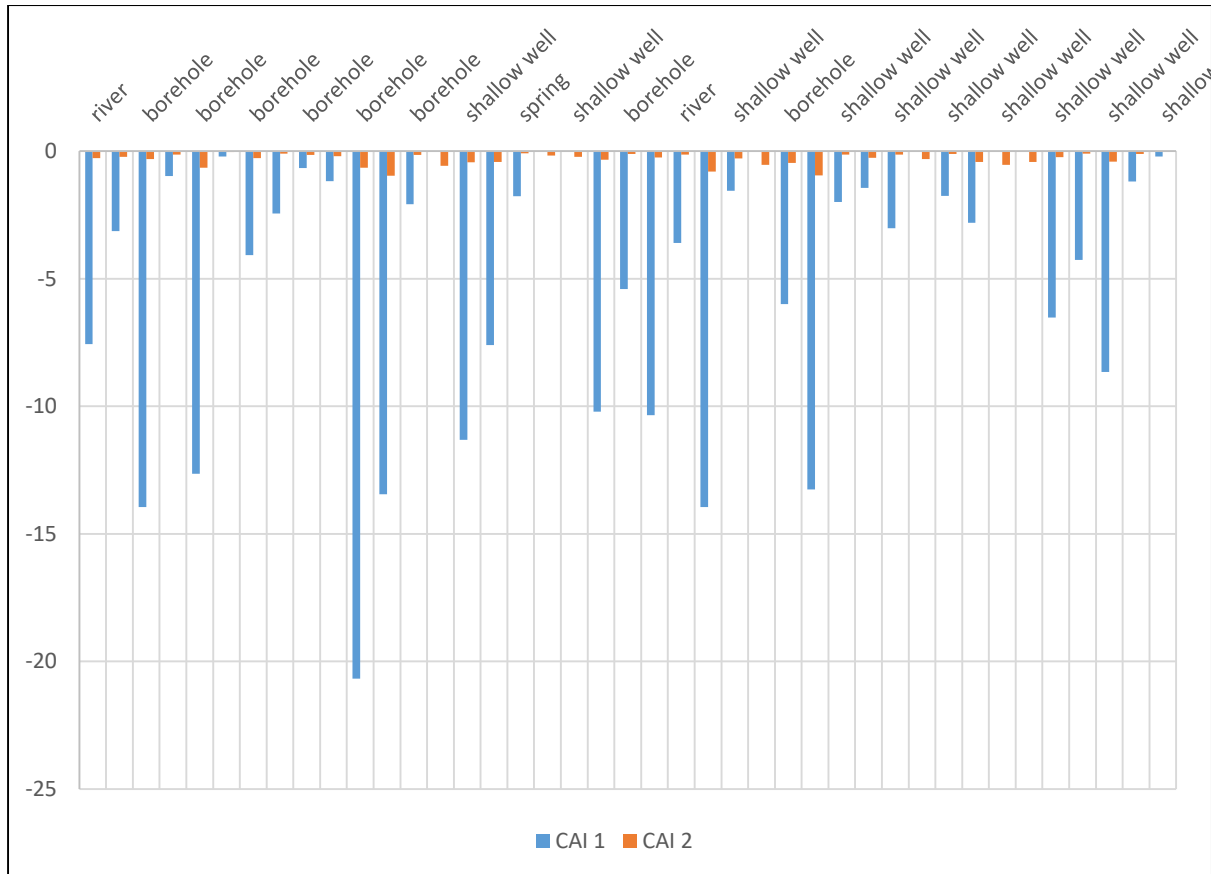
Figure 4.59. Chloro-alkaline indices (CAI 1and CAI 2) for Mt. Elgon water. All the water types are under saturated.

This shows that the dominant process in all water points in Mt Elgon is an exchange between Na^+ and K^+ in the aquifer material and Ca^{2+} and Mg^{2+} in groundwater (all negative indices). The water types dominating these ion exchanges are given in *Figure 4.60* and *Figure 4.61*.
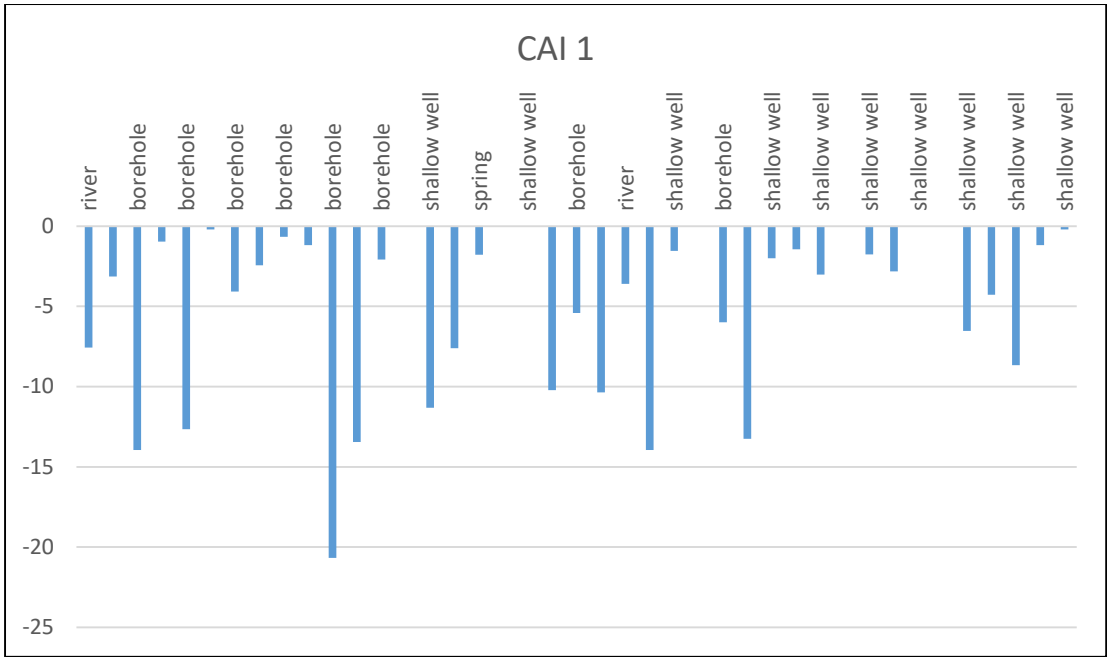
Figure 4.60. The main contributors of CAI 1 in Mt.Elgon are the boreholes
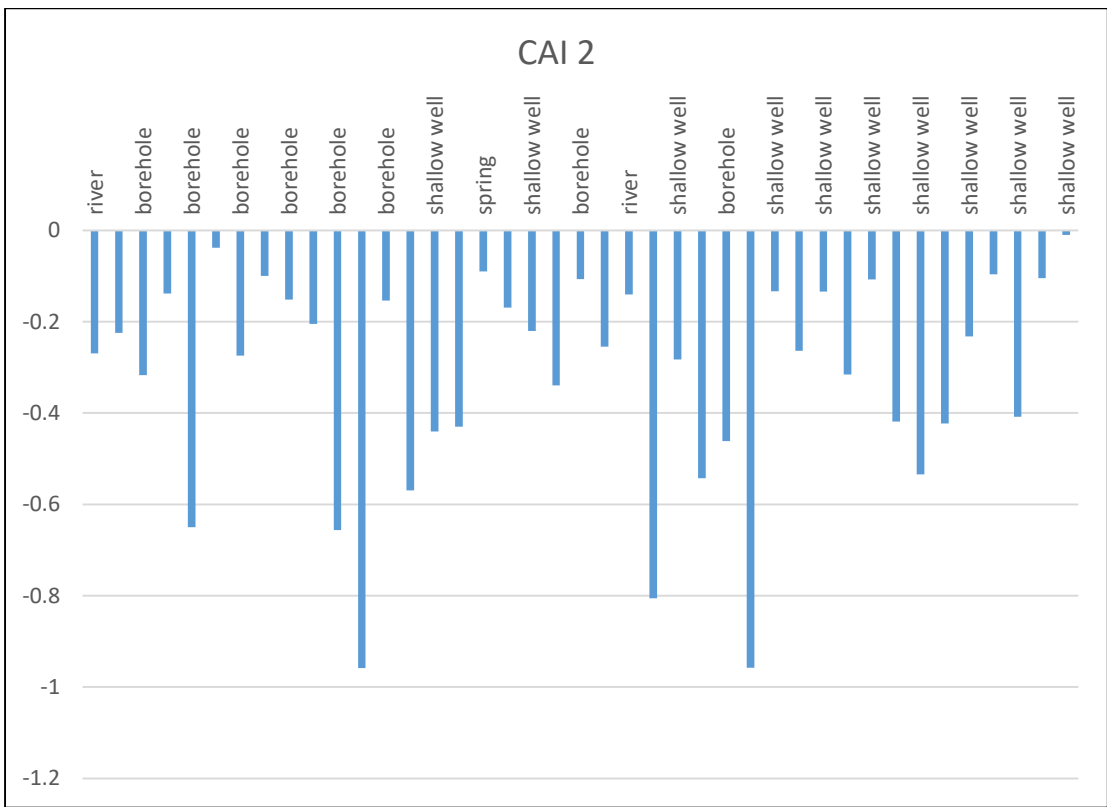
Figure 4.61. The main contributors of CAI 2 in Mt. Elgon are the boreholes

4.2.8   Results on the mineral saturation indices in Kisumu and Mt. Elgon aquifers

The saturation indices for the groundwater samples concerning the different mineral phases were evaluated. The full results of the saturation indices for Kisumu and Mt. Elgon are given in appendix 8 and 9, respectively. The Kisumu aquifer was under-saturated with all significant minerals apart from iron in all water sources apart from boreholes and aragonite in Kibos shallow well (*Figure 4.62*. The over-saturation in iron results in its precipitation.
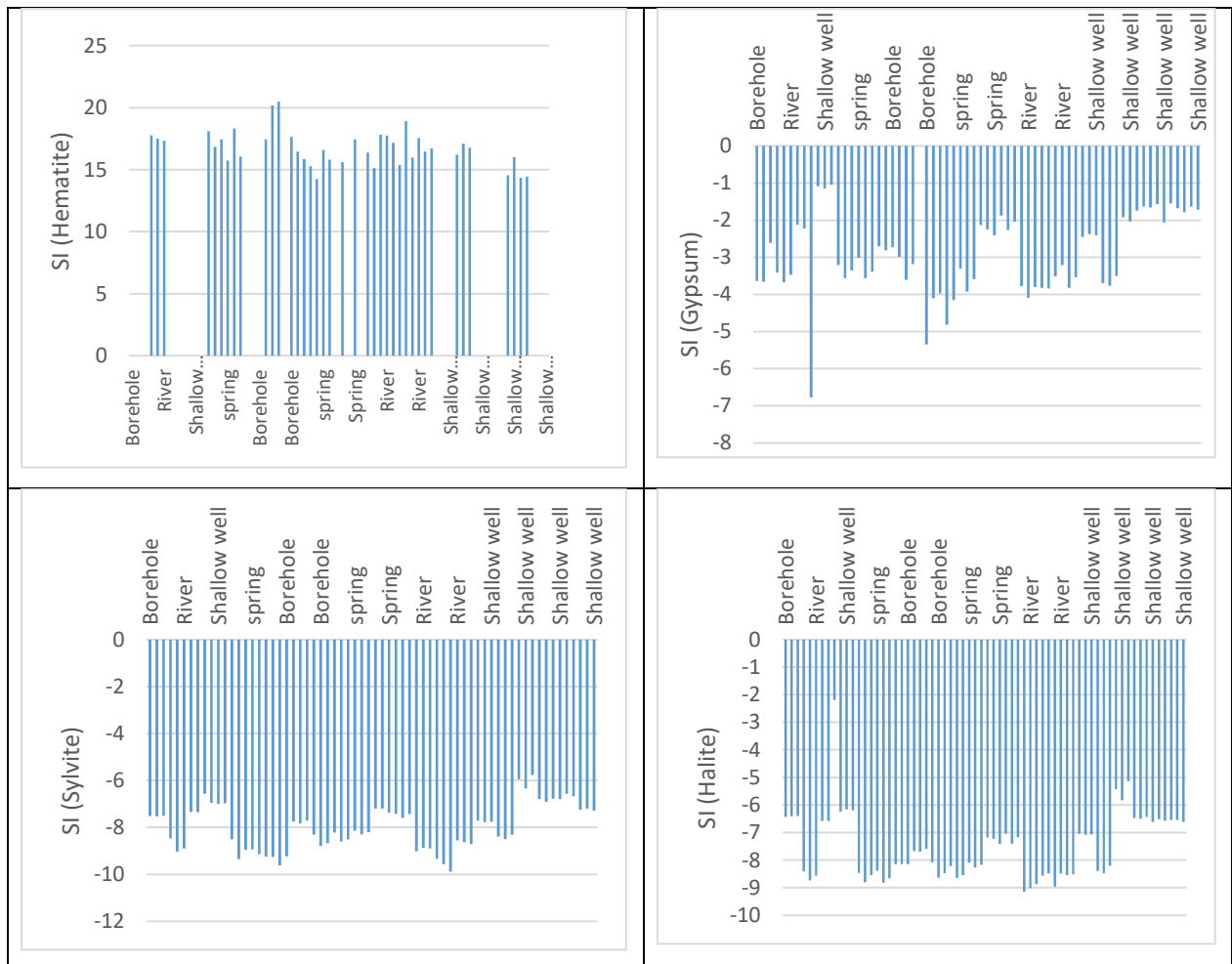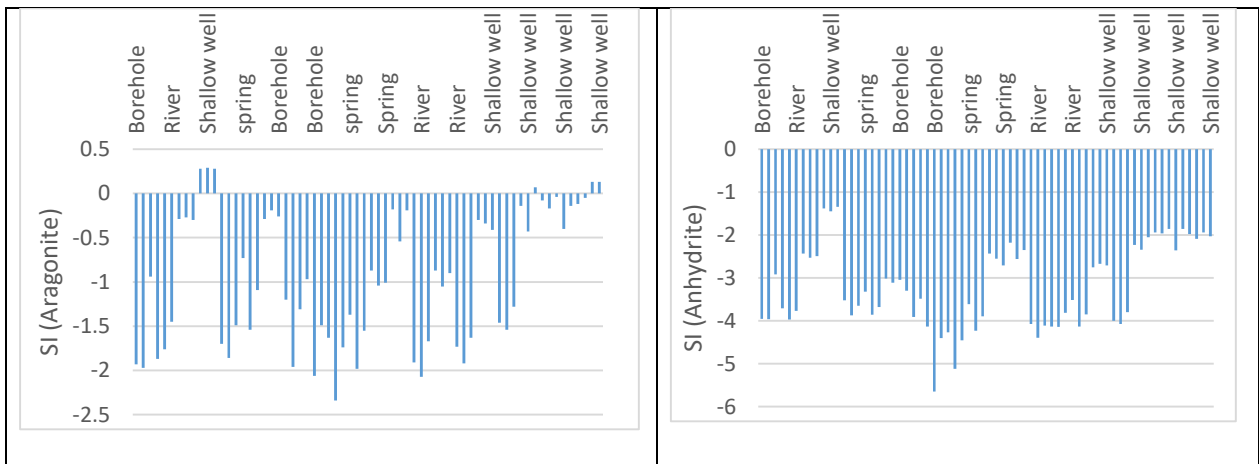
Figure 4.62. A plot of saturation indices of water samples from the Kisumu study site.

Kisumu water is under-saturated with major minerals apart from iron. The water sample from Kibo's shallow well is oversaturated with aragonite. The saturation index plots for the Mt. Elgon, *Figure 4.63*, similarly reveal under-saturation concerning main minerals, but aragonite, dolomite and sylvite are saturated in several samples. The SI of the carbonates helps define the thermodynamic stability of water and explain the geochemical behaviour of water (Arvidson and Mackenzie, 1999; Boon *et al*., 2020; Chidambaram *et al*., 2012; Hostetler, 1964).
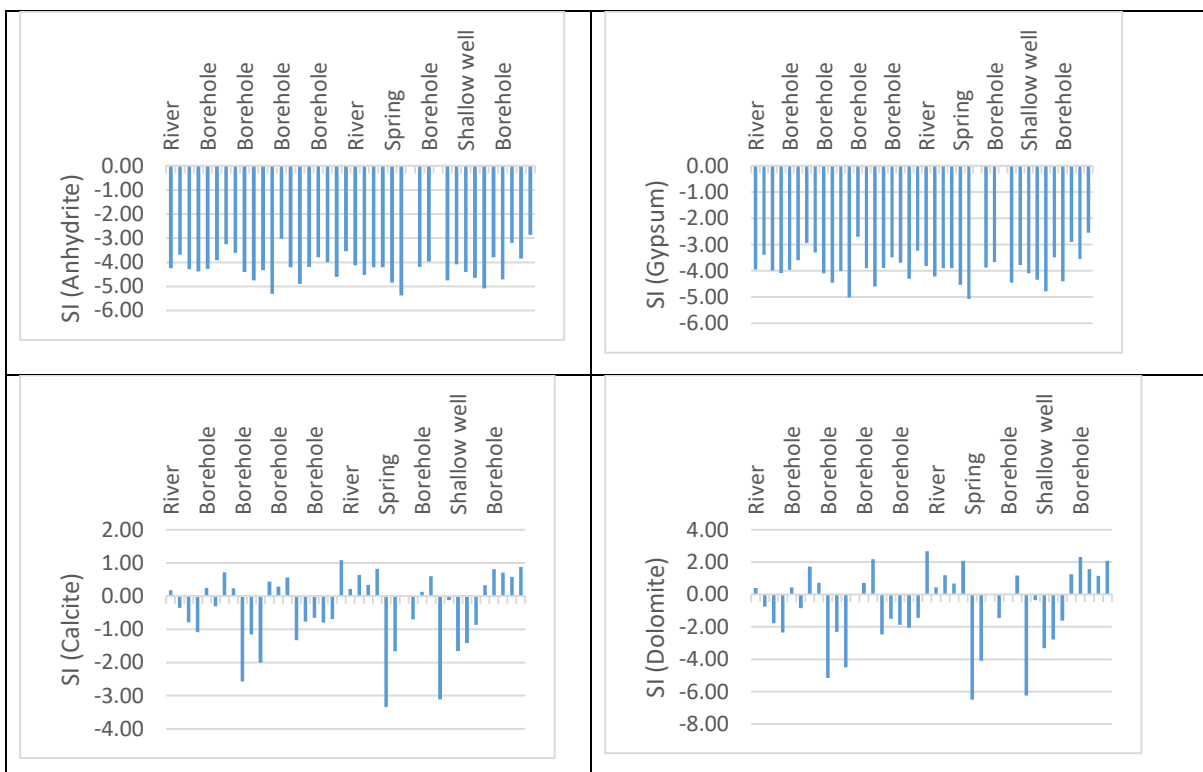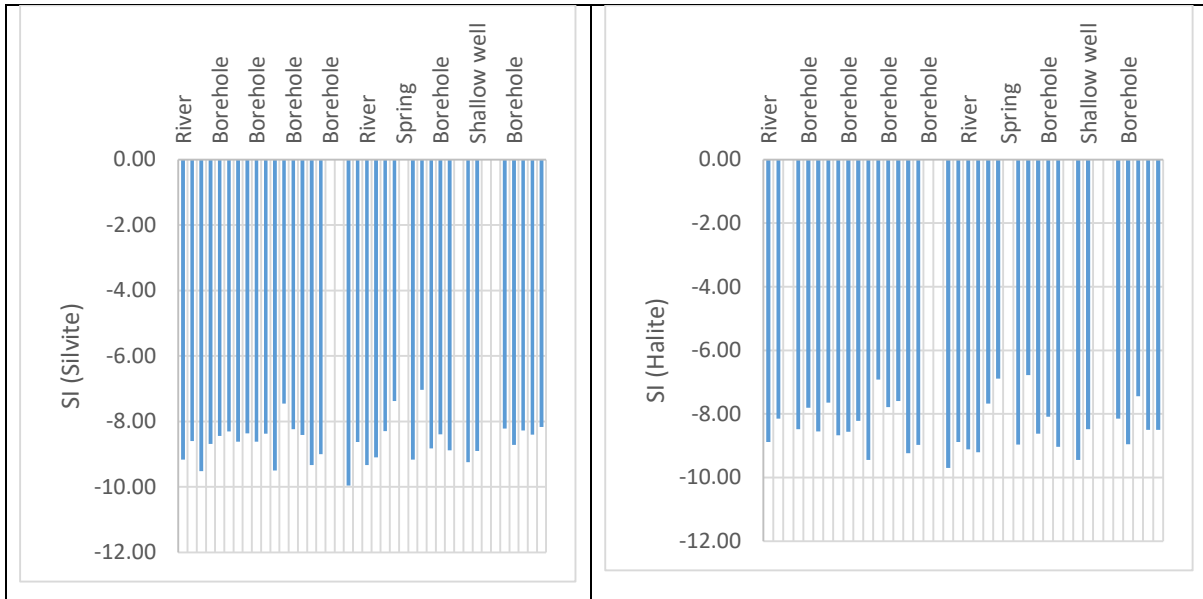
Figure 4.63. Saturation indices for Mt. Elgon water showing oversaturation with carbonates in some localities and undersaturation with halite, gypsum and anhydrite.

The Mt Elgon aquifer is undersaturated with halite, gypsum and anhydrite. It is, however, oversaturated with carbonates (dolomite and calcite) in some water points.

4.2.9   Results on the microbial contamination of groundwater in Kisumu

The conventional sewer system coverage is deficient, and therefore the most common human excreta disposal system in Kisumu is the unimproved pit latrine. The extensive usage of this mode of human waste disposal has resulted in the discharge of microbial contaminants, *Figure 4.64*, into the groundwater.
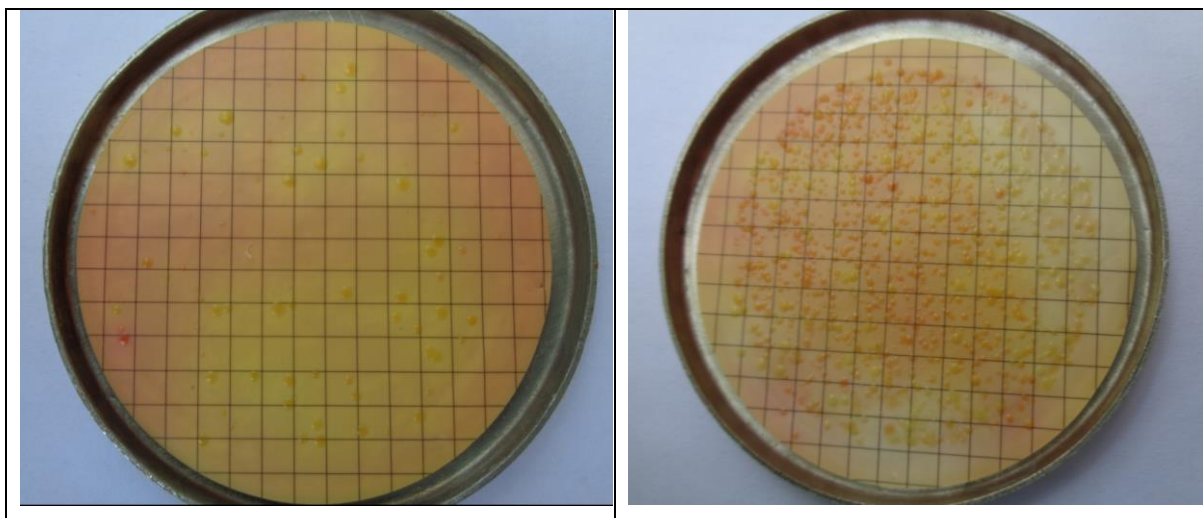
Figure 4.64. Typical thermotolerant colonies (TTC) enumerated after incubating the cultured media in an incubator

The enumerated colonies in samples analysed during March, June and September 2017, *Figure 4.65*, shows contamination of water in Kisumu with various degrees of loading.
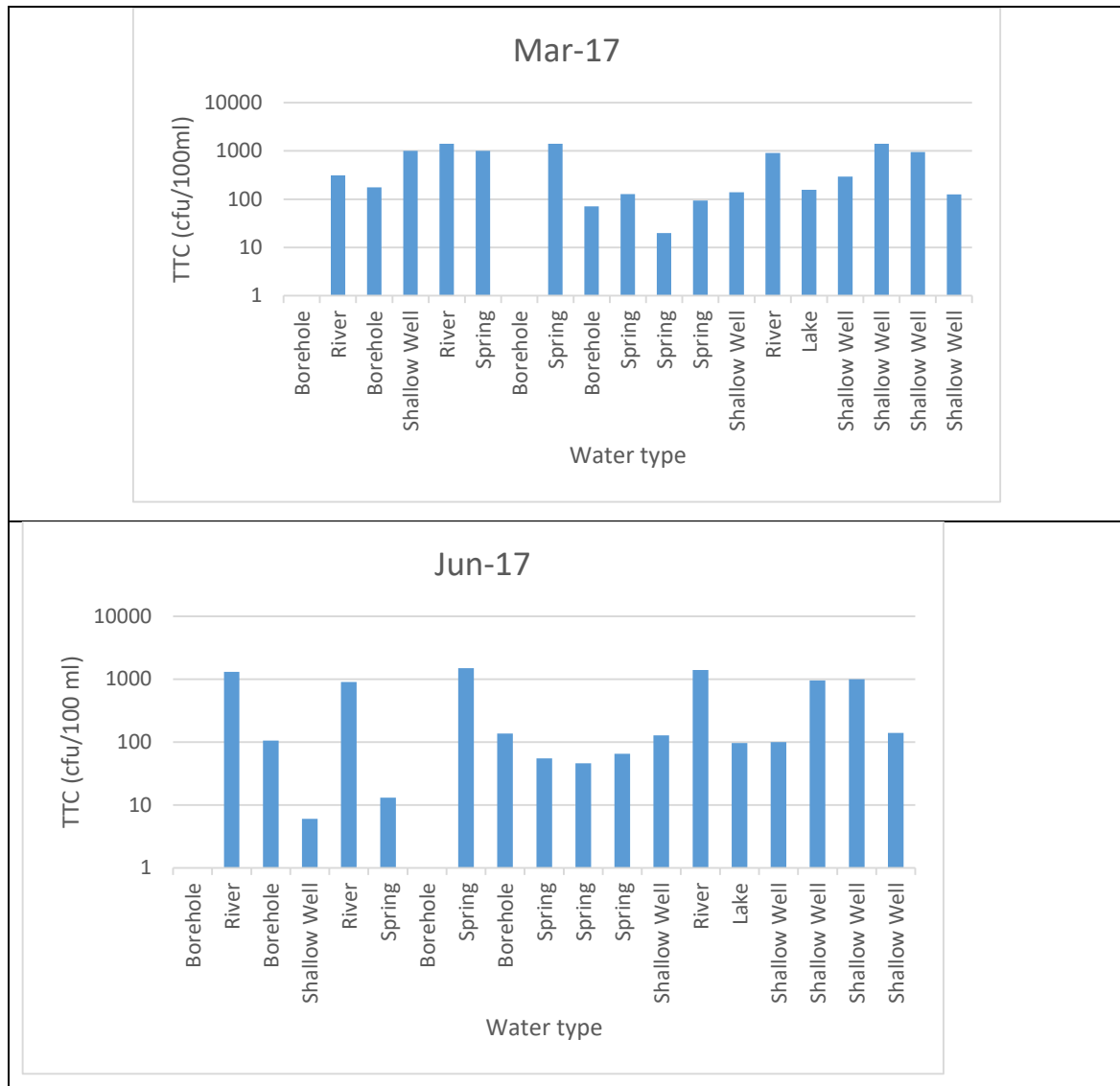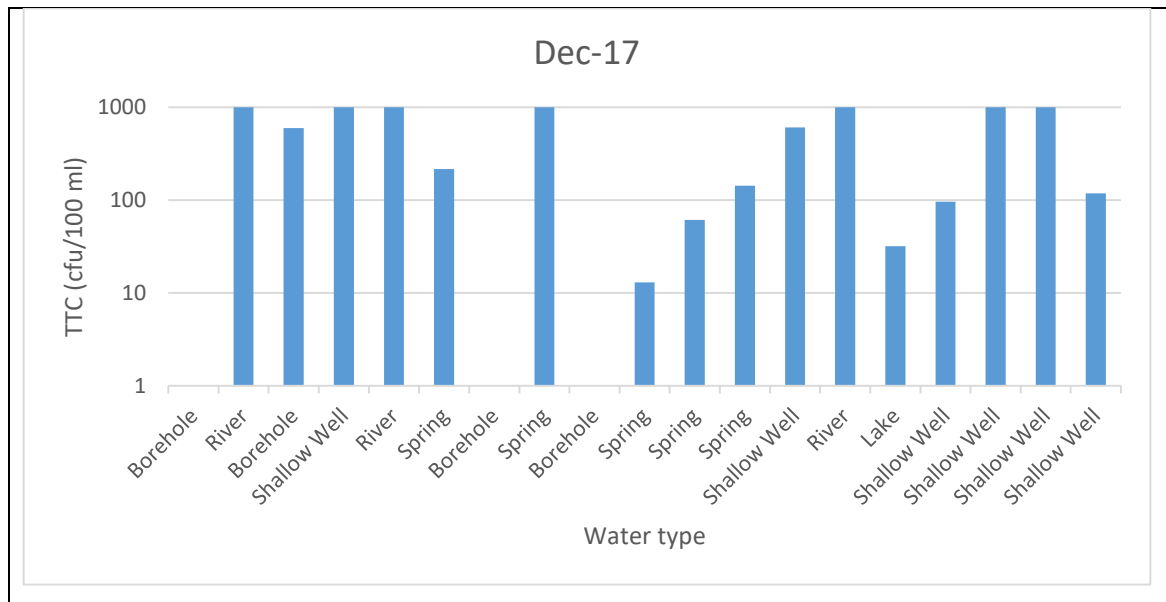
Figure 4.65. Variation of thermotolerant coliform bacteria in Kisumu water in March, June and December 2017(the y-axis is plotted on a logarithmic scale). The colonies are relatively lower during the June 2017 sampling campaign.

During June, the levels of coliform bacteria contamination were low compared to contamination during March and December. TTC counts were high during 2018, *Figure 4.66* when sampling and analysis were done after the long March-April rains. The water table is low, and the pit latrines are generally shallow because they are hand dug. Therefore, the spike in coliform can be explained by the interaction between groundwater and the pit latrines during the rainy season.
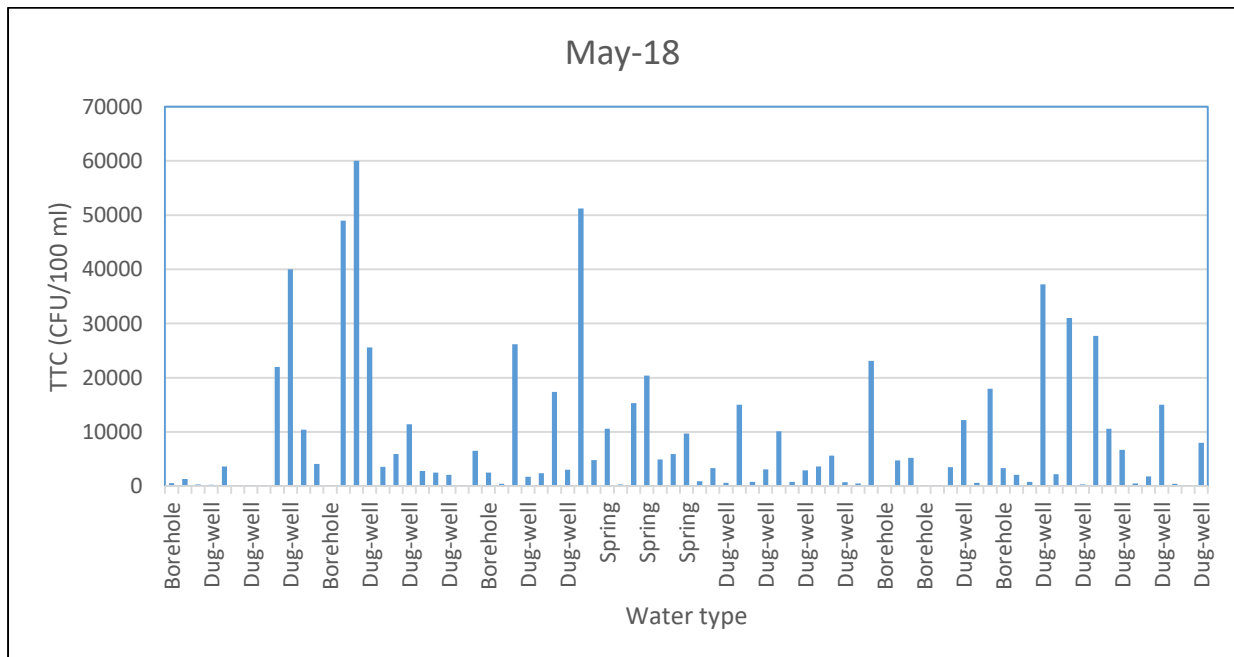
Figure 4.66. TTC contamination in May 2018. The levels of contamination are very high. May is toward the end of the rain season

158

The study has revealed that thermal-tolerant coliform (TTC) bacteria contaminate shallow wells and springs. The level of contamination was noted to be higher where toilets were located less than 50 meters from the water point and were upstream of the water source. The levels of groundwater contamination varied with seasons. The TTC counts were higher after the rains and during the dry season and lowered during the rainy season. This was interpreted as a consequence of dilution during the rainy seasons.

4.2.10 Results on the Kisumu aquifer vulnerability to contamination

TTCs in Kisumu water confirm that groundwater and surface water in Kisumu are vulnerable to pit latrines contamination. Coliform bacteria are found in the digestive system of warm-blooded animals. Since the population of livestock in densely populated peri-urban parts is low, the results suggest that the primary source of TTCs' in groundwater is from human faeces. Contamination can also be introduced into groundwater through geogenic processes. The ionic content is variable due to water-rock exchanges. This can result in ionic contents beyond the recommended KEBS and WHO limits.

4.2.10.1   *Geogenic contamination*

Geogenic groundwater pollution refers to naturally occurring elevated concentrations of certain groundwater elements with adverse health effects, *Table 4.47*.

Table 4.47. Summary of potential geogenic contaminants in Kisumu and likely impacts on human health (adapted from UNESCO, 2002)

Contaminant	Geogenic sources	Influencing factors	Health effects and guideline values
Fluoride	Fluorite, mica, apatite, amphiboles (hornblende)	F minerals, pH, temperature, anion exchange capacity of aquifer material, residency time depth,	Dental and skeletal fluorosis. The maximum WHO limit is 1.5 mg/L
Chloride	Natural weathering of bedrocks, volcanic rocks, atmospheric deposition	Availability of Cl sources, atmospheric precipitation	No health-based guidelines
sulphate	Sulphur bearing mineral, e.g. gypsum, anhydrite and pyrite	Availability of sulphate rich minerals in the aquifer, redox conditions	$SO_4 > 1000$ mg/L can cause laxative effects
Iron	Iron bearing minerals (ilmenite, magnetite and limonite)	An iron-bearing formation like laterite, redox conditions	Iron can lead to hemochromatosis, which can cause damage to the liver, heart, and pancreas. The maximum WHO limit is 1mg/L

In Kisumu, elevated levels of fluoride and iron were reported. Values as high as 21.3 mg/L (Fe^{3+}) and 7.29 mg/L (F^-) were found in groundwater. The concentrations are beyond the local KEBS and WHO maximum limits (KEBS, 2015; WHO, 2017).

4.2.10.2 *Anthropogenic contamination*

These are contaminants that can be attributed to human activities. Human groundwater contamination can be direct (e.g. faecal loading, accidental or non-accidental spillage of petroleum products, or indirect (inferior farming methods, excessive use of farm inputs, household products - detergents, aerosols, beauty products, and improper disposal of drugs, electronics and plastic products).

4.2.10.3 *Remedial measures of contaminated groundwater*

Groundwater contamination can be reversed in a few instances but irreversible in most cases. Remedial techniques include biological, chemical, and physical treatment technologies. The traditional approach is pump and treat, which physically means pumping out the contaminated groundwater using a pump and then purifying the groundwater using materials that absorb or destroy the contaminants. At the house level, water contaminated by bacteria can be made safe by boiling or using chemicals that kill them, e.g. chlorine. The two methods are widely used in both Kisumu and Mt. Elgon. Innovative technologies such as in situ bioremediation, in situ chemical oxidation (ISCO), in situ thermal treatment (ISTT) or monitored natural attenuation (MNA) are used to remedy contaminated aquifers. These technologies are, however, costly (EPA, 2018; IAEA, 1999).

4.3 Results on the isotopic signature of Kisumu groundwater

Understanding the sources and pathways of groundwater recharge to aquifers is critical to developing strategies to protect the quality and quantity of groundwater resources. In this section, the application of stable isotope ratios of oxygen and hydrogen to trace groundwater recharge to the volcano-sedimentary aquifer, widely developed to provide low-cost, on-site water supplies to low-income neighbourhoods, is presented.

4.3.1   Isotopic variation of rainfall from Kericho GNIP station

The relationship between delta δ^2H and delta $\delta^{18}O$ in precipitation at a site, known as the local meteoric water line (LMWL), and groundwater isotope signature can reveal the source of recharge water. Due to the absence of stable isotope measurements in rainfall from the study area, seasonal variations in the deuterium and oxygen-18 content of precipitation were inferred from historical data from Kericho (about 80 km east of Kisumu), collected every month between November 1967 and December 1969 by Global Network of Isotopes in Precipitation (GNIP). The station was one of the GNIP global monitoring stations operated jointly by WMO and IAEA (IAEA, 1981). Complete isotopic and precipitation data are shown in *Table 4.48.*

Table 4.48. A summary of Kericho isotope and precipitation data downloaded from IAEA wiser website (https://nucleus.iaea.org/wiser/index.aspx)

Site	WMO Code	Sample Name	Date	$\delta^{18}O$	δ^2H	Precipitation
KERICHO	6371401	196711	1967-11-15	-7.66	-49.8	58
KERICHO	6371401	196712	1967-12-15	-4.73	-27.3	10
KERICHO	6371401	196801	1968-01-15	0.6	23	4
KERICHO	6371401	196802	1968-02-15	-2.19	-1	136
KERICHO	6371401	196803	1968-03-15	-2.55	-6	70
KERICHO	6371401	196804	1968-04-15	-6.29	-33	249
KERICHO	6371401	196805	1968-05-15	-4.39	-18.6	18
KERICHO	6371401	196806	1968-06-15	-3.71	-12.6	76
KERICHO	6371401	196902	1969-02-15	-1.43	2.4	49
KERICHO	6371401	196903	1969-03-15	-3.84	-12.4	18
KERICHO	6371401	196904	1969-04-15	-0.84	4.8	41

KERICHO	6371401	196905	1969-05-15	-2.75	-10.6	95
KERICHO	6371401	196906	1969-06-15	0.81	19.3	23
KERICHO	6371401	196907	1969-07-15	-0.7	17.5	12
KERICHO	6371401	196908	1969-08-15	-0.1	7	1
KERICHO	6371401	196909	1969-09-15	-0.32	-11.4	16
KERICHO	6371401	196910	1969-10-15	-2.66	-10.7	44
KERICHO	6371401	196911	1969-11-15	-4.32	-18.3	46
KERICHO	6371401	196912	1969-12-15	-7.9	-53.1	41

A plot of average monthly rainfall and isotope content ($\delta^{18}O$ and δ^2H) shows a positive correlation between the amount of rain and its depletion in $\delta^{18}O$ and δ^2H, *Figure 4.67*.
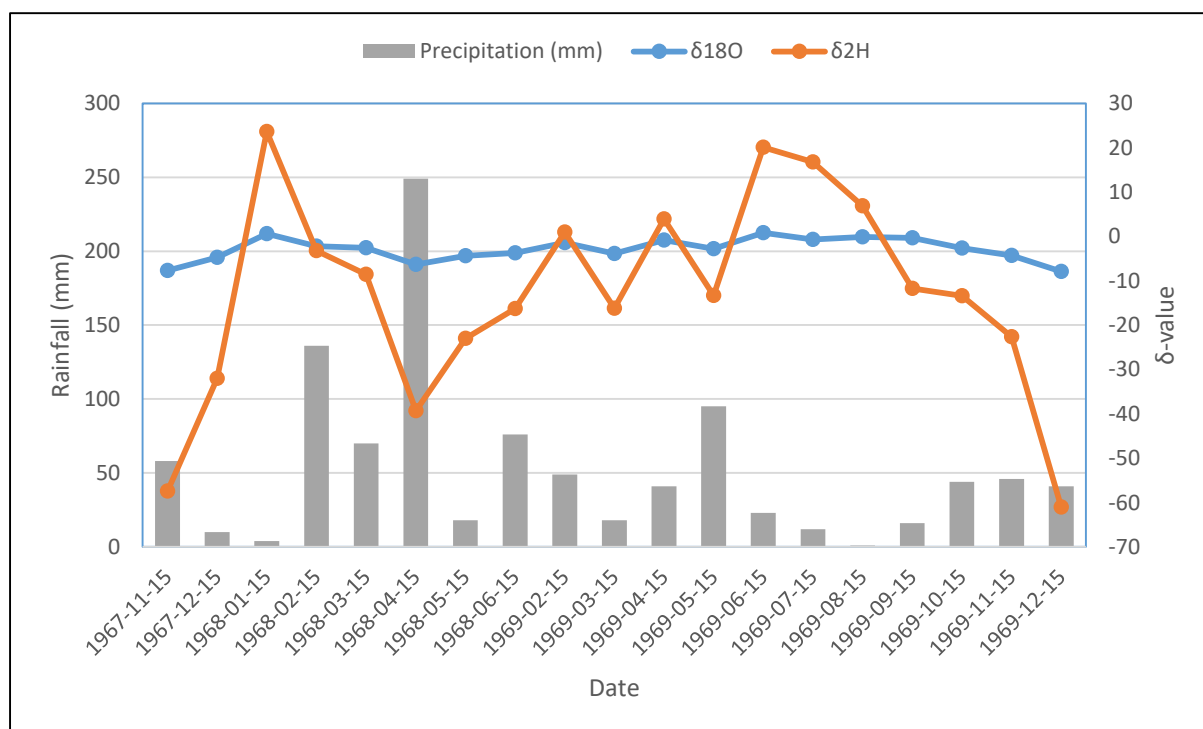
Figure 4.67. Annual distribution of rainfall and its δ18O and δ2H content at Kericho for the period November 1967 to December 1969

An inverse relationship between monthly rainfall and its isotopic composition (amount effect) can be interpreted. Heavy rainfall events correspond with depletion of both $\delta^{18}O$ and δ^2H. This implies that light rainfall in Kericho was subjected to evaporation which enriched their mean isotopic composition in heavier isotopes relative to non-evaporated, heavy rains. Meteoric waters which have not undergone significant evaporation show a consistent relationship between their deuterium and oxygen-18 content with a slope of eight (GMWL), whereas

evaporated, meteoric waters fall along a $\delta^2H/\delta^{18}O$ and a gradient of less than 8, *Figure 4.68*. The enriched isotopic composition of rainfall could be due to the enhanced evaporation that arises from dry atmospheric conditions, including low humidity (Levin *et al.*, 2009; Sklash and Mwangi, 1991; Taylor and Howard, 1996).
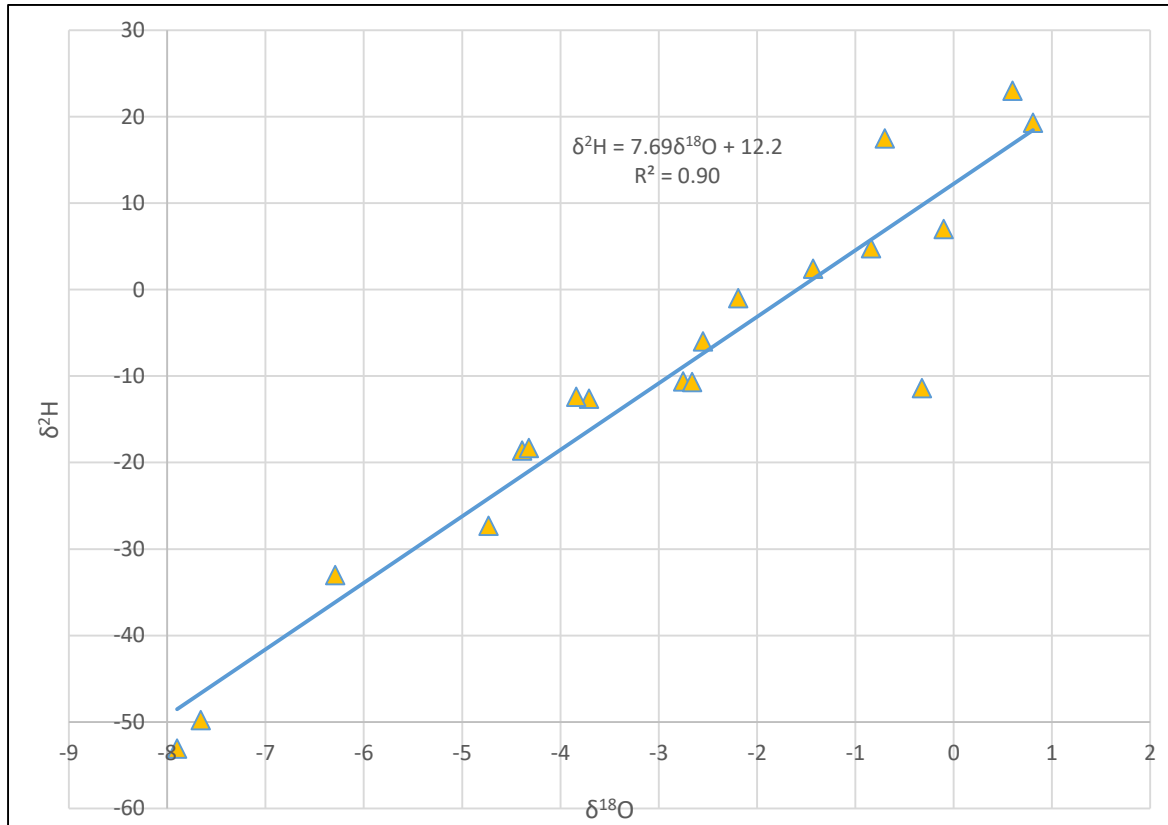
Figure 4.68. A plot of oxygen-18 against deuterium for Kericho GNIP station. The slope is less than 8 (slope for the global meteoric water line, GMWL, δ2H=8*δ18O+10) implying evaporation of rainfall due to dry atmospheric conditions (data downloaded from the IAEA WISER website (https://nucleus.iaea.org/wiser/index.aspx

4.3.2 Results on the relationship between rainfall and groundwater

Since the environmental isotopes of water are conservative, groundwater will retain the isotopic signature of recharging precipitation. The isotopic content of the recharge water is not affected by the vadose zone, and the source of recharge is restricted to the direct infiltration of rainfall. Significant evaporation before recharge may be revealed by plotting deuterium versus chloride in groundwater (Chandrasekharan *et al.*, 1997; Gaye and Edmunds, 1996; Subyani, 2004; Tamez-Meléndez *et al.*, 2016), *Figure 4.69*.
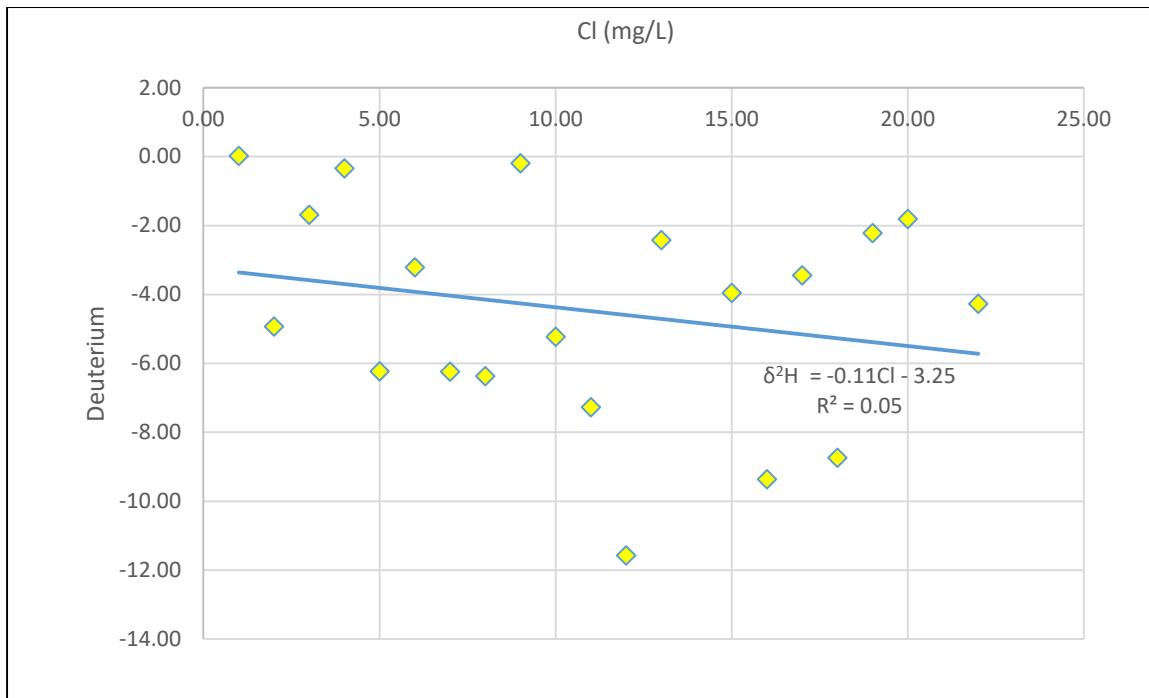
Figure 4.69.Chloride versus deuterium plot. The correlation is near zero implying that there is hardly any evaporation in the vadose zone

There was a slight or negligible negative correlation between deuterium and chloride. In general, high deuterium values are associated with lower anion concentrations. This indicate that evadose zone evaporation is not an important process in Kisumu (Chandrasekharan *et al*., 1997; Gaye an Edmunds, 1996; Subyani, 2004; Tamez-Meléndez *et al.,* 2016).

4.3.3   Results on the relationship between surface water and groundwater isotopic composition Kisumu

Lake Victoria water is highly evaporated and therefore enriched with oxygen-18 and deuterium, *Table 4.49,* and the Lake Victoria samples plot to the right of LMWL for Kericho, *Figure 4.70.* Groundwater and river water samples show a depleted isotopic signature. This indicates that groundwater and river water are meteoric since they plot along the LMWL for Kericho. Most river samples plot very close to groundwater samples. This may be due to high groundwater contribution (baseflow) to streams during the dry seasons or quick overland flow with an isotopic composition similar to precipitations during rainy seasons.

Table 4.49. Stable isotope of surface and groundwater in Kisumu collected by IAEA-funded project, RAF/8/042(IAEA, 2016)

Water type	δ¹⁸O	δ²H		Water type	δ¹⁸O	δ²H
Lake Victoria	4.6	33.04		River	-2.05	-4.84
Lake Victoria	3.33	25.35		River	-2.13	-5.05
Lake Victoria	4.58	24.53		River	-2.37	-6.76
Lake Victoria	3.11	23.92		River	-2.32	-6.96
Lake Victoria	3.3	25.4		River	-1.9	-1.53
Lake Victoria	3.37	25.27		River	-1.87	-3.02
Lake Victoria	3.51	27.92		River	-2.22	-4.62
Lake Victoria	2.79	20.41		River	-2.16	-3.88
Lake Victoria	2.78	20.89		River	-2.42	-6.8
Lake Victoria	3.57	24.29		Borehole	-3.38	-16.2
Lake Victoria	3.49	28.75		Borehole	-2.16	5.98
Lake Victoria	2.76	21.1		Borehole	-2.72	-12.47
Lake Victoria	2.74	21.15		Borehole	-2.96	-13.27
Lake Victoria	2.69	21.57		Borehole	-2.33	-12.48
Lake Victoria	1.49	12.87		Borehole	-2.26	-13.39
Lake Victoria	2.13	16.42		Borehole	-2.96	-13.45
Lake Victoria	3.59	27.2		Borehole	-3.11	-16.08
Lake Victoria	2.3	21.09		Borehole	-4.55	-23.26
Lake Victoria	1.42	14.16		Borehole	-2.09	-8.35
Lake Victoria	2.33	19.15		Borehole	-2.98	-11.84
shallow well	-3.3	-14.23		Borehole	-3.18	-14.31
shallow well	-3.26	-14.12		Borehole	-3.28	-14.73
shallow well	-3.14	-13.36		Borehole	-1.88	-6.48
shallow well	-3.1	-12.37		Borehole	-1.24	-0.95
shallow well	-2.99	-15		Borehole	-1.81	-6.26
shallow well	-3.14	-12.14		Borehole	-2.25	-5.07
shallow well	-3.89	-18.84		Borehole	-2.63	-8.9

The isotopic plot shows no interaction between Lake Victoria water and groundwater (*Figure 4.70*).
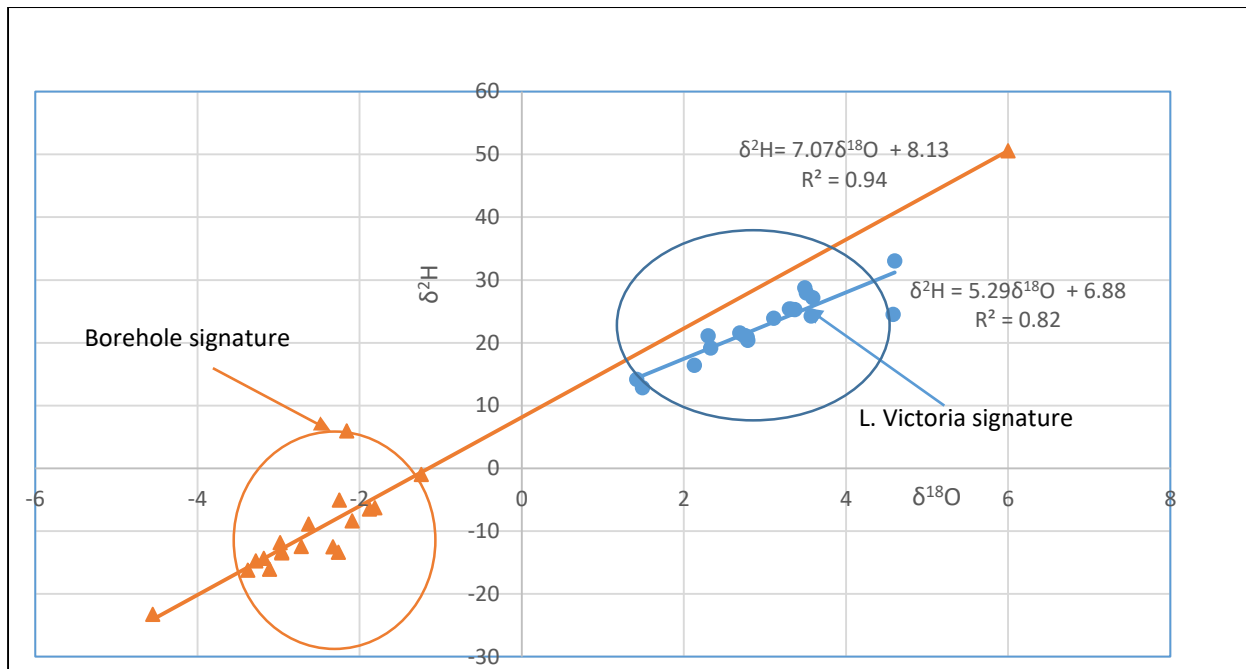
Figure 4.70. Comparison between the surface water and groundwater isotopic signature. The lake water is more enriched relative to groundwater (data from IAEA project, 2016)

Groundwater shows a consistent and marked depletion in its isotopic signature relative to surface waters. The separation in isotopic composition between groundwater and lake (surface) water suggests that little or no mixing occurs between them. The lake does not contribute significantly to aquifer recharge.

4.3.4 Results on the groundwater recharge mechanism in Kisumu

Although infiltrating rainfall represents the principal source of recharge in the Kisumu study site, the isotopic content of the groundwater is dominated by the isotopic composition of the rainfall falling during those months in which most recharge occurs. Groundwater timing of recharge corresponds to the heaviest rainfalls when rates of incoming precipitation temporarily exceed the intense evapotranspiration (Sklash and Mwangi, 1991; Taylor and Howard, 1996). The plot of the isotopic composition of Kericho GNIP precipitation (*Figure 4.71*) during the months of heavy rainfall (MAM and ND) has a slope close to 8.15, suggesting less evaporation. In contrast, the plot during light rains (JF and JJASO) has a slope of 6.91, indicating evaporated water. The global meteoric water line has a slope of 8.0.
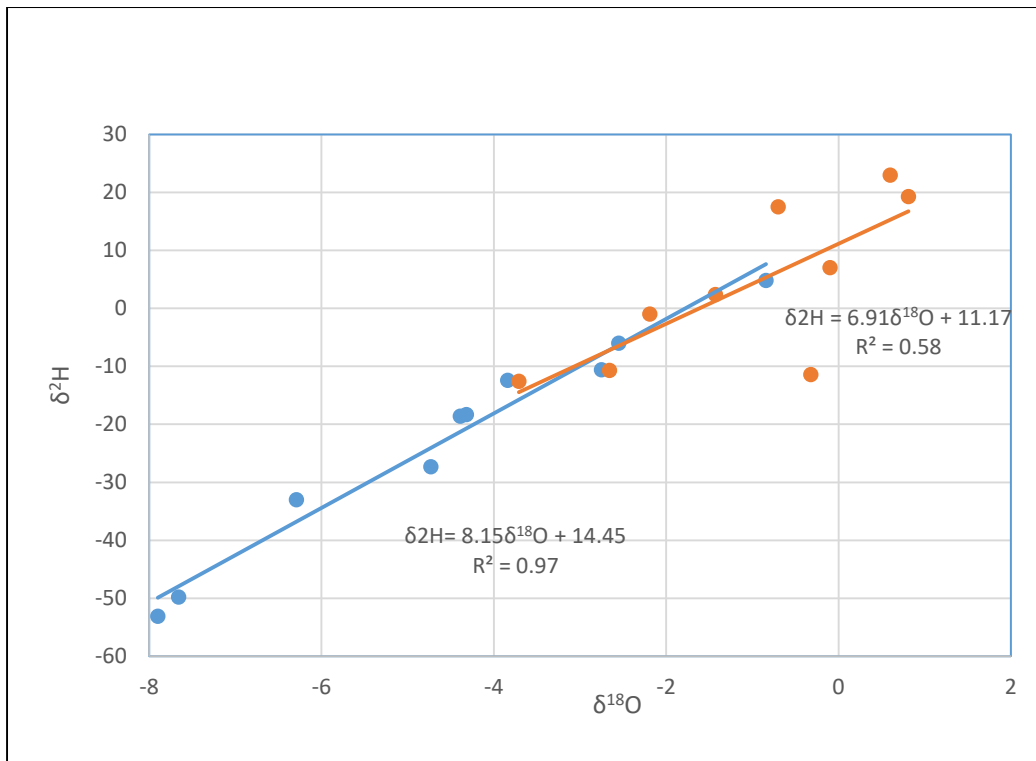
Figure 4.71. Isotopic signature during light and heavy rainfall in Kericho. The slope for light rain depicts evaporation (enrichment) in comparison to heavy rain signal (depletion). The blue regression line is for heavy rainfall months and the orange regression line is for the light rainfall months. (Data downloaded from https://nucleus.iaea.org/wiser/index.aspx)

The interpretation of the isotopic signal is that shallow groundwater in Kisumu is recharged directly and locally from heavy rainfall events. The light rain signal (slope = 6.91)) is evaporated in comparison to heavy rain (slope = 8.15) and groundwater signal in Kisumu (slope = 7.69). The isotopic signature for the spring shows a longer residence time since they are depleted in oxygen-18 and deuterium. These permanent springs probably come from deeper aquifer recharged in the uplands through numerous faults and fractures developed during the Kavirondo Rifting. They are all located along fault lines (Kisumu geological map).

The similarity between the isotopic composition of borehole, springs, river, and shallow well water samples implies that the water types are related (*Table 4.50*). However, the Maseno-Kombewa river water sample is highly evaporated, probably due to impounding and prolonged exposure to evaporation agents.

Table 4.50. Isotopic results for Kisumu water samples. All samples are depleted regarding oxygen 18 and deuterium, apart from river water from Maseno Kombewa that is highly evaporated.

Location	Water type	$\delta^{18}O$	δ^2H
Wandiege	Borehole	-0.68	0.02
Mbeme	Borehole	-1.90	-1.69
Korumba	Borehole	-1.70	-0.19
Kokelo	Borehole	-2.34	-6.24
Kokelo	spring	-1.73	-3.22
Kosinda	spring	-1.91	-5.23
Asengo	spring	-2.45	-7.27
Kogweno	spring	-2.36	-11.57
Kudho	spring	-2.49	-6.37
Maseno Kombewa	River	4.82	33.05
Kibos	River	-1.95	-6.23
Nyamasaria	River	-1.72	-4.93
Kisian Bridge	River	-2.63	-9.36
Kodiaga	Shallow well	-1.54	-2.42
Wandega	Shallow well	-1.68	-3.96
Lower Otonglo	Shallow well	-1.70	-2.22
Lower Otonglo	Shallow well	-1.52	-1.80
Upper Otonglo	Shallow well	1.06	9.19
Kodiaga	Shallow well	-1.44	-4.27
Kibos	Shallow well	-1.68	-0.34
Upper Otonglo	Shallow well	-1.46	-3.44

Generally, groundwater and other water type's isotopic composition fall along the Kericho local meteoric water line (LMWL), indicating that they have been recharged through precipitation (meteoric water), Figure 4.72 and Figure.4.73.
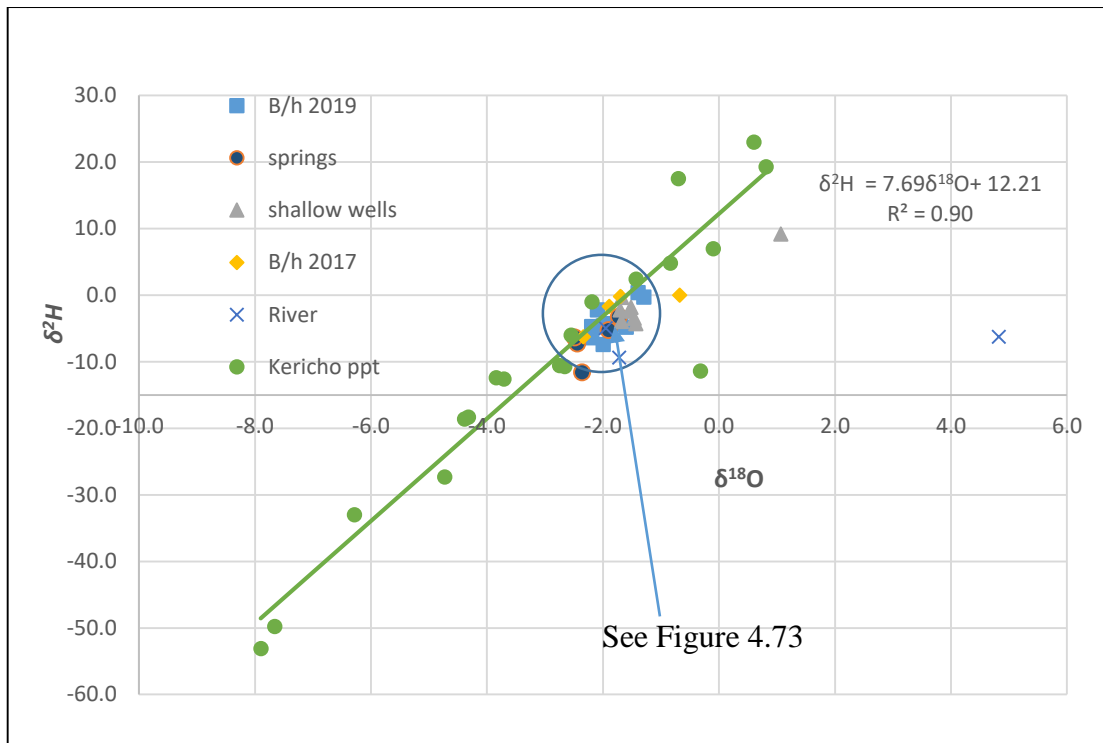
Figure 4.72. Local meteoric water line (LMWL) plotted using Kericho precipitation data and plots of isotope data from Kisumu sampling sites (2017) and in piezometers (2019). A close isotopic relationship between rainfall in Kericho and groundwater in Kisumu is revealed.
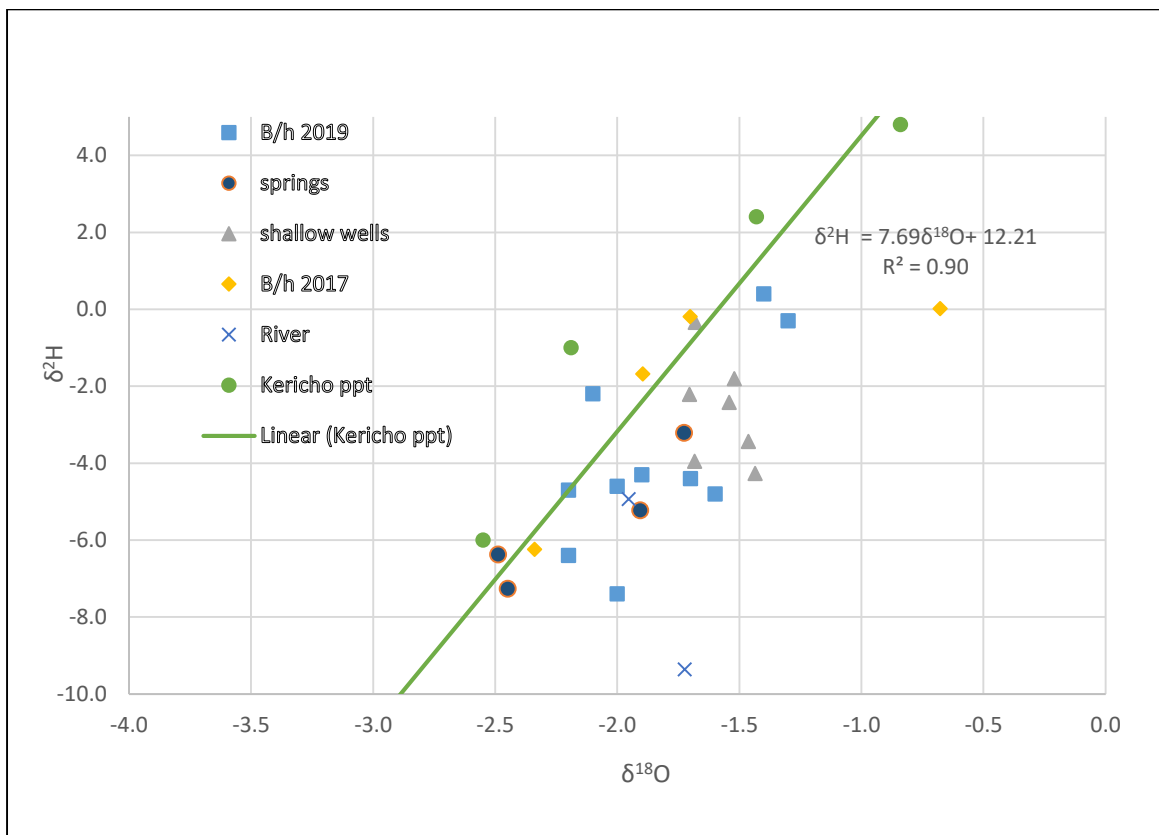
Figure 4.73. A close up of Figure 4.72 showing the isotope data for Kisumu from sampling points, excluding lake water. River and shallow wells samples are evaporated.

4.4 Discussion of the results

Groundwater problems are complicated to address due to complexity, mobility and differing perceptions of groundwater (Falkenmark, 1990). While previous studies in the study area (e.g. (Drangert *et al.*, 2002; Lapworth *et al.*, 2017; Nyilitya *et al.*, 2020; Okotto-Okotto *et al.*, 2015; Okotto *et al.*, 2015; Olago, 2019) focussed mainly on water quality and sanitation, this study encompassed a broad spectrum of issues ranging from the aquifer characteristics, rock-water interaction, water chemistry and, origin of recharge water.

The study has revealed that the shallow aquifer in the two study settings is heterogeneous. Most shallow volcano-sedimentary and volcanic aquifer studied in most parts of the world are homogeneous (Begashaw and Tafesse, 2017; De Vita *et al.*, 2018; Fenta *et al.*, 2020; Razack, Furi *et al.*, 2020; Vittecoq *et al.*, 2019). The study further showed that rock-water interactions and precipitation processes strongly influenced water chemistry. This observation concurs with studies conducted in other parts of Sub-Saharan Africa (Chilton and Foster, 1993; MacDonald *et al.*, 2010; Taylor and Howard, 2000; Xu *et al.*, 2019).

Like other aquifers in the world, the two aquifers are threatened by both geogenic and anthropogenic pollutants. Stable isotope studies revealed that the recharge water for the Kisumu aquifer was meteoric water and the timing of recharge coincided with heavy rainfall events. A similar observation was reported in Uganda by Taylor and Howard while developing a tectonic-geomorphic model of the deeply weathered crystalline rock aquifer (Taylor and Howard, 2000). The isotopic study has revealed no connection between groundwater and lake water despite being located on the shores of Lake Victoria.

4.4.1 Discussion of the results of the Kisumu Aquifer
4.4.1.1 Kisumu aquifer geometry and characteristics

The results of geological and geophysical investigations indicate that the Kisumu shallow volcano-sedimentary is heterogeneous. A heterogeneous aquifer in this context implies an aquifer whose hydraulic properties varies from one borehole to another within the same vicinity. This conclusion is supported by diverse aquifer materials encountered during drilling and the diversity of groundwater characteristics derived through pumping tests and geophysical profiles (Sánchez-Vila *et al.*, 1999; Upton *et al.*, 2019). Along the longitudinal axis of the

shallow Kisumu aquifer, the aquifer is likely to be hydraulically continuous, with groundwater flowing along the west to east direction beneath the recent sediments and screes. Groundwater from the shallow aquifer is discharged through numerous permanent springs (Kogweno, Kudho, Kosinda, Asengo and Kokelo) within the deposits. These springs ultimately combine to form streams that discharge into Lake Victoria.

Groundwater potential within the Nyanzian and the Paleogene and Neogene volcanic rocks are moderate but very low within the Kavirondian rocks. The Precambrian Nyanzian and Kavirondian system rocks are the oldest and widespread in the Kisumu study site. These rocks are very compact with very low porosity. In the absence of fractures or other geological structures, these rocks form very poor aquifers. The Palaeogene and Neogene volcanic rocks, mainly phonolite, have a weathered upper layer often covered by a porous material. The thickness of this layer is less than 10 meters. Most shallow wells within the volcanic zone are located within this zone. Within the meta-andesites of the Nyanzian period, the higher horizons of the weathered layer are clayey. This layer is evident on the pillow lavas located along the Kakamega Highway and range in depth from 0 to 10 meters (VES interpretation). Clays have high porosities and extremely low permeability, and, therefore, groundwater yields in these shallow wells is low. The water has high electrical conductivity (3510 µS/cm) in Otonglo due to interactions with clay minerals and contamination (well was highly contaminated by TTC). The sediments of the Pleistocene system north of Kisumu International Airport and alluvium deposits in Mbeme form the most productive shallow aquifer. These sediments are primarily sandy and gravely, as was evidenced by the geo-logs. These sediments are lacustrine in origin, and therefore indicate buried old river channels (Johnson *et al.*, 2000; Tryon *et al.*, 2016).

The main springs in Kisumu are located within andesite. Between the decomposed or weathered layer and the fresh andesitic bedrock, the weathered layer consists of less weathered, partly altered rock, with a higher permeability due to little clay material. The average thickness of this layer is between 10 and 20 meters, but in topographically low areas and along faults and fractures, the thickness is more than 50 meters. Moderate yielding boreholes (3 to 4 m^3/hour) have been drilled insignificant fault zones, while the surrounding areas have only a medium to low groundwater potential.

Faults zone within the topographically low area sometimes hosts high-yielding permanent springs. Good examples of such springs are the Kosinda and Asengo springs. Groundwater

yield within fault zones is high, but the yields fluctuate and are low during the prolonged dry season. This is because their permeability is high, and hence their storage capacity is low. However, weathering can penetrate much deeper within faults and fracture zones and create sub-vertical zones filled with coarse material having higher transmissivity values than the surrounding areas (Bense *et al.*, 2013; Gudmundsson, 2000). Groundwater, therefore, accumulates in these zones producing a steady recharge.

Almost all the topographically low areas in the study area consist of Pleistocene to Recent sediments. The Recent sediments occur along the Winam Gulf as alternating thin layers of sands and gravel. These deposits have high porosity, are well-sorted, and are suitable aquifers. These sediments include lacustrine and fluviatile deposits. The Pleistocene sediments host the best aquifer in the study area, as confirmed by boreholes located in Manyatta peri-urban area within the Kano plains. A good example is the Wandiege borehole that the Wandiege Water and Sanitation Company operate.

The Lake Basin Development Authority site, located on Pleistocene sediments, is another example of a borehole that demonstrated the heterogeneity of the shallow Kisumu aquifer. Drilling to a depth of 60 m yielded no substantial water apart from very wet fine-grained brown clays. Erastus Saye's site in Otonglo further provided evidence on the complexity of the Kisumu aquifer. Two boreholes were drilled 10 meters from each, and one yielded water while the other was dry. This was interpreted as fracture controlled groundwater system since the drilling logs for the two sites were the same. Additional evidence of fracture-controlled groundwater system was provided by the linear oozing of the drilling rig compressed air mixed with water (Gleeson, Novakowski, & Kurt Kyser, 2009; Ofterdinger, Macdonald, Comte, & Young, 2019).

The finding that the shallow Kisumu aquifer is extremely heterogeneous implies that contamination in one site is unlikely to affect other wells. Over-pumping in one location is also unlikely to affect neighbouring wells. These low-yielding water points can be utilized to meet the demands of local inhabitants but not for large-scale water schemes. The occurrence of groundwater is strongly influenced by geology and the amount of recharge. It would have been interesting to estimate the recharge in Kisumu using the groundwater fluctuation method, but delays in developing the piezometers and rainfalls rendered this futile. However, monitoring water table fluctuation and rainfall to construct long-term chronicles for future reference was established, and data collection is ongoing.

4.4.1.2   Discussion on the Relationship between groundwater quality, geology, environmental factors, and on-site sanitation

There was a slight or negligible monthly or seasonal fluctuation of temperature, pH, conductivity, and salinity. The minimally marked wet-dry season differences in the physico-chemical parameters suggest that recharge occurs over timescales longer than the seasonal cycles Turbidity was noted to change tremendously during rain seasons in river water, with a slight impact on groundwater. This indicates intensive deposition of silt into surface water during rainfall seasons (Hirpa *et al*., 2018; Li *et al*., 2020; Wu *et al*, 2019). The result concurs with similar findings in other parts of SSA (Lapworth *et al.,* 2017).

Geochemical plots and saturation indices classified Kisumu water into different water types, suggesting differences in the type of water-rock interactions. Gibbs plots indicate that the rock-water interaction dominance and precipitation are the main geochemical processes (Gibbs, 1970b). The dominant water type is the $NaHCO_3$ type. This is due to aragonite, dolomite, and sylvite saturation in several samples. The saturation index of the carbonates helps in defining the thermodynamic stability of water and to explain the geochemical behaviour of water (Arvidson and Mackenzie, 1999; Boon *et al*., 2020; Chidambaram *et al*., 2012; Hostetler, 1964).

Shallow groundwater is vulnerable to contamination from natural and anthropogenic contaminants (Fekkoul *et al*., 2013; IAEA, 1999; Khatri and Tyagi, 2015). Enumeration of coliform bacteria shows that the groundwater in Kisumu is contaminated with thermotolerant bacteria (TTC). The levels were high in water points located less than 10 meters from pit latrines and those found downslope from the toilets. Samples collected during March, June, and December show that the contamination levels are low during June. Coliform bacteria are hosted in the digestive tracks of warm-blooded animals. The numbers of domestic animals and livestock in the densely populated informal settlements led to the conclusion that the source of TTC in water is from human faecal matter.

Pit latrines are located within the same compound as shallow wells. Both structures are hand dug and mainly intercepted the shallow water table. Where open defecation is practised (e.g. along the railway line in Obunga and by small children in the villages and rural areas), the

waste is swept into water bodies during rain seasons. The faecal matter also percolates into the groundwater through rock fractures and faults. The results on TTC enumeration contributes a clearer understanding of the role of pit latrines in the faecal loading of the shallow aquifer in Kisumu. The study acknowledges the non-existence of guidelines on siting toilets and shallow wells.

Despite the TTC contamination, the Wilcox plot indicates that Kisumu groundwater is fit for domestic and irrigation use. Boiling and use of readily available chemicals can be used to kill TTC. Elevated values of fluorides and iron were confirmed in the groundwater. The elevated values of iron in Kudho (21.0 mg/L) and fluoride in Mbeme (7.3 mg/L) can have harmful effects on water consumers. Elevated and variable iron levels in groundwater could represent a potential risk. However, this risk has not been established with any certainty from recent studies elsewhere (e.g. Ghosh *et al.*, 2020). The high fluoride content of fluoride can cause borne and teeth defects. The high values are a consequence of rock-water interaction. Though the nitrates and sulphates content was within the maximum WHO and KEBS allowable levels, the concentrations were higher in shallow wells contaminated with TTC. The nitrates can therefore be considered to be contributed through faecal matter, in addition to geogenic sources.

The use of pit latrines, unregulated waste disposal and dilapidated sewer system pose a risk to residents using groundwater in Kisumu (Lapworth *et al.*, 2017; Okotto-Okotto *et al.*, 2015; Okotto *et al.*, 2015). Extensive fertiliser use and other farm inputs pose a risk to humans using groundwater in the Mt. Elgon region. The chloride and sodium plots show that chlorides come from rock water interactions and other anthropogenic sources. The isotopic plots show a close relationship between rainfall signature and signature from the borehole water. This suggests that groundwater is directly recharged from rainfall. The implication of this is that groundwater is vulnerable to anthropogenic activities and climate variability.

4.4.1.3   *Discussion on environmental isotopes and recharge sources*

Isotopic composition analysis provides evidence that the Kisumu aquifer is recharged directly through precipitation. The plots of $\delta^{18}O$ and δ^2H show that the isotopic signature falls within the local meteoric water line plotted using the IAEA GNIP Kericho station. There is a lack of precipitation isotopic signature data in SSA, and most studies use data jointly collected by IAEA and WMO. GNIP stations are operational in most developed countries but are no longer

functional in other countries, including Kenya. The precipitation isotopic data for Kericho was used to draw the local meteoric water line. The relationship between the rainfall and isotopic signature showed an inverse relationship. Heavy rainfall events correspond with depletion of both $\delta^{18}O$ and δ^2H. This implies that light rainfall in Kericho was subjected to evaporation which enriched their mean isotopic composition in heavier isotopes relative to non-evaporated, heavy rains.

Since the environmental isotopes of water are conservative, groundwater will retain the isotopic signature of recharging precipitation provided that the isotopic content of the recharge water is not affected by the vadose zone and the source of recharge is restricted to the direct infiltration of rainfall (Ben *et al*., 2014; Bonsor and MacDonald, 2010; Craig, 1961; Graham, 2008). Although infiltrating rainfall represents the principal source of recharge in the Kisumu study site, the isotopic content of the groundwater is dominated by the rainfall falling during those months in which most recharge occurs (April, April, October and November). Groundwater timing of recharge corresponds to the heaviest rainfalls when rates of incoming precipitation temporarily exceed the intense evapotranspiration (Sklash and Mwangi, 1991; Taylor and Howard, 1996).

Since isotopes signature suggest that groundwater in Kisumu is meteoric in origin, all anthropogenic activities within the larger catchment are likely to affect it negatively. The increase in population and demand for housing is slowly converting bare land into houses and accompanying infrastructural developments. One consequence of this land-use change is that surface land-off is increasing, and the portion of rainwater that percolates to recharge the aquifer is slowly becoming less. Secondly, the new settlements are mostly not connected to the sewer line and therefore use onsite sanitation. These activities compounded with climate variability will affect the amount and quality of groundwater in Kisumu.

4.4.1.4   *Results on the conceptual model for the Kisumu aquifer*

The main recharge contributing to the groundwater is the precipitation in the highlands and the hills north of Lake Victoria, *Figure 4.74*. The isotopic signature shows no interaction between groundwater and the Lake. There is, therefore, no recharge of groundwater from the Lake. The main discharge is naturally through springs and artificial shallow wells, and boreholes.
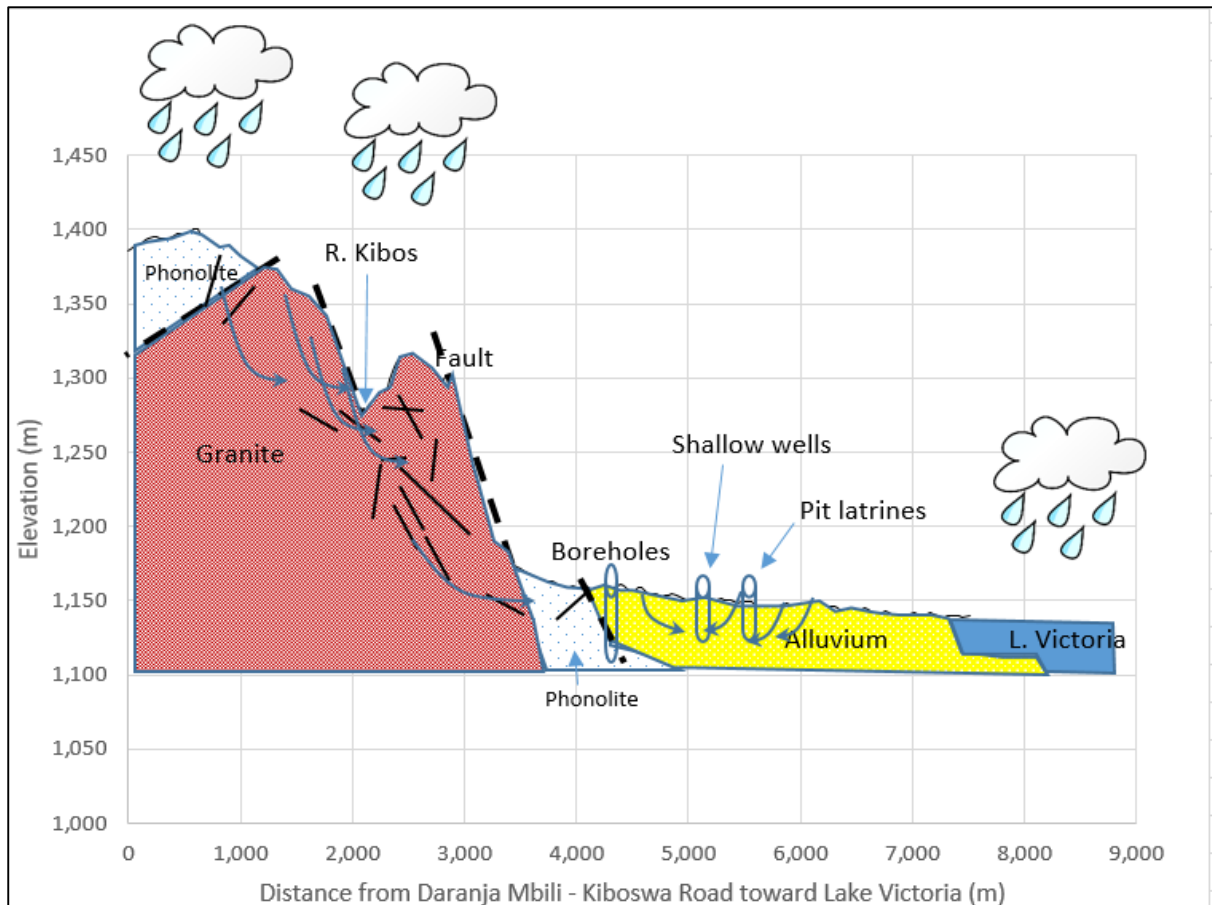
Figure 4.74. Geological profile along transect 1. The fractured and faulted granite form channels for rainwater percolation into the shallow aquifer. The water is trapped in the lowlands via shallow wells up to 2 meters in depth with the alluvium.

The transect passes through Otonglo peri-urban settlement that depends on shallow wells for water supply and pit latrines for sanitation. TTC highly contaminates the shallow aquifer. The second transect terminates into the Lake through an impervious meta-sedimentary rock outcrop (meta-grit), Figure 4.75.

177
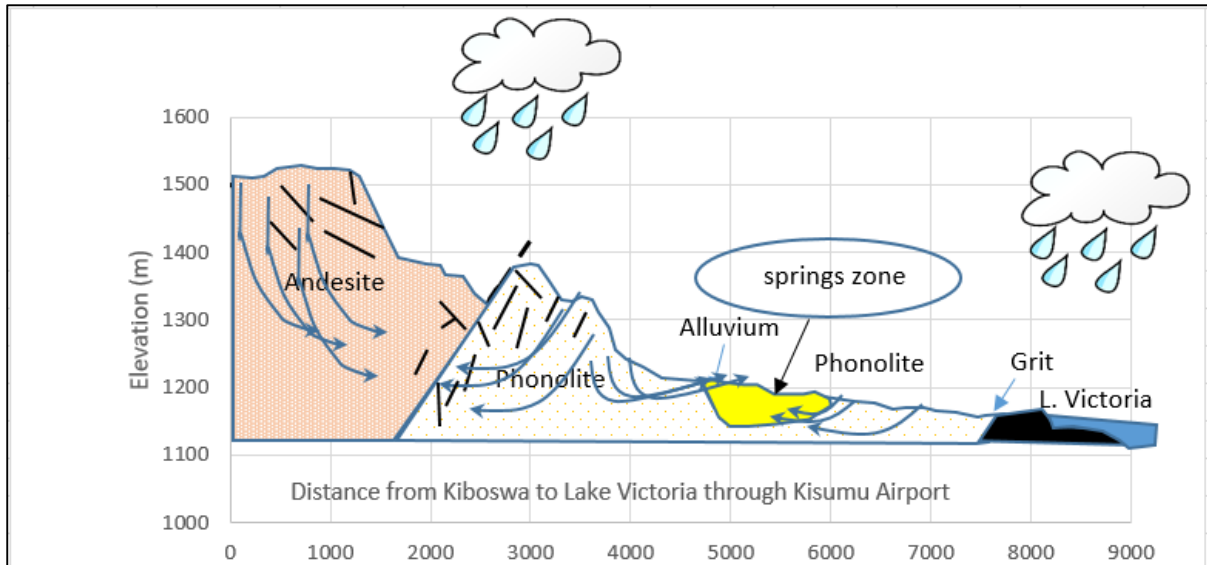
Figure 4.75. Geological profile through transect 2. The highlands consist of highly fractured and faulted meta-andesitic rocks. These are sites for precipitation percolation into the aquifer. Groundwater recharges through numerous springs within the alluvium and fractured phonolite.

This rock does not permeate groundwater flow into Lake Victoria, and water laterally flows eastwards to emerge as springs in Kogweno and Obunga. The third transect run from the Nandi Escarpment in Kokelo. This zone consists of highly fractured and faulted granite, *Figure 4.76*.
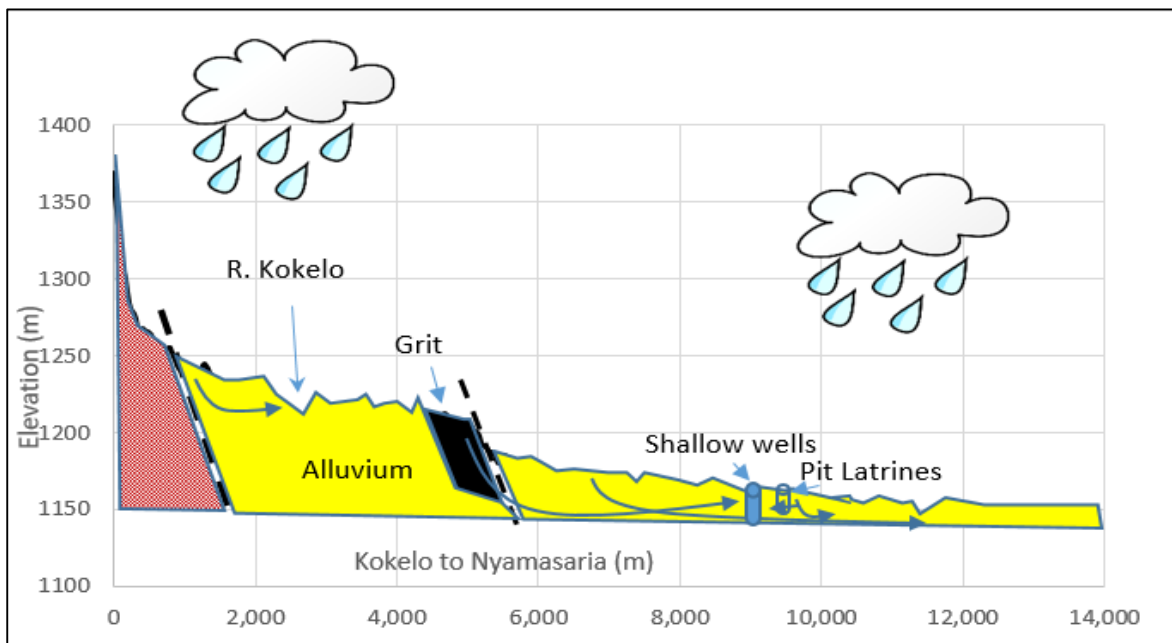
Figure 4.76. Geological profile along transect 3. Rainfall percolates through the faulted granite in Kokelo and recharges the shallow aquifer in the Kano plains. Mbeme and Wandiege are examples of boreholes fed by this groundwater system.

178

The fourth profile run from the Kisian to R. Kibos. This zone consists of alluvium. Springs and wetlands, Figure 4.77 dominate the zone.
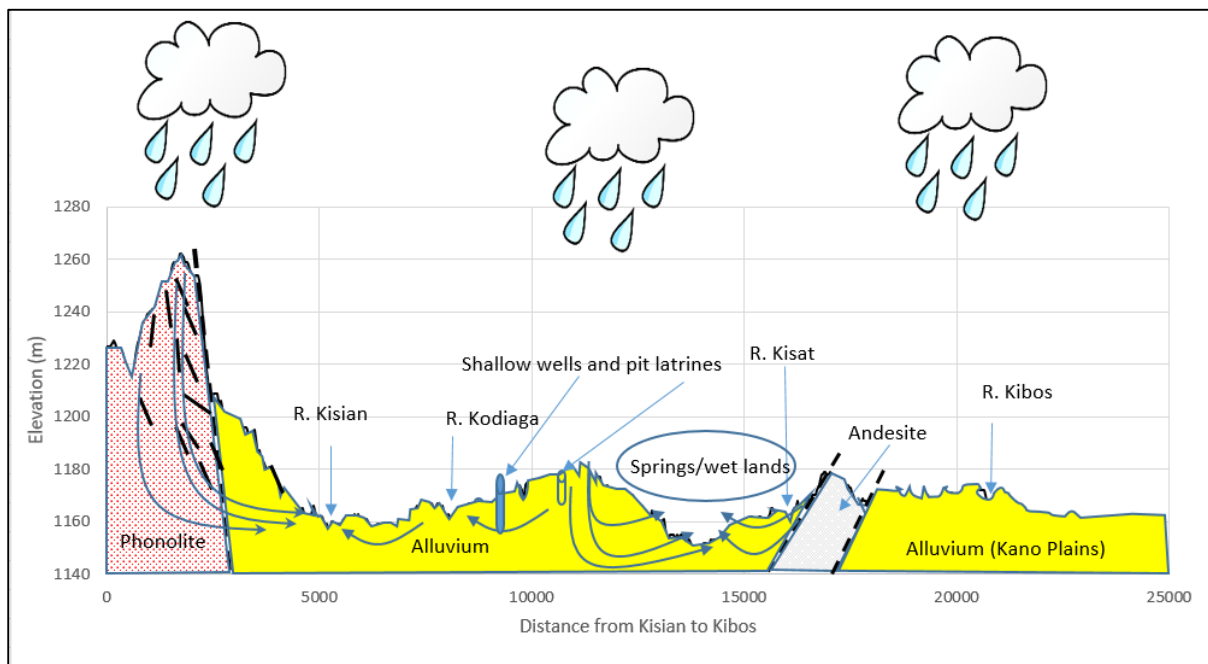
Figure 4.77. The West to East profile from Kisian to Kibos along the alluvium. Shallow groundwater flows along this line and discharges naturally as springs.

4.4.2   Discussion on the results of Mt. Elgon aquifer

4.4.2.1   Mt. Elgon aquifer geometry and characteristics

The geological mapping and geophysical surveys in Mt. Elgon show that the western side of Kitale comprises volcanic rocks. The volcanic rocks thickness reduces uniformly away from the mountain slopes towards the West Pokot lowlands and Kitale plains. The depth of the aquifer decreases eastward and is very shallow at the contact between the volcanic and metamorphic rocks (Odida, 2015). The aquifer characteristics are dependent and influenced by geology. For example, the transmissivity values range from 1.8 to 80.8 m^2/day, implying that the aquifer is heterogeneous. Boreholes located on successive old lava surfaces have high yields. Differences in the rocks or debris of the old lava surfaces in the volcanic successions result in contrasting aquifer characteristics. Faults that extend from the Neo-Proterozoic Mozambique belt rocks into the volcanic rocks form sites of very productive boreholes in West

Pokot and the Kitale plains. However, it is difficult to identify these buried faults within the Kitale plains using vertical electrical sounding.

The geophysical profiling showed that the Mt. Elgon Transboundary aquifer is shallow and occurs on the boundaries of successive basaltic lava flows, agglomerate and contacts of volcanic rocks and metamorphic rocks. The aquifer properties calculated from the existing borehole completion record showed that geology strongly influences the borehole yield. Boreholes located at the contacts between volcanic and metamorphic are examples of high yielding boreholes. Within the metamorphic rocks, productive boreholes are located on fault zones that emanate from the mountain slopes. However, locating these fault zones was difficult using the vertical electrical sounding. Identification of fault zone and hydro-geophysical characteristics of faulted and fractured aquifers are complicated because the structures are controlled by different factors (Kamal, 2018; Mansour, Omar *et al.*, 2018). The results agree with previous observations from other parts of sub-Saharan Africa (Xu *et al*., 2019).

4.4.2.2 *The relationship between groundwater quality, geology and environmental factors in Mt. Elgon aquifer*

The chemical and physico-chemical parameters are within the levels recommended by the local KEBS and WHO standards. However, fluoride levels beyond the maximum allowable value of 1.5 mg/L were noted in three samples (2.8, 2.3 and 5.1 mg/L, respectively). The residency time for groundwater is short within the volcanic rock. Therefore, the time for geochemical processes between rocks and water is reduced (Chenini *et al.*, 2010; Fouépé Takounjou *et al.*, 2020; Yousif and El-Aassar, 2018). The levels of nitrates and sulphates in groundwater are low, implying that anthropogenic influence on groundwater is low. In rural settings in Kenya, there is ample space to develop shallow wells and pit latrines. Further, the public health department ensures that the two are separated to avoid groundwater contamination (Nakagiri *et al*., 2016b; Ravenscroft *et al.*, 2017; SNV, 2018).

The stiff plot shows the dominance of bicarbonate water in the volcanic Mt. Elgon aquifer. The dominant cations are sodium and potassium. Calcium appears to dominate the shallow wells, while samples from borehole, rivers and springs have low values. Iron is released during the silicate weathering and oxidation of iron-rich minerals (mostly ilmenite, limonite and magnetite) (Kiczka *et al.*, 2011; Kump *et al*., 2000). The weathered and altered silicate products

from the andesite are extensive in the study area in laterite. This is the main source of iron in groundwater. Plots of Na^+ versus Cl^- revealed that most of the data clustered below the 1:1 line, illustrating the strong influence of the silicate weathering and ion exchanges within the groundwater. This supports the theory that ionic input into the groundwater system is most likely a consequence of geologic sources (Fetter, 2001; Todd and Mays, 1980). These geologic sources are the natural water-rock interactions, including weathering and dissolution of minerals in the aquifer. The relationship between total cations and alkali and total cations and alkali earth ions further confirms that silicate weathering contributes to groundwater ionic content.

Saturation indices and chemical composition of water samples from Mt. Elgon exhibited a normal distribution of major ions. Generally, water from volcanic rocks is dominated by carbonate dissolution (Fenta *et al*., 2020). However, water from metamorphic rocks is more mineralized, probably due to long travel from recharge areas within the mountain and longer residence time than groundwater near the recharge area (mountain). The boreholes within the metamorphic rocks were deep, up to 150 meters, and this indicates long flow paths as was concluded in similar studies (Kalbus *et al.*, 2006; Modica and Buxton, 1998). High mineralization is explained by long flow paths and residence time within the metamorphic rocks structures and regolith.

4.4.2.3   *Discussion of the conceptual model for the Mt. Elgon aquifer*

The recharge areas are located within the mountain and slopes, *Figure 4.78*. These areas are dominated by agglomeritic tuffs that are porous, allowing precipitation to percolate into the aquifer. Groundwater preferentially flows through old lava surface to emerge as springs on the slopes. The contact between the volcanic and metamorphic rocks are also dotted with all season springs.
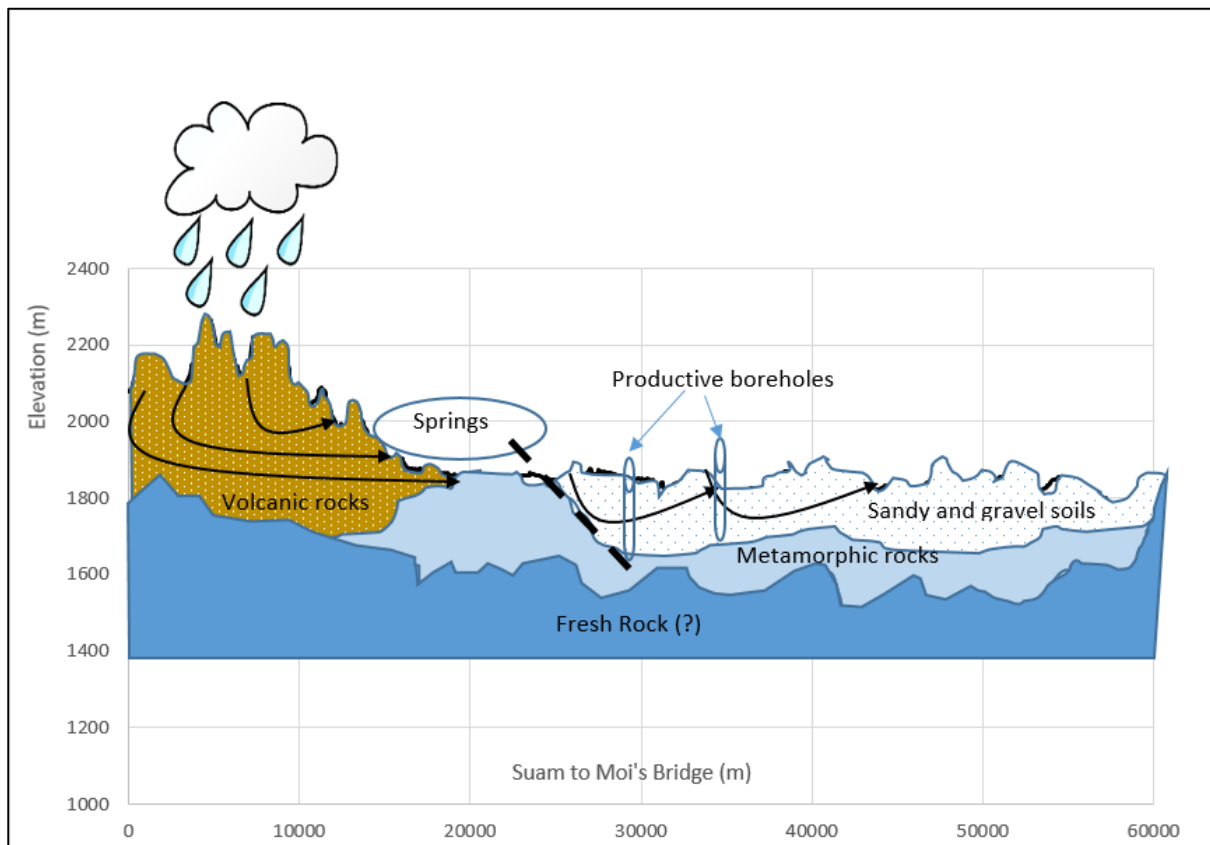
Figure 4.78. Geological profile north-west to the south-east from Suam to Moi's bridge. The main aquiferous zone is between sandy and gravel soils and the underlying metamorphic rocks.

CHAPTER 5 - CONCLUSION AND RECOMMENDATIONS

5.1 Conclusion

5.1.1 Introduction

Efforts have been made locally and internationally to address groundwater challenges. However, due to limited knowledge, groundwater problems are complicated to address holistically. Fragmented approaches in addressing groundwater locally and globally continue to threaten the available freshwater resources and the quest of humanity to achieve the UN Sustainable Development Goal No.6 by 2030. Changes in land use are slowly reducing recharge areas for groundwater systems dependent on direct rainfall recharge. In addition, deteriorating groundwater quality due to geogenic and anthropogenic sources poses a challenge to millions of people in sub-Saharan Africa. Urbanization coupled with population increases and enormous water demands for agriculture and industrial development continues to impose severe stress on available groundwater. This, therefore, requires careful management of the finite groundwater resources based on evidence derived through integrated research.

5.1.2 Conclusion based on objective 1 – Aquifer geometry and characteristics

Before this study, little was known about the aquifer geometries of the Kisumu and Mt. Elgon aquifers. The shallow Kisumu volcano-sedimentary and Mt. Elgon volcanic aquifers were thought to be reasonably homogeneous, and all the aquifer parameters were calculated or estimated based on this premise. The assumption that geophysical profiling alone could pinpoint groundwater drilling sites resulted in drilling dry wells or low yielding wells. Only boreholes located on Pleistocene alluvium deposits or along faults and main fractures yielded water. Therefore, a combination of geophysics and geological mapping methods could reduce the probability of missing aquiferous layers below the ground surface. In the Mt. Elgon aquifer, groundwater is influenced by old lava surfaces, cooling joints and fractures, and rock type. Agglomerates tuffs resting on metamorphic or igneous rocks formed sites for high yielding boreholes and permanent springs. The extreme heterogeneity of the Kisumu aquifer can be considered a blessing since activities (pumping and contamination) in one well hardly affect the neighbouring wells. However, the shallow aquifer cannot sustain extensive scale exploitation for public use. It can only serve individual demands or small scale community water schemes.

5.1.3 Conclusion based on objective 2 – Water chemistry and vulnerability to contamination

Water chemistry is influenced by many factors, including those of geogenic and anthropogenic origin. Silicate dissolution and weathering are the main processes identified to influence water chemistry in the two study sites. However, like other aquifers located within the tropics, evaporation plays a minimal role in modifying water chemistry. The constancy of physical parameters indicates that recharge occurs over timescales more prolonged than the seasonal cycles. This study has confirmed that rock-water interactions (dissolution and weathering) greatly influence water chemistry. A high concentration of dissolved minerals like fluorides and iron beyond the WHO and KEBS recommended upper limits can negatively impact water consumers.

Safe water and dignified sanitation are human rights in Kenya as enshrined in the bill of right to safe water and proper sanitation, Article 43 of the Kenya Constitution (Constitution, 2010). The County and National Governments are striving to achieve this. These efforts are masked by a lack of data and massive geographical inequalities, challenges in the supply system and high demand during the dry season when alternative sources are dry. Water shortages and lack of sewer services have led to constructing shallow wells (and boreholes by the rich) and pit latrines for self-service. The dual use of the underground as a water source and repository of human waste has numerous risks.

5.1.4 Conclusion based on objective 3 – Determination source of recharge water using stable isotope

Stable water isotopes confirmed that groundwater is of meteoric origin, and recharge occurs during the period of heavy rainfalls. This occurs during April – May and November December, though there is a shift of rainfall months due to climate variability. Low or light rainfall is depleted in deuterium and oxygen-18 due to evaporation. The isotope signature confirmed, further, that there is no interaction between Lake Victoria and groundwater. Discharge occurs through numerous springs in the topographically low area at various rock contacts. Groundwater form the base flow of the major streams and rivers.

5.2 Recommendations from the study

1. This study recommends constructing groundwater monitoring systems, including installing loggers for water table fluctuations monitoring and water chemistry monitoring, to better understand aquifer and water quality.

2. It is recommended that joint manuals for water surveillance involving all stakeholders, including Ministry of Water and Sanitation, Ministry of Health, NEMA, WARMA, WASREB, KEBS and other key water research institution. The Ministry of Water and Sanitation and the associated water institutions should develop strategies for analysing, summarizing and disseminating water-related data at national and county government levels. This information will inform policy on remedial actions to improve water safety, water source protection, household water treatment, pollution prevention and improved sanitation. It is recommended that siting and construction of pit latrines should be strictly controlled. The commonly used guideline is that the shallow wells should be located in an area higher than 15 m from the pit latrines and should be at least 2 m above the water table. To avoid sanitary risks and localized contamination of groundwater through the borehole head, a sound cement seal at least 5cm thick around the casing to the top of the intake screen.

3. The application of water isotopes in water resources management should be promoted since they provide information that cannot be obtained from other sources.

5.3 Contribution of the findings to science and residents of the study area

1. The research has revealed that the shallow Kisumu aquifer is heterogeneous, which poses a challenge in utilising the groundwater in the area. From an economic viewpoint, this revelation is essential since national, local or investment partners may develop boreholes targeting the shallow aquifer that will not last for long. Borehole completion record revealed heterogeneity of Mt. Elgon aquifer that is dictated by geology. The aquifer is multi-layered, and the high yielding boreholes can be drilled at the contact between the volcanic rocks and the metamorphic rocks or on old lava surfaces.

2. The research also established that the groundwater flows eastwards and not directly toward Lake Victoria. Direct flow into the lake is hindered by a geological formation,

a Kavirondian meta-sediment. There is, therefore, no Lake Victoria-groundwater interactions as evidenced by isotope studies.

3. The study has demonstrated that the main hydro-chemical processes in both Kisumu and Mt. Elgon aquifers are rock water interaction. This geogenic process has led to elevated levels of fluorides and iron that can be detrimental to human health. Other ions are within the range recommended by WHO and KEBS.

4. Groundwater in Kisumu is contaminated with TTC, and this revelation was shared with the residents. The advice is to boil water collected from these alternative sources before drinking. The study has also constructed six piezometers and two automatic rainfall stations to estimate the aquifer's recharge. These will continue monitoring water table fluctuation and rainfall beyond this study.

5. This study has demonstrated its usefulness in determining recharge, threats and vulnerability of groundwater. Groundwater in Kisumu is recharged by meteoric water from heavy rainfall events and is therefore considered modern water. It is vulnerable to anthropogenic activities and climate variability. Reduced precipitation will result in reduced recharge.

6. Further studies are needed to estimate the recharge and develop a numerical model for Kisumu and Mt. Elgon aquifers since these were not accomplished during this study. Estimation of recharge requires long term data of water table fluctuation and accompanying rainfall data. Other techniques of determining recharge, including the chloride mass balance (CMB) method, can be applied to estimate mean groundwater recharge. Over-pumping and contamination of aquifers can be studied using radiocarbon. It offers a technique to predict the over-pumping of the aquifer before it becomes contaminated or overexploited.

References

Abdou B, M. S., Orban, P., Ousmane, B., Favreau, G., Brouyère, S., & Dassargues, A. (2018). Characterization of recharge mechanisms in a Precambrian basement aquifer in semi-arid south-west Niger. *Hydrogeology Journal*, 1–17. https://doi.org/10.1007/s10040-018-1799-x

Abesser, C., Shand, P., Gooddy, D., & Peach, D. (2008). The role of alluvial valley deposits in groundwater-surface water exchange in a Chalk river. In *Proceedings of Symposium HS1002 at IUGG2007, Perugia, July 2007. IAHS Publ. 321, 2008* (pp. 11–20).

Abiye, T. A., Demlie, M., & Mengistu, H. (2015). Surface water and groundwater interaction in the Upper Crocodile River Basin, Johannesburg, South Africa: Environmental approach. *Environmental Earth Sciences*, 1–30. https://doi.org/https://doi.org/10.2113/gssajg.118.2.109

Abott, M., Lini, A., & Biermsn, P. (2000). $\delta 18O$, δD and 3H measurements constrain groundwater recharge patterns in an upland fractured bedrock aquifer, Vermont, USA. *Journal of Hydrology*, *228*, 101–112.

Adelana, S., Olasehinde, P., & Vrbka, P. (2011). Isotope and geochemical characterization of surface and subsurface waters in the semi-arid Sokoto Basin, Nigeria. *African Journal of Science and Technology*, *4*(2), 80–89. https://doi.org/10.4314/ajst.v4i2.15298

Adimalla, N., & Venkatayogi, S. (2018). Geochemical characterization and evaluation of groundwater suitability for domestic and agricultural utility in semi-arid region of Basara, Telangana State, South India. *Applied Water Science*, *8*(1), 44. https://doi.org/10.1007/s13201-018-0682-1

Adomako, D., Maloszewski, P., Stumpp, C., Osae, S., & Akiti, T. T. (2010). Estimation de la recharge des eaux souterraines à partir des profils en profondeur des isotopes de l'eau (d2H, d18O) dans le bassin de la Rivière Densu, Ghana. *Hydrological Sciences Journal*, *55*(8), 1405–1416. https://doi.org/10.1080/02626667.2010.527847

Ahialey, E. K., Kortatsi, B. K., Anornu, G. K., Kaka, E. A., & Dartey, G. (2016). Hydrogeochemical Processes Influencing Groundwater Quality in the Black Volta Basin of Ghana. *Research Journal of Applied Sciences, Engineering and Technology*, *11*(9), 975–982. https://doi.org/10.19026/rjaset.11.2137

Akotsi, E. (2004). *Changes in forest cover in Kenya's "water towers" 2000 - 2003*. Nairobi. Unpublished report. Downloaded from the site on 24th May 2021: https://allafrica.com/download/resource/main/main/idatcs/00010675:4e303c221b60c22e8b68ad05f8cc923d.pdf

Al-Ahmadi, M. E. (2013). Hydrochemical characterization of groundwater in wadi Sayyah, Western Saudi Arabia. *Applied Water Science*, *3*(4), 721–732. https://doi.org/10.1007/s13201-013-0118-x

Aladejana, J. A., Kalin, R. M., Sentenac, P., & Hassan, I. (2020). Assessing the impact of climate change on groundwater quality of the shallow coastal aquifer of Eastern Dahomey Basin, Southwestern Nigeria. *Water (Switzerland)*, *12*(1). https://doi.org/10.3390/w12010224

Alam, K., & Ahmad, N. (2014). Determination of aquifer geometry through geophysical methods: A case study from Quetta Valley, Pakistan. *Acta Geophysica*, *62*(1), 142–163. https://doi.org/10.2478/s11600-013-0171-8

Alsharhan, A. S., & Rizk, Z. E. (2020). *Water Resources and Integrated Management of the United Arab Emirates*. Springer Switzerland. ISBN 978-3-030-31683-9, ISBN 978-3-030-31684-6 (eBook). https://doi.org/10.1007/978-3-030-31684-6

Ammar, A. I., & Kamal, K. A. (2018). Resistivity method contribution in determining of fault

zone and hydro-geophysical characteristics of carbonate aquifer, eastern desert, Egypt. *Applied Water Science*, 8(1), 1–27. https://doi.org/10.1007/s13201-017-0639-9

Angienda, P. O., & Onyango, D. M. (2010). Epidemiology of Waterborne Diarrhoeal Diseases among Children Aged 6-36 Months Old in Busia - Western Kenya. *World Academy of Science, Engineering and Technology*, 37, 1158–1165.

APHA. (1999). Standard Methods for the Examination of Water and Wastewater; Part 4000; Inorganic Nonmetallic Constituents. *American Public Health Association, American Water Works Association, Water Environment Federation*.

APHA. (2017). *standard methods for the examination of water and wastewater*. (R. Baird, A. Eaton, & E. Rice, Eds.) (23rd Edition). https://doi.org/10.2105/SMWW.2882.216

Appelo, C., & Postma, D. (2005). Geochemistry, groundwater and pollution. Geochemistry, groundwater and pollution (2nd Editio). Amsterdam: *Balkema Publishers*. https://doi.org/10.1016/0016-7037(94)90585-1

ARGOSS. (2001). Guidelines for assessing the risk to Groundwater from On-Site Sanitation.British Geological Survey Commissioned Repor*t, CR/01/142. 97pp*.

Arnous, M. O., El-Rayes, A. E., Geriesh, M. H., Ghodeif, K. O., & Al-Oshari, F. A. (2020). Groundwater potentiality mapping of Tertiary volcanic aquifer in IBB basin, Yemen by using remote sensing and GIS tools. *Journal of Coastal Conservation*, 24(3). https://doi.org/10.1007/s11852-020-00744-w

Arvidson, R. S., & Mackenzie, F. T. (1999). The dolomite problem: Control of precipitation kinetics by temperature and saturation state. *American Journal of Science*, 299(4), 257–288. https://doi.org/10.2475/ajs.299.4.257

Awange, J. L., & Ong'ang'a, O. (2006). *Lake Victoria; Ecology, Resources, Environment*. Springer Verlag. https://doi.org/10.1007/978-1-4020-9726-3_12

Back, W. (1960). Origin of Hydrochemical Facies of Groundwater in the Atlantic Coastal Plains. In *International Geological Congress, 21st, Copenhagen, 1960, Report Part 1* (pp. 87–95).

Baker, B. H., Williams, L. A. J., Miller, J. A., & Fitch, F. J. (1970). Sequence and Geochronology of the Kenya Rift Volcanics. *Tectonophysics*, 11, 191–215.

Baker, B., Mitchell, G., & Williams, J. (1988). Stratigraphy, geochronology and volcano-tectonic evolution of the Kedong-Naivasha-Kinangop region, Gregory Rift Valley, Kenya. *Journal of the Geological Society, London*, 145, 107–116.

Bakker, B. H. (1997). Groundwater management in Kenya; The need for improved legislation, delegation of authority and independent decision making, Groundwater resources in Kenya. In A. Schrevel (Ed.), *ILRl workshop: Groundwater management: Sharing responsibility for an open access* (pp. 111–126). Wageningen.

Barbecot, F., Guillon, S., Pili, E., Larocque, M., Gibert-Brunet, E., Hélie, J.F., Meyzonnat, G. (2018). Using Water Stable Isotopes in the Unsaturated Zone to Quantify Recharge in Two Contrasted Infiltration Regimes. *Vadose Zone Journal*, 17(1), 1–13. https://doi.org/10.2136/vzj2017.09.0170

Barbieri, M. (2019). Isotopes in hydrology and hydrogeology. *Water (Switzerland)*, 11(2). https://doi.org/10.3390/w11020291

Beatty, M., Ochieng, J., Chege, W., Kumar, L., Okoth, G., Shapiro, R.,& Brooks, J. (2009). Sporadic paediatric diarrhoeal illness in urban and rural sites in Nyanza province, Kenya. *East African Medical Journal*, 86(8), 387–398. https://doi.org/10.4314/eamj.v86i8.54159

Begashaw, G., & Tafesse, N. T. (2017). Characteristics and Productivity of the Sediments and Volcanic Rocks Aquifers in Sunuta Sub-Basin, Northeast Ethiopia. *Asian Review of Environmental and Earth Sciences*, 4(1), 46–57. https://doi.org/10.20448/journal.506.2017.41.46.57

Ben, A., Mzali, H., Zouari, K., & Hezzi, H. (2014). Hydrochemical and isotopic assessment of groundwater quality in the Quaternary shallow aquifer, Tazoghrane region, north-eastern Tunisia. *Quaternary International*, *338*, 51–58. https://doi.org/10.1016/j.quaint.2014.01.023

Bennett, G. D., & Patten, E. P. (1962). Constant-head pumping test of a multiaquifer well to determine characteristics of individual aquifers. *US Geological Survey water-supply paper 1S36-G. Prepared in cooperation with the Pennsylvania Geological Survey. Department of Internal Affairs, Commo* (No. 1536- G).

Bense, V. F., Gleeson, T., Loveless, S. E., Bour, O., & Scibek, J. (2013). Fault zone hydrogeology. *Earth-Science Reviews*, *127*, 171–192. https://doi.org/10.1016/j.earscirev.2013.09.008

Benson, C., & Clay, E. J. (2004). *Understanding the economic and financial impacts of natural disasters. Risk Management Serie No. 4*.

Bershaw, J. (2018). Controls on deuterium excess across Asia. *Geosciences (Switzerland)*, *8*(7). https://doi.org/10.3390/geosciences8070257

Blanchette, D., Lefebvre, R., Nastev, M., & Cloutier, V. (2010). Groundwater Quality, Geochemical Processes and Groundwater Evolution in the Chateauguay River Watershed, Quebec, Canada. *Canadian Water Resources Journal*, *35*(4), 503–526. https://doi.org/10.4296/cwrj3504503

Blandenier, L. (2015). Recharge Quantification and Continental Freshwater lens Dynamics in Arid Regions: Application to the Merti Aquifer (Eastern Kenya*) PhD Thesis*. The University of Neuchâtel. Retrieved from www.unine.ch/sciences

Blomqvist, R. (1999). Hydrogeochemistry of deep groundwaters in the central part of the Fennoscandian Shield*, PhD Thesis*. Helsinki University of Technology.

Bonsor, H. C., & MacDonald, A. M. (2010). Groundwater and climate change in Africa: a review of aquifer properties data. *Groundwater Science Programmes, Internal Report IR/10/076*, 30. https://doi.org/IR/10/075

Bonsor, H., Shamsudduha, M., Marchant, B., MacDonald, A., & Taylor, R. (2018). Seasonal and Decadal Groundwater Changes in African Sedimentary Aquifers Estimated Using GRACE Products and LSMs. *Remote Sensing*, *10*(904), 1–20. https://doi.org/10.3390/rs10060904

Boon, M., Rickard, W. D. A., Rohl, A. L., & Jones, F. (2020). Stabilization of Aragonite: Role of Mg 2+ and Other Impurity Ions. *Crystal Growth & Design*, *20*(8), 5006–5017. https://doi.org/10.1021/acs.cgd.0c00152

Boretti, A., & Rosa, L. (2019). Reassessing the projections of the World Water Development Report. *Npj Clean Water*, *2*(1). https://doi.org/10.1038/s41545-019-0039-9

Bovolo, C. I., Parkin, G., & Sophocleous, M. (2009). Groundwater resources, climate and vulnerability. *Environmental Research Letters*, *4*(3). https://doi.org/10.1088/1748-9326/4/3/035001

Brand, W. A. (2004). Mass Spectrometer Hardware for Analyzing Stable Isotope Ratios. In P. A. de Groot (Ed.), *Handbook of Stable Isotope Analytical Techniques, Volume-1* (pp. 835–856). Elsevier B.V. https://doi.org/10.1016/B978-044451114-0/50040-5

Brielmann, H. (2008). Recharge and discharge mechanism and dynamics in the mountainous northern Upper Jordan River. PhD thesis. Ludwig-Maximilians-University, Munich.

Bruin, J., & Hudson, H. E. (1961). Selected Methods for Pumping Test Analysis*, Report of Investigation 25. Selected Method for Pumping Test Analysis*. https://core.ac.uk/download/pdf/161954118.pdf

Brundtland, H. (1988). The Brundtland Report: "Our Common Future.*" Report of the World Commission on Environment and Development: Our Common Future* (Vol. 4). https://doi.org/10.1080/07488008808408783

Brunner, P., & Kinzelbach, W. (2005). Management. *Encyclopedia of Hydrological Sciences*, 1–11.

Calow, Roger and Macdonald, A. (2009). *What will climate change mean for groundwater supply in Africa? Overseas Development Institute*.

Calow, R C, Robins, N. S., Macdonald, A. M., Macdonald, D. M. J., Gibbs, B. R., Orpen, W. R. G., & Appiah, S. O. (1997). Groundwater Management in Drought-prone Areas of Africa. *International Journal of Water Resources Development*, *13*(2), 241–262. https://doi.org/10.1080/07900629749863

Calow, Roger C., MacDonald, A. M., Nicol, A. L., & Robins, N. S. (2010). Ground water security and drought in Africa: Linking availability, access, and demand. *Ground Water*, *48*(2), 246–256. https://doi.org/10.1111/j.1745-6584.2009.00558.x

Carleton, G. B. (2010). Simulation of Groundwater Mounding Beneath Hypothetical Stormwater Infiltration Basins, 1–76. USGS Scientific Investigations Report 2010–5102 https://pubs.usgs.gov/sir/2010/5102/support/sir2010-5102.pdf

Carrera, J., & Tubau, I. (2010). An approach to identify urban groundwater recharge, 2085–2097. *Hydrol. Earth Syst. Sci.*, 14, 2085–2097. https://doi.org/10.5194/hess-14-2085-2010

Carter, R. C., & Parker, A. (2009). Climate change, population trends and groundwater in Africa. *Hydrological Sciences Journal*, *54*(4), 676–689. https://doi.org/10.1623/hysj.54.4.676

Carvalho Resende, T., Longuevergne, L., Gurdak, J. J., Leblanc, M., Favreau, G., Ansems, N., & Aureli, A. (2018). Assessment of the impacts of climate variability on total water storage across Africa: implications for groundwater resources management. *Hydrogeology Journal*. https://doi.org/10.1007/s10040-018-1864-5

Cerling, T. E. (2019). Pore Water Chemistry of an Alkaline Lake: Lake Turkana, Kenya. *The Limnology, Climatology and Paleoclimatology of the East African Lakes*, (November), 225–240. https://doi.org/10.1201/9780203748978-12

Chandrasekharan, H., Gupta, N., & Navada, S. V. (1997). Deuterium and oxygen-18 isotopes on groundwater salinization of adjoining salt pans in Porbandar coast, Gujarat, India. In *Hydrochemistry (Proceedings of the Rabat Symposium, April 1997) IAHS Publ. no. 244, 1997* (Vol. 244, pp. 207–215).

Chebet, E. B., Kibet, J. K., & Mbui, D. (2020). The assessment of water quality in river Molo water basin, Kenya. *Applied Water Science*, *10*(4), 1–10. https://doi.org/10.1007/s13201-020-1173-8

Chenini, I., Farhat, B., & Ben Mammou, A. B. (2010). Identification of major sources controlling groundwater chemistry from a multilayered aquifer system. *Chemical Speciation and Bioavailability*, *22*(3), 183–189. https://doi.org/10.3184/095422910X12829228276711

Chidambaram, S., Prasanna, M. V., Singaraja, C., Thilagavathi, R., Pethaperumal, S., & Tirumalesh, K. (2012). Study on the Saturation Index of the carbonates in the groundwater using WATEQ4F in layered coastal aquifers of Pondicherry. *Journal of the Geological Society of India*, *80*(6), 813–824. https://doi.org/10.1007/s12594-012-0210-0

Chilton, J., & Seiler, K.-P. (2006). Groundwater occurrence and hydrogeological environments. *Protecting Groundwater for Health: Managing the Quality of Drinking Water Resources*, 21–48.

Chilton, P., & Foster, S. (1993). Hydrogeological characterisation and water-supply potential of basement aquifers in tropical Africa. *Hydrogeology Journal*, *3*(1), 36–49.

Chirindja, F., Rosberg, J. E., & Dahlin, T. (2017). Borehole logging and slug tests for evaluating the applicability of electrical resistivity tomography for groundwater exploration in Nampula complex, Mozambique. *Water (Switzerland)*, *9*(2).

https://doi.org/10.3390/w9020095

Choo, S. (2019). The relationship between the total dissolved solids and the conductivity value of drinking water, surface water and wastewater. In *The 2019 International Academic Research Conference in Amsterdam* (pp. 11–16).

Chung, I. M., Kim, N. W., Lee, J., & Sophocleous, M. (2010). Assessing distributed groundwater recharge rate using integrated surface water-groundwater modelling: Application to Mihocheon watershed, South Korea. *Hydrogeology Journal*, *18*(5), 1253–1264. https://doi.org/10.1007/s10040-010-0593-1

Coetsiers, M., Kilonzo, F., & Walraevens, K. (2008). Hydrochemistry and source of high fluoride in groundwater of the Nairobi area, Kenya. *Hydrological Sciences Journal*, *53*(6), 1230–1240. https://doi.org/10.1623/hysj.53.6.1230

County Government of Trans Nzoia. (2018). *Trans Nzoia County Integrated Development Plan, 2018 - 2022*. Unpublished report

County Government of West Pokot. (2018). *West Pokot County Integrated Development Plan, 2018 - 2022*. Unpublished report

County Government of Kisumu. (2018a). *County Urban Institutional Development Strategy - Kisumu City*. Unpublished report

County Government of Kisumu. (2018b). *Kisumu county integrated development plan, 2018-2022*. Unpublished report

Craig, H. (1961). Isotopic Variations in Meteoric Waters. *Science, New Series*, *133*(3465), 1702–1703. https://doi.org/10.1126/science.133.3465.1702

Crawford, T. J., & Brackett, D. A. (1995). Groundwater in igneous and metamorphic rocks; Low-angle lithologic contacts related to site-specific control of groundwater occurrence. In *Proceedings of the 1995 Georgia Water Resources Conference, held April 11 and 12, 1995, at The University of Georgia.* (pp. 409–412).

Dansgaard, W. (1964). Stable isotopes in precipitation. *Tellus*, *16*(4), 436–468. https://doi.org/10.3402/tellusa.v16i4.8993

Davies, T. C. (1996). Chemistry and pollution of natural waters in western Kenya. *Journal of African Earth Sciences*, *23*(4), 547–563. https://doi.org/10.1016/S0899-5362(97)00018-3

De Leeuw, J., Said, M. Y., Kifugo, S., Musyimi, Z., Mutiga, J. K., & Peden, D. (2012). Benefits of riverine water discharge into the Lorian Swamp, Kenya. *Water (Switzerland)*, *4*(4), 1009–1024. https://doi.org/10.3390/w4041009

De Vita, P., Vincenzo, A., Celico, F., Fabbrocino, S., Cesaria, M., Giuseppina, M., & Pietro, C. (2018). Hydrogeology of continental southern Italy. *Journal of Maps*, *14*(2), 230–241. https://doi.org/10.1080/17445647.2018.1454352

Dedzo, M. G., Tsozué, D., Mimba, M. E., Teddy, F., Nembungwe, R. M., & Linida, S. (2017). Importance of rocks and their weathering products on groundwater quality in central-east Cameroon. *Hydrology*, *4*(2), 1–18. https://doi.org/10.3390/hydrology4020023

DHV Consultants. Rural Domestic Water Resources Assessment Kisumu District (1988). Retrieved from https://www.ircwash.org/sites/default/files/824-5816.pdf

Dos Santos, S., Adams, E. A., Neville, G., Wada, Y., de Sherbinin, A., Mullin Bernhardt, E., & Adamo, S. B. (2017). Urban growth and water access in sub-Saharan Africa: Progress, challenges, and emerging research directions. *Science of the Total Environment*, *607–608*, 497–508. https://doi.org/10.1016/j.scitotenv.2017.06.157

Dragon, K., & Gorski, J. (2015). Identification of groundwater chemistry origins in a regional aquifer system (Wielkopolska region, Poland). *Environmental Earth Sciences*, *73*(5), 2153–2167. https://doi.org/10.1007/s12665-014-3567-0

Drangert, J. O., Okotto-Okotto, J., Okotto, L. G. O., & Auko, O. (2002). Going small when

the city grows big new options for water supply and sanitation in rapidly expanding urban areas. *Water International*, *27*(3), 354–363. https://doi.org/10.1080/02508060208687015

Egboka, B. C. E., Nwankwor, G. I., Orajaka, I. P., & Ejiofor, A. O. (1989). Principles and problems of environmental pollution of groundwater resources with case examples from developing countries. *Environmental Health Perspectives*, *83*, 39–68. https://doi.org/10.1289/ehp.898339

Eggleston, J. R., Rojstaczer, S. A., & Peirce, J. J. (1996). Identification of hydraulic conductivity structure in sand and gravel aquifers: Cape Cod data set. *Water Resources Research*, *32*(5), 1209–1222. https://doi.org/10.1029/96WR00272

Eissa, M., Shawky, H., Samy, A., Khalil, M., & El Malky, M. (2018). Geochemical and Isotopic Evidence of Groundwater Salinization Processes in El Dabaa Area, Northwestern Coast, Egypt. *Geosciences*, *8*(11), 392. https://doi.org/10.3390/geosciences8110392

EPA. (2018). Examples of Groundwater Remediation at NPL Sites, EPA 542-R-18-002. available for viewing or downloading from https://www.epa.gov/remedytech, or http://www.cluin.org

Eugene, B., Skougstad, M., & Fishman, J. (1970). Methods for collection and analysis of water samples for dissolved minerals and gases. *Techniques of water-resources investigations of the United States geological survey. Book 5*. US Geological Survey. Techniques of Water-Resources Investigations 05-A1. https://doi.org/10.3133/twri05A1_1970

Ewusi, A. (2006). Groundwater Exploration and Management using Geophysics : Northern Region of Ghana. PhD thesis, Faculty of Environmental Sciences and Process Engineering, Brandenburg Technical University of Cottbus.

Fajana, A. O. (2020). Groundwater aquifer potential using electrical resistivity method and porosity calculation: a case study. *NRIAG Journal of Astronomy and Geophysics*, *9*(1), 168–175. https://doi.org/10.1080/20909977.2020.1728955

Falkenmark, M. (1990). Global Water Issues Confronting Humanity. *Journal of Peace Research*, *27*(2), 177–190.

Faye, S. C., Diongue, M. L., Pouye, A., Gaye, C. B., Travi, Y., Wohnlich, S.,& Taylor, R. G. (2019). Tracing natural groundwater recharge to the Thiaroye aquifer of Dakar, Senegal. *Hydrogeology Journal*, *27*(3), 1067–1080. https://doi.org/10.1007/s10040-018-01923-8

Fekkoul, A., Zarhloule, Y., Boughriba, M., Barkaoui, A. eddine, Jilali, A., & Bouri, S. (2013). Impact of anthropogenic activities on the groundwater resources of the unconfined aquifer of Triffa plain (Eastern Morocco). *Arabian Journal of Geosciences*, *6*(12), 4917–4924. https://doi.org/10.1007/s12517-012-0740-1

Fenn, M. E., Bytnerowicz, A., Schilling, S. L., & Ross, C. S. (2015). Atmospheric deposition of nitrogen, sulfur and base cations in jack pine stands in the Athabasca Oil Sands Region, Alberta, Canada. *Environmental Pollution*, *196*, 497–510. https://doi.org/10.1016/j.envpol.2014.08.023

Fenta, M. C., Anteneh, Z. L., Szanyi, J., & Walker, D. (2020). Hydrogeological framework of the volcanic aquifers and groundwater quality in Dangila Town and the surrounding area, Northwest Ethiopia. *Groundwater for Sustainable Development*, *11*(April). https://doi.org/10.1016/j.gsd.2020.100408

Ferrer, N., Folch, A., Lane, M., Olago, D., Odida, J., & Custodio, E. (2019). Groundwater hydrodynamics of an Eastern Africa coastal aquifer, including La Niña 2016–17 drought. *Science of the Total Environment*, *661*, 575–597. https://doi.org/10.1016/j.scitotenv.2019.01.198

Fetter, C. W. (2001). *Applied hydrogeology*. (L. Patrick, Ed.) (Fourth Edi). New Jersey:

Prentice-Hall, Inc.

Fiedler, K., & Doll, P. (2008). Global-scale modelling of groundwater recharge. *Hydrology and Earth System Sciences*, *12*(3), 863–885.

Foster, S., Bousquet, A., & Furey, S. (2018). Urban groundwater use in Tropical Africa - A key factor in enhancing water security? *Water Policy*, *20*(5), 982–994. https://doi.org/10.2166/wp.2018.056

Foster, S., Hirata, R., Gomes, D., D'Elia, M., & Paris, M. (2002). *Groundwater Quality Protection. A guide for water utilities, municipal authorities, and environmental agencies. The World Bank. Groundwater Quality Protection*. https://doi.org/10.1596/0-8213-4951-1

Foster, S. S. D. (1984). African groundwater development - The challenges for hydrogeological science. In *Proceedings of the Harare Symposium* (pp. 3–12).

Foster, T., Brozović, N., & Butler, A. P. (2017). Effects of initial aquifer conditions on economic benefits from groundwater conservation. *Water Resources Research*, *53*(1), 744–762. https://doi.org/10.1002/2016WR019365

Fouépé Takounjou, A., Takem Eyong, G., Kuitcha, D., Kringel, R., Fantong Yetoh, W., Ndjama, J., & Tejiobou, A. (2020). Hydrogeochemistry and groundwater flow mechanisms in shallow aquifer in Yaoundé, Cameroon. *Water Supply*, *20*(4), 1334–1348. https://doi.org/10.2166/ws.2020.050

Freeze, A., & Cherry, J. (1979). *Groundwater*. Prentice-Hall, Inc.

Gat, R., Mook, G., & Meijer, H. (2001). *Environmental Isotopes in the Hydrological Cycle - Principles and Applications, International Atomic Energy Agency* (Vol. 2).

Gaye, C. B., & Edmunds, W. M. (1996). Groundwater recharge estimation using chloride, stable isotopes and tritium profiles in the sands of northwestern Senegal. *Environmental Geology*, *27*(3), 246–251. https://doi.org/10.1007/BF00770438

Gaye, Cheikh B., & Tindimugaya, C. (2019). Review: Challenges and opportunities for sustainable groundwater management in Africa. *Hydrogeology Journal*, *27*(3), 1099–1110. https://doi.org/10.1007/s10040-018-1892-1

Ghosh, G. C., Khan, M. J. H., Chakraborty, T. K., Zaman, S., Kabir, A. H. M. E., & Tanaka, H. (2020). Human health risk assessment of elevated and variable iron and manganese intake with arsenic-safe groundwater in Jashore, Bangladesh. *Scientific Reports*, *10*(1), 1–9. https://doi.org/10.1038/s41598-020-62187-5

Gibbs, R. (1970b). Mechanisms Controlling World Water Chemistry. *Science, New Series*, *170*(3962), 1088–1090. Retrieved from http://www.jstor.org/stable/730827

Gibson, A. B. (1954). *Geology of the Broderick Falls area, Geological Survey of Kenya, Report No. 26*.

Gibson, A. B. (1954b). *Geology of the Broderick Falls area. Geological Survey of Kenya, Report No. 26*. Nairobi.

Gicheruh, C. (1993). Geophysical and Hydrological Investigations for Groundwater in the Lake Kenyatta Settlement Scheme, Lamu District, Coast Province, Kenya. MSc *Thesis*. The University of Nairobi.

Githui, F. W. (2008). *Assessing the Impacts of Environmental Change on the Hydrology of the Nzoia Catchment in the Lake Victoria Basin. PhD thesis*. Vrije Universiteit Brussel. Retrieved from http://twws6.vub.ac.be/hydr/wbauwens/PhD-Thesis/Thesis/PhD_Githui.pdf

Gleeson, T., Alley, W. M., Allen, D. M., Sophocleous, M. A., Zhou, Y., Taniguchi, M., & Vandersteen, J. (2012). Towards sustainable groundwater use: Setting long-term goals, backcasting, and managing adaptively. *Ground Water*, *50*(1), 19–26. https://doi.org/10.1111/j.1745-6584.2011.00825.x

Gleeson, T., Novakowski, K., & Kurt Kyser, T. (2009). Extremely rapid and localized

recharge to a fractured rock aquifer. *Journal of Hydrology*, *376*(3–4), 496–509. https://doi.org/10.1016/j.jhydrol.2009.07.056

Gok. (2016). *The Water Act, 2016.*

GoK. (2010). *Constitution of Kenya, 2010. National Council for Law Reporting.* https://doi.org/10.1364/OE.17.019075\r186571 [pii]

GoK. (2015). *Kenya Gazette Supplement No. 74 (Acts No. 5), The Environmental Management and Co-ordination (Amendment) Act 2015* (Vol. 74).

GoK. (2016). *The Climate Change Act No. 11 of 2016.*

Gonçalves, R., Teramoto, E., Engelbrecht, B., Alfaro Soto, M., Chang, H., & van Genuchten, M. (2019). Quasi-Saturated Layer: Implications for Estimating Recharge and Groundwater Modeling. *Groundwater*, 1–9. https://doi.org/10.1111/gwat.12916

González-Trinidad, J., Pacheco-Guerrero, A., Júnez-Ferreira, H., Bautista-Capetillo, C., & Hernández-Antonio, A. (2017). Identifying groundwater recharge sites through environmental stable isotopes in an alluvial aquifer. *Water (Switzerland)*, *9*(8), 1–12. https://doi.org/10.3390/w9080569

Gosselin, D. C., Headrick, J., Tremblay, R., Chen, X.-H., & Summerside, S. (1997). Domestic Well Water Quality in Rural Nebraska: Focus on Nitrate-Nitrogen, Pesticides, and Coliform Bacteria. *Groundwater Monitoring & Remediation*. https://doi.org/10.1111/j.1745-6592.1997.tb01280.x

Graham, M. T. (2008). The Hydrogeology of Northern Agago County in Pader District, Uganda. *British Geological Survey Groundwater Programme Open Report OR/08/040.*

Graham, M. T., Ball, D. F., Ó Dochartaigh, B. É., & MacDonald, A. M. (2009). Using transmissivity, specific capacity and borehole yield data to assess the productivity of Scottish aquifers. *Quarterly Journal of Engineering Geology and Hydrogeology*, *42*(2), 227–235. https://doi.org/10.1144/1470-9236/08-045

Green, T. R., Taniguchi, M., Kooi, H., Gurdak, J. J., Allen, D. M., Hiscock, K. M., & Aureli, A. (2011). Beneath the surface of global change: Impacts of climate change on groundwater. *Journal of Hydrology*, *405*(3–4), 532–560. https://doi.org/10.1016/j.jhydrol.2011.05.002

Greenway, P. j. (1973). A classification of the vegetation of East Africa. *Kirkia*, *9*(1), 1–68.

Gronwall, J., & Danert, K. (2020). Regarding Groundwater and Drinking Water Access through A Human Rights Lens : Self-Supply as A Norm. *Water*, *12*(419), 1–21. https://doi.org/10.3390/w12020419

Gross, E. S. (2008). Manual pumping test method for characterizing the productivity of drilled wells equipped with rope. *MSc thesis. Pumping Test Method. Michigan Technological University.*

Grutzmacher, G., Kumar, P. J. ., Rustler, M., Hannappel, S., & Sauer, U. (2013). Geogenic groundwater contamination – definition, occurrence and relevance for drinking water production. *Zbl.Geol.Palaont.Teil I*, *1*(Toran 1987), 69–75.

Gudda, F. O., Moturi, W. N., Oduor, O. S., Muchiri, E. W., & Ensink, J. (2019). Pit latrine fill-up rates: Variation determinants and public health implications in informal settlements, Nakuru-Kenya. *BMC Public Health*, *19*(1), 1–13. https://doi.org/10.1186/s12889-019-6403-3

Gudmundsson, A. (2000). Active fault zones and groundwater flow. *Geophysical Research Letters*, *27*(18), 2993–2996. https://doi.org/10.1029/1999GL011266

Gulyani, S., Talukdar, D., & Kariuki, R. M. (2005). Water for the Urban Poor : Water Markets, Household Demand, and Service Preferences in Kenya. *Water supply and Sanitation sector Board discussion Paper series, Paper No. 5. https://openknowledge.worldbank.org/handle/10986/17233*

Guppy, L., Uyttendaele, P., Villholth, K. G., & Smakhtin, V. (2018). Groundwater and

Sustainable Development Goals: Analysis of Interlinkages. UNU-INWEH Report Series, Issue 04. *United Nations University Institute for Water, Environment and Health. Hamilton, Canada*. Retrieved from http://inweh.unu.edu/publications/

Haines, D. S., Imana, C. A., Opondo, D. M., Ouma, D. G., & Rayner, P. S. (2017). Weather and climate knowledge for water security: institutional roles and relationships in Turkana. *REACH Working Paper*, (5), 22-pp. Retrieved from https://reachwater.org.uk/wp-content/uploads/2017/09/2017_10_WorkingPaper_Haines-et-al-1.pdf

Harbison, J. E. (2007). *Groundwater Chemistry and Hydrological Processes Within a Quaternary Coastal Plain : Pimpama, Southeast Queensland*. PhD thesis, School of Natural Resource Sciences, Queensland University of Technology.

Hellwig, J., Stoelzle, M., & Stahl, K. (2020). Stress-testing groundwater and baseflow drought responses to synthetic climate change-informed recharge scenarios. *Hydrology and Earth System Sciences Discussions*, (July), 1–26. https://doi.org/10.5194/hess-2020-211

Hem, D. (1985). Study and interpretation of the chemical characteristics natural water. U S Geological Survey - Water Supply Paper 2254. Retrieved from http://pubs.usgs.gov/wsp/wsp2254/pdf/wsp2254a.pdf

Hirji, R. (2000). Water resources management issues, challenges and options in Kenya: A Framework for a Strategy, Draft Issues Paper. https://www.ircwash.org/sites/default/files/824-KE00-16427.pdf

Hirpa, F. A., Dyer, E., Hope, R., Olago, D. O., & Dadson, S. J. (2018). Finding sustainable water futures in data-sparse regions under climate change: Insights from the Turkwel River basin, Kenya. *Journal of Hydrology: Regional Studies*, *19*(July), 124–135. https://doi.org/10.1016/j.ejrh.2018.08.005

Holman, I. P. (2006). Climate change impacts on groundwater recharge-uncertainty, shortcomings, and the way forward? *Hydrogeology Journal*, *14*(5), 637–647. https://doi.org/10.1007/s10040-005-0467-0

Hosseinizadeh, A., Zarei, H., Akhondali, A. M., Seyedkaboli, H., & Farjad, B. (2019). Potential impacts of climate change on groundwater resources: A multi-regional modelling assessment. *Journal of Earth System Science*, *128*(5). https://doi.org/10.1007/s12040-019-1134-5

Hostetler, P. B. (1964). The degree of saturation of magnesium and calcium carbonate minerals in natural waters. *US Geological Survey*, *64*, 34–49.

Houcine, J., Ammar, H., Kamel, A., Kamel, Z., & Aggoune, A. (2013). Study of Rejim Maatoug groundwater in southern Tunisia using isotope methods. *Journal of Hydro-Environment Research*. https://doi.org/10.1016/j.jher.2013.04.001

Howard, K. W. F., & Karundu, J. (1992). Constraints on the exploitation of basement aquifers in East Africa - water balance implications and the role of the regolith. *Journal of Hydrology*, *139*(1–4), 183–196. https://doi.org/10.1016/0022-1694(92)90201-6

Hubbert, M. K. (1957). Darcy's law and the field equations of the flow of underground fluids. *Hydrological Science Journal*, *2*(1), 23–59. https://doi.org/10.1080/02626665709493062

Hubert, E., & Wolkersdorfer, C. (2015). Establishing a conversion factor between electrical conductivity and total dissolved solids in South African mine waters. *Water SA*, *41*(4), 490–500. https://doi.org/10.4314/wsa.v41i4.08

Hulme, M., Doherty, R., Ngara, T., New, M., & Lister, D. (2001). African climate change: 1900-2100. *Climate Research*, *17*(2 SPECIAL 8), 145–168. https://doi.org/10.3354/cr017145

Hulme, M., & Turnpenny, J. (2004). Understanding and managing climate change: the UK experience. *The Geographical Journal*, *170*(2), 105–115.

Hunt, R. E. (2005). *Geotechnical Engineering Investigation Handbook* (Second edition). London: Taylor & Francis.

Hwang, J. Y., Park, S., Kim, H.-K., Kim, M.-S., Jo, H.-J., Kim, J.-I., & Kim, T.-S. (2017). Hydrochemistry for the assessment of groundwater quality in Korea. *Journal of Agricultural Chemistry and Environment*, *06*(01), 1–29. https://doi.org/10.4236/jacen.2017.61001

IAEA. (1981). *Statistical treatment of environmental isotope data in precipitation. IAEA technical reports series No. 206. STI/DOC/10/206.* https://inis.iaea.org/collection/NCLCollectionStore/_Public/26/076/26076354.pdf

IAEA. (1999). *Technical options for the remediation of contaminated groundwater. IAEA-TECDOC-1088* (Vol. 1). https://www-pub.iaea.org/MTCD/Publications/PDF/te_1088_prn.pdf

IAEA. (2016). *Mainstreaming Groundwater Consideration into the Integrated Management of the Nile River Basin. Kenya Report (RAF/8/042).* Unpublished report

IGRAC. (2018). *Groundwater Overview: Making the invisible visible*. *UN-water*. https://www.unwater.org/publications/groundwater-overview-making-the-invisible-visible/

IWMI. (2012). *Groundwater availability and use in Sub-Saharan Africa: A Review of 15 countries*. (T. Pavelic, Paul; Giordano, Mark; Keraita, Bernard; Rao, Ed.). Colombo, Sri Lanka: International Water Management Institute. https://doi.org/10.5337/2012.213

Izady, A., Davary, K., Alizadeh, A., Ziaei, A. N., Alipoor, A., Joodavi, A., & Brusseau, M. L. (2014). A framework toward developing a groundwater conceptual model. *Arabian Journal of Geosciences*, *7*(9), 3611–3631. https://doi.org/10.1007/s12517-013-0971-9

Jayakody, P., Parajuli, P. B., & Brooks, J. P. (2014). Evaluating Spatial and Temporal Variability of Fecal Coliform Bacteria Loads at the Pelahatchie Watershed in Mississippi. *Human and Ecological Risk Assessment: An International Journal*, *20*(4), 1023–1041. https://doi.org/10.1080/10807039.2013.784155

Jeon, C., Raza, M., Lee, J. Y., Kim, H., Kim, C. S., Kim, B., & Lee, S. W. (2020). Countrywide groundwater quality trend and suitability for use in key sectors of Korea. *Water (Switzerland)*, *12*(4), 1–22. https://doi.org/10.3390/W12041193

Jeong, C. H. (2001). Mineral-water interaction and hydrogeochemistry in the Samkwang mine area, Korea. *Geochemical Journal*, *35*(1), 1–12. https://doi.org/10.2343/geochemj.35.1

JICA. (2013). *The national water master plan 2030. Final Report, Volume 1. Executive Summary*. https://openjicareport.jica.go.jp/pdf/12146353_01.pdf

Johnson, A. I. (1967). *Specific Yield - Compilation of Specific Yields for Various Materials. Geological Survey Water Supply Paper 1662-D. USGS.* Retrieved from https://pubs.usgs.gov/wsp/1662d/report.pdf

Johnson, T. C., Kelts, K., & Odada, E. (2000). The Holocene history of Lake Victoria. *Ambio*, *29*(1), 2–11. https://doi.org/10.1579/0044-7447-29.1.2

Johnson, T., Kelts, K., & Odada, E. (2000). The Holocene history of Lake Victoria. *Ambio*, *29*(1), 2–11.

Joji, V. (2016). Major ion chemistry and identification of Hydrogeochemical Processes of Evolution of Ground Water in a Small Tropical Coral Island of Minicoy, Union Territory of Lakshadweep, India. *MOJ Ecology & Environmental Sciences*, *1*(2), 40–48. https://doi.org/10.15406/mojes.2016.01.00008

Jones, F. O. (1964). Influence of Chemical Composition of Water on Clay Blocking of Permeability. *Journal of Petroleum Technology*, *16*(4). https://doi.org/https://doi.org/10.2118/631-PA

Juntakut, P., Haacker, E. M. K., Snow, D. D., & Ray, C. (2020). Risk and cost assessment of

nitrate contamination in domestic wells. *Water (Switzerland)*, *12*(2), 6–8. https://doi.org/10.3390/w12020428

Kalbus, E., Reinstorf, F., & Schirmer, M. (2006). Measuring methods for groundwater-surface water interactions: a review. *Hydrology and Earth System Sciences*, *10*, 873–887. https://doi.org/10.5194/hess-10-873-2006

Kanda, I., & Suwai, J. (2013). Hydrogeochemistry of Shallow and Deep Water Aquifers of Menengai Geothermal Area, Kenya Rift Valley, *37*, 403–410.

Kaser, D., & Hunkeler, D. (2016). Contribution of alluvial groundwater to the outflow of mountainous catchments. *Water Resources Research.*, *52*, 680–697. https://doi.org/10.1002/2014WR016730

Kassune, M., Tafesse, N. T., & Hagos, M. (2018). Characteristics and Productivity of Volcanic Rock Aquifers in Kola Diba Well Field. *Universal Journal of Geoscience*, *2018*(4), 103–113. https://doi.org/10.13189/ujg.2018.060401

KEBS. (2015). *Kenya Standard; Potable water Specification, KS EAS 12:2014*. Retrieved from http://www.puntofocal.gov.ar/notific_otros_miembros/ken470_t.pdf

Kehinde, M. O., & Loehnert, E. P. (1989). Review of African groundwater resources. *Journal of African Earth Sciences*, *9*(1), 179–185. https://doi.org/10.1016/0899-5362(89)90019-5

Kempe, R. (2012). Urbanisation in Kenya. *African J. of Economic and Sustainable Development*, *1*(1), 24. https://doi.org/10.1504/ajesd.2012.045751

Kempton, J. P., Morse, W. J., & Visocky, A. P. (1982). Hydrogeologic Evaluation of Sand and Gravel Aquifers for Municipal Groundwater Supplies in East-Central Illinois. *Cooperative Groundwater Report (Illinois State Water Survey; Illinois State Geological Survey)*. http://library.isgs.illinois.edu/Pubs/pdfs/coops/coop08.pdf.

Kendall, R. L. (1969). An Ecological History of the Lake Victoria Basin. *Ecological Monographs*, *39*(2), 121–176. https://doi.org/10.2307/1950740

Kent, P. E. (1942). The country round the Kavirondo Gulf of Victoria Nyanza. *The Geographical Journal*, *100*(1), 22–31.

Kenya Water Tower Agency. (2019). *Policy Brief - Cherangany Hills water tower*. Unpublished report

Khatri, N., & Tyagi, S. (2015). Influences of natural and anthropogenic factors on surface and groundwater quality in rural and urban areas. *Frontiers in Life Science*, *8*(1), 23–39. https://doi.org/10.1080/21553769.2014.933716

Kiczka, M., Wiederhold, J. G., Frommer, J., Voegelin, A., Kraemer, S. M., Bourdon, B., & Kretzschmar, R. (2011). Iron speciation and isotope fractionation during silicate weathering and soil formation in an alpine glacier forefield chronosequence. *Geochimica et Cosmochimica Acta*, *75*(19), 5559–5573. https://doi.org/10.1016/j.gca.2011.07.008

King, B. C., le Bas, M. J., & Sutherland, D. S. (1972). The history of the alkaline volcanoes and intrusive complexes of Eastern Uganda and Western Kenya. *Journal of the Geological Society*, *128*(2), 173–205. https://doi.org/10.1144/gsjgs.128.2.0173

Kiptum, C. K., & Ndambuki, J. M. (2012). Well water contamination by pit latrines : A case study of Langas. *International Journal of Water Resources and Environmental Engineering*, *4*(2), 35–43. https://doi.org/10.5897/IJWREE11.084

Kjøller, C., Postma, D., & Larsen, F. (2004). Groundwater acidification and the mobilization of trace metals in a sandy aquifer. *Environmental Science and Technology*, *38*(10), 2829–2835. https://doi.org/10.1021/es030133v

KMD. (2018). Kisumu precipitation and temperature data. Unpublished report

KNBS. (2019). *2019 Kenya Population and Housing Census Volume 1: Population by County and Sub-County*. *2019 Kenya Population and Housing Census* (Vol. I).

Retrieved from https://www.knbs.or.ke/?wpdmpro=2019-kenya-population-and-housing-census-volume-i-population-by-county-and-sub-county

Konikow, L., August, L., & Voss, C. (2001). Effects of Clay Dispersion on Aquifer Storage and Recovery in Coastal Aquifers. *Transport in Porous Media*, *43*, 45–64.

Kopec, B. G., Feng, X., Posmentier, E. S., & Sonder, L. J. (2019). Seasonal Deuterium Excess Variations of Precipitation at Summit, Greenland, and their Climatological Significance. *Journal of Geophysical Research: Atmospheres*, *124*(1), 72–91. https://doi.org/10.1029/2018JD028750

Kothari, C. R. (2004). *Research Methodology, Methods and Techniques*. New Delhi: New Age International Publishers. ISBN: 9788122415223

Kouamé, A. A., Jaboyedoff, M., Tie, A. G. B., Derron, M. H., Kouamé, K. J., & Meier, C. (2019). Assessment of the potential pollution of the Abidjan unconfined aquifer by hydrocarbons. *Geosciences (Switzerland)*, *9*(2). https://doi.org/10.3390/geosciences9020060

Kraiem, Z., Zouari, K., Chkir, N., & Agoune, A. (2013). Geochemical characteristics of arid shallow aquifers in Chott Djerid. *Journal of Hydro-Environment Research*. https://doi.org/10.1016/j.jher.2013.06.002

Kruseman, G. P., & Ridder, N. A. (2000). *Analysis and evaluation of pumping test data, InternationalInstitute for land Reclamation and Improvement, Publication 47*. https://doi.org/10.1016/0022-1694(71)90015-1

Kumar, P. (2013). Interpretation of groundwater chemistry using piper and Chadha's diagrams: a comparative study from Perambalur Taluk. *Elixir Geosci*, *54*, 12208–12211.

Kumar, R. (2011). *Research Methodology - a step-by-step guide for beginners*. Sage Publications Ltd. ISBN 10: 1849203008

Kump, L. R., Brantley, S. L., & Arthur, M. A. (2000). Chemical weathering, atmospheric CO2, and climate. *Annual Review of Earth and Planetary Sciences*, *28*, 611–667. https://doi.org/10.1146/annurev.earth.28.1.611

Kuria, D. N., & Kamunge, H. N. (2013). Merti Aquifer Recharge Zones Determination Using. *Journal of Applied Sciences, Engineering and Technology for Development*, *1*(1), 24–31.

Kuria, Z. (2013). Groundwater Distribution and Aquifer Characteristics in Kenya. In *Kenya: A Natural Outlook* (1st ed., pp. 83–107). Elsevier B.V. https://doi.org/10.1016/B978-0-444-59559-1.00008-6

Kurth, A. (2014). *Investigation of Groundwater-Surface Water Interactions with Distributed Temperature Sensing (DTS), PhD thesis*. University of Neuchâtel.

Lantagne, D., Pezzi, C., & Mahamud, A. (2009). *Water Safety Plan : Dadaab Refugee Camps*. UNHCR working document, https://wash.unhcr.org/download/water-safety-plan-dadaab-refugee-camps-cdc-april-2009/

Lapworth, D. J., Nkhuwa, D. C. W., Okotto-Okotto, J., Pedley, S., Stuart, M. E., Tijani, M. N., & Wright, J. (2017). Urban groundwater quality in sub-Saharan Africa: current status and implications for water security and public health. *Hydrogeology Journal*, 1093–1116. https://doi.org/10.1007/s10040-016-1516-6

Lapworth, D. J., Nkhuwa, D. C. W., Pedley, S., Stuart, M. E., Okotto-Okotto, J., Tijani, M., & Wright, J. (2017). Urban groundwater quality in sub-Saharan Africa : current status and implications for water security and public health. *Hydrogeology Journal*, 1093–1116. https://doi.org/10.1007/s10040-016-1516-6

Lavina, B., Dera, P., & Downs, R. T. (2014). Modern X-ray diffraction methods in mineralogy and geosciences. *Reviews in Mineralogy and Geochemistry*, *78*, 1–31. https://doi.org/10.2138/rmg.2014.78.1

Le Bas, M. J., Le Maitre, R. N., Streckeisen, A., & Zanettin, B. (1986). A chemical

classification of volcanic rock based on total silica diagram. *Journal Petrology*, *27*(3), 745–750. Retrieved from http://petrology.oxfordjournals.org/

Le Treut, H. R., Somerville, U., Cubasch, Y., Ding, C., Mauritzen, A., Mokssit, T., & Prather, M. (2007). *Historical Overview of Climate Change Science. In: Climate Change 2007: The Physical Science Basis. Contribution of Working Group I to the Fourth Assessment Report of the Intergovernmental Panel on Climate Change [Solomon, S., D. Qin, M. Manning, Z. Chen, M. Marquis, K.B. Averyt, M. Tignor and H.L. Miller (eds.)]. Cambridge University Press, Cambridge, United Kingdom and New York, NY, USA. http://biblioteca.climantica.org/resources/37/05-ar4wg1-ch01-historicaloverview.pdf*

Leis, A., Dietzel, M., & Boch, R. (2018). Stable Isotope Network Austria Program & Abstracts, (December). https://opac.geologie.ac.at/wwwopacx/wwwopac.ashx?command=getcontent&server=images&value=BR0128.pdf

Levin, N. E., Zipser, E. J., & Ceding, T. E. (2009). Isotopic composition of waters from Ethiopia and Kenya: Insights into moisture sources for eastern Africa. *Journal of Geophysical Research Atmospheres*, *114*(23), 1–13. https://doi.org/10.1029/2009JD012166

Li, H., Lu, Y., Zheng, C., Zhang, X., Zhou, B., & Wu, J. (2020). Seasonal and inter-annual variability of groundwater and their responses to climate change and human activities in arid and desert areas: A case study in Yaoba Oasis, Northwest China. *Water (Switzerland)*, *12*(1). https://doi.org/10.3390/w12010303

Li, X., Wu, H., Qian, H., & Gao, Y. (2018). Groundwater chemistry regulated by hydrochemical processes and geological structures: A case study in Tongchuan, China. *Water (Switzerland)*, *10*(3). https://doi.org/10.3390/w10030338

Liu, Y., Wang, P., Ruan, H., Wang, T., Yu, J., Cheng, Y., & Kulmatov, R. (2020). Sustainable use of groundwater resources in the transboundary aquifers of the five central Asian countries: Challenges and perspectives. *Water (Switzerland)*, *12*(8). https://doi.org/10.3390/W12082101

Llamas, M. R., & Martínez-Santos, P. (2005). Intensive groundwater use: Silent revolution and potential source of social conflicts. *Journal of Water Resources Planning and Management*, *131*(5), 337–341. https://doi.org/10.1061/(ASCE)0733-9496(2005)131:5(337)

Loader, N. J., & Hemming, D. L. (2004). Palaeoclimate interpretation of stable isotope data from lake sediment archives. *Quaternary Science Reviews*, *23*, 893–900. https://doi.org/10.1016/j.quascirev.2003.06.015

Logan, J. (1964). Estimating transmissibility from routine production tests of water wells. *Ground Water*, *2*(1), 35–37. https://doi.org/https://doi.org/10.1111/j.1745-6584.1964.tb01744.x

Lohman, S. W. (1972). *Ground-Water Hydraulics*. Washington. Geological Survey Professional Paper 708. https://pubs.usgs.gov/pp/0708/report.pdf

Loke, M. H. (2000). *Electrical imaging surveys for environmental and engineering studies. A practical guide to 2-D and 3-D surveys*. Unpublished report. https://sites.ualberta.ca/~unsworth/UA-classes/223/loke_course_notes.pdf

Lovley, D. R., & Chapelle, F. H. (1995). Deep subsurface microbial processes. *Reviews of Geophysics*, *33*(3), 365–381. https://doi.org/10.1029/95RG01305

Lumumba, P. (2007). The Interpretation of the 1929 Treaty and its Legal Relevance and Implications for the Stability of the Region. *African Sociology Review*, *11*(1), 10–24.

MacDonald, A., Bonsor, H., Dochartaigh, B., & Taylor, R. (2012). Quantitative maps of groundwater resources in Africa. *Environmental Research Letters*, *7*(2).

https://doi.org/10.1088/1748-9326/7/2/024009

Macdonald, A., & Davies, J. (2000). *A brief review of groundwater for rural water supply in sub-Saharan. British Geological Survey Technical Report WC/00/33.* https://doi.org/WC/00/33

MacDonald, A., Davies, J., & Calow, R. (2010). *African hydrogeology and rural water supply. In: Adelana, Segun; MacDonald, Allan (eds.). Applied Groundwater Studies in Africa. IAH selected paper on hydrogeology, 13, pp 127-148.* https://doi.org/10.1201/9780203889497.pt2

MacDonald, A. M., & Davies, J. (2000). *A brief review of groundwater for rural water supply in sub-Saharan Africa. British Geological Survey Technical Report WC/00/33. BGS Keyworth UK.* Nottingham, United Kingdom. http://nora.nerc.ac.uk/id/eprint/501047/1/SSA_review_lr.pdf

Mailu, G. M. (1997). The impact of urbanization on groundwater quality in Wajir Town, Kenya. In *Freshwater Contamination (Proceedings of Rabat Symposium s4, April - May 1997.* (pp. 245–253).

Mandile, A. J., & Hutton, A. C. (1995). Quantitative X-ray diffraction analysis of mineral and organic phases in organic-rich rocks. *International Journal of Coal Geology*, *28*(1), 51–69. https://doi.org/10.1016/0166-5162(95)00004-W

Mansour, A. A.-G. (1996). *Direct Current Resistivity Investigation of Groundwater in the Lower Mesilla Valley, New Mexico and Texas, MSc thesis.* Colorado School of Mines, Golden, Colorado.

Mansour, K., Omar, K., Ali, K., & Abdel Zaher, M. (2018). Geophysical characterization of the role of fault and fracture systems for recharging groundwater aquifers from surface water of Lake Nasser. *NRIAG Journal of Astronomy and Geophysics*, *7*(1), 99–106. https://doi.org/10.1016/j.nrjag.2018.02.001

Marandi, A., Polikarpus, M., & Jõeleht, A. (2013). Applied Geochemistry A new approach for describing the relationship between electrical conductivity and major anion concentration in natural waters. *Applied Geochemistry*, *38*(2013), 103–109. https://doi.org/10.1016/j.apgeochem.2013.09.003

Marshall, S. (2011). *The Water Crisis in Kenya : Causes, Effects and Solutions. Global Majority E-Journal.* Global Majority E-Journal, Vol. 2, No. 1 (June 2011), pp. 31-45. https://www.american.edu/cas/economics/ejournal/upload/marshall_accessible.pdf

Martínez-Navarrete, C., Jiménez-Madrid, A., Sánchez-Navarro, I., Carrasco-Cantos, F., & Moreno-Merino, L. (2011). Conceptual framework for protecting groundwater quality. *International Journal of Water Resources Development*, *27*(1), 227–243. https://doi.org/10.1080/07900627.2010.532476

Maurice, L., Taylor, R. G., Tindimugaya, C., Macdonald, A. M., Johnson, P., Kaponda, A., & Sanga, H. (2018). Characteristics of high-intensity groundwater abstractions from weathered crystalline bedrock aquifers in East Africa. *Hydrogeology Journal*, 16. https://doi.org/10.1007/s10040-018-1836-9

Mavhura, E. (2019). Systems Analysis of Vulnerability to Hydrometeorological Threats: An Exploratory Study of Vulnerability Drivers in Northern Zimbabwe. *International Journal of Disaster Risk Science*, *10*(2), 204–219. https://doi.org/10.1007/s13753-019-0217-x

Maxwell, B., Brighid, D., Crane, E., Kirsty, U., & Imogen, B.-H. (2018). *Hydrogeology of Kenya. Africa Groundwater Atlas.* Retrieved from http://earthwise.bgs.ac.uk/index.php?title=Hydrogeology_of_Kenya&oldid=36288%0A http://earthwise.bgs.ac.uk/index.php/Hydrogeology_of_Kenya

Mboya, B. (1983). The genesis and tectonics of the N.E. Nyanza rift valley, Kenya. *Journal of African Earth Sciences (1983)*, *1*(3–4), 315–320. https://doi.org/Doi: 10.1016/s0731-

7247(83)80016-0

Mboya, B. (1984). The genesis and tectonics of the N.E. Nyanza rift valley, Kenya. *Journal of African Earth Sciences*, *1*(3–4), 315–320. https://doi.org/10.1016/S0731-7247(83)80016-0

Mbui, D., Chebet, E., Kamau, G., & Kibet, J. (2016). The state of water quality in Nairobi River, Kenya. *Asian Journal of Research in Chemistry*, *9*(11), 579. https://doi.org/10.5958/0974-4150.2016.00078.x

Meert, J., Voo, R. Van Der, & Patel, J. (1994). Paleomagnetism of the Late Archean Nyanzian System , western Kenya. *Precambrian Research*, *69*, 113–131.

Meinzer, O. E. (1923). *The occurrence of ground water in the United States, with a discussion of principles*. Washington. https://doi.org/10.3133/wsp489

Middlemost, E. (1991). *A classification of igneous rocks and glossary of terms*. *Journal of Volcanology and Geothermal Research* (Vol. 47). https://doi.org/10.1016/0377-0273(91)90012-o

Miller, J. M. (1956). *Geology of the Kitale-Cherangani Hills area. Geological Survey of Kenya, Report No. 35*.

Mishra, P. K., Vessilinov, V., & Gupta, H. (2012). On Simulation and Analysis of Variable-Rate Pumping Tests. *Ground Water*, *51*(3), 5. https://doi.org/10.1111/j.1745-6584.2012.00961.x

Modibo, A., Lin, X., & Kone, S. (2019). Assessing groundwater mineralization process, quality, and isotopic recharge origin in the Sahel region in Africa. *Water*, *11*(789), 1–19. https://doi.org/10.3390/w11040789

Modica, E., & Buxton, H. (1998). Evaluating the source and residence times of groundwater seepage to streams, New Jersy Coastal plain. *Water Resources Research*, *34*(11), 2797–2810. https://doi.org/10.1007/1-4020-4494-1_361

Mogaka, H., Gichere, S., Davis, R., & Hirji, R. (2006). Climate variability and water resources degradation in Kenya: Improving water resources development and management. *World Bank Working Paper No. 69. ISBN-10: 0-8213-6517-7 ISSN: 1726-5878, ISBN-13: 978-0-8213-6517-5,https://doi.org/10.1596/978-0-8213-6517-5*

Mohr, P. A., & Wood, C. A. (1976). Volcano spacings and lithospheric attenuation in the Eastern Rift of Africa. *Earth and Planetary Science Letters*, *33*, 126–144. https://doi.org/10.1016/0012-821X(76)90166-7

Mook, W. G. (2001). *Environmental Isotopes in the Hydrological Cycle - Principles and Applications. International Hydrological Programme Volume VI, Modelling*. Paris. UNESCO/IAEA Series

Mook, W. G. (2000). *Environmental Isotopes in the Hydrological Cycle. Principles and Applications. Volume II, Atmospheric Water*. Groningen. UNESCO/IAEA Series

Mook, W. G. (2000). *Environmental Isotopes in the Hydrological Cycle. Principles and Applications. Volume III, Surface Water*. Groningen. UNESCO/IAEA Series

Mook, W. G. (2000). *Environmental Isotopes in the Hydrological Cycle. Principles and Applications. Volume IV, Groundwater*. Groningen. UNESCO/IAEA Series

Mook, W. G. (2000). *Environmental Isotopes in the Hydrological Cycle. Principles and Applications. Volume V, Man's Impact on Groundwater Systems*. Groningen. UNESCO/IAEA Series

Mook, W. G. (2000). *Environmental Isotopes in the Hydrological Cycle - Principles and Applications. Volume 1, Introduction*. Groningen. UNESCO/IAEA Series

Moore, J. (2002). *Field Hydrogeology : A Guide for Site Investigations and Report Preparation*. Lewis Publishers. https://doi.org/10.1016/B978-0-12-373972-8.00050-4

Morales-Baquero, R., Pulido-Villena, E., & Reche, I. (2013). Chemical signature of Saharan dust on dry and wet atmospheric deposition in the south-western Mediterranean region.

Tellus, Series B: Chemical and Physical Meteorology, 65(1). https://doi.org/10.3402/tellusb.v65i0.18720

Morgan, K. (2018). Developing Water Supplies from Saprolite Regolith. *ASEG Extended Abstracts*, *2018*(1), 1–9. https://doi.org/10.1071/aseg2018abw9_2g

Morris, B., Lawrence, A., Chilton, P., Adams, B., Calow, R., & Klinck, B. (2003). *Groundwater and its susceptibility to degradation: A global assessment of the problem and options for management. Early warning and assessment report series, RS. 03-3. United Nations Environment Programme, Nairobi, Kenya.* http://nora.nerc.ac.uk/id/eprint/19395/

Morris, B., Lawrence, A. R., & Stuart, M. E. (1994). *The impacts of urbanization on groundwater quality (Project Summary Report), BGS Technical Report WC/94/56.* https://core.ac.uk/download/pdf/16748523.pdf

Mossmark, F. (2014). *Prediction of Groundwater Chemistry in Conjunction with Underground Constructions - Field Studies and Hydrochemical Modelling, PhD Thesis.* The Chalmers University of Technology. Gothenburg, Sweden.

Muchena, F. N., & Gachene, C. K. K. (1988). Soils of highland and mountainous areas of Kenya with special emphasis on agricultural soils. *Mountain Research & Development*, *8*(2–3), 183–191. https://doi.org/10.2307/3673446

Muhweezi, A. B., Sikoyo, G. M., & Chemonges, M. (2007). Introducing a Transboundary Ecosystem Management Approach in the Mount Elgon region. *Mountain Research and Development*, *27*(3), 215–219. https://doi.org/10.1659/0276-4741(2007)27[215:iatema]2.0.co;2

Mulwa, J., Gaciri, S., Barongo, J., Opiyo-Akech, N., & Kianji, G. (2010). Geological and structural influence on groundwater distribution and flow in Ngong area, Kenya. *African Journal of Science and Technology*, *6*(1), 105–115. https://doi.org/10.4314/ajst.v6i1.55166

Mungai, D. N. (1984). *Analysis of some seasonal rainfall characteristics in the lake victoria region of Kenya*. M.A thesis, Department of Geography, University of Nairobi.

Muricho, D. N., Otieno, D. J., Oluoch-Kosura, W., & Jirström, M. (2019). Building pastoralists' resilience to shocks for sustainable disaster risk mitigation: Lessons from West Pokot County, Kenya. *International Journal of Disaster Risk Reduction*, *34*(August 2018), 429–435. https://doi.org/10.1016/j.ijdrr.2018.12.012

Mussa, K. R., Mjemah, I. C., & Machunda, R. L. (2020). Open-source software application for hydrogeological delineation of potential groundwater recharge zones in the Singida semi-arid, fractured aquifer, central Tanzania. *Hydrology*, *7*(2). https://doi.org/10.3390/HYDROLOGY7020028

Muthoni, N. (2009). *Challenges of groundwater management in the city of Nairobi*. Master of Urban Management in the University Of Nairobi, School of the Built Environment.

Naik, P. K. (2017). Water crisis in Africa: myth or reality? *International Journal of Water Resources Development*, *33*(2), 326–339. https://doi.org/10.1080/07900627.2016.1188266

Nakagiri, A., Niwagaba, C. B., Nyenje, P. M., Kulabako, R. N., Tumuhairwe, J. B., & Kansiime, F. (2016a). Are pit latrines in urban areas of Sub-Saharan Africa performing? A review of usage, filling, insects and odour nuisances. *BMC Public Health*, *16*(1), 1–16. https://doi.org/10.1186/s12889-016-2772-z

Namboka, V. M., Nyangweso, P., Kipsat, M. (2017). Analysis of factors influencing demand for agricultural credit among farmers in Kapenguria, West Pokot, Kenya. *African Journal of Agriculture and Environment*, *3*(1), 22–51.

Nangulu, A. K. (2009). *Food security and coping mechanisms in marginal areas. The case of West Pokot, Kenya, 1920-1995. African Studies Centre Collection, vol. 15.*

Ndao, S., Babacar, D., Ba, A., & Bamba, E. (2019). The Thiaroye Aquifer in Senegal: Usable Groundwater Resources for Drinking or Irrigation? *International Journal of Advanced Research*, *7*(1), 667–676. https://doi.org/10.21474/ijar01/8375

Ngecu, W M, & Mathu, E. M. (1999). The El-Nino-triggered landslides and their socioeconomic impact on Kenya. *Environmental Geology*, *38*(4), 277–284.

Ngecu, Wilson M. (1991). *The geology of the Kavirondian Group of sediments, PhD thesis*. Department of Geology, University of Nairobi.

Njiru, P. K., Stanley, O., & Baraza, L. D. (2016). Sanitation In Relation To Prevalence of Waterborne Diseases in Mbeere, Embu County, Kenya. *IOSR Journal of Environmental Science Ver. I*, *10*(5), 2319–2399. https://doi.org/10.9790/2402-1005015965

Njuguna, J. (2019). Progress in sanitation among poor households in Kenya: Evidence from demographic and health surveys. *BMC Public Health*, *19*(1), 1–8. https://doi.org/10.1186/s12889-019-6459-0

Noy, I., & Yonson, R. (2018). Economic vulnerability and resilience to natural hazards: A survey of concepts and measurements. *Sustainability (Switzerland)*, *10*(8). https://doi.org/10.3390/su10082850

Nyaberi, D. M., Basweti, E., Barongo, J. O., Ogendi, G. M., & Kariuki, P. C. (2019). Mapping of Groundwater through the Integration of Remote Sensing and Vertical Electrical Sounding in ASALs: A Case Study of Turkana South Sub-County, Kenya. *Journal of Geoscience and Environment Protection*, *07*(11), 229–243. https://doi.org/10.4236/gep.2019.711017

Nyadawa, M. O., & Mwangi, J. K. (2011). Geomorphologic Characteristics of Nzoia River Basin. *Journal of Agriculture, Science and Technology*, *12*(2), 145–161. Retrieved from http://elearning.jkuat.ac.ke/journals/ojs/index.php/jagst/article/view/24

Nyilitya, B., Mureithi, S., & Boeckx, P. (2020). Tracking sources and fate of groundwater nitrate in Kisumu City and Kano Plains, Kenya. *Water*, *12*(401), 1–18.

Odida, J. (2015). *Aquifer geometry and structural controls on groundwater potential in Mt. Elgon aquifer, Trans Nzoia County, Kenya.*Department of Geology, The University of Nairobi.

Odira, M. A., M.O, N., Okelloh, N., Nelly, J., & John, O. (2010). Impact of Land Use /Cover dynamics on Streamflow: A Case of Nzoia River Catchment, Kenya. *Nile Basin Water Science& Engineering Journal, 3*(2), 64–78.

Ofterdinger, U., Macdonald, A. M., Comte, J. C., & Young, M. E. (2019). Groundwater in fractured bedrock environments: Managing catchment and subsurface resources – an introduction. *Geological Society Special Publication*, *479*(1), 1–9. https://doi.org/10.1144/SP479-2018-170

Oiro, S., Comte, J. C., Soulsby, C., MacDonald, A., & Mwakamba, C. (2020). Depletion of groundwater resources under rapid urbanisation in Africa: recent and future trends in the Nairobi Aquifer System, Kenya. *Hydrogeology Journal*, *28*(8), 2635–2656. https://doi.org/10.1007/s10040-020-02236-5

Oiro, S., Comte, J. C., Soulsby, C., & Walraevens, K. (2018). Using stable water isotopes to identify spatio-temporal controls on groundwater recharge in two contrasting East African aquifer systems. *Hydrological Sciences Journal*, *63*(6), 1–16. https://doi.org/10.1080/02626667.2018.1459625

Okayo, J., Odera, P., & Omuterema, S. (2015). Socio-economic characteristics of the community that determine ability to uptake precautionary measures to mitigate flood disaster in Kano Plains, Kisumu County, Kenya. *Geoenvironmental Disasters*, *2*(1). https://doi.org/10.1186/s40677-015-0034-5

Okello, C., Tomasello, B., Greggio, N., Wambiji, N., & Antonellini, M. (2015). Impact of population growth and climate change on the freshwater resources of Lamu Island,

Kenya. *Water (Switzerland)*, *7*(3), 1264–1290. https://doi.org/10.3390/w7031264

Okotto-Okotto, J., Okotto, L., Price, H., Pedley, S., & Wright, J. (2015). A longitudinal study of long-term change in contamination hazards and shallow well quality in two neighbourhoods of Kisumu, Kenya. *International Journal of Environmental Research and Public Health*, *12*(4), 4275–4291. https://doi.org/10.3390/ijerph120404275

Okotto, L., Okotto-Okotto, J., Price, H., Pedley, S., & Wright, J. (2015). Socio-economic aspects of domestic groundwater consumption, vending and use in Kisumu, Kenya. *Applied Geography*, *58*, 189–197. https://doi.org/10.1016/j.apgeog.2015.02.009

Olago, D. O. (2019). Constraints and solutions for groundwater development, supply and governance in urban areas in Kenya. *Hydrogeology Journal*, *27*(3), 1031–1050. https://doi.org/10.1007/s10040-018-1895-y

Olayinka, A., & Yaramanci, U. (2000). Assessment of the reliability of 2D inversion of apparent resistivity data. *Geophysical Prospecting*, *48*, 293–316.

Oliver, D. S. (1993). The influence of nonuniform transmissivity and storativity on drawdown. *Water Resources Research*, *29*(1), 169–178. https://doi.org/10.1029/92WR02061

Opande, G. O., Onyango, J. C., & Wagai, S. O. (2004). Lake Victoria: The water hyacinth (Eichhornia crassipes [MART.] SOLMS), its socio-economic effects, control measures and resurgence in the Winam Gulf. *Limnologica*, *34*(1–2), 105–109. https://doi.org/10.1016/S0075-9511(04)80028-8

Opisa, S., Odiere, M. R., Jura, W. G. Z. O., Karanja, D. M. S., & Mwinzi, P. N. M. (2012). Faecal contamination of public water sources in informal settlements of Kisumu City, western Kenya. *Water Science and Technology*, *66*(12), 2674–2681. https://doi.org/10.2166/wst.2012.503

Opiyo-Akech, N. (1988). *Geology and Geochemistry of the Late Archaean Greenstone Associations, Maseno Area, Kenya.* PhD thesis, University of Leicester.

Osiemo, M. M., Ogendi, G. M., & M'Erimba, C. (2019). Microbial Quality of Drinking Water and Prevalence of Water-Related Diseases in Marigat Urban Centre, Kenya. *Environmental Health Insights*, *13*. https://doi.org/10.1177/1178630219836988

Osman, A. D. (2012). *Groundwater quality in Wajir (Kenya) shallow aquifer : An examination of the association between water quality and water-borne diseases in children.* PhD thesis, La Trobe University.

Overmeeren, R. A. Van. (1981). A combination of electrical resistivity, seismic refraction, and gravity measurements for groundwater, exploration in Sudan. *Geophysics*, *46*(9), 1304–1313. https://doi.org/10.1016/0148-9062(83)91591-7

Pauling, L. (1948). The Modern Theory of Valency. The Liversidge Lecture, delivered before the Chemical Society in The Royal Institution on June 3rd, 1948. *Journal of Chemical Society*, 1461–1467. https://doi.org/10.1039/JR9480001461

Petersen-perlman, J., Megdal, S., Gerlak, A., Wireman, M., Zuniga-teran, A., & Robert, V. (2018). Critical Issues Affecting Groundwater Quality Governance and Management in the United States. *Water*, *10*(735), 1–17. https://doi.org/10.3390/w10060735

Pickford, M. (1986). Sedimentation and fossil preservation in the Nyanza Rift System, Kenya. *Geological Society Special Publication*, *25*, 345–362. https://doi.org/10.1144/GSL.SP.1986.025.01.29

Pierce, S. A., Sharp, J. M., Guillaume, J. H. A., Mace, R. E., & Eaton, D. J. (2013). Le continuum aquifère-débit comme guide typologique pour une gestion scientifique de l'eau souterraine. *Hydrogeology Journal*, *21*(2), 331–340. https://doi.org/10.1007/s10040-012-0910-y

Porowski, A. (2014). Isotope Hydrogeology. In L. Taylor & Francis Group (Ed.), *Handbook of Engineering Hydrology: Fundamentals and Applications* (pp. 345–377).

https://doi.org/10.1201/b15625-18

Prasanna, M. V., Chidambaram, S., & Srinivasamoorthy, K. (2010). Statistical analysis of the hydrogeochemical evolution of groundwater in hard and sedimentary aquifers system of Gadilam river basin, South India. *Journal of King Saud University - Science*, *22*(3), 133–145. https://doi.org/10.1016/j.jksus.2010.04.001

Pulfrey, W. (1960). *Shape of the sub-Miocene erosion bevel in Kenya. Geological Survey of Kenya, Bulletin No. 3*.

Rainwater, F. H., & Thatcher, L. L. (1960). *Methods for collection and analysis of water samples. USGS Water-Supply Paper 1454*. Retrieved from http://books.google.com/books?hl=en&lr=&id=e9jQAAAAMAAJ&oi=fnd&pg=PA1&dq=Methods+for+Collection+and+Analysis+of+Water+Samples&ots=Pwz1bhTr_q&sig=eBbZ5KrBsdDetjiQ5I6QV5ecN8g

Raith, M. M., Raase, P., & Reinhardt, J. (2011). *Guide to Thin Section Microscopy*. e-book, ISBN 978-3-00-033606-5 (PDF)

Rakama, S. O., Obiri, J. F., & Mugalavai, E. M. (2017). Evaluation of land use change pattern of Kajulu-Riat hill peri-urban area near Kisumu City, Kenya. *International Journal of Scientific Research and Innovative Technology*, *4*(7), 42–52.

Ravenscroft, P., Mahmud, Z. H., Islam, M. S., Hossain, A. K. M. Z., Zahid, A., Saha, G. C., & Islam, M. S. (2017). The public health significance of latrines discharging to groundwater used for drinking. *Water Research*, *124*(October 2018), 192–201. https://doi.org/10.1016/j.watres.2017.07.049

Razack, M., Furi, W., Fanta, L., & Shiferaw, A. (2020). Water resource assessment of a complex volcanic system under semi-arid climate using numerical modelling: The Borena Basin in Southern Ethiopia. *Water (Switzerland)*, *12*(1). https://doi.org/10.3390/w12010276

Rees, D., Momanyi, M., Wekundah, J., Kamau, M., Ndubi, J., Musembi, F., & Joldersma, R. (2000). Agricultural Knowledge and Information Systems in Kenya – Implications for Technology Dissemination and Development. *Agricultural Research & Extension Network*, (7), 107. Retrieved from https://www.odi.org/sites/odi.org.uk/files/odi-assets/publications-opinion-files/5120.pdf

Reinhard, K. (2009). *Groundwater Geophysics: A Tool for Hydrogeology* (Second Edi). Springer-Verlag. https://doi.org/10.1007/978-3-540-88405-7

Rendilicha, H., Home, P., & Raude, J. (2018). A Preliminary Review of Groundwater Vulnerability Assessment and Pollution Status in Kenya. *Italian Journal of Groundwater*, *AS25*(328), 7–13. https://doi.org/10.7343/as-2018-328

Richard, S. K., Chesnaux, R., Rouleau, A., Coupe, R. H., Richard, S. K., Chesnaux, R., & Coupe, R. H. (2016). Estimating the reliability of aquifer transmissivity values obtained from specific capacity tests : examples from the Saguenay-Lac-Saint-Jean aquifers, Canada. *Hydrological Sciences Journal*, *61*(1), 173–185. https://doi.org/10.1080/02626667.2014.966720

Richts, A., Struckmeier, W., & Zaepke, M. (2011). WHYMAP and the groundwater resources map of the World 1:25,000,000. *Sustaining Groundwater Resources*, 159–173. https://doi.org/10.1007/978-90-481-3426-7

Rompré, A., Servais, P., Baudart, J., De-Roubin, M. R., & Laurent, P. (2002). Detection and enumeration of coliforms in drinking water: current methods and emerging approaches. *Journal of Microbiological Methods*, *49*(1), 31–54. https://doi.org/10.1016/S0167-7012(01)00351-7

Rosenthal, E., Jones, B. F., & Weinberger, G. (1998). The chemical evolution of Kurnub Group paleowater in the Sinai- Negev province - a mass balance approach. *Applied Geochemistry*, *13*(5), 553–569.

Rozanski, K., Araguás-Araguás, L., & Gonfiantini, R. (2013). Isotopic Patterns in Modern Global Precipitation, 1–36. https://doi.org/10.1029/gm078p0001

SADC. (2011). *SADC Regional Groundwater Drought Vulnerability Mapping Final Report*. https://www.un-igrac.org/sites/default/files/resources/files/SADC%20Regional%20Groundwater%20Drought%20Risk%20Mapping.pdf

Saggerson, E. P. (1952). *Geology of the Kisumu District. Geological Survey of Kenya. Report number 21*.

Sajil Kumar, P. J., & James, E. J. (2016). Identification of hydrogeochemical processes in the Coimbatore district, Tamil Nadu, India. *Hydrological Sciences Journal*, *61*(4), 719–731. https://doi.org/10.1080/02626667.2015.1022551

Salami, R. O., von Meding, J. K., & Giggins, H. (2017). Urban settlements' vulnerability to flood risks in African cities: A conceptual framework. *Jamba: Journal of Disaster Risk Studies*, *9*(1), 1–9. https://doi.org/10.4102/jamba.v9i1.370

Sampat, P. (2000). Deep trouble: The hidden threat of groundwater pollution. *Worldwatch Paper*, (154), 28.

Sánchez-Vila, X., Meier, P. M., & Carrera, J. (1999). Pumping tests in heterogeneous aquifers: An analytical study of what can be obtained from their interpretation using Jacob's method. *Water Resources Research*, *35*(4), 943–952. https://doi.org/10.1029/1999WR900007

Sanders, L. (1963). *Geology of the Eldoret Area, Geological Survey of Kenya, Report No. 64*.

Sarin, M. M., Krishnaswami, S., Dilli, K., Somayajulu, B. L. K., & Moore, W. S. (1989). Major ion chemistry of the Ganga-Brahmaputra river system: Weathering processes and fluxes to the Bay of Bengal. *Geochimica et Cosmochimica Acta*, *53*(5), 997–1009. https://doi.org/10.1016/0016-7037(89)90205-6

Sarma, M., Bezbaruah, D., Goswami, T. K., & Baral, U. (2020). Geologic and Tectonic Evolution of the Yinkiong Group and Abor Volcanic Rocks in the Eastern Himalaya: An Overview of Geologic Data. *Geotectonics*, *54*(3), 395–409. https://doi.org/10.1134/S0016852120030097

Sarstedt, M., & Mooi, E. (2019). *Regression Analysis. In A Concise Guide to Market Research*. *A Concise Guide to Market Research*. https://doi.org/10.1007/978-3-662-56707-4

Schmoll, O. (2013). *Protecting Groundwater for Health: Managing the Quality of Drinking-water Sources. Water Intelligence Online* (Vol. 12). https://doi.org/10.2166/9781780405810

Sclar, G. D., Penakalapati, G., Amato, H. K., Garn, J. V., Alexander, K., Freeman, M. C., & Clasen, T. (2016). Assessing the impact of sanitation on indicators of faecal exposure along principal transmission pathways: A systematic review. *International Journal of Hygiene and Environmental Health*, *219*(8), 709–723. https://doi.org/10.1016/j.ijheh.2016.09.021

Searle, D. . (1952). *Geological map of the area North-West of Kitale Township, Geological Survey of Kenya, Report No.19*.

Seçkin, H., Meydan, İ., Özdek, U., Kömüroğlu, A. U., Kul, R., & Çibuk, S. (2018). Investigation of Coliform And E . Coli Bacteria And Nitrite And Nitrate Levels İn Drinking Waters of Van And Some Provinces. *IOSR Journal of Environmental Science, Toxicology and Food Technology*, *12*(4), 47–50. https://doi.org/10.9790/2402-1204014750

Selvakumar, S., Chandrasekar, N., & Kumar, G. (2017). Hydrogeochemical characteristics and groundwater contamination in the rapid urban development areas of Coimbatore, India. *Water Resources and Industry*, *17*(February), 26–33.

https://doi.org/10.1016/j.wri.2017.02.002

Sfinchez-vila, X., Meier, P. M., & Carrera, J. (1999). Pumping tests in heterogeneous aquifers: An analytical study of what can be obtained from their interpretation using Jacob's method. *Water Resources Research*, *35*(4), 943–952.

Shackleton, R. (1948). A contribution to the geology of the Kavirondo Rift Valley. *Quarterly Journal of the Geological Society*, *424*, 345–387.

Shah, T., Molden, D., Sakthivadivel, R., & Seckler, D. (2000). *The global groundwater situation: overview of opportunities and challenges. International Water Management Institute*. https://doi.org/10.5337/2011.0051

Shand, P., Edmunds, W. M., Lawrence, A. R., Smedley, P. L., & Burke, S. (2007). *The natural (baseline) quality of groundwater in England and Wales. BGS Research Report RR/07/06 and Technical Report NC/99/74/24*.

Sidle, W. C. (1998). Environmental isotopes for resolution of hydrology problems. *Environmental Monitoring and Assessment*, *52*(3), 389–410. https://doi.org/10.1023/A:1005922029958

Simiyu, S., Cairncross, S., & Swilling, M. (2018). Understanding Living Conditions and Deprivation in Informal Settlements of Kisumu, Kenya. *Urban Forum*. https://doi.org/10.1007/s12132-018-9346-3

Simonetti, A., & Bell, K. (1995). Nd, Pb and Sr isotopic data from the Mount Elgon volcano, eastern Uganda-western Kenya: Implications for the origin and evolution of nephelinite lavas. *Lithos*, *36*(2), 141–153. https://doi.org/10.1016/0024-4937(95)00011-4

Sindico, F., Hirata, R., & Manganelli, A. (2018). The Guarani Aquifer System: From a Beacon of hope to a question mark in the governance of transboundary aquifers. *Journal of Hydrology: Regional Studies*, (April), 0–1. https://doi.org/10.1016/j.ejrh.2018.04.008

Singh, A. (2014). Groundwater resources management through the applications of simulation modelling: A review. *Science of the Total Environment*, *499*, 414–423. https://doi.org/10.1016/j.scitotenv.2014.05.048

Singhal, B. (2008). Nature of Hard Rock Aquifers: Hydrogeological Uncertainties and Ambiguities. In *Groundwater dynamics in hard rock aquifer. Springer, Dordrecht* (pp. 20–39).

Sitoki, L., Gichuki, J., Ezekiel, C., Wanda, F., Mkumbo, O. C., & Marshall, B. E. (2010). The environment of Lake Victoria (East Africa): Current status and historical changes. *International Review of Hydrobiology*, *95*(3), 209–223. https://doi.org/10.1002/iroh.201011226

Sivaramakrishnan, J., Asokan, A., Sooryanarayana, K. R., Hegde, S. S., & Benjamin, J. (2015). Occurrence of Ground Water in Hard rock under distinct Geological setup. *Aquatic Procedia*, *4*(2015), 706–712. https://doi.org/10.1016/j.aqpro.2015.02.091

Sklash, M. G., & Mwangi, M. P. (1991). An isotopic study of groundwater supplies in the Eastern Province of Kenya. *Journal of Hydrology*, *128*(1–4), 257–275. https://doi.org/10.1016/0022-1694(91)90141-4

SNV. (2018). *Understanding the Effects of Poor Sanitation on Public Health, the Environment and Well-being Report of a study conducted in Homa Bay, Elgeyo Marakwet and Kericho counties in Kenya*. https://snv.org/cms/sites/default/files/explore/download/180006_snv_synthesis_report_lr.pdf

Sodemann, H. (2006). Stable Isotopes of Water (pp. 7–32). https://ethz.ch/content/dam/ethz/special-interest/usys/iac/iac-dam/documents/edu/courses/mesoscale_atmospheric_systems/Sodemann_Diss_ETH_16623_2006_Chap_2.pdf

Sokolov, A. A., & Chapman, T. G. (1974). Methods for water balance computations: an

international guide for research and practice. *The Unesco Press*.

Solder, J. E., Beisner, K. R., Anderson, J., & Bills, D. J. (2020). Rethinking groundwater flow on the South Rim of the Grand Canyon, USA: characterizing recharge sources and flow paths with environmental tracers. *Hydrogeology Journal*, *28*(5), 1593–1613. https://doi.org/10.1007/s10040-020-02193-z

Stallard, R. F., & Edmond, J. M. (1983). Geochemistry of the Amazon 2. The influence of geology and weathering environment on the dissolved load. *Journal of Geophysical Research*, *88*(C14), 9671–9688. https://doi.org/10.1029/JC088iC14p09671

Stefanakis, A. I., Zouzias, D., & Marsellos, A. (2015). Groundwater Pollution: Human and Natural Sources and Risks. *Environmental Sci. and Eng*, *4*(2017), 82–102. Retrieved from https://www.researchgate.net/publication/283017350_Groundwater_Pollution_Human_and_Natural_Sources_and_Risks

Stocker, M. D., Pachepsky, Y. a, Hill, R. L., & Shelton, D. R. (2015). Depth-Dependent Survival of Escherichia coli and Enterococci in Soil after Manure Application and Simulated Rainfall. *Applied and Environmental Microbiology*, *81*(14), 4801–4808. https://doi.org/10.1128/AEM.00705-15

Stoppelenbrug, F., Kovar, K., Pastoors, M., & Tiktak, A. (2005). *Modelling the interactions between transient saturated and unsaturated groundwater flow. Off-line coupling of LGM and SWAP*. RIVM report 500026001/2005. https://www.pbl.nl/sites/default/files/downloads/500026001.pdf

Subramani, T., Rajmohan, N., & Elango, L. (2010). Groundwater geochemistry and identification of hydrogeochemical processes in a hard rock region, Southern India. *Environmental Monitoring and Assessment*, *162*(1–4), 123–137. https://doi.org/10.1007/s10661-009-0781-4

Subyani, A. M. (2004). Use of chloride-mass balance and environmental isotopes for evaluation of groundwater recharge in the alluvial aquifer, Wadi Tharad, western Saudi Arabia. *Environmental Geology*, *46*(6–7), 741–749. https://doi.org/10.1007/s00254-004-1096-y

Suhada, R. A., & Hastuti, E. W. D. (2019). Petrogenesis study of quaternary volcanic rocks based on petrography analysis in Lubuk Nipis Village, Muara Enim District, South Sumatra. *IOP Conference Series: Materials Science and Engineering*, *620*(1). https://doi.org/10.1088/1757-899X/620/1/012122

Szymkiewicz, A., Gumuła-Kawęcka, A., Potrykus, D., Jaworska-Szulc, B., Pruszkowska-Caceres, M., & Gorczewska-Langner, W. (2018). Estimation of conservative contaminant travel time through vadose zone based on transient and steady flow approaches. *Water (Switzerland)*, *10*(10), 1–11. https://doi.org/10.3390/w10101417

Taherdoost, H., Sahibuddin, S., & Jalaliyoon, N. (2014). Exploratory factor analysis: Concepts and theory. *2nd International Conference on Mathematical, Computational and Statistical Sciences*, 375–382.

Tamez-Meléndez, C., Hernández-Antonio, A., Gaona-Zanella, P. C., Ornelas-Soto, N., & Mahlknecht, J. (2016). Isotope signatures and hydrochemistry as tools in assessing groundwater occurrence and dynamics in a coastal arid aquifer. *Environmental Earth Sciences*, *75*(9). https://doi.org/10.1007/s12665-016-5617-2

Tamunobereton-ari, I., Omubo-Pepple, V. B., & Amakiri, A. R. C. (2014). Characterization and Delineation of Aquifer in Part of Omoku, Rivers State, Nigeria. *IOSR Journal of Applied Geology and Geophysics*, *2*(4), 30–37. https://doi.org/10.9790/0990-0243037

Taweesin, K., Seeboonruang, U., & Saraphirom, P. (2018). The Influence of Climate Variability Effects on Groundwater Time Series in the Lower Central. *Water*, *10*(290), 23. https://doi.org/10.3390/w10030290

Taylor, R., & Howard, K. (2000). A tectono-geomorphic model of the hydrogeology of deeply weathered crystalline rock: Evidence from Uganda. *Hydrogeology Journal*, *8*(3), 279–294. https://doi.org/10.1007/s100400000069

Taylor, R G, Cronin, A., Lerner, D., Tellam, J., Bottrell, S., Rueedi, J., & Barrett, M. (2006). Hydrochemical evidence of the depth of penetration of anthropogenic recharge in sandstone aquifers underlying two mature cities in the UK. *Applied Geochemistry*, *21*, 1570–1592. https://doi.org/10.1016/j.apgeochem.2006.06.015

Taylor, Richard G., & Howard, K. W. F. (1996). Groundwater recharge in the Victoria Nile basin of East Africa: Support for the soil moisture balance approach using stable isotope tracers and flow modelling. *Journal of Hydrology*, *180*(1–4), 31–53. https://doi.org/10.1016/0022-1694(95)02899-4

Taylor, Richard G., Scanlon, B., Döll, P., Rodell, M., Van Beek, R., Wada, Y., & Treidel, H. (2013). Ground water and climate change. *Nature Climate Change*, *3*(4), 322–329. https://doi.org/10.1038/nclimate1744

Telford, W. M., Geldart, L. P., & Sheriff, R. E. (1990). Applied Geophysics. *Book*. https://doi.org/10.1180/minmag.1982.046.341.32

Tesfamichael, T. A. (2011). *Water-Rock Interaction and Geochemistry of Groundwater in Axum Area (Northern Ethiopia)*. PhD thesis. Institute of Applied Geosciences, Graz University of Technology.

Tessema, A., Nzotta, U., & Chirenje, E. (2014). *Assessment of Groundwater Potential in Fractured Hard Rocks Around Vryburg, North West Province, South Africa. WRC Report No. 2055/1/13*. http://www.wrc.org.za/wp-content/uploads/mdocs/2055-1-13.pdf

The World Bank. (2005). Sustainable Groundwater Groundwater Management : Management and Tools from Practice Kenya : The Role of Groundwater in the Water-Supply of Greater Nairobi, https://www.un-igrac.org/sites/default/files/resources/files/GWMATE%20case%20profile%20-%20Kenya.pdf.

Todd, K., & Mays, L. (1980). *Groundwater Hydrology*. John Wiley & Sons, Inc.

Tóth, J. (2009). Groundwater in igneous, metamorphic and sedimentary rocks. *Groundwater*, *I*, 1–10.

Trans Nzoia County Government. (2019). *Trans Nzoia County Annual Development Plan, 2019/2020*. Unpublished report

Tryon, C. A., Faith, J. T., Peppe, D. J., Beverly, E. J., Blegen, N., Blumenthal, S. A., & Sharp, W. D. (2016). The Pleistocene prehistory of the Lake Victoria basin. *Quaternary International*, *404*, 100–114. https://doi.org/10.1016/j.quaint.2015.11.073

Tsuchiya, N., Shibata, T., Koide, Y., Owada, M., Takazawa, E., Goto, Y., & Hariya, Y. (1989). Major Element Analysis of Rock Samples by X-ray Fluorescence Spectrometry, using Scandium Anode Tube. *Journal of the Faculty of Science, Hokkaido University*, *22*(3), 489–502.

Tuinhof, A., Foster, S., van Steenbergen, F., Talbi, A., & Wishart, M. (2011). *Appropriate groundwater management policy for Sub-Saharan Africa in face of demographic pressure and climatic variability. GW Mate, The World Bank*. https://openknowledge.worldbank.org/handle/10986/27363

TWAP. (2015). *AF39 – Mount Elgon Aquifer. Transboundary aquifer information sheet. TWAP Groundwater Indicators from Global Inventory. Transboundary waters assessment programme*. https://ggis.un-igrac.org/documents/1597/download

Ul Hadia, N., Abdullah, N., & Sentosa, I. (2016). An Easy Approach to Exploratory Factor Analysis: Marketing Perspective. *Journal of Educational and Social Research*, *6*(1), 215–223. https://doi.org/10.5901/jesr.2016.v6n1p215

UN-Habitant. (2005). *Situation Analysis of Informal Settlements in Kisumu. Cities without*

slums. Sub-Regional Programme for Eastern and Southern Africa.
https://digitallibrary.un.org/record/617637?ln=en

UN. (2012). *Management of Ground Water in Africa Including Transboundary Aquifers: Implications for Food Security, Livelihood and Climate Change Adaptation. Working paper 6. Climate Policy.* https://cgspace.cgiar.org/handle/10568/34895

UN. (1980). *Proclamation of the International Drinking Water Supply and Sanitation Decade. Resolutions adopted on the reports of the Second Committee.* Retrieved from http://undocs.org/a/res/35/18

UN. (2010). *The Human Rights to Water and Sanitation. Resolution adopted by General Assembly on 28th July 2010 (A/RES/64/292).* https://doi.org/10.4324/9781315471532-2

UN. (2015). *The 2030 Agenda for Sustainable Development. United Nations Department of Economic and Social Affairs.* https://doi.org/10.1080/02513625.2015.1038080

UN. (2019). *World Population Prospects 2019: Highlights (ST/ESA/SER.A/423).* Retrieved from http://www.ncbi.nlm.nih.gov/pubmed/12283219

UNEP/UNESCO. (2006). *Groundwater Pollution in Africa.* (Y. Xu & B. Usher, Eds.), *Balkema - Proceedings and Monographs in Engineering, Water and Earth Sciences.* London: Taylor & Francis. https://wedocs.unep.org/bitstream/handle/20.500.11822/9834/Groundwater_pollution_in_Africa.pdf?sequence=3&isAllowed=y

UNESCO. (2002). *Groundwater Contamination Inventory: A Methodological Guide. IHP-IV Series on Groundwater No.2. Unesco Ihp-Vi, Series on Groundwater* (Vol. 2). Retrieved from http://www.sepa.org.uk/land/land_publications.aspx

UNESCO. (2015). *A systematic review of emerging pollutants on human health and livelihoods of population living in the Lake Victoria Basin of Kenya. Case study report.* https://wedocs.unep.org/bitstream/handle/20.500.11822/7987/environment_development.pdf?sequence=3

Upton, K. A., Butler, A. P., Jackson, C. R., & Mansour, M. (2019). Modelling boreholes in complex heterogeneous aquifers. *Environmental Modelling and Software*, *118*(June 2018), 48–60. https://doi.org/10.1016/j.envsoft.2019.03.018

van Calsteren, P., & Schwieters, J. B. (1995). Performance of a thermal ionisation mass spectrometer with a deceleration lens system and post-deceleration detector selection. *International Journal of Mass Spectrometry and Ion Processes*, *146–147*(C), 119–129. https://doi.org/10.1016/0168-1176(95)04208-3

van Lopik, J. H., Hartog, N., & Schotting, R. J. (2020). Taking advantage of aquifer heterogeneity in designing construction dewatering systems with partially penetrating recharge wells. *Hydrogeology Journal.* https://doi.org/10.1007/s10040-020-02226-7

Varni, M., Comas, R., Weinzettel, P., & Dietrich, S. (2013). Application de la méthode de fluctuation du niveau piézométrique pour caractériser la recharge des eaux souterraines dans la plaine de la Pampa (Argentine). *Hydrological Sciences Journal*, *58*(7), 1445–1455. https://doi.org/10.1080/02626667.2013.833663

Vasu, D., Singh, S. K., Tiwary, P., Sahu, N., Ray, S. K., Butte, P., & Duraisami, V. P. (2017). Influence of geochemical processes on hydrochemistry and irrigation suitability of groundwater in part of semi-arid Deccan Plateau, India. *Applied Water Science*, *7*(7), 3803–3815. https://doi.org/10.1007/s13201-017-0528-2

Vearncombe, J. R. (1983). A dismembered ophiolite from the Mozambique Belt, West Pokot, Kenya. *Journal of African Earth Sciences*, *1*(2), 133–143. https://doi.org/10.1016/0899-5362(83)90005-2

Vittecoq, B., Reninger, P. A., Lacquement, F., Martelet, G., & Violette, S. (2019). Hydrogeological conceptual model of andesitic watersheds revealed by high-resolution heliborne geophysics. *Hydrology and Earth System Sciences*, *23*(5), 2321–2338.

https://doi.org/10.5194/hess-23-2321-2019

Wadsworth, W. B., & Baird, A. K. (1989). Modal analysis of granitic rocks by X-Ray Diffraction. *Canadian Minerologist*, *27*, 323–341.

Waldner, P., Marchetto, A., Thimonier, A., Schmitt, M., Rogora, M., Granke, O., … Lorenz, M. (2014). Detection of temporal trends in atmospheric deposition of inorganic nitrogen and sulphate to forests in Europe. *Atmospheric Environment*, *95*, 363–374. https://doi.org/10.1016/j.atmosenv.2014.06.054

Walliman, N. (2011). *Research Methods, the basics*. London and New York: Routledge.

Walter, J., Chesnaux, R., Cloutier, V., & Gaboury, D. (2017). The influence of water/rock − water/clay interactions and mixing in the salinization processes of groundwater. *Journal of Hydrology: Regional Studies*, *13*(June), 168–188. https://doi.org/10.1016/j.ejrh.2017.07.004

Walton, N. (1989). Electrical Conductivity and Total Dissolved Solids-What is Their Precise Relationship ? *Desalination*, *72*(1989), 275–292.

Wang, L., Dochartaigh, B. Ó., & Macdonald, D. (2010). *A literature review of recharge estimation and groundwater resource assessment in Africa. British Geological Survey Internal Report, IR/10/051*. http://nora.nerc.ac.uk/id/eprint/14145/1/BGS_Report-A_literature_review_of_recharge_estimation.pdf

Wang, L., Dang, J., Zhao, Y., Zhu, Y., Qiao, P., & Feng, C. (2020). Effects of Urbanization on Water Quality and the Macrobenthos Community Structure in the Fenhe River, Shanxi Province, China. *Journal of Chemistry*, *2020*. https://doi.org/10.1155/2020/8653486

Weingärtner, L., Jaime, C., Todd, M., Levine, S., Mcdowell, S., & Macleod, D. (2019). *Reducing flood impacts through forecast-based action. Entry points for social protection systems in Kenya. Working paper 553. WISER*. https://www.anticipation-hub.org/Documents/Research_Reports/Reducing_flood_impacts_through_forecast-based_action.pdf

WHO. (2003). *Assessing Microbial Safety of Drinking Water. Improving approaches and methods*. https://doi.org/10.1787/9789264099470-en

WHO. (2007). *Combating waterborne disease at the household level*. https://www.who.int/household_water/advocacy/combating_disease.pdf

WHO. (2009). Calcium and Magnesium in Drinking-water: Public Health Significance, 194. https://doi.org/10.1080/00207230903208415

WHO. (2017). *Guidelines for drinking-water quality: The fourth edition incorporating the first addendum. WHO Library Cataloguing-in-Publication Data* (Fourth edition). https://doi.org/10.1016/S1462-0758(00)00006-6

WHO and UNICEF. (2017). *Progress on Drinking Water, Sanitation and Hygiene - 2017 Update and SDG Baselines. Geneva*. https://doi.org/10.1007/s12686-011-9397-4

Wilcox, L. V. (1955). *Classification and use of irrigation water. Agricultural circular No 969, DC: USDA*. https://doi.org/USDA Circular No. 969.

Wilhelm, S., & Jean, M. (1995). *Hydrogeological maps: a guide and a standard legend. International Association of Hydrogeologist, International contributions to hydrogeology, vol. 17* (Vol. 17).

William Black. (1966). Hydrochemical facies and ground-water flow patterns in Northern part of Atlantic Coastal Plain. Geological Survey Professional Paper 498-A. US Government Printing Office. *Hydrology of Aquifer Systems*, Page 1-50.

Williams, K., Chamberlain, J., Buontempo, C., & Bain, C. (2015). Regional climate model performance in the Lake Victoria basin. *Climate Dynamics*, *44*(5–6), 1699–1713. https://doi.org/10.1007/s00382-014-2201-x

Willis, W. (2008). *Hydrogeology Field Manual* (Second Edi). Montana: McGraw-Hill.

https://doi.org/10.1036/0071477497

Winchester, J. A., & Floyd, P. A. (1977). Geochemical discrimination of different magma series and their differentiation products using immobile elements. *Chemical Geology*, *20*(C), 325–343. https://doi.org/10.1016/0009-2541(77)90057-2

Winter, T., Harvey, J., Franke, O., & Alley, W. (1998). *Interaction of ground water and surface water in different landscapes. Ground Water and Surface Water A Single Resource, USGS Circular 1139.*

Wirmvem, M. J., Ohba, T., Kamtchueng, B. T., Taylor, E. T., Fantong, W. Y., & Ako, A. A. (2017). Variation in stable isotope ratios of monthly rainfall in the Douala and Yaounde cities, Cameroon: local meteoric lines and relationship to regional precipitation cycle. *Applied Water Science*, *7*(5), 2343–2356. https://doi.org/10.1007/s13201-016-0413-4

Wisén, R., Christiansen, A. V., Dahlin, T., & Auken, E. (2008). Experience from two resistivity inversion techniques applied in three cases of geotechnical site investigation. *Journal of Geotechnical and Geoenvironmental Engineering*, *134*(12), 1730–1742. https://doi.org/10.1061/(ASCE)1090-0241(2008)134:12(1730)

Wohlgemuth, L., Bintakies, E., Kück, J., Conze, R., & Harms, U. (2004). Integrated deep drilling, coring, downhole logging, and data management in the Chicxulub Scientific Drilling Project (CSDP), Mexico. *Meteoritics and Planetary Science*, *39*(6), 791–797. https://doi.org/10.1111/j.1945-5100.2004.tb00929.x

Wood, W. W. (2019). Geogenic groundwater solutes: the myth. *Hydrogeology Journal*, *27*(8), 2729–2738. https://doi.org/10.1007/s10040-019-02057-1

World Bank. (2011a). *Guide to Climate Change Adaptation in Cities. Guide to Climate Change Adaptation in Cities.* https://doi.org/10.1596/27396

World Bank. (2011b). *Kenya Groundwater Governance case study. Water papers No. 71726* (Vol. 71726). Retrieved from http://documents.worldbank.org/curated/en/2011/06/16583819/kenya-groundwater-governance-case-study

World Bank. (2016). *Kenya urbanization review.* Retrieved from http://documents.worldbank.org/curated/en/639231468043512906/pdf/AUS8099-WP-P148360-PUBLIC-KE-Urbanization-ACS.pdf

WRC. (2017). *Groundwater sampling manual. Water Research Commission (WRC). WRC Report No. TT 733/17. Pretoria, South Africa.*

Wright, E. P., & Burgess, W. G. (1992). The hydrogeology of crystalline basement aquifers in Africa. *The Hydrogeology of Crystalline Basement Aquifers in Africa*, (66), 1–27.

Wright, J. B. (1963). A Note on Possible Differentiation Trends in Tertiary to Recent Lavas of Kenya. *Geological Magazine*, *100*(2), 164–180. https://doi.org/10.1017/S0016756800055369

Wu, Q., Si, B., He, H., & Wu, P. (2019). Determining regional-scale groundwater recharge with GRACE and GLDAS. *Remote Sensing*, *11*(2). https://doi.org/10.3390/rs11020154

Xing, L., Huang, L., Yang, Y., Xu, J., Zhang, W., Chi, G., & Hou, X. (2018). The blocking effect of clay in groundwater systems: A case study in an Inland plain area. *International Journal of Environmental Research and Public Health*, *15*(1816), 1–17. https://doi.org/10.3390/ijerph15091816

Xu, Y., Seward, P., Gaye, C., Lin, L., & Olago, D. (2019). Preface : Groundwater in Sub-Saharan Africa. *Hydrogeology Journal*, *27*, 815–822. https://doi.org/https://doi.org/10.1007/s10040-019-01977-2

Yang, L., Qi, Y., Zheng, C., Andrews, C. B., Yue, S., Lin, S., … Li, H. (2018). A modified water-table fluctuation method to characterize regional groundwater discharge. *Water (Switzerland)*, *10*(4), 1–16. https://doi.org/10.3390/w10040503

Yang, W., Seager, R., Cane, M. A., & Lyon, B. (2014). The East African long rains in

observations and models. *Journal of Climate*, *27*(19), 7185–7202. https://doi.org/10.1175/JCLI-D-13-00447.1

Yang, X., Steward, D. R., de Lange, W. J., Lauwo, S. Y., Chubb, R. M., & Bernard, E. A. (2010). Data model for system conceptualization in groundwater studies. *International Journal of Geographical Information Science*, *24*(5), 677–694. https://doi.org/10.1080/13658810902967389

Yeh, H. F., Lin, H. I., Lee, C. H., Hsu, K. C., & Wu, C. S. (2014). Identifying seasonal groundwater recharge using environmental stable isotopes. *Water (Switzerland)*, *6*(10), 2849–2861. https://doi.org/10.3390/w6102849

Yim, O., & Ramdeen, K. T. (2015). Hierarchical Cluster Analysis: Comparison of Three Linkage Measures and Application to Psychological Data. *The Quantitative Methods for Psychology*, *11*(1), 8–21. https://doi.org/10.20982/tqmp.11.1.p008

Yousif, M., & El-Aassar, A. H. M. (2018). Rock-water interaction processes based on geochemical modelling and remote sensing applications in hyper-arid environment: cases from the southeastern region of Egypt. *Bulletin of the National Research Centre*, *42*(1). https://doi.org/10.1186/s42269-018-0004-7

Yu, W., Yao, T., Tian, L., Ma, Y., Kurita, N., Ichiyanagi, K., & Sun, W. (2007). Stable Isotope Variations in Precipitation and Moisture Trajectories on the Western Tibetan Plateau, China. *Arctic, Antarctic, and Alpine Research*, *39*(4), 688–693. https://doi.org/10.1657/1523-0430(07-511)[yu]2.0.co;2

Yurtsever, Y., & Araguas Araguas, L. (1993). Environmental isotope applications in hydrology: an overview of the IAEA's activities, experiences, and prospects. In *Tracers in hydrology. Proc. international symposium, Yokohama, 1993* (pp. 3–20).

Zhang, G., Feng, G., Li, X., Xie, C., & Pi, X. (2017). Flood effect on groundwater recharge on a typical silt loam soil. *Water (Switzerland)*, *9*(7). https://doi.org/10.3390/w9070523

Zhou, Z., Ansems, N., & Torfs, P. (2015). *A Global Assessment of Nitrate Contamination in Groundwater. International Groundwater Resources Assessment Centre.* https://www.un-igrac.org/resource/global-assessment-nitrate-contamination-groundwater

Zhu, B.-Q., & Ren, X.-Z. (2018). Direct or indirect recharge on groundwater in the middle-latitude desert of Otindag, China? *Hydrology and Earth System Sciences Discussions*, (March), 1–43. https://doi.org/10.5194/hess-2018-71

List of publications

1. Kanoti *et al.,* 2020. Sanitation challenges, groundwater perspectives and their intertwined relationships in Kisumu, Kenya. **Kenya Policy Briefs, 1(1), 15-16.** Retrieved from: **https://uonresearch.org/journal/index.php/kpb/article/view/7**

2. Kanoti *et al.,* 2019. Microbial and Physical Chemical Indicators of Groundwater Contamination in Kenya: A Case Study of Kisumu Aquifer System, Kenya. **Journal of Water Resource and Protection 11(04):404-418;** DOI: 10.4236/jwarp.2019.114024

3. Kanoti *et al.,* 2019. Characterization of Major Ion Chemistry and Hydro-Geochemical Processes in Mt. Elgon Trans-Boundary Aquifer and Their Impacts on Public Health. **Journal of Environment and Earth Sciences**. DOI: 10.7176/JEES/9-4-06

Appendices

Appendix 1. Full chemical results for Kisumu water samples (mg/L)

Fe²⁺	Mn²⁺	Ca²⁺	Mg²⁺	Na⁺	K⁺	HCO₃⁻	Cl⁻	F.	NO₂⁻	NO₃²⁻	SO₄²⁻
0	0	0.85	0.28	309.00	9.36	829.60	46.60	4.13	0.73	3.23	83.90
0.00	0.00	0.78	0.14	321.00	8.94	845.46	47.40	3.79	0.74	3.28	91.10
0.00	0.00	8.78	1.67	323.00	9.27	801.54	48.70	3.43	1.09	4.83	89.90
0.79	1.13	8.57	2.33	10.90	3.39	58.56	11.90	0.53	1.48	6.55	7.01
0.58	0.71	9.43	2.68	10.60	2.00	68.44	5.64	0.39	1.15	5.09	3.42
0.50	0.23	18.10	3.89	13.00	2.19	74.54	6.95	0.23	1.35	5.98	3.06
0.00	0.00	40.10	3.86	246.00	15.70	753.96	41.00	5.62	0.50	2.21	59.90
0.00	0.00	36.30	2.87	248.00	15.50	871.08	41.20	7.29	0.39	1.73	53.00
0.00	0.00	38.20	3.85	258.00	16.30	772.26	40.80	5.98	0.23	1.02	54.20
0.00	0.16	186.00	41.00	150.00	10.60	723.46	159.00	0.85	9.31	41.20	209.00
0.00	0.02	188.00	34.50	162.00	8.59	734.44	177.00	0.91	13.60	60.20	179.00
0.00	1.03	193.00	42.40	162.00	10.20	691.74	159.00	0.73	6.48	28.70	223.00
1.17	1.12	16.70	3.49	11.10	3.55	45.63	10.40	0.28	1.69	7.48	5.90
0.27	0.46	8.70	2.65	12.20	1.24	58.93	4.28	0.32	1.00	4.43	4.64
0.56	0.34	16.40	3.76	12.90	1.81	75.15	7.43	0.20	1.24	5.49	4.40
0.09	0.66	35.00	10.30	28.80	2.90	228.14	5.07	0.31	0.94	4.16	5.51
1.54	0.14	11.00	3.54	14.80	2.52	97.72	3.47	0.37	0.28	1.24	3.89
0.12	0.14	22.30	6.21	22.30	2.03	143.96	3.40	0.34	0.16	0.71	3.24
0.00	0.57	60.40	22.10	38.60	1.10	401.38	6.63	0.73	1.05	4.65	7.88
0.00	0.72	64.40	21.60	36.10	0.45	489.22	7.09	0.84	1.49	6.60	6.08
0.00	0.64	61.30	22.30	39.20	1.16	424.56	6.47	0.77	0.86	3.81	7.28
0.60	0.41	20.80	3.93	34.80	10.30	124.44	21.10	0.66	1.84	8.15	8.96
13.20	0.09	4.82	1.64	34.90	8.92	90.89	19.90	1.06	1.72	7.61	8.81
21.30	0.20	11.20	3.20	41.90	11.50	191.54	21.60	0.83	1.23	5.44	11.40
0.00	0.00	16.70	3.19	58.90	12.50	278.16	4.92	0.26	0.63	2.79	1.71
0.72	0.00	3.02	0.89	28.50	7.09	109.31	2.77	0.29	1.89	8.37	0.23
0.20	0.00	7.29	1.88	43.40	9.74	179.34	2.67	0.21	1.05	4.65	1.86
0.09	0.07	12.70	2.16	19.60	6.99	71.86	10.70	0.34	2.96	13.10	1.38
0.04	0.04	2.85	0.73	16.00	6.14	58.80	4.76	0.36	2.51	11.10	0.78
0.01	0.04	9.58	1.86	19.50	7.40	72.59	4.94	0.28	2.56	11.30	1.17
0.22	0.05	18.10	3.36	30.10	9.66	95.40	9.29	0.30	3.60	15.90	4.85
0.09	0.01	4.86	1.24	22.90	7.69	83.69	7.96	0.43	3.86	17.10	3.92
0.00	0.02	11.10	2.35	27.70	9.13	99.67	8.26	0.28	2.65	11.70	3.86
0.08	0.17	36.60	6.65	54.90	19.40	173.24	43.00	0.90	1.68	7.44	45.50
0.00	0.06	28.20	5.56	43.00	17.00	145.18	48.10	0.85	1.49	6.60	41.90
0.66	0.07	25.60	5.49	43.30	17.20	169.58	31.40	0.81	1.64	7.26	31.20
0.00	0.00	62.70	12.30	132.00	20.20	583.16	26.10	3.50	0.29	1.28	62.90
0.23	0.00	61.10	10.50	80.90	19.70	264.74	18.60	3.13	42.60	189.00	28.10
0.06	0.00	63.80	12.60	110.00	22.10	535.58	22.80	2.33	0.76	3.36	40.10
0.82	0.17	7.32	2.39	6.69	3.19	60.51	3.56	0.49	0.28	1.24	3.30
0.75	0.38	5.28	1.62	4.96	2.56	56.85	6.30	0.39	0.60	2.66	2.16
0.39	0.21	12.90	3.26	7.61	2.63	61.49	5.80	0.34	0.68	3.01	1.83
0.06	0.02	23.50	13.10	21.70	1.32	235.46	4.37	0.98	0.39	1.73	1.17
3.39	0.02	18.40	10.00	19.10	0.56	193.98	5.98	0.97	0.60	2.66	1.38
0.12	0.00	23.80	11.90	22.70	1.00	219.60	1.64	1.02	0.21	0.93	2.37
0.61	0.32	14.90	3.02	12.60	3.96	47.09	8.63	0.42	1.32	5.84	6.53
0.18	0.50	5.29	1.59	9.21	2.69	84.79	10.30	0.45	1.86	8.23	4.25
0.24	0.34	12.50	3.02	12.10	2.79	70.52	8.37	0.34	1.43	6.33	3.57
0	0	43.20	8.31	122.00	9.47	600.24	27.40	0.85	0.28	1.24	21.90
0.00	0.00	44.30	7.63	111.00	8.08	525.82	27.70	1.44	0.25	1.11	25.20
0.00	0.00	41.80	8.28	121.00	8.97	464.82	26.10	1.38	0.23	1.02	23.80

Fe^{2+}	Mn^{2+}	Ca^{2+}	Mg^{2+}	Na$^+$	K$^+$	HCO$_3^-$	Cl$^-$	F$^-$	NO$_2^-$	NO$_3^{2-}$	SO$_4^{2-}$
0.14	0.13	11.60	3.67	18.10	6.58	115.66	7.48	0.73	0.27	1.20	2.73
0.39	0.37	11.10	3.46	17.00	5.86	101.87	6.73	0.67	4.57	20.20	2.61
0.27	0.12	19.20	5.10	20.00	5.68	108.58	10.70	0.58	0.82	3.63	2.79
0	0.03	131.00	17.00	286.00	30.40	345.26	538.00	0.87	1.82	8.06	37.10
0.00	0.03	88.30	9.85	173.00	19.70	237.90	331.00	0.99	2.75	12.20	34.20
0.00	0.19	196.00	23.00	412.00	34.90	423.34	752.00	1.40	0.59	2.61	46.10
0	0	78.70	9.19	166.00	29.60	631.96	77.40	3.50	1.44	6.37	99.80
0.00	0.00	69.20	7.73	156.00	22.00	568.52	78.70	2.85	2.10	9.30	104.00
0.04	0.01	89.10	10.40	179.00	29.20	629.52	80.60	3.20	1.88	8.32	109.00
0.16	0	49.70	8.27	117.00	28.30	425.78	76.60	1.85	2.79	12.40	49.10
0.02	0.00	97.80	12.40	94.50	29.90	425.78	125.00	1.73	1.79	7.92	93.50
0.03	0.01	86.50	13.00	104.00	29.60	495.32	99.90	1.93	1.82	8.06	77.90
0.00	0.00	87.00	17.90	147.00	10.80	588.04	73.20	3.07	0.34	1.51	61.10
0.00	0.00	109.00	21.10	141.00	11.80	747.86	77.60	1.85	2.18	9.65	76.40
0.00	0.01	106.00	21.40	151.00	11.50	762.50	63.70	2.19	0.21	0.93	62.60

Appendix 2. Full chemical results for Mt. Elgon water samples (mg/L)

Sample No	Fe²⁺	Mn²⁺	Ca²⁺	Mg²⁺	Na⁺	K⁺	HCO₃⁻	Cl⁻	F⁻	NO₃²⁻	SO₄²⁻
EL 21	0.0	0.0	30.4	12.2	24.9	3.2	212.3	10.0	0.1	6.7	2.9
EL 3	0.0	0.1	13.6	3.9	7.5	3.7	85.5	1.0	0.1	2.2	1.2
EL 4	0.0	0.0	18.4	5.8	11.3	2.5	95.2	10.0	0.1	7.7	0.8
EL 8	0.0	0.0	9.6	3.9	67.3	5.8	248.9	8.0	0.1	2.0	2.3
EL 9	0.0	0.0	25.6	6.8	7.4	4.7	95.2	13.0	0.1	2.2	1.8
EL 13	0.0	0.0	28.0	23.8	51.4	2.0	366.0	16.0	0.1	0.7	10.8
EL 10	0.0	0.0	36.0	28.7	11.0	7.9	278.2	7.0	0.2	0.6	3.5
EL 15	0.0	0.0	12.8	5.4	9.1	2.9	48.8	10.0	0.0	8.5	1.0
EL 18	0.0	0.0	23.2	10.7	16.0	4.0	87.8	13.0	0.1	18.3	0.3
EL 25	0.0	0.0	10.4	1.5	11.8	3.8	43.9	1.0	0.1	6.9	1.4
EL 26	0.0	0.0	0.8	0.0	212.3	21.0	514.8	24.0	2.8	2.3	16.1
EL 32	0.0	0.0	52.8	33.1	33.4	4.3	373.3	18.0	0.6	1.0	10.6
EL 2	0.0	0.0	2.1	1.5	6.2	0.6	29.3	0.0	0.1	0.5	0.6
EL 12	0.0	0.0	8.8	43.7	85.0	4.7	456.3	11.0	2.3	5.1	4.5
EL 24	0.0	0.0	8.0	5.4	9.5	2.8	43.9	2.0	0.1	7.8	4.5
EL 27	0.0	0.0	25.6	12.2	7.5	2.5	153.7	5.0	0.3	5.0	1.0
EL 16	0.0	0.0	20.0	2.4	4.0	2.9	85.4	0.0	0.1	0.6	2.7
EL 17	0.0	0.0	15.2	2.4	4.0	2.5	61.0	0.0	0.1	2.3	2.1
EL 19	0.0	0.0	7.2	2.9	6.5	1.3	48.8	1.0	0.1		1.0
EL 11	0.0	0.0	30.4	42.8	12.0	7.8	331.8	4.0	0.6	1.6	5.7
EL 1	0.0	0.0	17.6	8.8	15.0	2.8	136.6	3.0	1.1	1.4	1.2
ELB 1	0.2	0.0	19.2	8.8	13.0	2.9	134.2	2.0	1.2	0.1	1.5
ELB 5	0.2	0.0	23.2	8.3	7.0	3.3	124.4	3.0	0.2	1.8	0.5
ELB 6	0.0	0.0	12.8	5.4	83.0	7.1	244.0	9.0	0.2	5.9	2.1
ELB 7	0.9	0.0	33.6	40.4	86.5	10.2	422.1	56.0	0.2	7.3	1.2
ELB 8	0.0	0.0	4.0	2.9	7.0	2.1	34.2	0.0	0.1	4.9	1.0
ELB 10	0.0	0.0	12.8	1.0	12.0	2.7	58.6	3.0	0.1	3.1	0.1
ELB 13	0.4	0.0	2.1	1.0	250.0	46.0	641.7	30.0	5.1	3.1	13.8
ELB 14	0.0	0.0	29.6	11.7	12.0	2.7	158.6	7.0	0.3	8.1	0.9
ELB 16	0.0	0.0	24.0	5.9	20.0	3.6	90.3	14.0	0.1	15.1	1.7
ELB 17	1.0	0.1	22.4	9.3	8.0	4.1	146.4	4.0	0.2	1.4	0.0
ELB 18	0.2	0.2	4.8	2.0	2.4	2.1	24.4	0.0	0.1	5.0	1.0
ELB19	0.0	0.0	15.2	5.4	4.0	2.3	73.2	3.0	0.1	3.5	1.8
ELB 21	0.0	0.0	13.6	6.3	16.0	2.2	58.6	7.0	0.1	9.1	1.0
ELB22	0.0	0.0	5.6	2.9	10.0	1.5	48.8	0.0	0.1	3.8	1.2
ELB 24	0.2	0.0	4.8	2.9	7.0	2.0	48.8	0.0	0.2	2.0	0.5
ELB 26	0.0	0.0	29.6	50.1	33.0	10.2	366.0	8.0	0.4	2.6	3.3
ELB 27	0.0	0.0	17.6	36.0	10.0	6.2	295.2	4.0	0.6	2.0	0.6
ELB 28	0.1	0.1	56.0	34.1	91.0	4.8	500.2	15.0	3.1	12.0	7.3
ELB 29	0.1	0.0	30.4	13.1	11.2	5.0	170.8	10.0	0.6	3.7	2.0
ELB 30	0.0	0.0	69.6	64.7	8.0	6.3	488.0	15.0	1.3	7.4	14.8

Appendix 3. Charge balance calculation for Kisumu anions and cations

Meq/l Calculations for Cations				Total Major Cations	Meq/l Calculations for Anions						Total Anions	Charge Balance Difference
Ca^{2+}	Mg^{2+}	Na^+	K^+		HCO_3^-	SO_4^-	Cl^-	F^-	NO_2^-	NO_3^{2-}		
0.04	0.02	13.43	0.24	13.74	13.60	1.75	1.31	0.22	0.02	0.05	16.94	-10.43
0.04	0.01	13.96	0.23	14.24	13.86	1.90	1.34	0.20	0.02	0.05	17.36	-9.88
0.44	0.14	14.04	0.24	14.86	13.14	1.87	1.37	0.18	0.02	0.08	16.66	-5.73
0.43	0.19	0.47	0.09	1.18	0.96	0.15	0.34	0.03	0.03	0.11	1.61	-15.26
0.47	0.22	0.46	0.05	1.20	1.12	0.07	0.16	0.02	0.03	0.08	1.48	-10.25
0.91	0.32	0.57	0.06	1.85	1.22	0.06	0.20	0.01	0.03	0.10	1.62	6.56
2.01	0.32	10.70	0.40	13.42	12.36	1.25	1.15	0.30	0.01	0.04	15.10	-5.89
1.82	0.24	10.78	0.40	13.23	14.28	1.10	1.16	0.38	0.01	0.03	16.96	-12.35
1.91	0.32	11.22	0.42	13.86	12.66	1.13	1.15	0.31	0.01	0.02	15.27	-4.83
9.30	3.37	6.52	0.27	19.47	11.86	4.35	4.48	0.04	0.20	0.66	21.60	-5.19
9.40	2.84	7.04	0.22	19.50	12.04	3.73	4.99	0.05	0.30	0.97	22.07	-6.16
9.65	3.49	7.04	0.26	20.44	11.34	4.65	4.48	0.04	0.14	0.46	21.10	-1.58
0.84	0.29	0.48	0.09	1.70	0.75	0.12	0.29	0.01	0.04	0.12	1.34	11.88
0.44	0.22	0.53	0.03	1.22	0.97	0.10	0.12	0.02	0.02	0.07	1.29	-3.09
0.82	0.31	0.56	0.05	1.74	1.23	0.09	0.21	0.01	0.03	0.09	1.66	2.30
1.75	0.85	1.25	0.07	3.92	3.74	0.11	0.14	0.02	0.02	0.07	4.10	-2.19
0.55	0.29	0.64	0.06	1.55	1.60	0.08	0.10	0.02	0.01	0.02	1.83	-8.19
1.12	0.51	0.97	0.05	2.65	2.36	0.07	0.10	0.02	0.00	0.01	2.56	1.78
3.02	1.82	1.68	0.03	6.55	6.58	0.16	0.19	0.04	0.02	0.08	7.07	-3.82
3.22	1.78	1.57	0.01	6.58	8.02	0.13	0.20	0.04	0.03	0.11	8.53	-12.90
3.07	1.84	1.70	0.03	6.63	6.96	0.15	0.18	0.04	0.02	0.06	7.41	-5.54
1.04	0.32	1.51	0.26	3.14	2.04	0.19	0.59	0.03	0.04	0.13	3.03	1.85
0.24	0.13	1.52	0.23	2.12	1.49	0.18	0.56	0.06	0.04	0.12	2.45	-7.16
0.56	0.26	1.82	0.29	2.94	3.14	0.24	0.61	0.04	0.03	0.09	4.14	-16.99
0.84	0.26	2.56	0.32	3.98	4.56	0.04	0.14	0.01	0.01	0.05	4.81	-9.41
0.15	0.07	1.24	0.18	1.65	1.79	0.00	0.08	0.02	0.04	0.14	2.07	-11.33
0.36	0.15	1.89	0.25	2.66	2.94	0.04	0.08	0.01	0.02	0.08	3.16	-8.70
0.64	0.18	0.85	0.18	1.84	1.18	0.03	0.30	0.02	0.06	0.21	1.80	1.18
0.14	0.06	0.70	0.16	1.06	0.96	0.02	0.13	0.02	0.05	0.18	1.37	-12.83
0.48	0.15	0.85	0.19	1.67	1.19	0.02	0.14	0.01	0.06	0.18	1.61	1.95
0.91	0.28	1.31	0.25	2.74	1.56	0.10	0.26	0.02	0.08	0.26	2.28	9.20
0.24	0.10	1.00	0.20	1.54	1.37	0.08	0.22	0.02	0.08	0.28	2.06	-14.51
0.56	0.19	1.20	0.23	2.19	1.63	0.08	0.23	0.01	0.06	0.19	2.21	-0.47
1.83	0.55	2.39	0.50	5.26	2.84	0.95	1.21	0.05	0.04	0.12	5.20	0.57
1.41	0.46	1.87	0.44	4.17	2.38	0.87	1.35	0.04	0.03	0.11	4.79	-6.89
1.28	0.45	1.88	0.44	4.06	2.78	0.65	0.88	0.04	0.04	0.12	4.51	-5.30
3.14	1.01	5.74	0.52	10.40	9.56	1.31	0.74	0.18	0.01	0.02	11.81	-6.34
3.06	0.86	3.52	0.51	7.94	4.34	0.59	0.52	0.16	0.93	3.05	9.59	-9.39
3.19	1.04	4.78	0.57	9.58	8.78	0.84	0.64	0.12	0.02	0.05	10.45	-4.35
0.37	0.20	0.29	0.08	0.94	0.99	0.07	0.10	0.03	0.01	0.02	1.21	-12.91
0.26	0.13	0.22	0.07	0.68	0.93	0.05	0.18	0.02	0.01	0.04	1.23	-28.91
0.65	0.27	0.33	0.07	1.31	1.01	0.04	0.16	0.02	0.01	0.05	1.29	0.82
1.18	1.08	0.94	0.03	3.23	3.86	0.02	0.12	0.05	0.01	0.03	4.09	-11.79

218

Meq/l Calculations for Cations					219							
				Total Major Cations	Meq/l Calculations for Anions						Total Anions	Charge Balance Difference
Ca²⁺	Mg²⁺	Na⁺	K⁺		HCO₃⁻	SO₄⁻	Cl⁻	F⁻	NO₂⁻	NO₃²⁻		
0.92	0.82	0.83	0.01	2.59	3.18	0.03	0.17	0.05	0.01	0.04	3.48	-14.75
1.19	0.98	0.99	0.03	3.18	3.60	0.05	0.05	0.05	0.00	0.02	3.77	-8.43
0.75	0.25	0.55	0.10	1.64	0.77	0.14	0.24	0.02	0.03	0.09	1.30	11.81
0.76	0.13	0.40	0.07	1.36	1.39	0.09	0.29	0.02	0.04	0.13	1.97	-18.03
0.63	0.25	0.53	0.07	1.47	1.16	0.07	0.24	0.02	0.03	0.10	1.62	-4.72
2.16	0.68	5.30	0.24	8.39	9.84	0.46	0.77	0.04	0.01	0.02	11.14	-14.06
2.22	0.63	4.83	0.21	7.88	8.62	0.53	0.78	0.08	0.01	0.02	10.02	-11.99
2.09	0.68	5.26	0.23	8.26	7.62	0.50	0.74	0.07	0.01	0.02	8.94	-3.95
0.58	0.30	0.79	0.17	1.84	1.90	0.06	0.21	0.04	0.01	0.02	2.23	-9.57
0.56	0.28	0.74	0.15	1.73	1.67	0.05	0.19	0.04	0.10	0.33	2.37	-15.71
0.96	0.42	0.87	0.15	2.39	1.78	0.06	0.30	0.03	0.02	0.06	2.25	3.21
6.55	1.40	12.43	0.78	21.16	5.66	0.77	####	0.05	0.04	0.13	21.80	-1.48
4.42	0.81	7.52	0.51	13.25	3.90	0.71	9.32	0.05	0.06	0.20	14.24	-3.61
9.80	1.89	17.91	0.89	30.50	6.94	0.96	####	0.07	0.01	0.04	29.21	2.16
3.94	0.76	7.22	0.76	12.67	10.36	2.08	2.18	0.18	0.03	0.10	14.93	-8.21
3.46	0.64	6.78	0.56	11.44	9.32	2.17	2.22	0.15	0.05	0.15	14.05	-10.21
4.46	0.86	7.78	0.75	13.84	10.32	2.27	2.27	0.17	0.04	0.13	15.20	-4.68
2.49	0.68	5.09	0.73	8.98	6.98	1.02	2.16	0.10	0.06	0.20	10.52	-7.89
4.89	1.02	4.11	0.77	10.79	6.98	1.95	3.52	0.09	0.04	0.13	12.70	-8.17
4.33	1.07	4.52	0.76	10.68	8.12	1.62	2.81	0.10	0.04	0.13	12.83	-9.15
4.35	1.47	6.39	0.28	12.49	9.64	1.27	2.06	0.16	0.01	0.02	13.17	-2.63
5.45	1.74	6.13	0.30	13.62	12.26	1.59	2.19	0.10	0.05	0.16	16.33	-9.06
5.30	1.76	6.57	0.29	13.92	12.50	1.30	1.79	0.12	0.00	0.02	15.73	-6.10

Appendix 4. Charge balance calculation for Mt. Elgon ions and cations

Cations (Meq/L)					Anions (Meq/L)						
Ca	Mg	Na	K	Total Major Cations	HCO3	SO4	Cl	F	NO3	Total Anions	Charge Balance Diffrence
0.88	0.72	0.65	0.07	2.32	2.24	0.03	0.08	0.06	0.02	2.43	-2.20
1.52	1.00	1.08	0.08	3.69	3.48	0.06	0.28	0.01	0.11	3.94	-3.24
0.68	0.32	0.33	0.09	1.42	1.15	0.03	0.03	0.01	0.04	1.24	6.64
0.92	0.48	0.49	0.06	1.96	1.56	0.02	0.28	0.00	0.12	1.98	-0.71
0.48	0.32	2.93	0.15	3.87	4.08	0.05	0.23	0.00	0.03	4.39	-6.22
1.28	0.56	0.32	0.12	2.28	1.56	0.04	0.37	0.00	0.04	2.00	6.52
1.40	1.96	2.23	0.05	5.65	6.00	0.23	0.45	0.01	0.01	6.69	-8.47
1.80	2.36	0.48	0.20	4.84	4.56	0.07	0.20	0.01	0.01	4.85	-0.06
0.64	0.44	0.40	0.07	1.55	0.80	0.02	0.28	0.00	0.14	1.24	11.07
1.16	0.88	0.70	0.10	2.84	1.44	0.01	0.37	0.00	0.30	2.11	14.74
0.52	0.12	0.51	0.10	1.25	0.72	0.03	0.03	0.00	0.11	0.89	16.84
0.04	0.00	9.23	0.54	9.81	8.44	0.34	0.68	0.15	0.04	9.63	0.91
2.64	2.72	1.45	0.11	6.92	6.12	0.22	0.51	0.03	0.02	6.89	0.24
0.11	0.12	0.27	0.02	0.51	0.48	0.01	0.00	0.00	0.01	0.51	0.49
0.44	3.60	3.70	0.12	7.86	7.48	0.09	0.31	0.12	0.08	8.09	-1.45
0.40	0.44	0.41	0.07	1.33	0.72	0.09	0.06	0.01	0.13	1.00	13.85
1.28	1.00	0.33	0.06	2.67	2.52	0.02	0.14	0.02	0.08	2.78	-1.97
1.00	0.20	0.17	0.07	1.45	1.40	0.06	0.00	0.01	0.01	1.47	-0.76
0.76	0.20	0.17	0.06	1.20	1.00	0.04	0.00	0.01	0.04	1.09	4.87
0.36	0.24	0.28	0.03	0.92	0.80	0.02	0.03	0.01	0.00	0.85	3.46
1.52	3.52	0.52	0.20	5.76	5.44	0.12	0.11	0.03	0.03	5.72	0.34
0.96	0.72	0.57	0.07	2.32	2.20	0.03	0.06	0.06	0.00	2.35	-0.66
1.16	0.68	0.30	0.08	2.23	2.04	0.01	0.08	0.01	0.03	2.17	1.34
0.64	0.44	3.61	0.18	4.87	4.00	0.04	0.25	0.01	0.10	4.40	5.10
1.68	3.32	3.76	0.26	9.02	6.92	0.03	1.58	0.01	0.12	8.65	2.12
0.20	0.24	0.30	0.05	0.80	0.56	0.02	0.00	0.01	0.08	0.67	9.01
0.64	0.08	0.52	0.07	1.31	0.96	0.00	0.08	0.01	0.05	1.10	8.63
0.12	0.08	10.87	1.18	12.25	10.52	0.29	0.85	0.27	0.05	11.96	1.17
1.48	0.96	0.52	0.07	3.03	2.60	0.02	0.20	0.01	0.13	2.96	1.23
1.20	0.48	0.87	0.09	2.64	1.48	0.04	0.39	0.01	0.24	2.16	10.09
1.12	0.76	0.35	0.11	2.33	2.40	0.00	0.11	0.01	0.02	2.55	-4.33
0.24	0.16	0.10	0.05	0.56	0.40	0.02	0.00	0.01	0.08	0.51	4.80
0.76	0.44	0.17	0.06	1.43	1.20	0.04	0.08	0.01	0.06	1.38	1.77
0.68	0.52	0.70	0.06	1.95	0.96	0.02	0.20	0.01	0.15	1.33	18.93
0.28	0.24	0.43	0.04	0.99	0.80	0.02	0.00	0.01	0.06	0.89	5.44
0.24	0.24	0.30	0.05	0.84	0.80	0.01	0.00	0.01	0.03	0.85	-0.85
1.48	4.12	1.43	0.26	7.30	6.00	0.07	0.23	0.02	0.04	6.36	6.89
0.88	2.96	0.43	0.16	4.43	4.84	0.01	0.11	0.03	0.03	5.03	-6.28
2.80	2.80	3.96	0.12	9.68	8.20	0.15	0.42	0.16	0.19	9.13	2.95
1.52	1.08	0.49	0.13	3.22	2.80	0.04	0.28	0.03	0.06	3.21	0.10
3.48	5.32	0.35	0.16	9.31	8.00	0.31	0.42	0.07	0.12	8.91	2.19

Appendix 5. Field analysis in Kisumu of TTC in May 2018.

Date	ID	longitude	latitude	Elevation	Water type	TTC	NO$_3^{2-}$	EC (µS/cm)	pH	Temp
14-May	L1	34.75872	-0.118301	1158	Borehole	570	23.8	373	6.1	27.7
14-May	L2	34.764235	-0.119955	1145	Spring	1320	90.4	724	6.16	25.9
15-May	L3	34.707561	-0.060481	1235	Dug-well	330	0.2	665	7.15	25.4
15-May	L4	34.706851	-0.062652	1219	Dug-well	270	51.6	1450	6.98	25.8
15-May	L5	34.707652	-0.081887	1154	Dug-well	3600	10.0	1057	7.66	28.7
15-May	L6	34.706304	-0.086372	1145	Dug-well	50	2.4	2160	8.09	26.9
15-May	L7	34.717918	-0.066739	1203	Dug-well	187	19.0	1160	7.06	26.1
15-May	L8	34.76126	-0.075681	1156	Spring	20	1.2	205	6.64	25.8
15-May	L9	34.742522	-0.074886	1161	Spring	22000	16.8	448	6.48	25.4
15-May	L10	34.742297	-0.0739	1164	Dug-well	40000	46.4	549	6.5	25.8
16-May	L12	34.751585	-0.069903	1173	Dug-well	10400	35.7	477	6.42	27.2
16-May	L13	34.742261	-0.047684	1367	Spring	4100	5.5	103.9	5.72	24.3
16-May	L14	34.747264	-0.040929	1427	Borehole	17	6.3	89.7	6.75	23.2
16-May	L15	34.724466	-0.060779	1236	Dug-well	49000	3.2	222	7.03	22.8
16-May	L16	34.727763	-0.066097	1205	Dug-well	60000	8.6	565	6.98	26.7
16-May	L17	34.727584	-0.066051	1206	Dug-well	25600	11.3	808	7.27	26.4
17-May	L18	34.764754	-0.075373	1160	Dug-well	3560	5.0	139	6.68	26.3
17-May	L19	34.766487	-0.079198	1160	Dug-well	5900	5.0	3640	7.52	25.7
17-May	L20	34.766568	-0.080202	1160	Dug-well	11400	133.3	1021	6.53	26.7
17-May	L21	34.767377	-0.079497	1161	Dug-well	2800	132.3	111	6.65	25.3
17-May	L22	34.767161	-0.079614	1161	Dug-well	2500	182.6	1277	6.46	27.6
17-May	L23	34.766344	-0.080275	1160	Dug-well	2100	178.6	1108	6.35	26.3
17-May	L24	34.783373	-0.013546	1281	Borehole	0	2.6	566	6.95	23.9
17-May	L25	34.808552	-0.071981	1171	Dug-well	6500	0.6	1836	6.9	26.1
17-May	L26	34.799624	-0.096957	1158	Borehole	2500	0.3	1281	7.64	27.4
18-May	L27	34.769804	-0.113363	1147	Dug-well	400	1.5	2600	7.21	26.5
18-May	L28	34.770208	-0.112992	1147	Dug-well	26200	171.6	2360	7.27	24.9
18-May	L29	34.769615	-0.113119	1148	Dug-well	1700	101.3	1115	7.08	26.2
18-May	L30	34.768376	-0.115198	1148	Dug-well	2400	159.6	1866	7.15	24.4
18-May	L31	34.768313	-0.113616	1150	Dug-well	17400	66.2	6490	6.47	27.8
18-May	L32	34.768097	-0.115036	1148	Dug-well	3000	67.8	625	6.41	28.4
19-May	L33	34.765349	-0.114774	1154	Dug-well	51200	92.4	981	6.74	25.6
19-May	L34	34.765744	-0.117288	1147	Dug-well	4800	100.9	389	6.29	26.1
19-May	L35	34.766849	-0.117188	1145	Spring	10600	134.7	485	6.2	26.3
19-May	L36	34.765196	-0.118038	1147	Dug-well	300	158.5	593	6.39	26.5
19-May	L37	34.765528	-0.11811	1145	Dug-well	15300	160.9	620	6.84	25.2
19-May	L38	34.765133	-0.118572	1146	Spring	20400	128.1	493	6.18	26.2
19-May	L39	34.764639	-0.117722	1148	Dug-well	4900	113.0	492	6.29	27.5
19-May	L40	34.763902	-0.115208	1156	Dug-well	5900	28.1	201	6.26	27.6
19-May	L41	34.763615	-0.120652	1145	Spring	9700	71.4	482	6.75	26.5
19-May	L42	34.762968	-0.118834	1148	Dug-well	900	80.0	312	6.13	26.8
19-May	L43	34.76251	-0.119024	1147	Dug-well	3300	63.5	251	6.17	27
19-May	L44	34.76272	-0.118807	1148	Dug-well	600	73.1	648	6.05	27.3
19-May	L45	34.759762	-0.124504	1144	Spring	15000	60.4	708	6.25	25.7
20-May	L46	34.758765	-0.123944	1145	Spring	800	45.9	538	6.37	24.4
20-May	L47	34.758756	-0.124323	1144	Dug-well	3100	0.3	1104	7.32	24
20-May	L48	34.759052	-0.124134	1144	Dug-well	10100	62.2	623	6.49	26.6
20-May	L49	34.758514	-0.124875	1144	Spring	800	56.9	637	6.28	26.6
20-May	L50	34.758361	-0.123582	1147	Dug-well	2900	53.8	607	6.34	27.6
20-May	L51	34.75934	-0.123419	1148	Dug-well	3600	118.6	845	6.19	27.7
20-May	L52	34.750681	-0.124631	1147	Dug-well	5600	24.5	579	6.42	28.8
20-May	L53	34.783601	-0.116753	1147	Dug-well	700	30.6	1660	7.27	27.4

Date	ID	longitude	latitude	Elevation	Water type	TTC	NO_3^{2-}	EC (µS/cm)	pH	Temp
20-May	L54	34.783664	-0.115143	1145	Dug-well	500	42.9	3240	8.49	26.7
20-May	L55	34.784167	-0.114845	1146	Dug-well	23100	55.3	1131	7.41	27
21-May	L56	34.781202	-0.109709	1146	Borehole	2	2.5	1313	7.91	30.2
21-May	L57	34.778831	-0.110396	1146	Dug-well	4733	3.0	947	7.75	24.3
21-May	L58	34.786709	-0.114411	1146	Dug-well	5200	224.0	1316	6.58	26.6
21-May	L59	34.793032	-0.11687	1149	Borehole	0	2.2	1305	7.33	27.7
21-May	L60	34.792269	-0.11573	1149	Dug-well	88	2.2	1038	7.56	27.5
21-May	L61	34.792107	-0.115423	1148	Dug-well	3500	16.5	911	7.28	27.5
21-May	L62	34.791847	-0.115595	1149	Dug-well	12200	30.9	1131	8.76	28.7
21-May	L63	34.792431	-0.115631	1148	Dug-well	600	25.8	609	8.19	27.6
21-May	L64	34.783763	-0.115207	1146	Dug-well	17950	18.0	1853	7.38	27
22-May	L65	34.801179	-0.116915	1150	Borehole	3350	1.5	2310	7.98	26.3
22-May	L66	34.809282	-0.119202	1151	Dug-well	2100	1.4	1053	7	26.9
22-May	L67	34.784975	-0.11498	1146	Dug-well	800	49.8	3230	8.09	27.4
22-May	L68	34.78281	-0.115776	1145	Dug-well	37200	33.7	4430	7.26	25.7
22-May	L69	34.77814	-0.115406	1143	Dug-well	2200	1.4	1047	6.81	26.5
22-May	L70	34.777466	-0.114918	1143	Dug-well	31000	10.2	634	6.75	25.3
22-May	L71	34.779505	-0.115134	1142	Dug-well	300	109.6	1579	6.7	26.7
22-May	L72	34.780556	-0.114999	1140	Dug-well	27700	4.0	792	6.94	27.3
22-May	L73	34.781454	-0.114284	1143	Dug-well	10600	34.4	1746	7.34	26.3
22-May	L74	34.780511	-0.115668	1143	Dug-well	6700	14.2	1507	7.6	26
22-May	L75	34.780843	-0.116744	1142	Dug-well	500	0.3	1265	6.6	27.1
22-May	L76	34.779676	-0.116247	1145	Dug-well	189000	0.1	418	7.87	25.7
23-May	L77	34.77893	-0.115695	1144	Dug-well	15000	2.4	1256	7.3	25.7
23-May	L78	34.779532	-0.116527	1145	Dug-well	400	0.3	1110	7.05	27.3
23-May	L79	34.780044	-0.117468	1141	Dug-well	40	0.3	1108	6.91	26.8
23-May	L80	34.779245	-0.118327	1140	Dug-well	8000	0.3	963	7.21	26.4

Appendix 6. Physico-chemical results for Kisumu sites

ID	Water type	Date	Temp (°C)	EC (µS/cm)	DO (mg/L)	pH (Units)	Salinity (PSS)	DO (%)	Turbidity (NTU)
1	Borehole	24-Nov-16	30.65	1110.00	3.02	7.79	0.55	50.00	0.00
1	Borehole	28-Jan-17	30.15	1150.00	4.22	8.08	0.59	61.30	4.40
1	Borehole	1-Mar-17	30.75	1128.00	5.39	7.93	0.57	70.00	6.20
1	Borehole	6-Apr-17	30.27	1135.00	6.22	7.87	0.56	56.60	5.40
1	Borehole	28-Apr-17	30.53	1152.00	4.89	7.89	0.57	62.10	7.20
1	Borehole	3-Jun-17	30.40	1161.00	7.12	8.02	0.58	60.10	14.60
1	Borehole	1-Jul-17	30.37	1170.00	5.85	8.00	0.58	76.60	12.60
1	Borehole	28-Jul-17	30.06	1156.00	3.79	8.15	0.58	51.50	4.90
1	Borehole	11-Sep-17	30.64	1162.00	3.65	8.21	0.58	56.70	8.90
1	Borehole	8-Oct-17	29.86	1154.00	4.13	8.35	0.58	58.80	6.10
1	Borehole	8-Dec-17	30.68	1161.00	4.35	8.38	0.59	61.00	8.60
1	Borehole	7-Jan-18	30.32	1197.00	3.51	8.10	0.60	47.10	8.10
2	River	24-Nov-16	24.90	128.00	5.26	7.40	0.02	72.20	89.90
2	River	28-Jan-17	23.73	332.00	2.65	7.67	0.16	34.70	46.30
2	River	1-Mar-17	23.40	83.00	5.61	7.36	0.04	71.00	765.00
2	River	6-Apr-17	26.91	167.00	5.00	7.83	0.08	66.00	270.00
2	River	28-Apr-17	23.64	68.00	10.26	7.94	0.04	92.90	2000.00
2	River	3-Jun-17	22.40	88.00	8.76	8.33	0.05	74.90	690.00
2	River	30-Jun-17	22.94	68.00	5.67	7.91	0.04	72.70	627.00
2	River	28-Jul-17	24.76	98.00	5.59	7.80	0.05	74.60	166.00
2	River	10-Sep-17	22.74	89.00	5.16	8.04	0.05	68.20	136.00
2	River	8-Oct-17	26.78	104.00	4.17	7.71	0.05	57.70	124.00
2	River	5-Nov-17	24.28	93.00	5.60	8.16	0.05	75.00	180.00
2	River	8-Dec-17	23.30	87.00	4.46	7.89	0.05	57.30	186.00
2	River	6-Jan-18	23.32	174.00	2.33	7.85	0.09	30.60	514.00
3	Borehole	24-Nov-16	27.62	1003.00	2.96	7.35	0.50	42.40	3.20
3	Borehole	28-Jan-17	27.90	1023.00	4.48	7.34	0.51	62.50	2.40
3	Borehole	1-Mar-17	27.95	1043.00	3.67	7.36	0.52	47.20	9.50
3	Borehole	6-Apr-17	28.95	1071.00	4.97	7.64	0.53	52.90	4.30
3	Borehole	28-Apr-17	27.37	1081.00	5.61	7.51	0.54	56.00	10.60
3	Borehole	1-Jun-17	28.24	1102.00	4.01	7.57	0.55	44.50	4.40
3	Borehole	30-Jun-17	27.89	1025.00	3.02	7.53	0.51	43.90	6.60
3	Borehole	28-Jul-17	28.95	1047.00	4.20	7.60	0.52	57.20	6.50
3	Borehole	10-Sep-17	27.52	1073.00	3.23	7.69	0.63	45.10	11.80
3	Borehole	3-Oct-17	28.22	1042.00	2.64	7.74	0.52	40.70	7.70
3	Borehole	8-Dec-17	27.33	1086.00	3.27	7.81	0.54	39.10	7.40
3	Borehole	6-Jan-18	27.66	1042.00	3.49	7.75	0.52	48.00	8.60
4	Shallow Well	26-Nov-16	26.16	1490.00	1.18	6.75	0.75	23.20	9.10
4	Shallow Well	28-Jan-17	26.37	1480.00	5.13	6.85	0.74	31.90	16.40
4	Shallow Well	1-Mar-17	26.39	1510.00	2.47	6.85	0.76	30.30	6.00
4	Shallow Well	6-Apr-17	26.38	1580.00	4.61	6.72	0.79	31.80	5.60
4	Shallow Well	28-Apr-17	25.86	1272.00	5.23	7.14	0.64	42.00	36.20
4	Shallow Well	2-Jun-17	26.15	1550.00	2.01	6.90	0.78	26.80	8.10
4	Shallow Well	30-Jun-17	25.99	1540.00	2.00	6.91	0.77	25.30	13.90
4	Shallow Well	28-Jul-17	26.03	1480.00	2.33	6.95	0.74	29.90	16.20
4	Shallow Well	10-Sep-17	25.98	1560.00	1.79	6.78	0.78	22.20	16.70
4	Shallow Well	8-Oct-17	26.06	1670.00	1.75	6.85	0.84	23.30	8.30
4	Shallow Well	5-Nov-17	26.64	1600.00	1.99	7.10	0.80	26.00	11.10
4	Shallow Well	8-Dec-17	25.72	1770.00	1.94	7.16	0.89	25.00	13.60
4	Shallow Well	6-Jan-18	25.61	1770.00	1.81	7.05	0.89	19.60	11.20
5	River	26-Nov-16	21.16	71.00	5.55	7.24	0.04	69.20	788.00
5	River	28-Jan-17	24.60	279.00	1.41	7.30	0.14	17.70	56.50
5	River	1-Mar-17	24.23	80.00	5.56	7.62	0.04	69.60	1112.00
5	River	6-Apr-17	25.68	158.00	8.31	7.60	0.08	58.10	263.00
5	River	28-Apr-17	21.09	59.00	7.13	8.04	0.03	76.00	2000.00
5	River	1-Jun-17	23.43	96.00	7.88	7.64	0.05	65.00	169.00
5	River	30-Jun-17	21.07	64.00	6.45	7.70	0.04	80.00	1125.00
5	River	28-Jul-17	22.69	148.00	5.65	7.74	0.07	72.20	171.00
5	River	10-Sep-17	21.41	93.00	5.27	8.26	0.05	66.50	150.00
5	River	8-Oct-17	24.22	98.00	4.51	7.63	0.05	60.80	157.00
5	River	5-Nov-17	22.50	91.00	5.38	7.71	0.05	65.80	219.00

ID	Water type	Date	Temp (°C)	EC (µS/cm)	DO (mg/L)	pH (Units)	Salinity (PSS)	DO (%)	Turbidity (NTU)
5	River	8-Dec-17	22.60	91.00	4.70	7.86	0.05	55.60	164.00
5	River	6-Jan-18	22.85	135.00	1.46	7.62	0.07	17.60	141.00
6	Spring	28-Nov-16	23.85	256.00	3.07	6.66	0.12	41.80	12.90
6	Spring	28-Jan-17	24.78	265.00	4.43	6.87	0.13	57.60	10.50
6	Spring	1-Mar-17	25.33	268.00	4.02	6.78	0.13	55.30	15.00
6	Spring	6-Apr-17	25.54	213.00	5.07	6.95	0.10	61.50	77.00
6	Spring	28-Apr-17	24.64	135.00	2.34	6.15	0.07	14.80	38.00
6	Spring	1-Jun-17	24.17	120.00	0.68	6.13	0.01	8.80	34.00
6	Spring	30-Jun-17	23.70	142.00	1.13	6.14	0.07	12.40	8.00
6	Spring	28-Jul-17	23.95	208.00	4.13	7.22	0.10	55.30	17.00
6	Spring	8-Sep-17	26.65	168.00	4.14	7.09	0.08	60.80	53.20
6	Spring	8-Oct-17	26.26	167.00	3.62	7.07	0.08	47.20	83.40
6	Spring	5-Nov-17	23.64	197.00	4.56	7.09	0.10	60.10	22.30
6	Spring	6-Dec-17	25.39	184.00	3.55	7.17	0.09	46.70	29.70
6	Spring	6-Jan-18	23.81	222.00	4.11	7.29	0.11	54.00	10.50
7	Borehole	28-Nov-16	23.00	491.00	2.79	6.92	0.24	35.40	5.50
7	Borehole	28-Jan-17	25.00	500.00	1.78	6.71	0.24	21.10	4.10
7	Borehole	1-Mar-17	24.00	500.00	3.89	6.90	0.24	41.10	6.20
7	Borehole	6-Apr-17	24.62	507.00	6.99	6.76	0.25	52.60	8.60
7	Borehole	28-Apr-17	24.54	504.00	3.90	6.90	0.24	45.20	9.60
7	Borehole	1-Jun-17	23.90	506.00	4.08	6.95	0.25	51.60	5.10
7	Borehole	30-Jun-17	23.21	508.00	3.46	6.97	0.24	43.10	6.10
7	Borehole	28-Jul-17	23.53	512.00	3.51	6.99	0.24	42.30	7.80
7	Borehole	8-Sep-17	23.02	503.00	2.51	6.98	0.24	31.60	11.30
7	Borehole	8-Oct-17	23.37	512.00	1.94	6.94	0.25	25.80	66.00
7	Borehole	5-Nov-17	23.31	512.00	2.96	7.05	0.25	38.40	7.20
7	Borehole	6-Dec-17	23.21	505.00	2.97	7.10	0.24	35.60	7.90
7	Borehole	6-Jan-18	24.57	513.00	3.27	7.13	0.25	43.40	6.80
8	Spring	6-Dec-16	27.26	201.00	2.12	6.54	0.10	26.50	225.00
8	Spring	28-Jan-17	29.77	252.00	3.84	7.07	0.12	53.50	6.40
8	Spring	2-Mar-17	27.68	188.00	2.16	6.25	0.09	31.10	456.00
8	Spring	5-Apr-17	27.45	152.00	1.17	6.47	0.08	14.80	211.00
8	Spring	27-Apr-17	27.00	149.00	2.12	6.48	0.07	25.00	220.00
8	Spring	1-Jun-17	26.10	185.00	0.96	6.49	0.09	11.00	102.00
8	Spring	30-Jun-17	26.07	201.00	2.24	7.19	0.10	18.30	66.10
8	Spring	28-Jul-17	26.10	218.00	1.52	6.52	0.11	20.30	63.30
8	Spring	8-Sep-17	26.30	217.00	1.31	6.51	0.11	17.40	245.00
8	Spring	7-Oct-17	27.10	216.00	1.75	6.74	0.11	24.20	126.00
8	Spring	4-Nov-17	26.97	193.00	1.13	6.79	0.10	14.90	146.00
8	Spring	6-Dec-17	26.56	186.00	1.26	6.58	0.09	17.20	139.00
9	Borehole	7-Dec-16	23.52	228.00	4.81	7.39	0.11	60.50	5.50
9	Borehole	28-Jan-17	30.64	275.00	4.28	7.38	0.13	58.80	3.50
9	Borehole	2-Mar-17	23.42	214.00	6.51	7.30	0.10	67.00	5.10
9	Borehole	6-Apr-17	24.93	165.00	8.71	6.49	0.08	72.10	12.50
9	Borehole	28-Apr-17	23.66	145.00	5.91	7.18	0.07	67.80	18.10
9	Borehole	1-Jun-17	24.71	143.00	7.77	6.70	0.07	80.10	15.20
9	Borehole	30-Jun-17	21.06	164.00	4.54	7.03	0.08	56.20	14.20
9	Borehole	28-Jul-17	22.26	225.00	5.31	7.13	0.11	66.20	9.90
9	Borehole	8-Sep-17	21.99	208.00	4.88	7.01	0.10	61.10	12.20
9	Borehole	8-Oct-17	26.11	261.00	4.54	7.83	0.13	63.30	10.50
9	Borehole	5-Nov-17	22.39	266.00	4.88	7.06	0.13	61.30	8.00
9	Borehole	6-Dec-17	24.02	221.00	4.66	7.45	0.11	63.40	11.40
9	Borehole	6-Jan-18	22.52	198.00	5.29	6.95	0.10	68.70	9.20
10	Spring	7-Dec-16	24.22	0.05	1.83	23.10	0.11	5.65	17.60
10	Spring	28-Jan-17	24.94	0.05	4.43	41.70	0.11	5.59	15.10
10	Spring	2-Mar-17	24.81	0.05	1.30	16.06	0.10	5.53	77.80
10	Spring	6-Apr-17	24.68	0.05	1.42	13.60	0.10	5.52	25.30
10	Spring	28-Apr-17	24.69	0.05	1.95	15.30	0.10	5.66	57.40
10	Spring	1-Jun-17	24.24	0.05	1.14	11.50	0.10	5.55	17.20
10	Spring	30-Jun-17	23.94	0.05	1.09	13.40	0.10	5.67	21.60
10	Spring	28-Jul-17	23.90	0.05	0.87	9.80	0.11	5.61	19.10
10	Spring	8-Sep-17	24.12	0.05	0.78	9.90	0.11	5.56	35.80
10	Spring	3-Oct-17	24.22	0.06	1.77	22.00	0.11	5.59	16.40

ID	Water type	Date	Temp (°C)	EC (µS/cm)	DO (mg/L)	pH (Units)	Salinity (PSS)	DO (%)	Turbidity (NTU)
10	Spring	5-Nov-17	24.18	0.06	0.74	9.40	0.11	5.59	45.00
10	Spring	6-Dec-17	24.52	107.00	1.02	5.70	0.05	11.30	16.10
10	Spring	6-Jan-18	24.29	109.00	1.51	5.81	0.06	19.40	26.30
11	Spring	7-Dec-16	24.39	170.00	3.75	6.01	0.08	50.60	30.00
11	Spring	28-Jan-17	24.65	192.00	5.01	6.31	0.09	65.40	20.40
11	Spring	2-Mar-17	24.64	168.00	1.48	5.76	0.08	19.90	50.30
11	Spring	6-Apr-17	24.47	148.00	1.60	5.90	0.07	18.40	46.20
11	Spring	27-Apr-17	24.63	159.00	1.68	5.92	0.08	13.90	72.70
11	Spring	1-Jun-17	24.31	142.00	2.17	5.98	0.07	25.20	47.20
11	Spring	30-Jun-17	24.01	146.00	3.57	6.11	0.07	29.00	23.40
11	Spring	29-Jul-17	24.29	158.00	2.49	6.11	0.08	32.60	20.20
11	Spring	8-Sep-17	24.20	157.00	1.02	5.90	0.08	12.50	34.70
11	Spring	8-Oct-17	24.22	161.00	2.57	5.93	0.08	31.00	30.80
11	Spring	5-Nov-17	24.10	157.00	2.25	6.05	0.08	28.60	196.00
11	Spring	6-Dec-17	24.33	159.00	2.82	6.05	0.08	35.20	28.50
11	Spring	6-Jan-18	24.35	173.00	2.98	6.23	0.08	38.90	38.70
12	Spring	28-Nov-16	25.61	318.00	2.53	6.43	0.15	32.30	16.60
12	Spring	29-Jan-17	26.39	311.00	3.92	6.51	0.15	31.60	7.30
12	Spring	2-Mar-17	25.42	410.00	4.62	6.35	0.20	21.70	13.60
12	Spring	5-Apr-17	25.83	461.00	1.87	6.40	0.22	22.70	6.80
12	Spring	27-Apr-17	25.70	429.00	1.66	6.45	0.21	15.60	17.60
12	Spring	2-Jun-17	25.67	392.00	4.97	6.89	0.19	36.00	16.20
12	Spring	29-Jun-17	25.28	367.00	4.94	6.80	0.18	34.00	10.90
12	Spring	28-Jul-17	24.77	362.00	1.53	6.38	0.18	18.90	14.50
12	Spring	8-Sep-17	24.84	351.00	1.88	6.45	0.17	24.60	36.10
12	Spring	7-Oct-17	26.15	326.00	1.69	6.55	0.16	22.30	13.40
12	Spring	4-Nov-17	25.77	352.00	2.20	6.64	0.17	27.50	27.00
12	Spring	8-Dec-17	25.71	374.00	1.87	6.67	0.18	26.00	16.50
12	Spring	5-Jan-18	26.00	340.00	1.97	6.77	0.16	27.10	16.20
13	Shallow Well	6-Mar-17	25.42	819.00	3.89	7.39	0.40	47.70	18.60
13	Shallow Well	5-Apr-17	25.66	784.00	9.05	7.72	0.38	76.50	19.70
13	Shallow Well	27-Apr-17	26.26	626.00	5.81	7.43	0.31	49.50	60.40
13	Shallow Well	2-Jun-17	25.51	646.00	5.75	7.23	0.31	55.80	22.30
13	Shallow Well	29-Jun-17	25.13	696.00	3.06	7.31	0.34	34.60	9.50
13	Shallow Well	29-Jul-17	25.83	745.00	2.83	7.31	0.37	37.20	10.50
13	Shallow Well	9-Sep-17	25.16	737.00	3.13	7.50	0.35	41.20	17.30
13	Shallow Well	7-Oct-17	25.25	739.00	4.12	7.63	0.36	53.40	8.90
13	Shallow Well	4-Nov-17	25.20	708.00	3.72	7.86	0.35	50.20	14.50
13	Shallow Well	7-Dec-17	25.21	740.00	3.43	7.89	0.36	42.00	15.20
13	Shallow Well	5-Jan-18	25.35	762.00	3.08	7.73	0.37	42.20	19.80
14	River	5-Dec-16	20.61	639.00	7.99	7.58	0.03	94.50	406.00
14	River	29-Jan-17	21.51	93.00	5.82	7.70	0.05	73.40	25.30
14	River	3-Mar-17	22.63	69.00	6.53	7.70	0.04	80.10	83.40
14	River	5-Apr-17	21.97	77.00	5.53	7.21	0.04	69.70	56.60
14	River	27-Apr-17	22.39	55.00	6.72	7.79	0.03	85.60	326.00
14	River	2-Jun-17	23.23	56.00	10.83	8.06	0.03	88.10	259.00
14	River	29-Jun-17	20.37	71.00	7.83	8.33	0.04	86.10	56.70
14	River	29-Jul-17	20.33	73.00	6.56	8.46	0.04	75.60	36.80
14	River	9-Sep-17	22.98	68.00	5.54	8.26	0.04	74.10	71.50
14	River	7-Oct-17	22.85	75.00	6.42	8.15	0.04	80.60	48.80
14	River	4-Nov-17	22.35	73.00	6.43	8.17	0.04	81.00	51.50
14	River	7-Dec-17	21.97	68.00	5.72	8.31	0.04	71.20	83.40
15	Shallow Well	5-Dec-16	23.90	232.00	3.49	6.48	0.01	33.20	18.00
15	Shallow Well	30-Jan-17	24.38	250.00	3.94	6.63	0.12	41.10	8.40
15	Shallow Well	3-Mar-17	24.24	247.00	2.19	6.51	0.12	28.30	10.20
15	Shallow Well	5-Apr-17	24.10	248.00	2.02	6.44	0.12	26.40	9.20
15	Shallow Well	27-Apr-17	23.43	229.00	5.90	6.64	0.11	27.00	53.40
15	Shallow Well	2-Jun-17	23.42	203.00	2.16	6.46	0.10	18.10	70.00
15	Shallow Well	29-Jul-17	22.87	221.00	4.01	6.82	0.11	29.50	30.80
15	Shallow Well	29-Jul-17	22.67	245.00	2.36	6.84	0.12	29.50	8.50
15	Shallow Well	9-Sep-17	22.99	244.00	1.94	6.80	0.12	24.50	12.50
15	Shallow Well	7-Oct-17	23.42	240.00	2.50	6.79	0.12	32.20	14.10
15	Shallow Well	4-Nov-17	23.50	248.00	1.96	6.75	0.12	25.90	8.30

225

ID	Water type	Date	Temp (°C)	EC (µS/cm)	DO (mg/L)	pH (Units)	Salinity (PSS)	DO (%)	Turbidity (NTU)
15	Shallow Well	7-Dec-17	23.61	244.00	1.77	6.86	0.12	23.00	11.10
16	River	29-Jan-17	23.98	125.00	5.21	7.96	0.06	71.50	62.60
16	River	3-Mar-17	26.11	79.00	4.96	7.86	0.04	68.10	184.00
16	River	5-Apr-17	23.59	95.00	5.53	7.94	0.05	73.00	125.00
16	River	27-Apr-17	23.95	54.00	10.24	7.74	0.03	95.60	1701.00
16	River	2-Jun-17	25.16	68.00	9.78	8.06	0.04	89.60	398.00
16	River	29-Jun-17	21.58	77.00	9.57	8.01	0.04	84.30	402.00
16	River	29-Jul-17	22.51	90.00	6.92	8.37	0.05	86.40	108.00
16	River	9-Sep-17	24.25	79.00	5.47	8.15	0.04	75.00	173.00
16	River	7-Oct-17	25.35	89.00	6.15	8.36	0.05	83.20	104.00
16	River	4-Nov-17	24.77	84.00	5.74	8.24	0.04	77.30	132.00
16	River	7-Dec-17	24.88	84.00	5.60	8.40	0.04	74.20	211.00
16	River	5-Jan-18	21.19	88.00	5.92	8.62	0.05	72.80	172.00
17	Shallow Well	2-Dec-16	25.73	665.00	2.01	7.19	0.32	26.70	3.70
17	Shallow Well	29-Jan-17	26.01	667.00	3.06	7.20	0.32	31.80	3.70
17	Shallow Well	3-Mar-17	25.92	660.00	2.07	7.23	0.32	26.70	5.10
17	Shallow Well	5-Apr-17	25.97	662.00	2.05	7.24	0.32	25.50	4.60
17	Shallow Well	27-Apr-17	25.93	663.00	2.44	7.35	0.32	27.60	4.50
17	Shallow Well	2-Jun-17	26.05	664.00	4.56	7.48	0.32	32.00	6.00
17	Shallow Well	29-Jun-17	25.92	665.00	2.39	7.40	0.32	30.90	8.90
17	Shallow Well	29-Jul-17	25.86	656.00	2.40	7.55	0.32	28.90	8.20
17	Shallow Well	9-Sep-17	25.92	646.00	2.53	7.61	0.32	33.40	10.10
17	Shallow Well	7-Oct-17	25.98	653.00	2.45	7.55	0.32	32.30	6.00
17	Shallow Well	4-Nov-17	25.95	650.00	1.89	7.58	0.32	26.80	7.30
17	Shallow Well	7-Dec-17	25.89	651.00	2.33	7.64	0.32	31.50	9.40
17	Shallow Well	6-Jan-18	25.86	648.00	2.00	7.53	0.32	27.00	9.10
18	Lake	29-Jan-17	23.71	331.00	1.03	6.33	0.16	11.00	27.90
18	Lake	4-Mar-17	26.12	140.00	2.98	7.84	0.07	21.50	95.80
18	Lake	5-Apr-17	29.48	150.00	3.43	7.52	0.07	50.90	69.70
18	Lake	24-Apr-17	26.70	155.00	1.77	7.17	0.08	16.40	91.90
18	Lake	2-Jun-17	26.31	140.00	3.10	7.96	0.07	21.60	65.00
18	Lake	29-Jun-17	25.25	152.00	3.94	7.16	0.08	43.40	95.20
18	Lake	29-Jul-17	24.87	149.00	4.42	8.79	0.07	57.30	75.20
18	Lake	9-Sep-17	25.27	134.00	3.32	8.31	0.07	43.80	88.60
18	Lake	7-Oct-17	26.16	139.00	5.25	8.59	0.07	67.40	103.00
18	Lake	4-Nov-17	27.02	130.00	4.20	7.92	0.07	57.40	102.00
18	Lake	7-Dec-17	26.17	125.00	3.40	8.13	0.06	44.90	80.60
18	Lake	5-Jan-18	24.31	131.00	3.30	7.80	0.07	42.50	93.20
19	Shallow Well	2-Dec-16	26.38	2800.00	2.53	7.00	2.01	29.80	1.50
19	Shallow Well	29-Jan-17	26.93	3510.00	5.60	7.11	1.87	53.10	4.20
19	Shallow Well	4-Mar-17	25.60	1920.00	4.41	7.09	0.97	45.60	11.10
19	Shallow Well	5-Apr-17	26.51	1650.00	3.17	7.27	0.83	35.70	7.80
19	Shallow Well	27-Apr-17	25.44	1073.00	6.47	7.24	0.53	42.20	73.60
19	Shallow Well	2-Jun-17	26.35	1240.00	7.11	7.73	0.62	52.80	12.60
19	Shallow Well	29-Jun-17	26.12	1660.00	4.52	7.45	0.84	53.60	20.00
19	Shallow Well	29-Jul-17	26.21	2260.00	2.71	7.18	1.16	30.20	15.20
19	Shallow Well	9-Sep-17	26.27	2730.00	1.79	7.21	1.41	24.10	14.50
19	Shallow Well	7-Oct-17	26.40	2970.00	1.63	7.28	1.54	23.90	9.70
19	Shallow Well	4-Nov-17	26.36	3050.00	1.98	7.25	1.59	25.70	11.70
19	Shallow Well	7-Dec-17	26.27	2990.00	3.25	7.57	1.55	40.50	14.70
19	Shallow Well	5-Jan-18	26.30	3260.00	1.89	7.29	1.71	25.80	15.80
20	Shallow Well	2-Dec-16	25.98	800.00	4.20	7.44	0.39	57.00	12.20
20	Shallow Well	29-Jan-17	27.42	1101.00	3.40	7.18	0.55	43.60	5.00
20	Shallow Well	4-Mar-17	27.30	1084.00	2.82	7.33	0.54	37.80	7.80
20	Shallow Well	5-Apr-17	27.53	1047.00	1.68	7.28	0.53	23.90	5.40
20	Shallow Well	27-Apr-17	27.10	1030.00	3.33	7.50	0.50	38.30	10.90
20	Shallow Well	2-Jun-17	26.92	980.00	6.22	7.83	0.48	58.60	10.90
20	Shallow Well	29-Jun-17	26.65	1059.00	7.57	7.49	0.53	44.90	9.20
20	Shallow Well	29-Jul-17	29.74	1071.00	3.60	7.70	0.52	48.80	12.10
20	Shallow Well	9-Sep-17	26.84	1085.00	2.87	7.46	0.54	39.30	54.30
20	Shallow Well	7-Oct-17	26.95	1101.00	1.98	7.52	0.55	28.10	8.20
20	Shallow Well	4-Nov-17	26.94	1058.00	2.85	7.77	0.53	35.20	9.80
20	Shallow Well	7-Dec-17	26.83	1091.00	2.46	7.66	0.53	31.90	14.40

ID	Water type	Date	Temp (°C)	EC (µS/cm)	DO (mg/L)	pH (Units)	Salinity (PSS)	DO (%)	Turbidity (NTU)
20	Shallow Well	5-Jan-18	26.84	1100.00	2.78	7.46	0.55	36.20	18.00
21	Shallow Well	2-Dec-16	25.98	800.00	4.20	7.44	0.39	57.00	12.20
21	Shallow Well	29-Jan-17	25.96	746.00	5.02	5.51	0.36	63.60	45.50
21	Shallow Well	4-Mar-17	25.77	743.00	7.23	7.37	0.36	52.00	22.50
21	Shallow Well	5-Apr-17	25.91	769.00	4.00	7.72	0.37	62.70	17.70
21	Shallow Well	27-Apr-17	26.42	800.00	5.37	7.28	0.39	61.50	14.80
21	Shallow Well	2-Jun-17	26.80	969.00	3.11	7.19	0.47	41.90	27.10
21	Shallow Well	29-Jun-17	25.88	1067.00	3.19	7.20	0.53	37.80	7.90
21	Shallow Well	29-Jul-17	25.84	1045.00	2.47	7.23	0.52	30.90	9.20
21	Shallow Well	9-Sep-17	25.95	896.00	2.63	7.31	0.44	35.60	16.70
21	Shallow Well	7-Oct-17	25.90	872.00	2.37	7.27	0.42	31.60	8.60
21	Shallow Well	4-Nov-17	25.96	876.00	2.33	7.31	0.43	28.40	19.40
21	Shallow Well	8-Dec-17	25.84	874.00	1.88	7.42	0.43	27.10	11.00
21	Shallow Well	5-Jan-18	25.88	773.00	2.59	7.49	0.38	36.20	15.60
22	Shallow Well	6-Mar-17	26.39	969.00	4.26	7.54	0.48	67.00	5.80
22	Shallow Well	5-Apr-17	26.43	1019.00	5.25	7.54	0.50	62.70	1.10
22	Shallow Well	27-Apr-17	26.29	1045.00	5.25	7.21	0.52	49.10	12.60
22	Shallow Well	2-Jun-17	26.02	1090.00	0.70	7.03	0.54	8.30	7.70
22	Shallow Well	29-Jun-17	25.54	1118.00	1.98	7.08	0.55	24.10	5.20
22	Shallow Well	27-Jul-17	25.32	1093.00	2.01	7.15	0.54	26.00	9.30
22	Shallow Well	9-Sep-17	25.38	1075.00	2.01	7.17	0.53	28.60	13.40
22	Shallow Well	7-Oct-17	25.50	1038.00	4.36	7.71	0.51	60.70	9.20
22	Shallow Well	4-Nov-17	25.36	964.00	3.74	7.76	0.47	45.20	47.50
22	Shallow Well	7-Dec-17	25.58	1028.00	3.29	7.57	0.51	44.00	15.40
22	Shallow Well	5-Jan-18	25.56	979.00	3.26	7.84	0.48	44.00	239.00

Appendix 7. Physico-chemical data Mt. Elgon water sites

Date	Sample No	Temperature (ºC)	pH	pH (pH scale)	Turbidity (N.T.U)	EC (at 25ºC)
30/10/2014	EL 21	23.1	7.08	7.34	2.2	370.0
28/10/2014	EL 3	22.8	6.90	7.64	1.1	142.5
28/10/2014	EL 4	24.0	6.72	7.07	4.3	196.3
28/10/2014	EL 8	22.8	8.55	8.25	1.8	388.0
28/10/2014	EL 9	22.7	7.42	7.68	1.7	229.0
29/10/2014	EL 13	24.9	7.82	8.21	3.1	567.0
29/10/2014	EL 10	26.2	8.31	7.74	0.9	487.0
30/10/2014	EL 15	22.5	6.09	6.31	1.9	155.6
30/10/2014	EL 18	24.0	6.65	7.01	4.4	285.0
1/11/2014	EL 25	23.3	6.60	6.78	1.2	12.5
1/11/2014	EL 26	23.6	11.54	10.61	5.0	981.0
3/11/2014	EL 32	28.1	7.35	7.45	2.2	696.0
27/10/2014	EL 2	13.8	8.44	7.3	4.9	40.8
29/10/2014	EL 12	28.2	7.51	8.45	4.0	791.0
1/11/2014	EL 24	22.4	6.43	7.54	5.8	133.0
1/11/2014	EL 27	23.0	7.10	7.10	0.1	268.0
30/10/2014	EL 16	23.0	6.70	7.47	0.0	142.4
30/10/2014	EL 17	23.0	6.85	7.58	16.6	118.5
30/10/2014	EL 19	22.4	6.94	8.05	3.4	90.8
29/10/2014	EL 11	28.0	7.53	8.61	19.5	580.0
18/3/2015	ELB 1	16.2	8.53	8.21	1.5	232.0
18/3/2015	ELB 5	21.6	8.17	8.55	9.1	221.0
18/3/2015	ELB 6	26.3	8.16	8.27	0.0	487.0
18/3/2015	ELB 7	26.7	8.23	8.23	56.5	907.0
20/3/2015	ELB 8	22.2	6.40	6.16	10.7	79.2
20/3/2015	ELB 10	23.4	6.25	6.86	6.4	129.2
20/3/2015	ELB 13	27.3	11.87	11.26	9.8	1214.0
20/3/2015	ELB 14	23.4	7.25	7.10	0.8	302.0
21/3/2015	ELB 16	22.3	7.06	8.23	0.7	264.0
21/3/2015	ELB 17	21.0	8.42	8.48	83.3	232.0
21/3/2015	ELB 18	23.8	6.38	6.44	18.7	56.1
21/3/2015	ELB19	23.0	7.14	8.20	3.2	135
21/3/2015	ELB 21	22.2	6.65	6.91	4.1	193.6
21/3/2015	ELB22	24.0	7.40	7.46	1.6	95.7
21/3/2015	ELB 24	23.4	6.77	8.09	12.6	83.6
21/3/2015	ELB 26	25.9	8.05	7.76	0.0	725.0
21/3/2016	ELB 27	28.8	7.53	8.59	4.3	447.0
21/3/2017	ELB 28	28.1	7.65	7.79	2.4	970.0
21/3/2018	ELB 29	31.1	9.05	8.31	7.2	323.0
21/3/2019	ELB 30	27.6	7.66	7.90	0.0	914.0

Appendix 8. Saturation indices for Kisumu water samples

Main minerals

Water type	Anhydrite	Aragonite	Calcite	Halite	Sylvite	Fluorite	Gypsum
B/hole	-3.95	-1.93	-1.79	-6.43	-7.51	-1.78	-3.64
B/hole	-3.96	-1.97	-1.82	-6.41	-7.53	-1.90	-3.65
B/hole	-2.92	-0.94	-0.79	-6.40	-7.50	-0.93	-2.61
River	-3.71	-1.87	-1.73	-8.41	-8.48	-2.31	-3.41
River	-3.97	-1.76	-1.62	-8.74	-9.03	-2.53	-3.67
River	-3.77	-1.45	-1.31	-8.57	-8.9	-2.72	-3.47
B/hole	-2.43	-0.29	-0.14	-6.58	-7.34	0.18	-2.12
B/hole	-2.53	-0.27	-0.13	-6.58	-7.35	0.35	-2.22
B/hole	-2.49	-0.30	-0.15	-2.19	-6.57	0.21	-6.77
S/well	-1.38	0.28	0.43	-6.24	-6.95	-0.88	-1.08
S/well	-1.45	0.29	0.44	-6.16	-7.00	-0.82	-1.14
S/well	-1.34	0.28	0.42	-6.20	-6.97	-1.00	-1.04
River	-3.52	-1.70	-1.56	-8.46	-8.52	-2.58	-3.21
River	-3.87	-1.86	-1.71	-8.80	-9.35	-2.73	-3.56
River	-3.65	-1.49	-1.35	-8.54	-8.96	-2.88	-3.35
spring	-3.32	-0.73	-0.59	-8.38	-8.94	-2.23	-3.01
Spring	-3.86	-1.54	-1.40	-8.81	-9.14	-2.51	-3.56
Spring	-3.68	-1.09	-0.95	-8.65	-9.25	-2.31	-3.38
B/hole	-3.01	-0.29	-0.15	-8.15	-9.26	-1.30	-2.70
B/hole	-3.11	-0.19	-0.05	-8.15	-9.62	-1.17	-2.81
B/hole	-3.04	-0.26	-0.12	-8.15	-9.24	-1.25	-2.73
spring	-3.30	-1.20	-1.06	-7.67	-7.76	-1.78	-2.99
Spring	-3.91	-1.96	-1.82	-7.69	-7.84	-1.99	-3.60
Spring	-3.48	-1.31	-1.16	-7.59	-7.71	-1.87	-3.18
B/hole	-4.13	-0.97	-0.82	-8.08	-8.32	-3.83	
B/hole	-5.65	-2.06	-1.92	-8.63	-8.79	-3.29	-5.35
B/hole	-4.40	-1.49	-1.34	-8.47	-8.68	-3.22	-4.10
spring	-4.27	-1.63	-1.48	-8.21	-8.22	-2.54	-3.97
Spring	-5.12	-2.34	-2.20	-8.64	-8.61	-3.11	-4.82
Spring	-4.45	-1.74	-1.59	-8.54	-8.52	-2.82	-4.15
spring	-3.61	-1.37	-1.23	-8.09	-8.14	-2.52	-3.30
Spring	-4.23	-1.98	-1.83	-8.27	-8.30	-2.75	-3.92
Spring	-3.89	-1.55	-1.41	-8.17	-8.21	-2.78	-3.59
spring	-2.43	-0.87	-0.72	-7.18	-7.19	-1.33	-2.13
Spring	-2.55	-1.04	-0.90	-7.23	-7.20	-1.48	-2.25
Spring	-2.71	-1.01	-0.87	-7.41	-7.38	-1.55	-2.41
S/well	-2.18	-0.18	-0.04	-7.04	-7.42	-0.01	-1.88
S/well	-2.56	-0.54	-0.39	-7.41	-7.59	-0.13	-2.26

Water type	Anhydrite	Aragonite	Calcite	Halite	Sylvite	Fluorite	Gypsum
S/well	-2.35	-0.19	-0.05	-7.17	-7.43	-0.33	-2.04
River	-4.07	-1.91	-1.77	-9.14	-9.02	-2.42	-3.77
River	-4.39	-2.07	-1.93	-9.02	-8.87	-2.76	-4.09
River	-4.11	-1.67	-1.52	-8.87	-8.90	-2.51	-3.80
S/well	-4.13	-0.87	-0.73	-8.56	-9.34	-1.39	-3.82
S/well	-4.14	-1.05	-0.91	-8.48	-9.57	-1.49	-3.84
S/well	-3.81	-0.90	-0.75	-8.96	-9.88	-1.34	-3.51
River	-3.51	-1.73	-1.59	-8.49	-8.55	-2.27	-3.21
River	-4.13	-1.92	-1.78	-8.54	-8.64	-2.66	-3.82
River	-3.85	-1.63	-1.49	-8.52	-8.72	-2.53	-3.54
S/well	-2.75	-0.30	-0.16	-7.05	-7.72	-1.37	-2.45
S/well	-2.67	-0.34	-0.20	-7.08	-7.78	-0.89	-2.37
S/well	-2.71	-0.41	-0.27	-7.07	-7.76	-0.94	-2.41
Lake	-4.00	-1.46	-1.31	-8.39	-8.39	-1.91	-3.70
Lake	-4.07	-1.54	-1.40	-8.47	-8.50	-2.02	-3.76
Lake	-3.80	-1.28	-1.13	-8.20	-8.31	-1.90	-3.50
S/well	-2.23	-0.14	0.00	-5.42	-5.96	-0.97	-1.92
S/well	-2.34	-0.43	-0.28	-5.83	-6.34	-0.97	-2.03
S/well	-2.05	0.07	0.22	-5.14	-5.77	-0.44	-1.74
S/well	-1.94	-0.08	0.06	-6.48	-6.79	0.05	-1.63
S/well	-1.96	-0.17	-0.03	-6.50	-6.91	-0.17	-1.66
S/well	-1.86	-0.04	0.11	-6.43	-6.78	0.02	-1.56
S/well	-2.36	-0.40	-0.26	-6.62	-6.8	-0.64	-2.06
S/well	-1.86	-0.14	0.00	-6.51	-6.57	-0.44	-1.55
S/well	-1.98	-0.12	0.02	-6.57	-6.67	-0.40	-1.67
S/well	-2.09	-0.05	0.10	-6.55	-7.25	0.01	-1.78
S/well	-1.94	0.13	0.27	-6.55	-7.19	-0.37	-1.63
S/well	-2.03	0.13	0.27	-6.61	-7.29	-0.22	-1.72

Minor minerals

Water type	Manganite	Fe(OH)3	Goethite	Hausmannite	Hematite	Jarosite-K	Melanterite	Pyrochroite	Pyrolusite	Rhodochrosite	Siderite
River	-5.14	1.99	7.88	-11.44	17.77	-3.69	-7.12	-6.00	-10.18	-0.13	-0.66
River	-5.35	1.86	7.75	-12.05	17.5	-4.94	-7.56	-6.21	-10.39	-0.26	-0.73
River	-5.85	1.78	7.67	-13.56	17.35	-5.27	-7.71	-6.71	-10.89	-0.73	-0.77
S/well	-6.37			-15.12				-7.23	-11.41	-0.30	
S/well	-7.27			-17.83				-8.13	-12.31	-1.20	
S/well	-5.55			-12.67				-6.41	-6.41	-10.59	0.49
River	-5.15	2.16	8.05	-11.45	18.11	-3.34	-7.04	-6.01	-10.19	-0.24	-0.6
River	-5.53	1.53	7.42	-12.59	16.85	-5.86	-7.76	-6.39	-10.57	-0.51	-1.12
River	-5.68	1.83	7.72	-13.05	17.45	-4.88	-7.50	-6.54	-10.72	-0.56	-0.71
spring	-5.49	0.97	6.86	-12.48	15.73	-7.17	-8.31	-6.35	-10.53	0.11	-1.10
Spring	-6.07	2.27	8.16	-14.22	18.32	-3.51	-7.10	-6.93	-11.11	-0.83	-0.16

Water type	Manganite	Fe(OH)3	Goethite	Hausmannite	Hematite	Jarosite-K	Melanterite	Pyrochroite	Pyrolusite	Rhodochrosite	Siderite
Spring	-6.11	1.13	7.02	-14.34	16.05	-7.23	-8.35	-6.97	-11.15	-0.70	-1.14
B/hole	-5.64			-12.93				-6.50	-10.68	0.19	
B/hole	-5.57			-12.73				-6.43	-10.61	0.35	
B/hole	-5.60			-12.81				-6.46	-10.64	0.26	
spring	-5.65	1.83	7.72	-12.95	17.44	-3.59	-7.22	-6.51	-10.69	-0.31	-0.51
Spring	-6.29	3.19	9.08	-14.89	20.16	0.47	-5.85	-7.15	-11.33	-1.09	0.72
Spring	-5.99	3.35	9.24	-13.99	20.49	1.23	-5.60	-6.85	-11.03	-0.48	1.20
B/hole		-2.71									
B/hole		1.93	7.82		17.65	-6.52	-8.66				-0.45
B/hole		1.34	7.23		16.47	-6.38	-8.37				-0.83
spring	-6.40	1.04	6.93	-15.21	15.87	-7.68	-8.79	-7.26	-11.44	-1.30	-1.53
Spring	-6.62	0.74	6.63	-15.87	15.27	-9.06	-9.31	-7.48	-11.66	-1.60	-1.91
Spring	-6.62	0.23	6.12	-15.86	14.25	-10.2	-9.66	-7.48	-11.66	-1.51	-2.33
spring	-6.56	1.4	7.3	-15.68	16.6	-5.39	-7.9	-7.42	-11.60	-1.33	-1.04
Spring	-7.11	1.02	6.91	-17.33	15.82	-6.78	-8.35	-7.97	-12.15	-1.93	-1.48
Spring	-6.87			-16.62				-7.73	-11.91	-1.63	
spring	-6.09	0.92	6.81	-14.27	15.62	-4.72	-7.47	-6.95	-11.13	-0.61	-1.28
Spring	-6.50			-15.52				-7.36	-11.54	-1.10	
Spring	-6.44	1.84	7.73	-15.32	17.46	-2.29	-6.69	-7.30	-11.48	-0.97	-0.37
S/well	-7.37	1.30	7.19		16.39	-4.16					-0.73
S/well		0.68	6.57		15.14	-5.61	-7.82				-1.04
River	-5.95	2.02	7.91	-13.87	17.82	-4.26	-7.41	-6.81	-10.99	-0.92	-0.62
River	-5.60	1.98	7.87	-12.81	17.75	-4.82	-7.62	-6.46	-10.64	-0.59	-0.68
River	-5.87	1.69	7.58	-13.62	17.16	-5.87	-8.01	-6.73	-10.91	-0.83	-0.94
S/well	-6.96	0.79	6.69	-16.89	15.38	-9.33	-9.14	-7.82	-12	-1.35	-1.26
S/well	-7.05	2.56	8.45	-17.16	18.92	-4.23	-7.29	-7.91	-12.09	-1.52	0.43
S/well		1.10	6.99		15.99	-7.92	-8.52				-0.98
River	-5.69	1.88	7.77	-13.07	17.55	-4.04	-7.27	-6.55	-10.73	-0.77	-0.87
River	-5.51	1.34	7.23	-12.54	16.47	-6.16	-7.98	-6.37	-10.55	-0.33	-1.15
River	-5.67	1.47	7.36	-13.03	16.72	-5.94	-7.94	-6.53	-10.71	-0.58	-1.10
Lake	-6.12	1.21	7.11	-14.36	16.22	-6.57	-8.31	-6.98	-11.16	-0.81	-1.14
Lake	-5.67	1.66	7.55	-13.01	17.1	-5.36	-7.9	-6.53	-10.71	-0.41	-0.76
Lake	-6.16	1.5	7.39	-14.48	16.78	-5.8	-8.04	-7.02	-11.2	-0.87	-0.89
S/well	-7.05			-17.14				-7.91	-12.09	-1.30	
S/well				-16.68			-6.89	-7.75	-11.93	-1.30	
S/well	-6.23			-14.7				-7.09	-11.27	-0.41	
S/well	-7.37	0.39	6.28	-18.13	14.56	-5.58	-7.72	-8.23	-12.41	-1.36	-1.26
S/well		1.12	7.01		16.02	-3.99	-7.28				-0.7
S/well		0.28	6.17		14.34	-6.02	-7.88				-1.54
S/well	-7.36	0.33	6.22	-18.08	14.45	-6.00	-7.90	-8.22	-12.40	-1.44	-1.42
S/well	-7.47			-18.41				-8.33	-12.51	-1.37	

Appendix 9. Saturation indices for Mt. Elgon water samples

Lab No.	Water type	Anhydrite	Aragonite	Calcite	Dolomite	Fluorite	Gypsum	Halite	Sylvite
El 1	River	-4.25	0.04	0.18	0.41	-1.42	-3.95	-8.88	-9.17
EL 21	Spring	-3.69	-0.50	-0.35	-0.75	-3.31	-3.39	-8.15	-8.60
EL 3	Borehole	-4.29	-0.94	-0.79	-1.78	-3.57	-3.99		-9.52
EL 4	Borehole	-4.38	-1.24	-1.09	-2.34	-3.46	-4.08	-8.48	-8.69
EL 8	Borehole	-4.27	0.09	0.24	0.44	-3.81	-3.96	-7.81	-8.44
EL 9	Borehole	-3.91	-0.46	-0.31	-0.85	-3.33	-3.60	-8.55	-8.31
EL 13	Borehole	-3.25	0.57	0.72	1.72	-3.43	-2.94	-7.65	-8.62
EL 10	Borehole	-3.61	0.09	0.23	0.72	-2.69	-3.30	-8.67	-8.37
EL 15	Borehole	-4.40	-2.71	-2.57	-5.16		-4.10	-8.56	-8.62
EL 18	Borehole	-4.75	-1.31	-1.16	-2.31	-3.39	-4.45	-8.22	-8.38
EL 25	Borehole	-4.32	-2.15	-2.00	-4.50	-3.66	-4.01	-9.45	-9.50
EL 26	Borehole	-5.31	0.30	0.44		-2.76	-5.01	-6.92	-7.46
EL 32	Borehole	-3.02	0.14	0.28	0.72	-1.61	-2.71	-7.79	-8.24
EL 12	Shallow well	-4.20	0.41	0.56	2.18	-1.28	-3.90	-7.60	-8.42
EL 24	Spring	-4.89	-1.47	-1.33	-2.47	-3.79	-4.59	-9.24	-9.33
EL 27	Spring	-4.19	-0.91	-0.77	-1.50	-2.40	-3.89	-8.97	-9.00
EL 16	Borehole	-3.79	-0.80	-0.65	-1.88	-3.40	-3.48		
EL 17	Shallow well	-3.99	-0.94	-0.80	-2.05	-3.51	-3.69		
EL 19	Spring	-4.61	-0.84	-0.69	-1.43	-3.82	-4.30	-9.70	-9.96
EL 11	Borehole	-3.54	0.93	1.08	2.67	-1.88	-3.23	-8.88	-8.63
ELB 1	River	-4.12	0.07	0.21	0.43	-1.31	-3.81	-9.12	-9.33
ELB 5	River	-4.52	0.50	0.64	1.20	-2.79	-4.22	-9.21	-9.10
ELB 6	Borehole	-4.21	0.20	0.34	0.67	-3.10	-3.90	-7.68	-8.30
ELB 7	Shallow well	-4.20	0.68	0.82	2.08	-2.81	-3.90	-6.89	-7.38
ELB 8	Spring	-4.84	-3.50	-3.35	-6.50	-4.06	-4.54		
ELB 10	Spring	-5.38	-1.81	-1.67	-4.09	-3.57	-5.07	-8.96	-9.17
ELB 13	Borehole							-6.78	-7.04
ELB 14	Spring	-4.19	-0.84	-0.70	-1.45	-2.35	-3.88	-8.62	-8.83
ELB 16	Borehole	-3.97	-0.01	0.13	0.00	-3.37	-3.67	-8.09	-8.40
ELB 17	River		0.45	0.60	1.17	-2.81		-9.03	-8.88
ELB 18	Borehole	-4.75	-3.25	-3.11	-6.25	-3.97	-4.45		
ELB 19	Borehole	-4.09	-0.27	-0.12	-0.35	-3.53	-3.78	-9.45	-9.25
ELB 21	Shallow well	-4.40	-1.80	-1.66	-3.31	-3.58	-4.09	-8.48	-8.90
ELB 22	Spring	-4.64	-1.57	-1.42	-2.78	-3.93	-4.34		
ELB 24	Shallow well	-5.08	-1.01	-0.87	-1.61	-3.39	-4.78		
ELB 26	Borehole	-3.79	0.19	0.33	1.25	-2.24	-3.49	-8.15	-8.22
ELB 27	Borehole	-4.71	0.67	0.81	2.31	-2.09	-4.40	-8.95	-8.72
ELB 28	Borehole	-3.20	0.57	0.71	1.56	-0.20	-2.90	-7.44	-8.28
ELB 29	Borehole	-3.85	0.44	0.58	1.15	-1.75	-3.55	-8.50	-8.41
ELB 30	Borehole	-2.86	0.74	0.88	2.09	-0.91	-2.55	-8.50	8.17

232

Appendix 10. Pumping test data for Kisumu Piezometers

Pumping test - Mbeme						
12/11/2018						
Total depth = 40 m						
Calculated Yield = 2.8 m³/hr						
Constant drawdown				Recovery test		
Time (Min)	Water Level	Drawdown		Time	water level	Recovery
0	10.4	0.0		0	31.5	0.0
5	15.0	4.6		5	21.7	9.8
10	16.7	6.3		10	19.4	2.3
15	18.3	7.9		15	17.4	2.0
20	19.6	9.2		20	16.6	0.8
25	20.1	9.7		25	16.2	0.4
30	21.3	10.9		30	15.0	1.2
35	22.5	12.1		35	14.1	0.9
40	25.8	15.4		40	13.6	0.5
45	26.0	15.6		45	13.3	0.3
50	27.0	16.6		50	13.2	0.1
55	28.5	18.1				
60	29.2	18.8				
70	29.7	19.3		Physico- chemical quality		
80	30.7	20.3		Temperature	28.75	
90	32.7	22.3		eC	1094	
100	31.8	21.4		DO	2.16	
110	32.4	22.0		pH	7.25	
120	31.5	21.1		Salinity	0.55	
140	31.5	21.1		Turbidity	104	
160	31.5	21.1				
180	31.5	0.0				
200	31.5	0.0				
220	31.5	0.0				
240	31.5	0.0				
Pumping test - Kudho						
14/11/2018						
Total depth = 40 m						
Calculated Yield = 1.0 m³/hr						
Constant drawdown				Recovery test		
Time (Min)	Water Level	Drawdown		Time	water level	Recovery
0	1.0	0.0		0	38.5	0.0
5	11.0	10.0		5	27.6	10.9
10	19.4	18.4		10	20.7	6.9
15	23.0	22.0		15	12.5	8.2
20	23.0	22.0		20	10.9	1.6
25	23.6	22.6		25	4.0	6.9
30	23.6	22.6		30	2.0	2.0
35	23.9	22.9				

40	23.9	22.9				
45	24.0	23.0				
50	24.7	23.7				
55	25.3	24.3				
60	26.0	25.0				
70	34.0	33.0		Physico-chemical quality		
80	36.0	3.50		Temperature	26.2	
90	39.0	38.0		eC	330	
100	37.0	36.0		DO	9.01	
110	36.7	35.7		pH	7.24	
120	36.5	35.5		Salinity	0.16	
140	36.0	35.0		Turbidity	332	
160	35.9	34.9				
180	35.0	34.0				
200	35.3	34.3				
220	35.1	34.1				
240	35.4	34.4				
300	38.2	37.2				
360	38.2	37.2				
420	36.4	35.4				
480	38.4	37.4				
500	38.5	37.5				
520	38.5	37.5				
540	38.5	37.5				
560	38.5	37.5				

Pumping test - Kogweno

13/11/2018						
Total depth = 40 m						
Calculated Yield = 0.2 m³/hr						
Constant drawdown				Recovery test		
Time (Min)	Water Level	Drawdown		Time	water level	Recovery
0	1.5	0.0		0	21.2	0.0
5	15.3	13.8		5	19.4	1.8
10	23.7	22.2		10	18.3	1.1
15	33.6	32.1		15	17.4	0.9
20	36.0	34.5		20	16.5	0.9
25	35.3	33.8		25	15.5	1.0
30	34.2	32.7		30	14.4	1.1
35	33.0	31.5		35	14.0	0.4
40	32.0	30.5		40	13.4	0.6
45	31.0	29.5		45	12.7	0.7
50	30.0	28.5		50	11.1	1.6
55	29.0	27.5		55	11.9	
60	28.0	26.5		60	11.4	
70	26.7	25.2		Physico-chemical quality		
80	25.0	23.5		Temperature	27.78	

90	24.5	23.0		eC	655	
100	23.5	22.0		DO	6.47	
110	23.8	22.3		pH	7.33	
120	22.3	20.8		Salinity	0.32	
140	20.7	19.2		Turbidity	30.4	
160	21.2	19.7				
180	21.2	19.7				
200	21.2	19.7				
220	21.2	19.7				
240	21.2	19.7				
Pumping test - Wandiege						
Total depth = 40 m						
Yield = 0.05 m^3/hr						
Constant drawdown						
Time (Min)	Water Level	Drawdown				
0	4.0	0.0				
5	15.3	11.3				
10	20.6	5.3				
15	22.0	1.4				
20	22.4	0.4				
25	33.0	10.6				
30	40.0	7.0				
40	40.0	0.0				
				Physico-chemical quality quality		
				Temperature	27.51	
				eC	4070	
				DO	2.63	
				pH	6.91	
				Salinity	2.15	
				Turbidity	830	

235